Synthesis of Novel Quinoline Derivatives and their Cytotoxicity in A549 Lung Cancer Cells

Thesis submitted in fulfilment of the requirements for the Degree of Master of Science, Chemistry, in the Faculty of Applied Sciences at Durban University of Technology

By

S'BUSISO MFAN'VELE NKOSI

2017

Supervisor : Professor Rorbet M Gengan **Date:** 25/08/2017

Co-Supervisor: Professor Anil A Chuturgoon **Date:** 25/08/2017

Declaration

I, Sõbusiso Mfanôvele Nkosi, hereby declare that this dissertation entitled ñ**Synthesis of Novel Quinoline Derivatives and their Cytotoxicity in A549 Lung Cancer Cell Lines''**, submitted to Durban University of Technology, in fulfilment of the requirements for the award of the Degree of Master of Technology, Organic Chemistry, in the Faculty of Applied Sciences, is the result of my own work and that all sources used or quoted have been indicated and acknowledged by means of complete references.

Signed [redacted] Sõbusiso Mfanôvele Nkosi

Date : 25/08/2017

Signed [redacted] Professor R M Gengan (Supervisor)

Date : 25/08/2017

Signed [redacted] . Professor A Chuturgoon (Co Supervisor)

Date : 25/08/2017 .

Dedication

This dissertation is dedicated to:

- my late twin sisters **Sihle** and **Esihle Nkosi (1988-1990),** may their soul rest in peace
- my sister **Nomathemba Nkosi (1981-2014)** who died of cancer, may her soul be in peace.
- my father **Lazaros Nkosi,** who gave me direction in this world.
- my mother **Espa Mhlophe Madi** who brought me in this world and made sure that I am well looked after until I was able to fend for myself.

Acknowledgements

My heartfelt thanks to **God Almighty** for providing me the inner strength to complete this project. Words can hardly substitute the immense depth of gratitude to my supervisor, **Professor RM Gengan** of the Department of Chemistry, Durban University of Technology for his guidance, never-ending encouragement, unlimited support and provision of all the requirements which allowed me to gain a wide range of experience. His patience and editing skills is also highly appreciated. My sincere thanks to **Professor AA Chuturgoon**, Discipline of Medical Biochemistry and Chemical Pathology, University of KwaZulu-Natal, University of KwaZulu-Natal, for his guidance, assistance and suggestions regarding cancer studies.

I acknowledge my senior **Dr Anand Krishnan,** Post-Doctoral Fellow, Durban University of Technology, who generously provided me with the technical skills and advice during the tenure of my study. His kindness and good wishes is highly appreciated.

My thanks extends to my colleagues **Talent Makhanya, Muthu Thangaraj, Arul Murugesan, Sureshkumar Mahalingum, Sandy Zondo, Hlengiwe Ndaba** and **Bipath Nivarshini** of the Department of Chemistry, Durban University of Technology for their constant encouragement and assistance at various stages of my study.

I acknowledge **Dilip Jagjivan** from the **University of KwaZulu-Natal** for providing all NMR analysis. My thanks to **NRF** for their financial support and **Durban University of Technology** for allowing me to pursue my studies.

Mere acknowledgement may not redeem the depth for the blessings and sacrifices from my parents and family members. Special thanks to my mother **Mhlophe Madi**, my step mother **Joyce Zwane** and my dad **Lazaros Nkosi** for their motivation at all stages of my study: you are great people in my life.

Abstract

Quinoline and its derivatives represent an important class of nitrogen-containing heterocylces as they are useful intermediates in organic synthesis and possess a broad spectrum of biological activities, such as anti-asthmatic, anti-inflammatory and anti-malarial activity. Hence, synthesis of novel compounds with potent biological activities is important in medicine. Significant research is directed into the development of new quinoline based structures and new methods for their preparations. In the past, synthesis of complex molecules was accomplished by step-wise reaction. This was time consuming and yield was generally low. Nowadays, multi-component reactions (MCRs) are being used since three or more substrates can be reacted in a one-pot reaction. Therefore yields are higher and the reaction is more efficient. In this research investigation novel quinoline derivatives, using the multi-component reaction protocol, were synthesized. After characterization of the product by several spectroscopic techniques, the biological potential of these compounds were assessed using lung cancer cell lines, bacteria and molecular modeling in an enzymatic system.

In the synthetic part of this study, the first step was the preparation of the starting compound 2-chloro-3-formyl quinoline for which the Vilsmeier-Haack cyclisation protocol was used. The cyclisation was carried out by combining DMF and $POCl_3$ at 5°C to form an electrophile which then reacted *in situ* with N-phenylacetamide at 100ºC to afford 2-chloro-3-formyl quinoline in high yield (95%). This was followed by the synthesis of a series of novel quinoline derivatives in a MCR system comprising 2-chloro-3-formyl quinoline, malononitrile, aromatic amines and dimethyl acetylenedicarboxylate in the presence of a catalytic amount of triethylamine. Valuable features of this routine included high yields, extensive substrate range and straight forward procedures. Eight novel poly-functionalised dihydropyridine quinoline derivatives were synthesized, purified and characterized. The outline for the synthesis of poly-functionalised dihydropyridine quinoline derivatives is presented graphically in **Scheme 1**. **Scheme 2** shows the eight compounds synthesized and used subsequently for further studies.

.

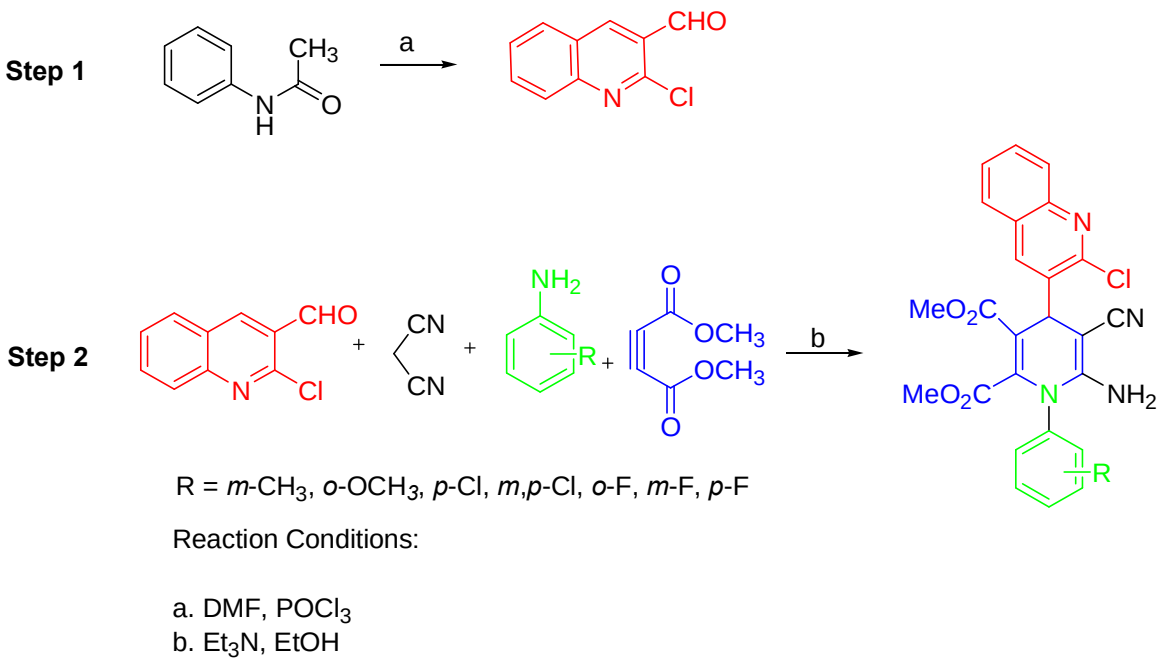

Scheme 1: Graphical representation for the synthesis of poly-functionalised dihydropyridine quinoline derivatives

The novel eight compounds were screened for their potential activity in lung cancer cell lines. A549 cells were incubated for 24 hours with a range of concentrations of each compound, in triplicate, in a micro-titre plate together with an untreated control. Each experiment was conducted twice on separate occasions; the results from the first set matched the repeated experiment. The cells were then incubated (37ºC, 5% CO_2) with the MTT substrate for 4 hours. Thereafter all supernatants were aspirated and DMSO was added to the wells. Finally the optical density was measured at 570 nm at a reference wavelength of 690 nm with an ELISA plate reader. The net MTT dependant absorbance (optical density) of each sample was calculated by subtracting the average absorbance of the blank from the average absorbance of each sample. Data were represented as mean optical density plus or minus the standard deviation. Four of the synthesized compounds (**A1-A8**) were evaluated for their cytotoxicity activities. The anti-cancer assay indicated that poly-functionalised dihydropyridine quinoline compounds, **A2, A3** and **A4** have good potential as anti-cancer drugs. Among them, **A2** and **A4** proved to be dose dependent with **A4** having the highest toxicity at 250 µM and **A8** having the highest toxicity at 125, 250 and 500 µM, whereas **A1, A5, A6 and A7** were not cytotoxic.

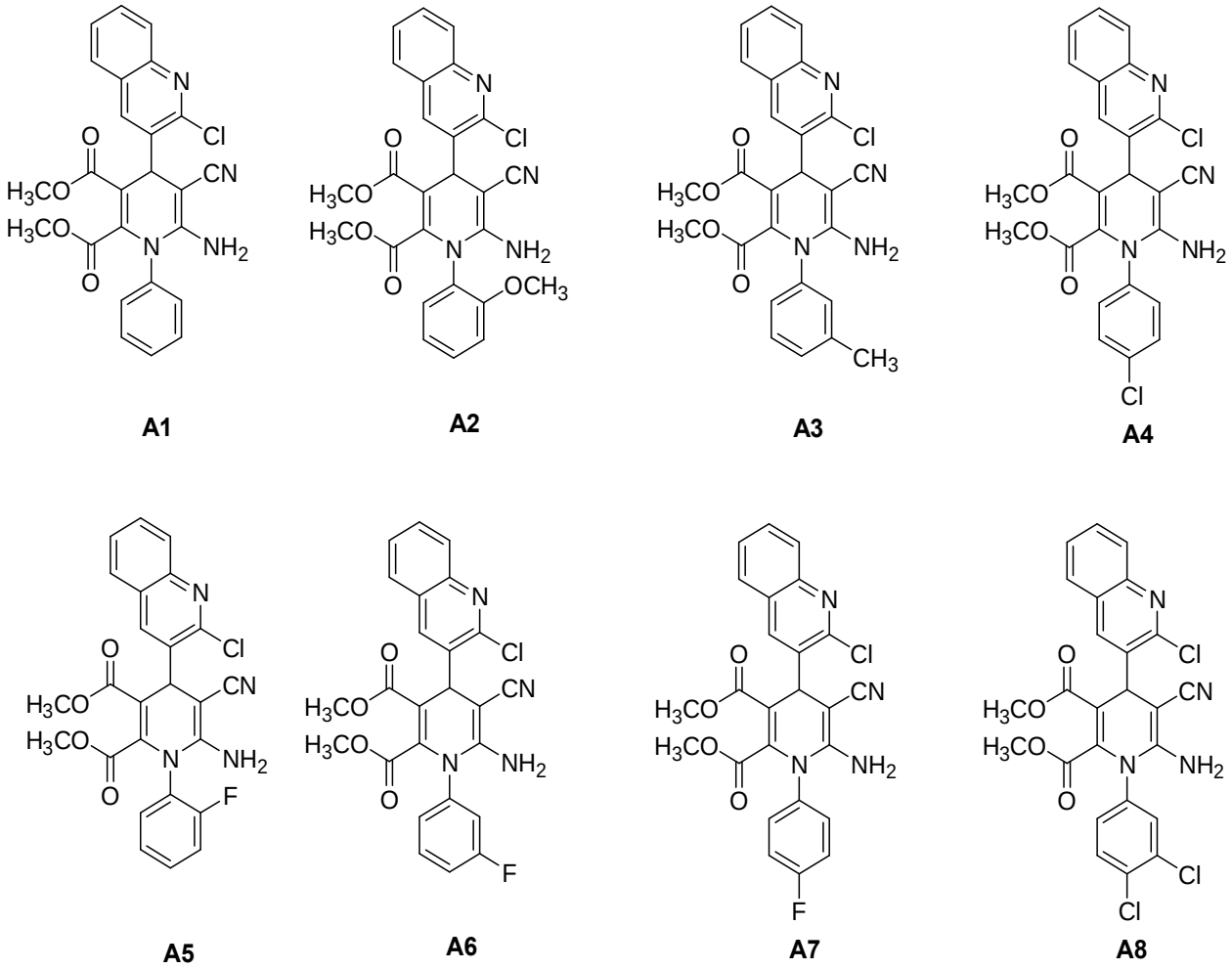

Scheme 2: Structures of novel poly-functionalised dihydropyridine quinoline derivatives by MCRs

Since molecular docking is a key tool in structural molecular biology and computer-assisted drug design, these compounds were subjected to molecular docking and the binding mode for the compounds, within the active site of the protein, was analyzed. Docking of **A1** to Human mdm2 protein provided insights into the binding regions. Three hydrogen bonds were formed between GLU 25 (2.7 Å distance), LEU 27 (3.2 Å distance) and LEU 54 (3.2 Å distance) atoms with binding energy of -8.91 kcal/mol. Docking of **A1** with Human mdm2 indicated the lowest binding energy thereby showing strong affinity of the ligand molecule with the receptor which has been stabilized by strong hydrogen bond interactions in the binding pocket. This confirms that **A1** is a better inhibitor for E3 ubiquitin-protein ligase mdm2 than all the other compounds tested (A2-A8).

Further, the eight novel poly-functionalised dihydropyridine quinoline derivatives were evaluated for their antibacterial activity. This was performed using the MABA method against three strains i.e.

Gram negative; *Pseudomonas aeruginosa* (ATCC 27853), *Escherichia coli* (ATCC 25922) and Gram positive; *Staphylococcus aureus* (ATCC 29213) using the broth micro dilution method. Standard antibiotics (ciprofloxacin and nalidixic acid) were used as positive controls and DMSO was used as a negative control. The results obtained from the anti-bacterial assay showed that compounds **A4, A7** and **A8** have high activity, whereas **A2** and **A3** showed poor activity against all the tested bacterial strains. Compound **A6** showed no activity against *S. aureus* and *E. coli*.

Table of Content

Synthesis of Novel Quinoline Derivatives and their Cytotoxicity in A549 Lung Cancer Cellsé é é é é i

Acknowledgementsé ..iv

Abstracté .v

List of Schemesé xii

List of Figuresé .xiv

Chapter One: Introductioné .1

Referencesé ..5

Chapter Two: Literature Reviewé ...7

2.1. Importance of Organic Chemistry.. 7

2.2. Multi-Component Reactions.. 8

2.3. Heterocyclic Chemistry 13

2.3.1. Five-Membered Heterocycles.. 14

2.3.2. Six-Membered Heterocycles.. 17

2.3.3. Polycyclic Six-Membered Heterocycles 18

2.3.4. Seven-Membered Heterocycles 20

2.4. Some Important Applications of Quinolines and Quinolonesé é é é é é é é é é é é é é é ..21

2.4.1. Cancer Studies.. 21

2.4.1.1. Quinoline based alkaloids as DNA intercalators... 21

2.4.1.2. Some Anti-Cancer Agents and their Reaction Schemes.. 21

2.4.2. Molecular Docking Studiesé 24

2.4.2.1. Some Molecular Docking Properties and Their Reaction Schemes............................... 25

2.4.3. Bacterial Studiesé 27

2.4.3.1. History of Bacteria 27

2.4.3.2. Anti-microbial Activity of Quinoline 27

2.4.3.3 Some Quinolones and Quinolines Anti-bacterial Drugs and their Reaction Schemes................... 28

Referencesé 35

Chapter Three: Synthesis of Poly-Functional Dihydropyridine Quinoline Derivativesé é é é é .42

3.1. Introduction... 42

3.2. Experimentalé .43

3.2.1. Instrumental 43
3.3. Results and Discussion 45
3.3.1. Synthesis of 2-Chloro-3-Formyl Quinoline 46
3.3.2. The Spectroscopic Data (A1-A8) 59
3.3.3. Conclusion 63
Chapter Four: Biological studiesé ..65
4.1.1. Introduction 65
4.1.2. Experimental 65
4.1.2.1. Materials and Methods 65
4.1.2.2. Maintenance of A549 Cells in Culture 65
4.1.3 Results and Discussion 66
4.1.4. Conclusion 72
4.2. Molecular Docking Studyé .72
4.2.1. Introduction 72
4.2.2. Experimental 73
4.2.2.1. Materials and Methods 73
4.2.2.2. Ligand Preparation 73
4.2.3. Results and Discussion 73
4.2.4. Conclusion 78
4.3. Bacterial Studiesé ...79
4.3.1. Introduction 79
4.3.1.1. Experimental 79
4.3.1.2. Materials & Methods 79
4.3.1.3. The Preparation of Media 79
4.3.1.4. The Preparation of the Nutrient Broth 79
4.3.1.5. Microbial Cultures 80
4.3.1.6. Preparation of Reagent: Microplate Alamar Blue Assay (MABA) 80
4.3.2. Results and Discussion 80
4.3.3. Conclusion 81
Chapter Five: Summary 82
APPENDICESé .85
PUBLISHED RESEARCH PAPERé ..132

List of Tables

Table 1: ^{1}H and ^{13}C NMR structural elucidation of 4k 33
Table 2: ^{1}H NMR and ^{13}C NMR data of 2-chloro-formylquinoline 48
Table 3: Physicochemical data for quinoline derivatives 49
Table 4: ^{1}H NMR chemical shifts for compounds A1-A8, ŭ of ^{1}H (*J*, Hz) 57
Table 5: ^{13}C NMR chemical shifts (ŭ in ppm) for compounds A1-A8 58
Table 6: Glide extra-precision (XP) results for 8 compounds (A1-A8) with human mdm2 75
Table 7: Antibacterial activities of quinoline derivatives: Minimum Inhibitory Concentration (µM) 81

List of Schemes

Scheme 1: Graphical representation for the synthesis of poly-functionalised dihydropyridine quinoline derivatives vi
Scheme 2: Synthesis of pyrimidinones from ethyl aceto acetate, aldehyde and urea 9
Scheme 3: Synthesis of hydroxyquinolinones from dihydropyrimidine, aldehydes and urea 9
Scheme 4: Synthesis of tetrazoloquinoline carbaldehydes from aldehydes, dimedone and urea 9
Scheme 5: Mannich reaction for the synthesis of 7-(4-benzenesulfonyl-piperazin-1-ylmethyl)-quinolin-8-ol 10
Scheme 6: Mannich reaction for the synthesis of 3-(2-chloroquinolin-3-yl)-1-phenyl-3-(phenylamino)propan-1-one 10
Scheme 7: Passerini reaction for the synthesis of Ŭ-acyloxy amides 10
Scheme 8: Gewald reaction for the synthesis of poly-substituted 2-amino-thiophene 11
Scheme 9: Gewald reaction for the synthesis of 2-aminothiophene-3-carboxamides 11
Scheme 10: Ugi reaction for the synthesis of Ŭ-aminoacyl amide derivatives 12
Scheme 11: Synthesis of spiro [indole-3,4-pyrano(3,2)-c]quinolones from isatins, malononitrile and 4-hydroxyquinoline-2(1*H*)-one 12
Scheme 12: Synthesis of benzonaphthyridine from aniline, aldehydes and *N*-alkyl-1,4-dihydropyridine. 13
Scheme 13: Synthesis of 3-oxo-isoindlones from 2-chloro-3-formyquinoline, 2-halo-5-nitrobenzoic acid, (4-methoxy-phenyl)methanamine, aniline and isonitrile 13
Scheme 14: Synthesis for pyrroles acyclo-condensation reaction 14
Scheme 15: Furan example for the synthesis of bis(aminofuran)bicinchroninicamides 14
Scheme 16: Synthesis of quinoline-attached furan-2(3*H*)-ones 15
Scheme 17: Synthesis of fully substituted 1,2,3-triazoles 15
Scheme 18: A synthesis of quinoline coupled [1,2,3]-triazoles 15
Scheme 19: Synthesis for highly substituted 2(2-azaaryl) imidazoles 16
Scheme 20: Synthesis of quinoline-imidazolium based compounds 16
Scheme 21: Fisher-indole synthesis from arylhydrazine and ketone 16
Scheme 22: Pyridines reaction for the synthesis of 2,2-bipyridine and unsymmetrical 2,4,6-triarylpyridine derivatives 17
Scheme 23: Diels-Alder reaction between aza-olefins and aza-dicarboxylic for the synthesis of tetrazines 17
Scheme 24: Prins-Friedel-Crafts reaction for the synthesis of 4-aryltetrahydropyran derivatives 18

Scheme 25: Synthesis of 4-aryl-8-arylidene-5,6,7,8-tetrahydro-2-quinolinones 19
Scheme 26: Hantzsch reaction for the synthesis of polyhydroquinolines..... 19
Scheme 27: Steroselective synthesis of *N*,*N*-bis[(2-chloroquinoline-3-yl)methylene]-1-diamine..... 19
Scheme 28: An example of quinolines c-arylation nucleophilic substitution reaction..... 19
Scheme 29: An example of quinolines nucleophilic substitution reaction 20
Scheme 30: An example of quinolines Aza Wittig reaction 20
Scheme 31: An example of quinolines Crossed Cannizaro reaction..... 20
Scheme 32: Synthesis of polysubstituted 1,4-benzodiazepin-3-ones by isocyanide 20
Scheme 33: Synthesis for quinoline-rhodanine derivatives 2-chloro-3-formylquinoline and rhodanine... 22
Scheme 34: Biginelli reactions for the synthesis of 4-(2-chloro-3-quinolinyl)-2-thio/oxo-pyrimidine 22
Scheme 35: Synthesis 1-methoxy-3-phenyl-1*H*-pyrano[4,3-*b*]- quinoline from 2-chloro-3-formylquinoline and phenyl acetylene..... 23
Scheme 36: Synthesis of quinoline isoxazole derivatives..... 25
Scheme 37: Synthesis of 1-aryl/hetryl-1,2,4-triazolo[4,3-*a*]pyridines 28
Scheme 38: Synthesis of synthesis of 1-(5-(2-chloroquinolin-3yl)3-phenyl-1*H*-pyazol-1-yl)etha-none derivatives..... 29
Scheme 39: Synthesis of 3-Formyl-2-(3-hydroxy-1,4-naphthoquinon-2-yl)-quinoline from 2-chloro-3-fomylquinoline and 2-hydroxy-1,4-naphthoquinone 30
Scheme 40: 2-(2-chloro-6-quinolin-3-yl)-2,3,4,12-tetrahydro-1*H*-benzothiazolo[2,3-b]quinazolin-1-one 2-chloro-3-formylquinoline 2-amino-6-methoxybenzothiazole and 5-dimethyl-1,3-cyclohexanedione..... 30
Scheme 41: Synthesis of 2-amino-4-(2-chloroquinolin-3-yl)-5-oxo-4,5-dihydropyrano[3,2]chromene-3-carbonitrile derivatives..... 31
Scheme 42: Synthesis of synthesis of substituted 2-[2-amino-6-(2-chloroquinolin-3-yl)-5,6-dihydropyrimidine-4-yl]phenol 31
Scheme 43: Synthesis of biquinoline derivatives 32
Scheme 44: The reaction of DMF and $POCl_3$ 46
Scheme 45: The reaction mechanism illustrating the formation of an electrophile [1]..... 46
Scheme 46: Synthesis of 2-chloro-3-formyl quinoline 46
Scheme 47: A possible reaction mechanism for 2-chloro-3-formyl quinoline [2] 47
Scheme 48: General reaction for the synthesis of A1-A8. 49
Scheme 49: The postulated reaction mechanism for the synthesised poly-functionalised dihydropyridine quinoline derivatives 50
Scheme 50: Proposed fragments of A1 54

List of Figures

Figure 1: General Tandem multi-component strategy 8
Figure 2: Typical examples of important quinolines from natural products 18
Figure 3: Schematic diagram of DNA intercalation [63] 21
Figure 4: Molecules with anti-cancer activity 23
Figure 5: Schematic diagram for the mechanism of action for anticancer drugs [70] 24
Figure 6: Docking of a small molecule ligand to a protein receptor to produce a complex [72] 25
Figure 7: A small molecule docked to a protein [72] 25
Figure 8: Example for B-DNA molecular docking [73] 26
Figure 9: Binding interactions of compounds at the active site where the non-peptide interact with the receptor ligand (green), Hydrogen bonds are expressed as dotted lines (purple), and active site residues are demonstrated in orange [74] 26
Figure 10: An overview of bacterial infections in the human body [77] 27
Figure 11: Selected HMBC correlations for dispiro substituted benzo[*H*]quinoline compounds 34
Figure 12: Novel poly-functionalised dihydropyridine quinoline derivatives 45
Figure 13: Aromatic amines A1a-A8a 49
Figure 14: Selected HMBC correlations for A1 53
Figure 15: The cytotoxic effects of A1 in the A549 lung cancer cell line 68
Figure 16: The cytotoxic effects of A2 in the A549 lung cancer cell line 68
Figure 17: The cytotoxic effects of A3 in the A549 lung cancer cell line 69
Figure 18: The cytotoxic effects of A4 in the A549 lung cancer cell line 69
Figure 19: The cytotoxic effects of A5 in the A549 lung cancer cell line 70
Figure 20: The cytotoxic effects of A6 in the A549 lung cancer cell line 70
Figure 21: The cytotoxic effects of A7 in the A549 lung cancer cell line 71
Figure 22: The cytotoxic effects of A8 in the A549 lung cancer cell line 71
Figure 23 : Hydrogen bond formation of A1 between GLU 25, LEU 27 and LEU 54 atoms 76
Figure 24 : Hydrogen bond formation and bond length of docking A1 compound to human mdm2 77
Figure 25: Binding mode of A1 compound with E3 ubiquitin-protein ligase Mdm2 78
Figure 26: ^{1}H NMR Spectrum of 2-chloro-3-formylquinoline 86
Figure 27: ^{13}C NMR Spectrum of 2-chloro-3-formylquinoline 87
Figure 28: IR Spectrum of 2-chloro-3-formylquinoline 88

Figure 29: ^{1}H NMR Spectrum of A1, dimethyl 6-amino-4-(2-chloroquinolin-3-yl)-5-cyano-1-phenyl-1,4-dihydropyridine-2,3-dicarboxylate 89
Figure 30: ^{1}H NMR Expanded spectrum of A1, dimethyl 6-amino-4-(2-chloroquinolin-3-yl)-5-cyano-1-phenyl-1,4-dihydropyridine-2,3-dicarboxylate 90
Figure 31: COSY Spectrum of A1, dimethyl 6-amino-4-(2-chloroquinolin-3-yl)-5-cyano-1-phenyl-1,4-dihydropyridine-2,3-dicarboxylate 91
Figure 32: HSQC Spectrum of A1, dimethyl 6-amino-4-(2-chloroquinolin-3-yl)-5-cyano-1-phenyl-1,4-dihydropyridine-2,3-dicarboxylate 92
Figure 33: NOESY Spectrum of A1, dimethyl 6-amino-4-(2-chloroquinolin-3-yl)-5-cyano-1-phenyl-1,4-dihydropyridine-2,3-dicarboxylate 93
Figure 34: HMBC Spectrum of A1, dimethyl 6-amino-4-(2-chloroquinolin-3-yl)-5-cyano-1-phenyl-1,4-dihydropyridine-2,3-dicarboxylate 94
Figure 35: ^{13}C NMR Spectrum of A1, dimethyl 6-amino-4-(2-chloroquinolin-3-yl)-5-cyano-1-phenyl-1,4-dihydropyridine-2,3-dicarboxylate 95
Figure 36: The IR Spectrum of A1, dimethyl 6-amino-4-(2-chloroquinolin-3-yl)-5-cyano-1-phenyl-1,4-dihydropyridine-2,3-dicarboxylate 96
Figure 37: The Mass Spectrum of A1, dimethyl 6-amino-4-(2-chloroquinolin-3-yl)-5-cyano-1-phenyl-1,4-dihydropyridine-2,3-dicarboxylate 97
Figure 38: ^{1}H NMR Spectrum of A2, dimethyl 6-amino-4-(2-chloroquinolin-3-yl)-5-cyano-1-(2-methoxyphenyl)-1,4-dihydropyridine-2,3-dicarboxylate 98
Figure 39: ^{1}H NMR Expanded spectrum of A2, dimethyl 6-amino-4-(2-chloroquinolin-3-yl)-5-cyano-1-(2-methoxyphenyl)-1,4-dihydropyridine-2,3-dicarboxylate 99
Figure 40: ^{13}C NMR Spectrum of A2, dimethyl 6-amino-4-(2-chloroquinolin-3-yl)-5-cyano-1-(2-methoxyphenyl)-1,4-dihydropyridine-2,3-dicarboxylate 100
Figure 41: The IR Spectrum of A2, dimethyl 6-amino-4-(2-chloroquinolin-3-yl)-5-cyano-1-(2-methoxyphenyl)-1,4-dihydropyridine-2,3-dicarboxylate 101
Figure 42: The Mass Spectrum of A2, dimethyl 6-amino-4-(2-chloroquinolin-3-yl)-5-cyano-1-(2-methoxyphenyl)-1,4-dihydropyridine-2,3-dicarboxylate 102
Figure 43: ^{1}H NMR Spectrum of A3, dimethyl 6-amino-4-(2-chloroquinolin-3-yl)-5-cyano-1-m-tolyl-1,4-dihydropyridine-2,3-dicarboxylate 103
Figure 44: ^{1}H NMR Expanded spectrum of A3, dimethyl 6-amino-4-(2-chloroquinolin-3-yl)-5-cyano-1-m-tolyl-1,4-dihydropyridine-2,3-dicarboxylate 104
Figure 45: ^{13}C NMR Spectrum of A3, dimethyl 6-amino-4-(2-chloroquinolin-3-yl)-5-cyano-1-m-tolyl-1,4-dihydropyridine-2,3-dicarboxylate 105

Figure 46: The IR Spectrum of A3, dimethyl 6-amino-4-(2-chloroquinolin-3-yl)-5-cyano-1-m-tolyl-1,4-dihydropyridine-2,3-dicarboxylate 106
Figure 47: Mass spectrum of A3, dimethyl 6-amino-4-(2-chloroquinolin-3-yl)-5-cyano-1-m-tolyl-1,4-dihydropyridine-2,3-dicarboxylate 107
Figure 48: ^{1}H NMR Spectrum of A4, dimethyl 6-amino-1-(4-chlorophenyl)-4-(2-chloroquinolin-3-yl)-5-cyano-1,4-dihydropyridine-2,3-dicarboxylate 108
Figure 49: ^{1}H NMR Expanded spectrum of A4, dimethyl 6-amino-1-(4-chlorophenyl)-4-(2-chloroquinolin-3-yl)-5-cyano-1,4-dihydropyridine-2,3-dicarboxylate 109
Figure 50: ^{13}C NMR Spectrum of A4, dimethyl 6-amino-1-(4-chlorophenyl)-4-(2-chloroquinolin-3-yl)-5-cyano-1,4-dihydropyridine-2,3-dicarboxylate 110
Figure 51: The IR Spectrum of A4, dimethyl 6-amino-1-(4-chlorophenyl)-4-(2-chloroquinolin-3-yl)-5-cyano-1,4-dihydropyridine-2,3-dicarboxylate 111
Figure 52: The Mass Spectrum of A4, dimethyl 6-amino-1-(4-chlorophenyl)-4-(2-chloroquinolin-3-yl)-5-cyano-1,4-dihydropyridine-2,3-dicarboxylate 112
Figure 53: ^{1}H NMR Spectrum of A5, dimethyl 6-amino-4-(2-chloroquinolin-3-yl)-5-cyano-1-(2-fluorophenyl)-1,4-dihydropyridine-2,3-dicarboxylate 113
Figure 54: ^{13}C NMR Spectrum of A5, dimethyl 6-amino-4-(2-chloroquinolin-3-yl)-5-cyano-1-(2-fluorophenyl)-1,4-dihydropyridine-2,3-dicarboxylate 114
Figure 55: The IR Spectrum of A5, dimethyl 6-amino-4-(2-chloroquinolin-3-yl)-5-cyano-1-(2-fluorophenyl)-1,4-dihydropyridine-2,3-dicarboxylate 115
Figure 56: ^{1}H NMR Spectrum of A6, dimethyl 6-amino-4-(2-chloroquinolin-3-yl)-5-cyano-1-(3-fluorophenyl)-1,4-dihydropyridine-2,3-dicarboxylate 116
Figure 57: ^{1}H NMR Expanded spectrum of A6, dimethyl 6-amino-4-(2-chloroquinolin-3-yl)-5-cyano-1-(3-fluorophenyl)-1,4-dihydropyridine-2,3-dicarboxylate 117
Figure 58: ^{19}F NMR Spectrum of A6, dimethyl 6-amino-4-(2-chloroquinolin-3-yl)-5-cyano-1-(3-fluorophenyl)-1,4-dihydropyridine-2,3-dicarboxylate 118
Figure 59: ^{13}C NMR Spectrum of A6, dimethyl 6-amino-4-(2-chloroquinolin-3-yl)-5-cyano-1-(3-fluorophenyl)-1,4-dihydropyridine-2,3-dicarboxylate 119
Figure 60: The IR Spectrum of A6, dimethyl 6-amino-4-(2-chloroquinolin-3-yl)-5-cyano-1-(3-fluorophenyl)-1,4-dihydropyridine-2,3-dicarboxylate 120
Figure 61: The Mass Spectrum of A6, dimethyl 6-amino-4-(2-chloroquinolin-3-yl)-5-cyano-1-(3-fluorophenyl)-1,4-dihydropyridine-2,3-dicarboxylate 121
Figure 62: ^{1}H NMR Spectrum of A7, dimethyl 6-amino-4-(2-chloroquinolin-3-yl)-5-cyano-1-(4-fluorophenyl)-1,4-dihydropyridine-2,3-dicarboxylate 122

Figure 63: ^{19}F NMR Spectrum of A7, dimethyl 6-amino-4-(2-chloroquinolin-3-yl)-5-cyano-1-(4-fluorophenyl)-1,4-dihydropyridine-2,3-dicarboxylate 123
Figure 64: ^{13}C NMR Spectrum of A7, dimethyl 6-amino-4-(2-chloroquinolin-3-yl)-5-cyano-1-(4-fluorophenyl)-1,4-dihydropyridine-2,3-dicarboxylate 124
Figure 65: The IR Spectrum of A7, dimethyl 6-amino-4-(2-chloroquinolin-3-yl)-5-cyano-1-(4-fluorophenyl)-1,4-dihydropyridine-2,3-dicarboxylate 125
Figure 66: The Mass Spectrum of A7, dimethyl 6-amino-4-(2-chloroquinolin-3-yl)-5-cyano-1-(4-fluorophenyl)-1,4-dihydropyridine-2,3-dicarboxylate 126
Figure 67: ^{1}H NMR Spectrum of A8, dimethyl 6-amino-4-(2-chloroquinolin-3-yl)-5-cyano-1-(3,4-dichlorophenyl)-1,4-dihydropyridine-2,3-dicarboxylate 127
Figure 68: ^{1}H NMR Expanded spectrum of A8, dimethyl 6-amino-4-(2-chloroquinolin-3-yl)-5-cyano-1-(3,4-dichlorophenyl)-1,4-dihydropyridine-2,3-dicarboxylate 128
Figure 69: ^{13}C NMR Spectrum of A8, dimethyl 6-amino-4-(2-chloroquinolin-3-yl)-5-cyano-1-(3,4-dichlorophenyl)-1,4-dihydropyridine-2,3-dicarboxylate 129
Figure 70: IR Spectrum of A8, dimethyl 6-amino-4-(2-chloroquinolin-3-yl)-5-cyano-1-(3,4-dichlorophenyl)-1,4-dihydropyridine-2,3-dicarboxylate 130
Figure 71: The Mass Spectrum of A8, dimethyl 6-amino-4-(2-chloroquinolin-3-yl)-5-cyano-1-(3,4-dichlorophenyl)-1,4-dihydropyridine-2,3-dicarboxylate 131

Abbreviations

MCR- Multi-Component Reactions

$POCl_3$- Phosphorus Trichloride Oxide

$CHCl_3$- Chloroform

$CDCl_3$ï Deuterated Chloroform

CO_2- Carbon Dioxide

DMF- Dimethylformamide

NaOH- Sodium Hydroxide

VHR- Vilsmeier-Haack Reaction

TLC- Thin Layer Chromatography

NMR- Nuclear Magnetic Resonance

^{1}H ï Proton

^{13}C ï Carbon 13

OH^- ï Hydroxide

ºC ï Degrees Celsius

s ï Second

IR ï Infra-Red

g ï Grams

mg- Milligrams

% - Percentage

mol - Mole

ppm ï Part Per Million

MS ï Mass Spectrometer

mL ï Milli Litre

m.p ï Melting Point

nm ï Nanometer

dm ï Decimeter

min. ï Minute

Hzï Hertz

UV- Ultra Violet

ATR- Attenuated Total Reflectance

TMS- Tetramethylsilane

Mdm2-E3 Ubiquitin Protein

GLU 25- Glutamic Acid

LEU ï Leucine (27/54)

RMSD- Root-Mean-Square Deviation

A549 - Adenocarcinomic Human Alveolar Basal Epithelial Cells

PEG- Poly Ethylene Glycol

WHO- World Health Organization

DNA- Deoxyribonucleic Acid

LGA- Genetic Algorithm

PDB- Protein Data Bank

OD- Optical Density

CCM- Complete Culture Media

EDTA- Ethylenediaminetetraacetic Acid

MTT- (3-(4,5-Dimethylthiazol-2-yl)-2,5-diphenyltetrazolium Bromide

PBS- Phosphate Buffer Solutions

ANOVA- Analysis of Variance

TOF-MS- Time of Flight Mass Spectrometry

Chapter One: Introduction

Chemistry occupies an extraordinary place in our understanding of the universe and its composition; it is the science of molecules present in matter and space. But organic chemistry, even though a branch of chemistry is an exciting and dynamic field of science which literally creates itself as it grows. The study of organic chemistry often involves a study of new molecules that give information either available or unavailable from the molecules actually present in living things [1]. In this field of chemistry, the physical and chemical properties of carbon-containing compounds, which are either known or novel, are studied. In the quest for knowledge and biological research, organic chemists, biochemists and other academics are developing new strategies to satisfy their research aims.

Numerous organic compounds have been synthesized in research laboratories and used for biological applications. However, not all organic compounds display properties suitable for application beneficial to mankind. It is important for the new generation synthetic organic chemists to address issues such as:

- cost of the starting material
- environmental impact
- time extent of the synthesis
- overall yield of the preferred product
- possibility of scale-up of the reaction
- possibility of application

Quinoline and their derivatives represent an important class of nitrogen-containing heterocycles as they are useful dyes and intermediates in organic synthesis [2]. In recent years, much attention has been focused on their synthesis as they possess useful biological activities such as anti-malarial [3], anti-inflammatory [4], bactericidal [5], fungicidal [6] and anti-cancer [7]. Because of their important role in the pharmaceutical field [8], the profiles of quinolines, their anti-microbial, anti-cancer, anti-malarial and anti-inflammatory properties are documented [9-10]. Significant research is directed into the development of new quinoline based structures and new methods for their preparation. In this study, we investigated quinoline derivatives which could be synthesized from readily available starting compounds and hence provide a better synthetic route by using a multi-component reaction system.

Multi-component reactions (MCRs) are reactions using more than two starting materials that form a product which contains the key parts of all of the starting materials [11] in a few *in-situ* reaction steps. Compared with conventional organic reactions, MCRs are more profitable and requires minimum energy to complete the reaction. Several MCRs are known which include the Ugi 4 component condensation of amine, ketone, carboxylic acid and isocyanide [12]. The Strecker reaction, documented in 1850, was the first MCR described; [13]. Recently, there has been a tremendous development in three and four-component reactions and huge attempts have been and still are being made to discover and amplify new MCRs. Therefore, the development of new synthetic approaches using MCRs remains an active research area of study. [14]

Cancer, an epidemic and one of the leading causes of death in developed countries, is responsible for about 25% of all deaths [15]. The identification of lung cancer in humans can be detrimental, confronting them with changes in identity, social interactions and presenting them with an uncertain future [16]. At the beginning of the 20th century the diagnosis of lung cancer was rarely made. Now it is the leading disease both in rate and mortality. Every year, 1.2 million new cases of lung cancer are diagnosed (12.3% of all cancers worldwide) and 1.1 million patients die due to lung cancer (17.8% of all cancer deaths worldwide) [17]. Regardless of the fact that effective anti-cancer drugs exist, drug resistance has become a substantial crisis. This has necessitated the search for novel and cost-effective drugs with high structural variation.

Ever since the beginning of civilization, humans have searched for substances that can cure or ease the symptoms of the disease. During these times, extracts from plants and animal parts were used to treat the disease, and the discovery of such remedies was driven empirically. Starting in the early 1900s, drug discovery was increasingly focused on discovering and developing chemical entities that on their own have a desired pharmaceutical effect. Initially this was fuelled by attempts to extract and identify the active component in extracts from natural products that were being used to treat illness. A number of developments, however, have resulted in the multi-disciplinary science that drug discovery is today, including molecular biology [18]. Increasingly, as the structures of more and more potential compounds are becoming available, molecular docking is progressively being studied for pharmacologically or biologically active chemical compounds [19]. Docking is a method which predicts the preferred orientation of one molecule to a second when bound to each other to form a stable complex; it is a key tool in structural molecular biology and computer-assisted drug design. The goal of ligand-protein docking is to predict the predominant binding mode of a ligand with a protein of known three-dimensional structure [20].

Viruses like bacteria are becoming resistance to anti-microbial treatment because of acquired resistance genes in the DNA of the micro-organism. Therefore, the antibiotic resistance problem demands continuous discovery and development of new anti-bacterial agents that could be used for the effective treatment of infectious diseases. This is an urgent biomedical need [21]. Quinoline and its derivatives are known for their anti-bacterial and therapeutic properties, applications of quinoline derivatives has spread rapidly from being in anti-bacterial drugs, to almost every branch of medicinal chemistry [22]. Realizing the medicinal importance of quinoline based compounds, we undertook an investigation to synthesize novel quinoline derivatives and study their application in biological systems. The aim of this study is to synthesize novel poly-functionalised dihydropyridine quinoline derivatives, assess their bacterial and anti-cancer potential and undertake molecular docking evaluation of selected compounds.

The objectives of this study were to:

- synthesize novel quinoline derivatives, viz. poly-functionalised dihydropyridine type molecules from readily available, simple and cost effective starting compounds.
- purify compounds by chromatographic techniques and characterize them by spectroscopy.
- to assess and compare their potential as anti-cancer drugs in A549 lung cancer cell lines.
- evaluate selected compounds for their molecular modeling properties.
- evaluate the anti-microbial activity of the synthesized poly-functionalised quinoline derivatives.

The outcome of our research study is summarized in **Five Chapters** as presented below:

In **Chapter 2,** the importance of organic chemistry, multi-component reactions, heterocyclic chemistry, quinolines as anti-microbial agents, history of bacteria and quinolines as anti-bacterial drugs, structural elucidation, quinoline base alkaloids as DNA intercalators and molecular docking is described and discussed.

In **Chapter 3**, we describe and discuss the synthesis of one of the starting compounds 2-chloro-3-formylquinoline using readily available and cost effective starting compounds. The discussion also includes the use of Vilsmeier reagent that is used to synthesize 2-chloro-3-formylquinoline. We also examine the preparation of an electrophile and the mechanism illustrating the formation of an electrophile. This compound is then used to synthesize the novel poly-functionalised dihydropyridine quinoline moiety. We also describe a possible mechanism when a catalytic amount of triethylamine is used; this is a Knoevenagel condensation reaction. In this reaction, three other substrates were used in a

one pot 4 component reaction. We also analyse and interpret the IR, NMR and GCMS data for poly-functionalised dihydropyridine quinoline derivatives.

In **Chapter 4**, we outline the biological studies. In cancer studies, the text contains:

ÅRaw Data from biological assays (cell viability by MTT assay)

ÅAnalyzed data with means and standard deviations

ÅStatistical analysis for each treatment compared to the corresponding control with p-values and a summary of One way ANOVA

ÅA full description of cell culture protocol and an outline of the principle of the MTT assay.

In molecular docking studies, the text contains:

ÅLigand preparations

ÅGlide extra-precision (XP) data for **A1-A8** with human mdm2.

ÅHydrogen bond formation of A1 between GLU 25, LEU 27, and LEU 54 atoms.

ÅHydrogen bond formation and bond length of docking **A1** to human mdm2.

ÅBinding mode of **A1** with E3 ubiquitin-protein ligase mdm2.

In anti-microbial studies, the text contains:

ÅThe preparation of Media, Microplate Alamar Blue Assay and microbial cultures.

ÅAnti-bacterial activities of poly-functionalised dihydropyridine quinoline derivatives i.e, Minimum Inhibitory Concentration (MICøs).

In **Chapter 5**, we outline the summary and the future work of the study.

References

1. J P Clayden, P D Wothers, N Greeves, S Warren, Organic Chemistry (1st Ed). *Oxford*, **2001**, 19-25.
2. M M Heravi, M H Tehrani, K Bhakhtiari, H A Oskooie, Synthesis of 2,4,5-triaryl-imidazoles catalyzed by $NiCl_2 \cdot 6H_2O$ under heterogeneous system, *Catal. Commun.* 8, **2007**, 1341-1344.
3. J C Craig, P E Person, Potential anti-malarials, tribromomethylquinolines and positive halogen compounds, *J. Med. Chem*. 14, **1971**, 1221-1228.
4. R D Dillard, D E Pravey, D N Benslay, Synthesis and anti-inflammatory activity of some 2,2-dimethyl-1,2-dihydroquinolines, *J. Med. Chem*. 16, **1973**, 251-260.
5. H V Patel, K V Vyas, P S Fernandes, Synthesis of substituted 6-(3ô,5ô-4-dimethyl-1*H* Pyrazol-yl) quinolines and evaluation of their biological activity, *Indian J. Chem*. 29, **1990**, 836-840.
6. V Nadaraj, S T Selvi, Synthesis and characterization of some quinoline bearing isoxazoles nucleus, *J. Chem. Pharm. Res*. 4, **2012**, 2850-2855.
7. R V Solomon, H Lee, Quinoline as a privileged scaffold in cancer drug discovery, *Curr. Med. Chem.* 18, **2011**, 1508-1510.
8. V P Litvinov, Thienopyrimidines: synthesis, properties, and biological activity, *Russ. Chem. Bull.* 53, **2004**, 487-490.
9. B Pati, S Banerjee, Indispensability of quinoline moiety in the field of medicinal chemistry research, *J. PharmaSciTech*, 3, **2014**, 65-72.
10. S Kumar, S Bawa, H Gupta, Biological activities of quinoline derivatives, *Mini Rev. Med. Chem.* 9, **2009**, 1654-1660.
11. M K Sinha, K Khoury, E Herdtweck, A Domling, Tricycles by a new Ugi variation and Pictet-Spengler reaction in one pot, *Eur. J. Chem*. 19, **2013**, 8048-8053.
12. I Ugi, The solution phase synthesis of diketopiperazine libraries via the Ugi reaction: novel application of Armstrong's convertible isonitrile, *Angew. Chem. Int. Ed. Engl*. 1, **1962**, 8-10.
13. A G Degussa, Catalytic enantioselective Strecker reactions and analogous syntheses, *Chem. Rev.* 103, **2003**, 2795-2798.
14. A M Shestopalov, D H Evans, One-step synthesis of substituted 6-Amino-5-cyanospiro-4-(piperidine-4')-2*H*,4*H*-dihydropyrazolo [3,4-*b*]pyrans, *Org. Lett*. 16, **2002**, 423-434.
15. G Bepler. Preoperative exercise Vol.2 Measurement for lung resection candidates: results of cancer and leukemia group B protocol 9238, *J. Thoracic Oncology*, 2, **2007**, 619-625.
16. P Hytiroglou, N D Theise, M Schwartz, E Mor, C Miller, S N Thung. Macro regenerative nodules in a series of adult cirrhotic liver explant issues of classification and nomenclature, *Hepatology,* 21, **1995**, 703-707.

17. N Brooijmans, Docking methods, ligand design and validating data sets in the structural genomics era, *Struct. Biol.* 2, **2009**, 635-640.
18. K B Shoichet, L S McGovern, Molecular docking and high-throughput screening for novel inhibitors of protein tyrosine phosphatase-1B, *J. Med. Chem.* 45, **2002**, 2213-2218.
19. H Clauben, C Buninga, M Rareya, T Lengauera, Efficient molecular docking considering protein structure variations, *J. Mol. Biol.* 308, **2001**, 377-380.
20. R Kharb,Y M Shahar, Recent advances and future perspectives of triazole analogs as promising antiviral agents, *Rev. Med. Chem.,* 11, **2011**, 84-90.
21. B Kalluraya, A D'Souza, B S Holla, Synthesis and structural characterization of some nitrothienyltriazolo[3,4-*b*]-1,3,4-thiadiazines, *Indian J. Chem*. 34, **1995**, 939-942.

Chapter Two: Literature Review

2.1. Importance of Organic Chemistry

Organic chemistry is the science of the rules on how chemical entities react with each other to form new molecules. The importance of a precise reaction may be judged on its capability to deliver interesting products with high yield, chemo-, regio-, stereo- or enantioselectivity [1].

Prior to 1828 it was theorized that organic compounds may probably be produced only by living organisms, but in 1828 Friedrich Wöhler, by an unexpected reaction, synthesized an organic compound from an inorganic compound in a test tube; urea, a constituent of urine was synthesized from ammonium cyanate. This synthesis is a landmark achievement in the history of science since it disproved and undermined the vital force theory. Another great discovery was made in 1856 by William Henry Perkin. As he was trying to manufacture quinine, he accidentally manufactured the organic dye called Perkin's mauve. The industrial application of this product generated a huge amount of money thereby stimulating greater interest in organic chemistry [2].

The development of new procedures for the production of nitrogen-containing heterocycles is of great importance in organic chemistry since these types of compounds are used as drugs to ease various diseases in man. One such type is quinoline which belongs to the alkaloid category. Organic chemists have fixed their interest to the synthesis of quinoline and isoquinoline type compounds for more than a century. In most cases, classical synthetic routes suffer from numerous disadvantages such as harsh reaction conditions, long reaction time and poor yield due to the fact that they are limited to certain substitution patterns [3]. Hence, MCRs are considered as interesting variants of organic reactions. Recently, they have become very popular in the context of combinatorial chemistry [4]. It can be shown that they are extremely useful in producing a variety of highly diverse libraries of small drug-like organic compounds [5].

Owing to the enormous demand by society for new medicinal drugs, cosmetics, foods, dyes and other allied commodities, research in synthetic organic chemistry has grown rapidly resulting in the formation of several sub-disciplines such as photo-chemical, sono-chemical, microwave organic synthesis and MCRs [5].

2.2. Multi-Component Reactions

Tandem multi-component reactions, in which multiple reactions are simulated in one synthetic operation, have been used comprehensively to form carbon-carbon bonds [6]. Such reactions offer a wide range of possibilities for the efficient formation of highly complex molecules in a single operation. Thus, these reactions avoid the need for several work-up and purification operations as in the case of the conventional step wise reaction. Therefore MCRôs provide a great saving of solvents and reagents and give higher yields of the desired product. Additionally, they frequently occur with superior regio-, diastereo-, and even enantio-selectivity. All reactions proceed either jointly or step by step as shown in **Figure 1**. Hence, tandem or cascade reactions are powerful tools for synthetic conversions and are the focus of modern interest [7]. There are many named MCRôs which are extensively used for organic synthesis.

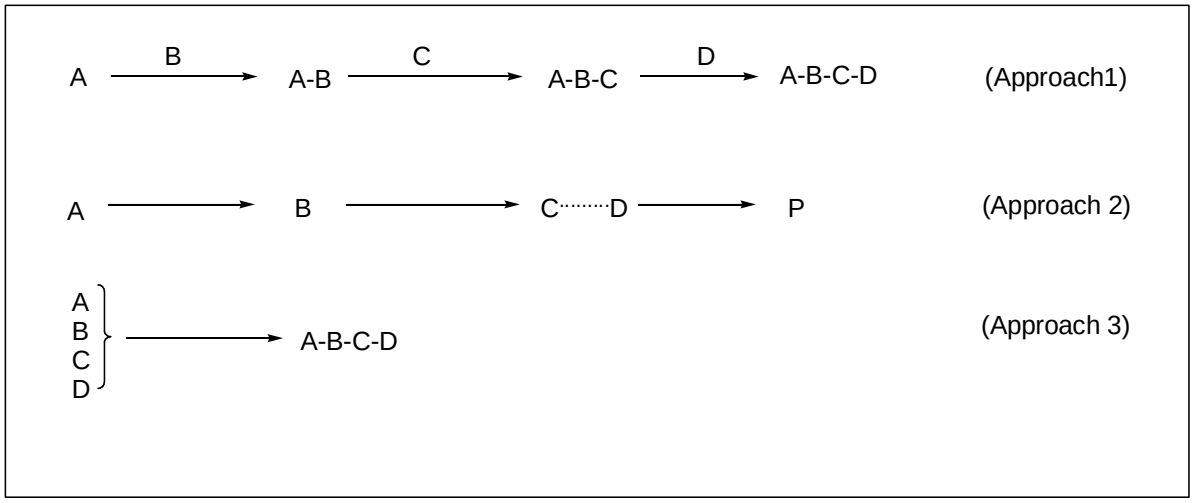

Figure 1: General Tandem multi-component strategy

2.2.1. Biginelli Reaction

The Biginelli reaction is a MCR that creates 3,4-dihydropyrimidin-2(1*H*)-ones **(4)** from ethyl acetoacetate **(1)**, aryl aldehyde **(2)** and urea **(3)**. Dihydropyrimidinones are widely used in the pharmaceutical industry as calcium channel blockers, anti-hypertensive agents and alpha-1-a-antangonists [8].

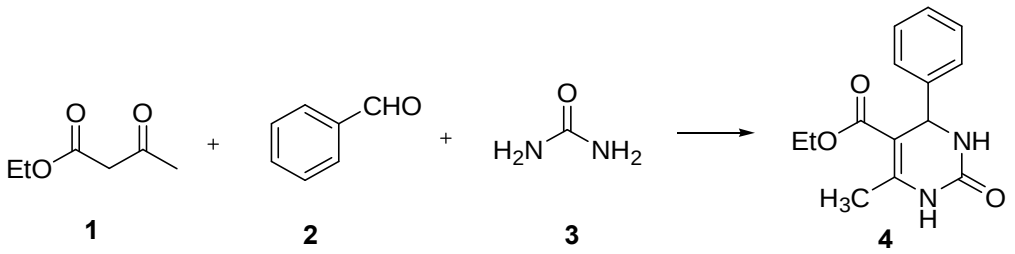

1 2 3 4

Scheme 2: Synthesis of pyrimidinones from ethyl aceto acetate, aldehyde and urea

Nadaraj *et. al*. [9] reported a based catalysed, three-component one pot synthesis of quinoline fused dihydropyrimidine **(8)** by the Biginelli reaction of 4-hydroxyquinolin-2(1*H*)-ones **(5)** with aromatic aldehydes **(6)** and thiourea **(7)**. The reaction was carried out in solvent free conditions under microwave irradiation.

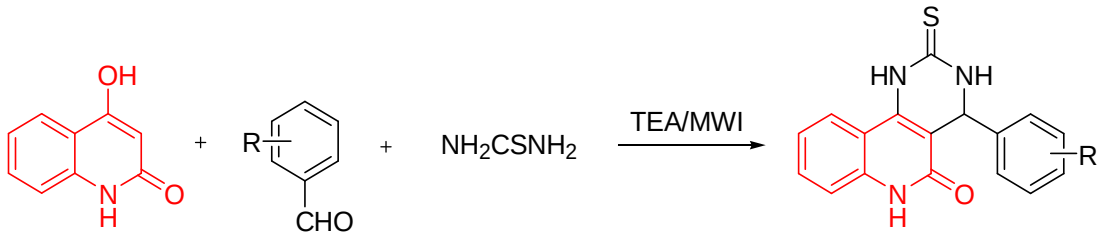

5 6 7 8

R = H, *o*-Cl, *p*-Cl, *m*-Cl, *o*-OH, *p*-OH, *m*-NO_2

Scheme 3: Synthesis of hydroxyquinolinones from dihydropyrimidine, aldehydes and urea

A convenient procedure for the synthesis of octahydroquinazolinones **(12)** in good yields was developed by Ladani *et. al*. [10] The synthesis was achieved by the reaction between tetrazolo[1,5-a]quinoline-4-carbaldehyde **(10)**, dimedone **(11)** and urea **(3)** in the presence of concentrated hydrochloric acid in ethanol.

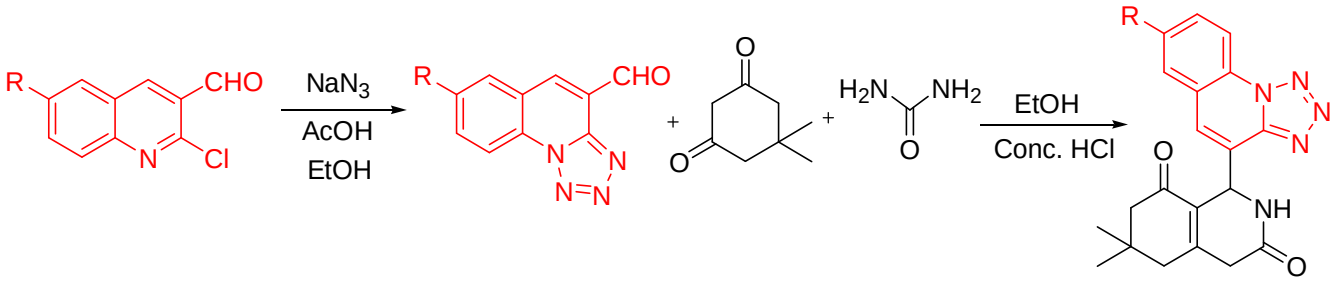

9 10 11 3 12

R = H, CH_3

Scheme 4: Synthesis of tetrazoloquinoline carbaldehydes from aldehydes, dimedone and urea

2.2.2. Mannich Reactions

The Mannich reactions involve amino alkylation of an acidic proton placed next to a carbonyl functional group by formaldehyde and a primary or secondary amine or ammonia. It is employed in the organic synthesis of natural compounds such as peptides, nucleotides, antibiotics and alkaloids. Subramaniapillai [12] gave an insight of new applications of Mannich reaction and its variants in the construction of bioactive molecules such as 7-(4-benzenesulfonyl-piperazin-1-ylmethyl)-quinolin-8-ol **(16)**.

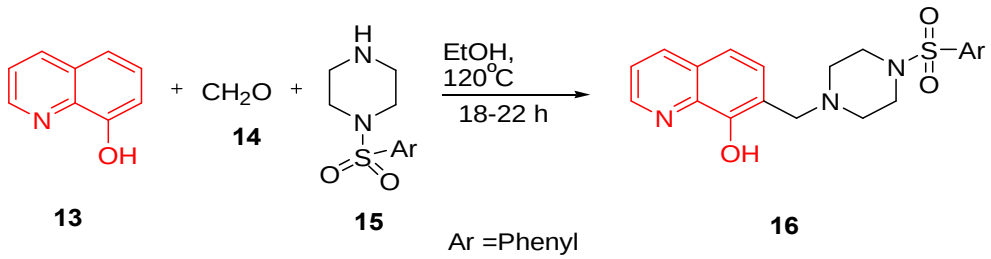

Scheme 5: Mannich reaction for the synthesis of 7-(4-benzenesulfonyl-piperazin-1-ylmethyl)-quinolin-8-ol

A direct three component Mannich-type reaction of 2-chloro-3-formylquinoline **(17)**, aniline **(19)** and acetophenone **(18)** was efficiently catalysed by an yttria-zircona based strong Lewis acid and in aqueous acetonitrile to give 3-(2-chloroquinolin-3-yl)-1-phenyl-3-(phenylamino)propan-1-one **(20)** [13].

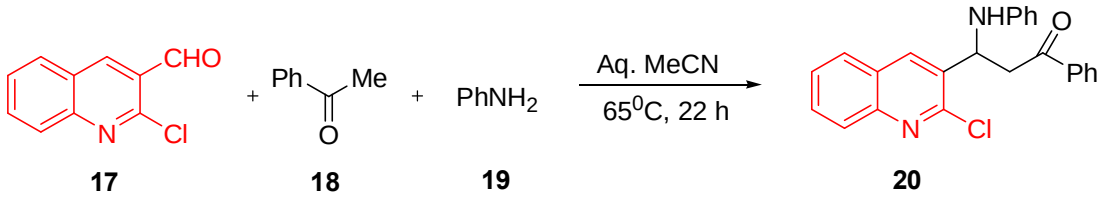

Scheme 6: Mannich reaction for the synthesis of 3-(2-chloroquinolin-3-yl)-1-phenyl-3-(phenylamino)propan-1-one

2.2.3. Passerini Reaction

The Passerini reaction is a chemical reaction involving isocyanide **(23)**, aldehyde or ketone **(22)** and a carboxylic acid **(21)** to form Ŭ-acyloxy amide **(24)**. It is the first isocyanide based MCR developed and currently plays a central role in combinational chemistry [14].

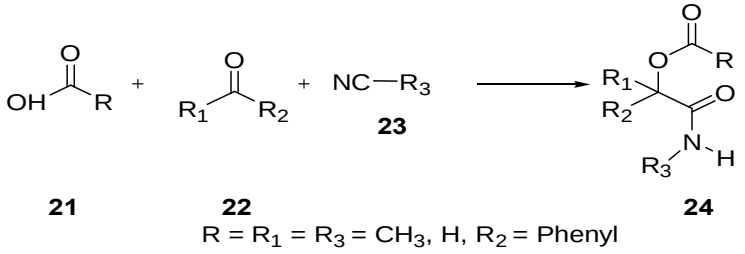

Scheme 7: Passerini reaction for the synthesis of α-acyloxy amides

2.2.4. Gewald Reactions

The Gewald reactions [15] involve the condensation of ketone **(25)** or aldehyde with Ŭ-cyanoester **(26)** in the presence of elemental sulphur and base to give a poly-substituted 2-amino-thiophene **(27)**.

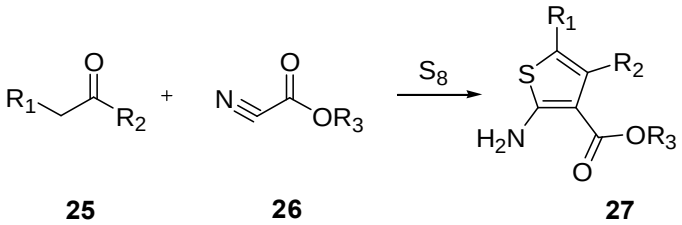

25 **26** **27**

$R_1 = R_2 = R_3 = CH_3$, Aryl, H

Scheme 8: Gewald reaction for the synthesis of poly-substituted 2-amino-thiophene

Wang *et. al*. [16] described valuable general protocols for the synthesis of arrays of 2-aminothiophene-3-carboxamides **(30)** from cyanoacetamides **(28)**, aldehydes or ketones **(29)** via Gewald-3CR variation and phenol-thiophene based biosisosterie between the drugs olanzapine **(31)** and clozapine **(32)**.

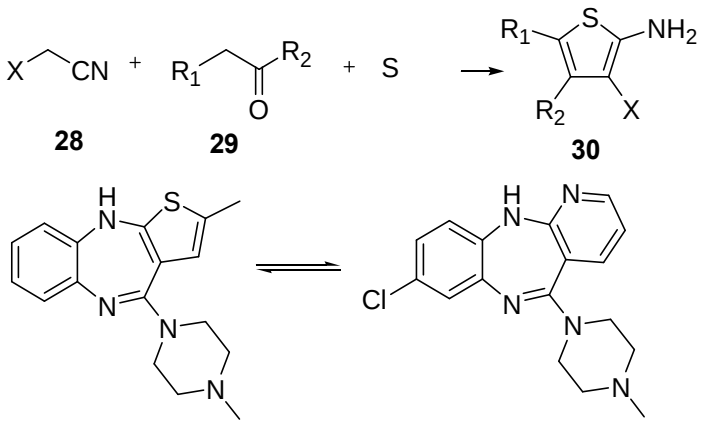

28 **29** **30**

31 **32**

$R_1 = R_2$ = H, alkyl, aryl, X = Cl, Br

Scheme 9: Gewald reaction for the synthesis of 2-aminothiophene-3-carboxamides

2.2.5. Ugi Reactions

The Ugi reaction is an isonitrile based reaction that provides a quick route for Ŭ-aminoacyl amide derivatives **(36)**. It is a four component condensation of an amine **(33)**, ketone **(22)**, carboxylic acid **(35)** and an isocyanide **(23)**. It is the most acknowledged and versatile MCR [17].

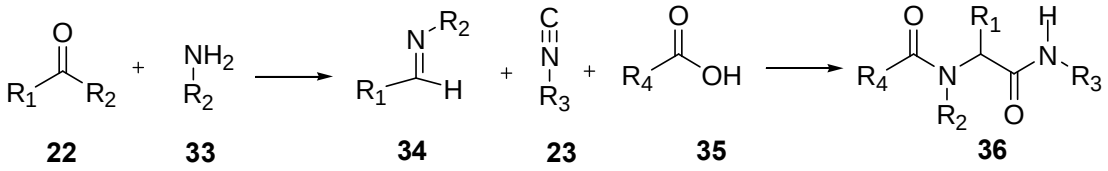

Scheme 10: Ugi reaction for the synthesis of α-aminoacyl amide derivatives

The Ugi reaction can be joined with a post condensation reaction to add to the number of possible pharmacologically imperative scaffolds. An example is the Heck reaction. Umkehrer *et. al.* [18] demonstrated that the Ugi/Heck combination works well for high-throughput combinatorial collection production of indol-2-ones having four points of diversity. This scaffold is of interest because it has shown biological activity as anti-tumor compounds **(37)** and tyrosine kinase **(38)** inhibitors.

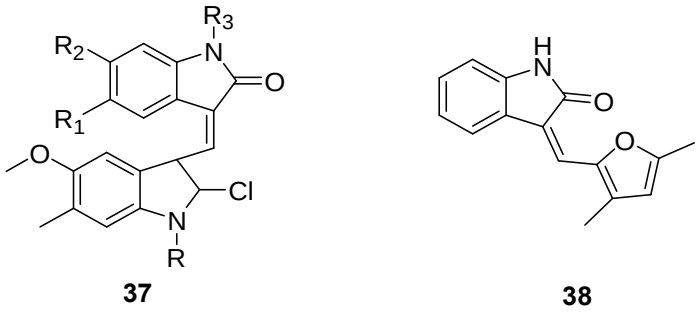

Michail *et. al.* [19] disclosed an electro catalytic multi-component chain conversion of isatins **(39)**, malononitrile **(40)** and 4-hydroxyquinoline-2(1*H*)-one **(41)** into spiro [indole-3,4-pyrano(3,2)-c]quinolones **(42)** by the combined electrolysis in an undivided cell.

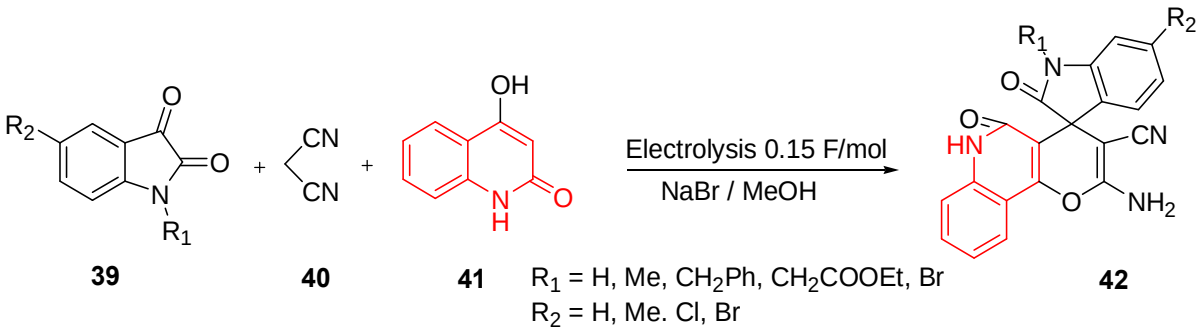

Scheme 11: Synthesis of spiro [indole-3,4-pyrano(3,2)-c]quinolones from isatins, malononitrile and 4-hydroxyquinoline-2(1*H*)-one

Rodolfo Lavilla *et. al.* [20] documented a versatile route for the synthesis of substituted tetrahydroquinolines, which has elicited enormous interest in modern times. The three component interaction of aniline **(43)** with an aldehyde **(44)** and *N*-alkyl-1,4-dihydropyridine **(45)** results in a benzonaphthyridine **(46).**

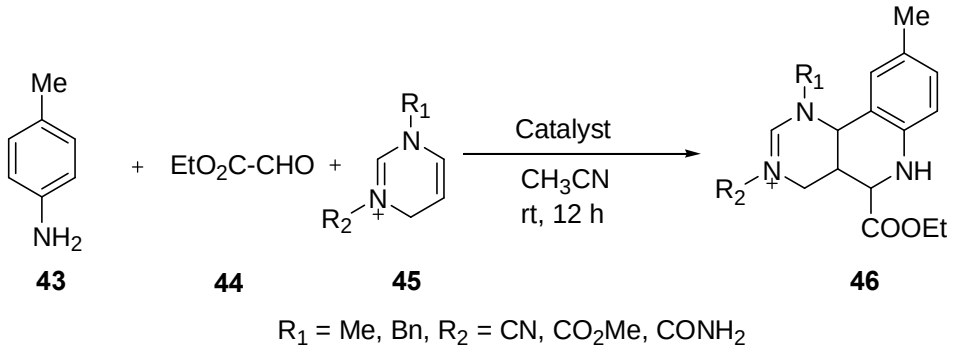

Scheme 12: Synthesis of benzonaphthyridine from aniline, aldehydes and *N*-alkyl-1,4-dihydropyridine

The Ugi [21] four-component reaction of 2-chloro-3-formyquinoline **(17)**, 2-halo-5-nitrobenzoic acid, (4-methoxy-phenyl)methanamine **(47)**, aniline **(48)** and isonitrile **(49)** resulted in a formation of classical 3-oxo-isoindlone adduct **(50)** which showed good anti-bacterial assays.

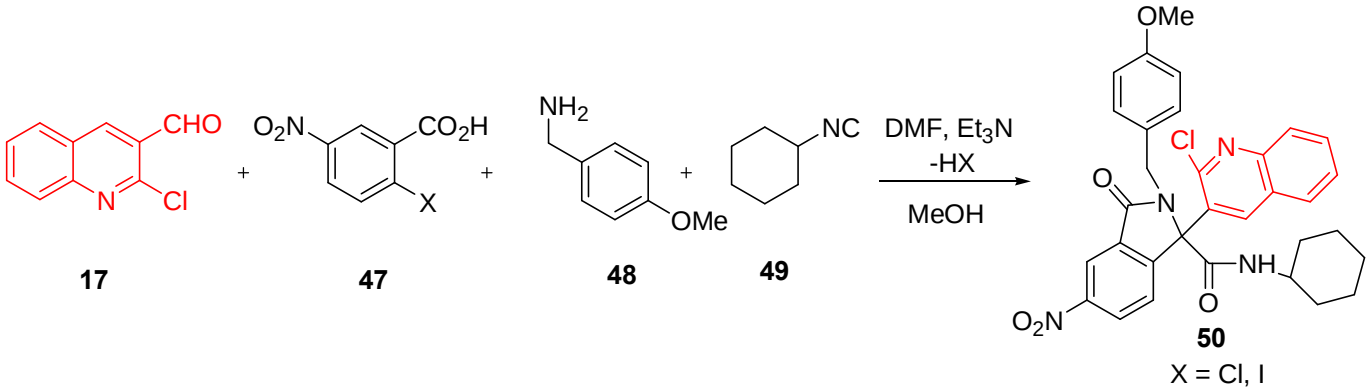

Scheme 13: Synthesis of 3-oxo-isoindlones from 2-chloro-3-formyquinoline, 2-halo-5-nitrobenzoic acid, (4-methoxy-phenyl)methanamine, aniline and isonitrile

2.3. Heterocyclic Chemistry

The type of compounds classified as heterocyclic probably constitutes the largest and most varied family of organic compounds. Literature on the subject is correspondingly plenty; nearly six million compounds have been recorded in chemical abstracts and approximately half of those are heterocyclic. Heterocyclic compounds are very widely distributed in nature and are essential to life as they play a vital role in the metabolism of all living cells [22].

2.3.1. Five-Membered Heterocycles

2.3.1.1. Pyrroles

Pyrrole is a five-membered ring with the formula C_4H_4NH [23]. An example of a MCR of acyclo-condensation reaction was reported by Alizadeh *et. al.* [24] under solvent-free conditions at room temperature to afford penta-substituted pyrroles **(53).**

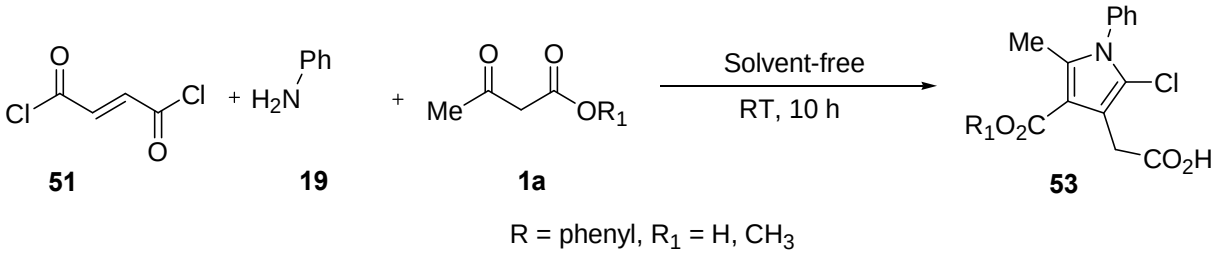

Scheme 14: Synthesis for pyrroles acyclo-condensation reaction

Despite the fact that the effect of the substituents has been investigated by means of pyrrole-quinoline derivatives [25-26], Ohshiro *et. al.* [27] focused their attention on the structural importance of these skeletons **(54-57)**.

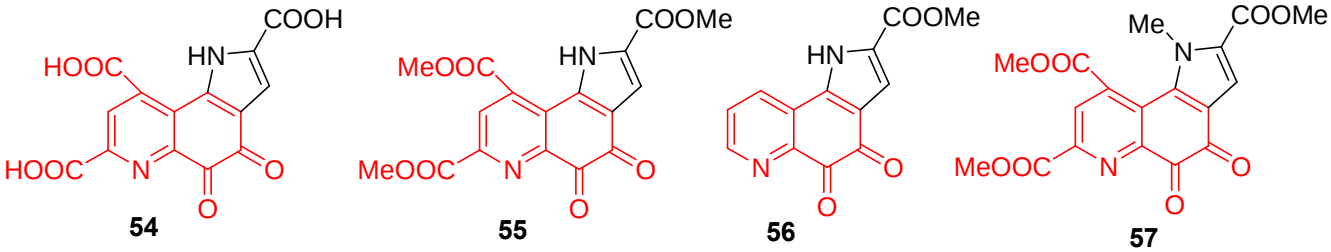

2.3.1.2. Furans

Furan is a five-membered aromatic ring with four carbon atoms and one oxygen atom. Examples are tetrahydrofuran, 2,5-dimethylfuran, benzofuran etc [28]. Alizadeh *et. al.* [29] reported a simple isocyanide-based MCR synthesis of bis(aminofuran)bicinchroninicamide derivatives **(60)**

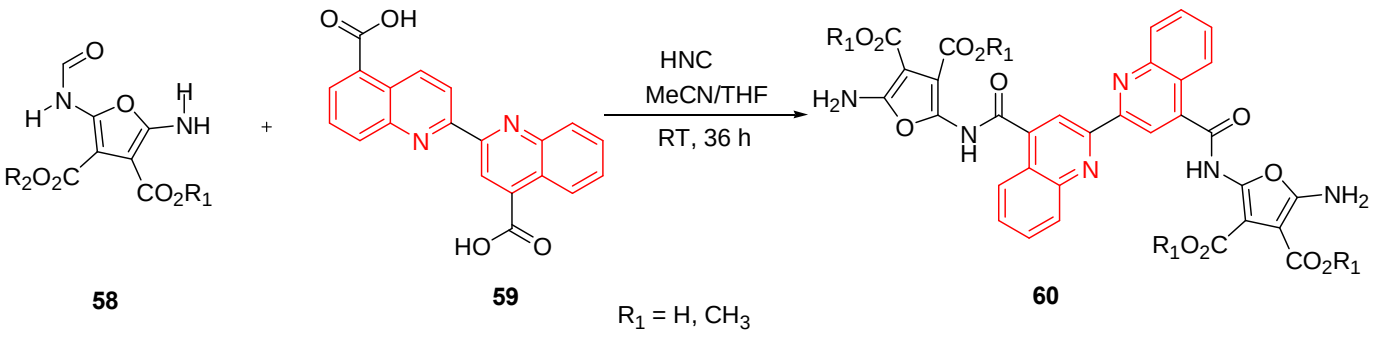

Scheme 15: Synthesis of bis(aminofuran)bicinchroninicamides

Synthesis of quinoline-attached furan-2(3*H*)-ones **(63)** having anti-inflammatory and anti-bacterial properties with reduced gastro-intestinal toxicity and lipid peroxidation was synthesized by Alam *et. al.* [30] by condensing different aldehydes **(62)** with a 3-(substituted benzoyl)propionic acid **(61)** in the presence of triethylamine and acetic anhydride under anhydrous conditions.

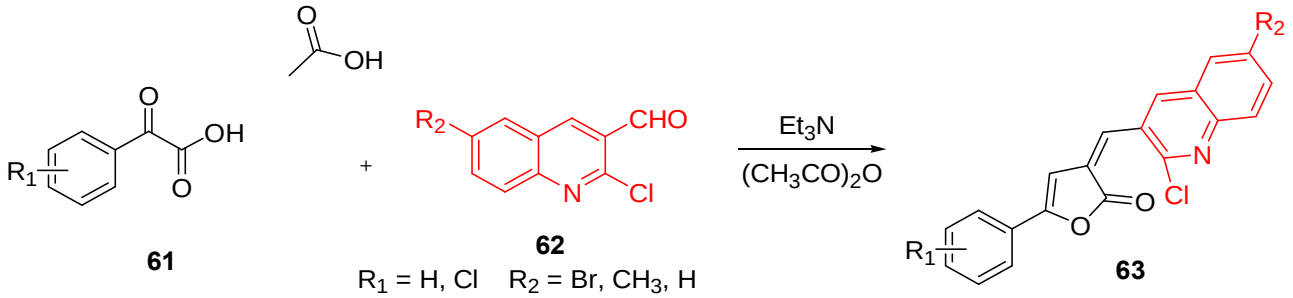

Scheme 16: Synthesis of quinoline-attached furan-2(3*H*)-ones

2.3.1.3. Triazoles

Triazole refers to either one of a pair of isomeric chemical compounds with molecular formula $C_2H_3N_3$, having a five-membered ring of two carbon atoms and three nitrogen atoms [31]. Ackerman *et. al.* [32] developed an elegant modular synthesis of fully substituted 1,2,3-triazoles (**60**) through a chemo- and regio-selective one-pot, four-component coupling of alkynes **(56)** with sodium azide **(57)**.

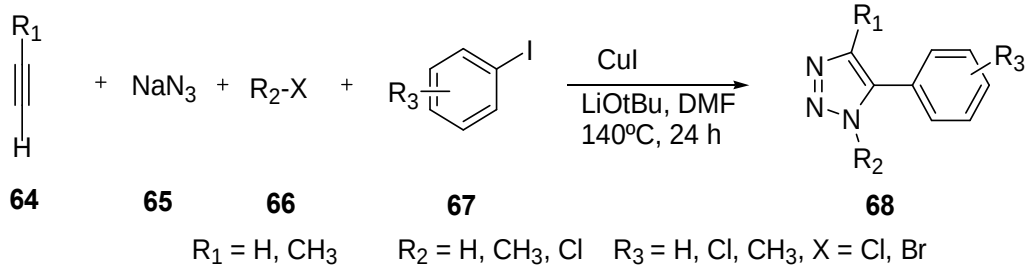

Scheme 17: Synthesis of fully substituted 1,2,3-triazoles

A synthesis of quinoline coupled [1,2,3]-triazoles **(70)** as a promising class of anti-tubercolosis agents from azidemethyl quinoline **(69)** with different alkynes **(64)** was prepared by Kumar *et. al.* [33]

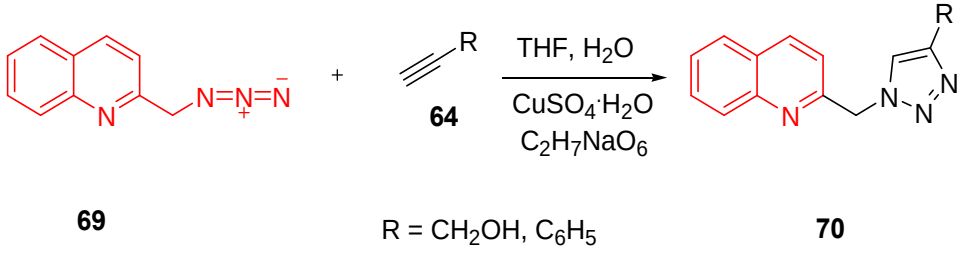

Scheme 18: Synthesis of quinoline coupled [1,2,3]-triazoles

2.3.1.4. Imidazoles

Imidazole is an organic compound with the formula $(CH)_2N(NH)CH$. It is an aromatic heterocycle, classified as a diazole and as an alkaloid [34]. Jiang *et. al.* [35] established a concise and efficient four-component domino approach to highly substituted 2(2-azaaryl) imidazoles **(73)** under solvent-free and microwave irradiation conditions.

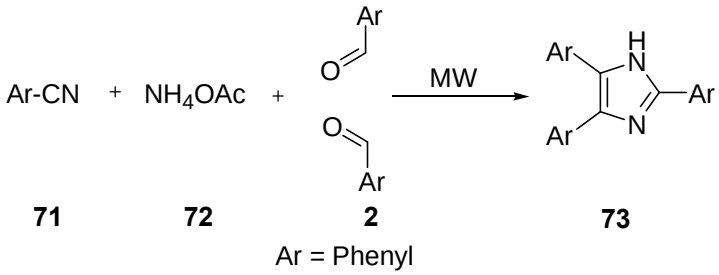

Scheme 19: Synthesis for highly substituted 2(2-azaaryl) imidazoles

A quinoline-imidazolium **(76)** based compound was synthesized by Desai *et. al.* [36] as a symmetrically saturated bis(1,3-quinoline)imidazolium adduct **(75)**.

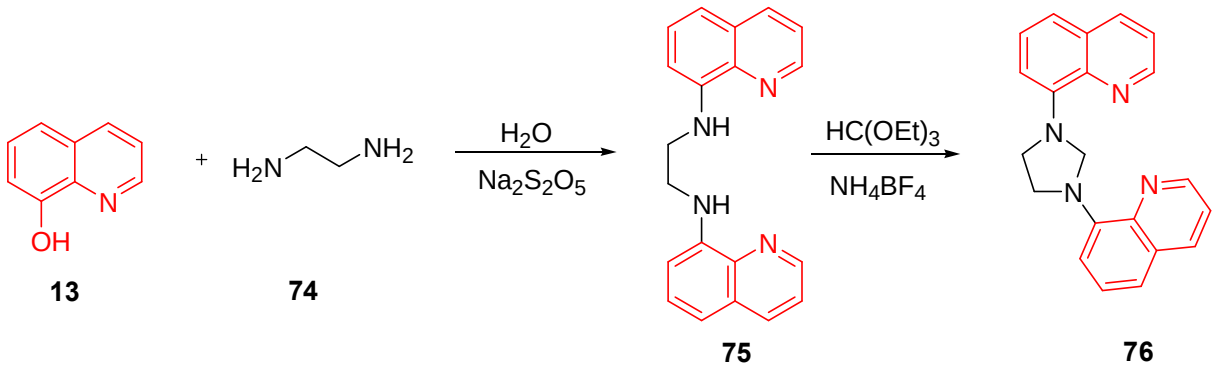

Scheme 20: Synthesis of quinoline-imidazolium based compounds

2.3.1.5. Indoles

Indole is an aromatic heterocyclic organic compound. It has a bicyclic structure consisting of a six-membered ring fused to a five-membered nitrogen-containing pyrrole ring [37]. Sridar *et. al.* [38] presented a classical Fisher-indole synthesis using an arylhydrazine **(77)** and a ketone **(78)**.

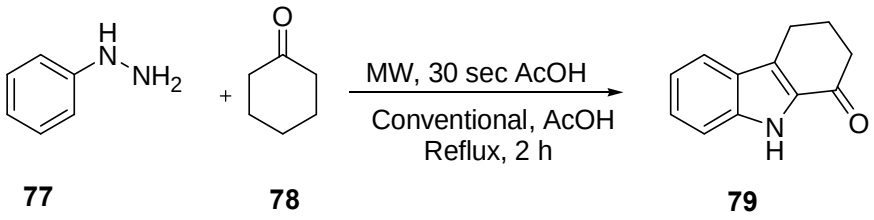

Scheme 21: Fisher-indole synthesis from arylhydrazine and ketone

2.3.2. Six-Membered Heterocycles

2.3.2.1. Pyridines

Pyridine is a basic heterocyclic organic compound with the chemical formula C_5H_5N [39]. Jiang *et. al.* [40] described an efficient reagent-controlled regio-specific synthesis of 2,2-bipyridine and unsymmetrical 2,4,6-triarylpyridine derivatives **(82)** at high temperature by microwave-assisted aqueous MCRôs of aromatic aldehydes, 3-aryl-3-oxo-propanenitrile, 2-acetylpyridine, or aromatic ketones and ammonium acetate.

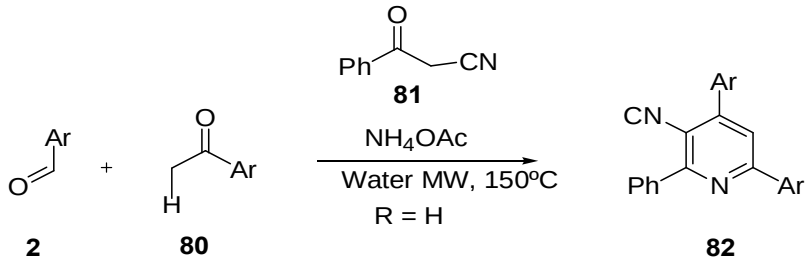

Scheme 22: Pyridines reaction for the synthesis of 2,2-bipyridine and unsymmetrical 2,4,6-triarylpyridine derivatives

2.3.2.2. Tetrazines

Tetrazine is an unstable compound that consists of a six-membered aromatic ring containing four nitrogen atoms with the molecular formula $C_2H_2N_4$. The Diels-Alder reaction between aza-olefins **(83)** and aza-dicarboxylic ester **(84)** to give tetrazines **(85)** was reported by Avalos *et. al.* [41]

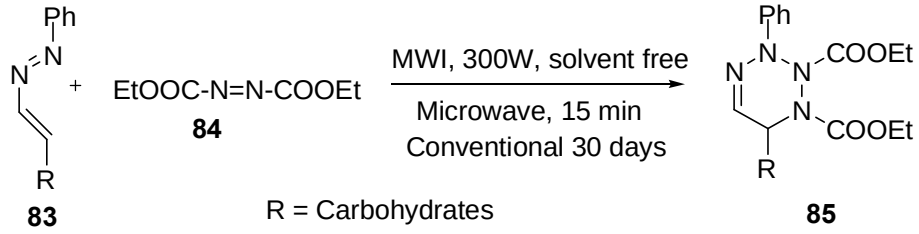

Scheme 23: Diels-Alder reaction between aza-olefins and aza-dicarboxylic for the synthesis of tetrazines

2.3.2.3. Pyrans

Pyran is a six-membered heterocyclic, non-aromatic ring consisting of five carbon atoms and one oxygen atom and containing two double bonds with a molecular formula C_5H_5O [42]. Laloo *et. al.* [43] presented a diastereo selective three-component Prins-Friedel-Crafts reaction for the synthesis of 4-aryltetrahydropyran derivatives **(89)**.

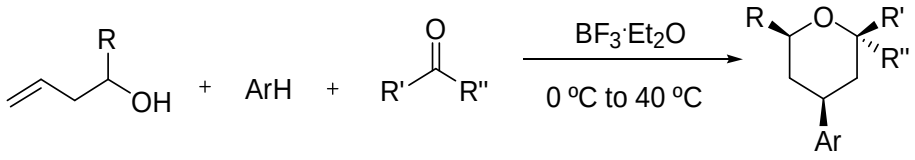

86 **87** **88a,b,c** **89**

R' = H, alkyl, aryl R'' = H, alkyl, aryl

Scheme 24: Prins-Friedel-Crafts reaction for the synthesis of 4-aryltetrahydropyran derivatives

2.3.3. Polycyclic Six-Membered Heterocycles

2.3.3.1. Quinolines

The quinoline moiety is an essential core structure of several natural and synthetic heterocyclic compounds that exhibit outstanding medicinal performances [44]. The quinoline skeleton structure is presented below:

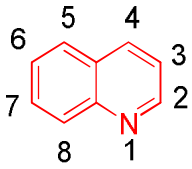

In particular, quinolines have played a unique role in the design and synthesis of novel biologically-active compounds. They have been studied as anti-bacterial, anti-flammatory, anti-malarial, anti-asthmatic, anti-tuberculosis, and anti-hypertensive agents [45-50]. Apart from the above mentioned applications, quinoline and quinolinone ring systems are present in the diverse array of natural products such as tecleabine **(90)**, tecleoxine **(91)**, plakinidine **(92)** and quinine **(93)**. Some of the representatives are shown in **Figure. 2**

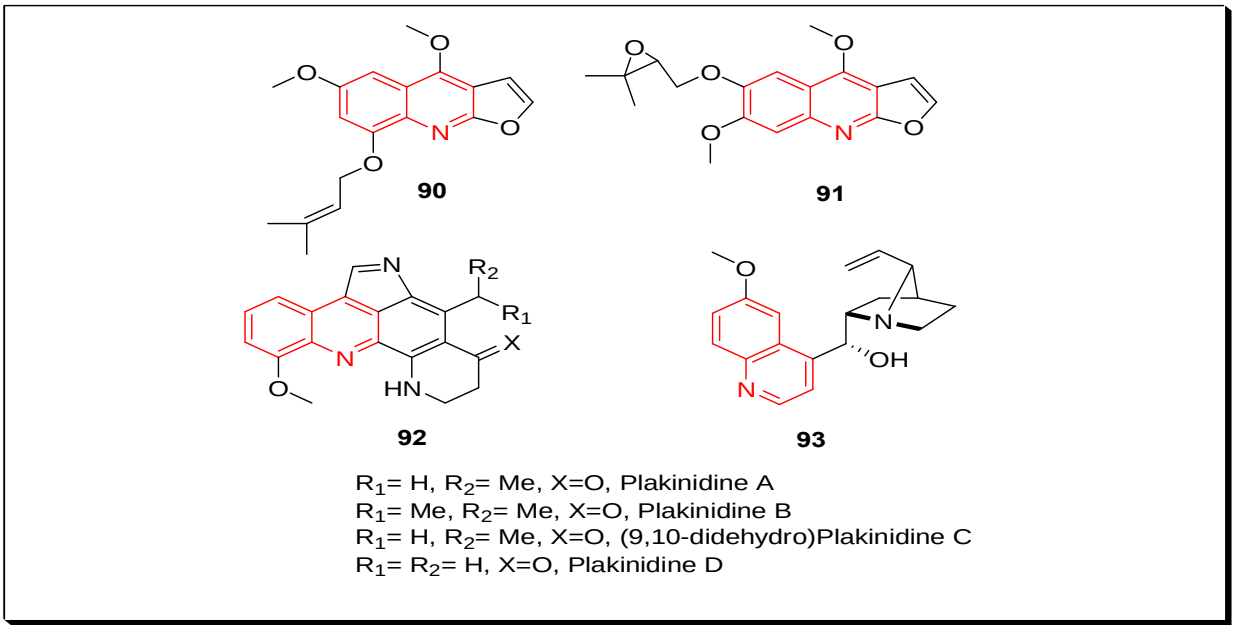

Figure 2: Typical examples of important quinolines from natural products

A one pot route for the synthesis of 4-aryl-8-arylidene-5,6,7,8-tetrahydro-2-quinolinones (**95**) was developed by Yan *et. al*. [51] based on a cyclocondensation reaction with cyclohexanone.

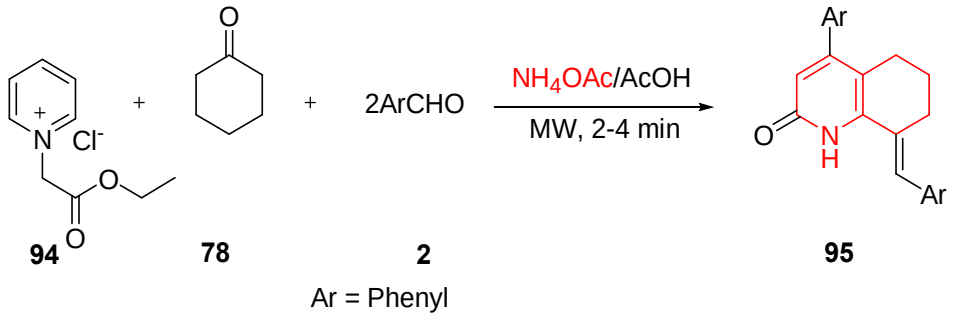

Scheme 25: Synthesis of 4-aryl-8-arylidene-5,6,7,8-tetrahydro-2-quinolinones

Zhang *et. al*. [52] described an efficient Hantzsch reaction for the synthesis of polyhydroquinolines (**97**) applying a solvent-free microwave-assisted one pot four-component reaction of poly(ethylene glycol)-bound acetoacetate **(96)**, 1,3-cyclohexanedione **(11)**, aromatic aldehyde **(2)** and ammonium acetate.

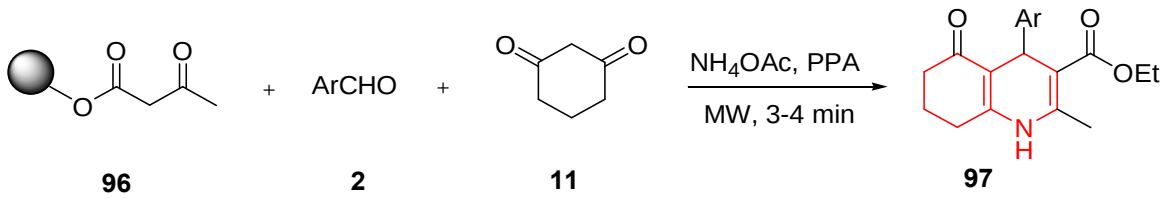

Scheme 26: Hantzsch reaction for the synthesis of polyhydroquinolines

Steroselective synthesis of *N*,*N*-bis[(2-chloroquinoline-3-yl)methylene]-1-diamine **(98)** was reported by reaction of 2-chloro-3-formylquinoline **(17)** with ethylenediamine **(74)** in ethanol at 120ºC [53].

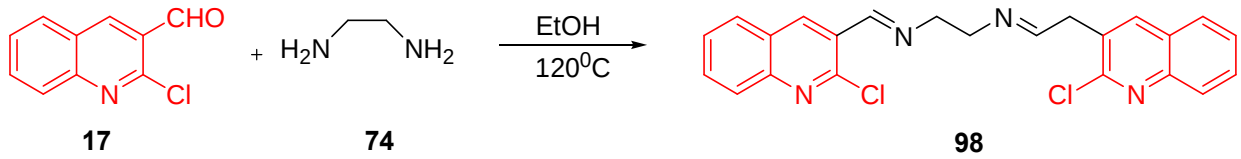

Scheme 27: Steroselective synthesis of *N*,*N*-bis[(2-chloroquinoline-3-yl)methylene]-1-diamine

Other types of heterocyclic reactions such as heterocyclic *C*-alkylations and heterocyclic *N*-alkylations and other typical reactions are presented below.

C-arylation nucleophilic substitution [54]

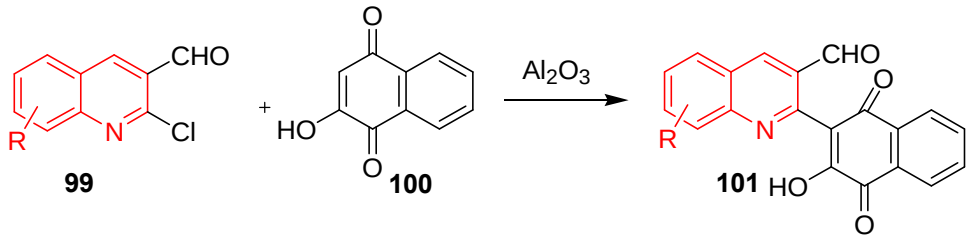

Scheme 28: An example of quinolines c-arylation nucleophilic substitution reaction

Nucleophilic substitution [55]

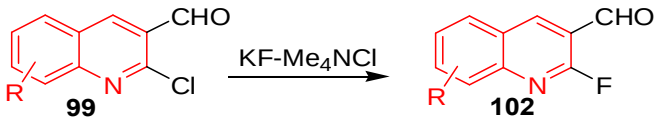

Scheme 29: An example of quinolines nucleophilic substitution reaction

Aza Wittig reaction [56]

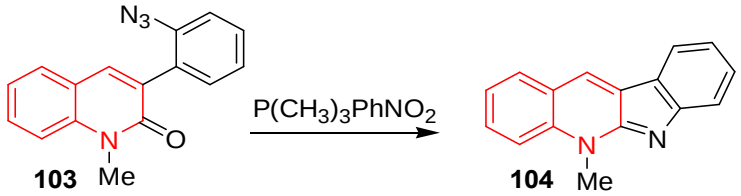

Scheme 30: An example of quinolines Aza Wittig reaction

Crossed Cannizaro reaction [57- 58]

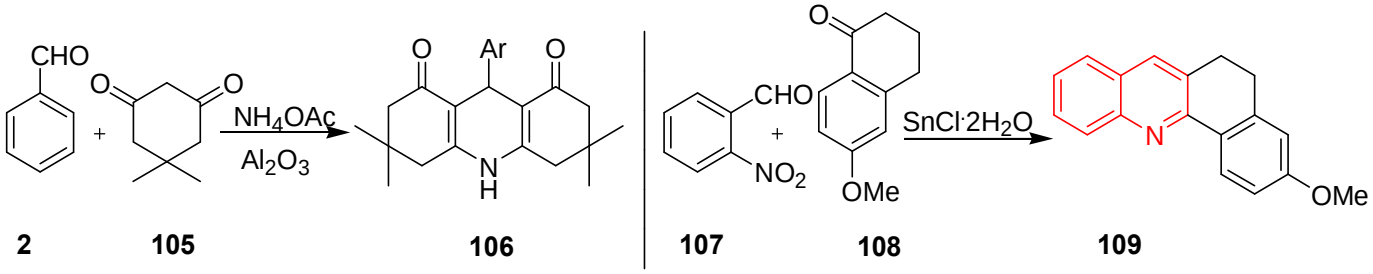

Scheme 31: An example of quinolines Crossed Cannizaro reaction

2.3.4. Seven-Membered Heterocycles

The polysubstituted 1,4-benzodiazepin-3-ones **(100)** and **(101)** were synthesized by Silva *et. al.* [59] by isocyanide based MCR.

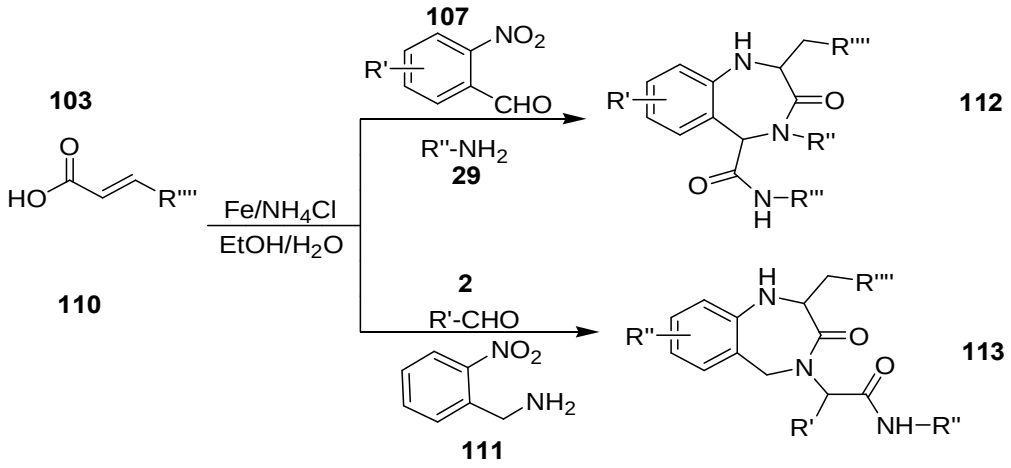

Scheme 32: Synthesis of polysubstituted 1,4-benzodiazepin-3-ones by isocyanide

2.4. Some Important Applications of Quinolines and Quinolones

2.4.1. Cancer Studies

2.4.1.1. Quinoline based alkaloids as DNA intercalators

Watson and Crickôs assertion that genetic substances structurally exist as a double helix are well established characteristics [60]. Its role in the control of cellular functions immediately made it an excellent target for treating illness of genetic origin, such as cancer. The first compound discovered to act on DNA were the sulphur mustards, but their high toxicity prompted the search for less toxic and more efficient compounds [61]. In the 1960s, some compounds with cytoxic activity were discovered to act as anti-cancer agents, although their mechanism of action was unknown. Interestingly, after Lerman reported the occurrence of a non-covalent interaction between acridine and DNA, suggesting an intercalative process, it was established that some of these anti-cancer agents worked by interacting with DNA [62].

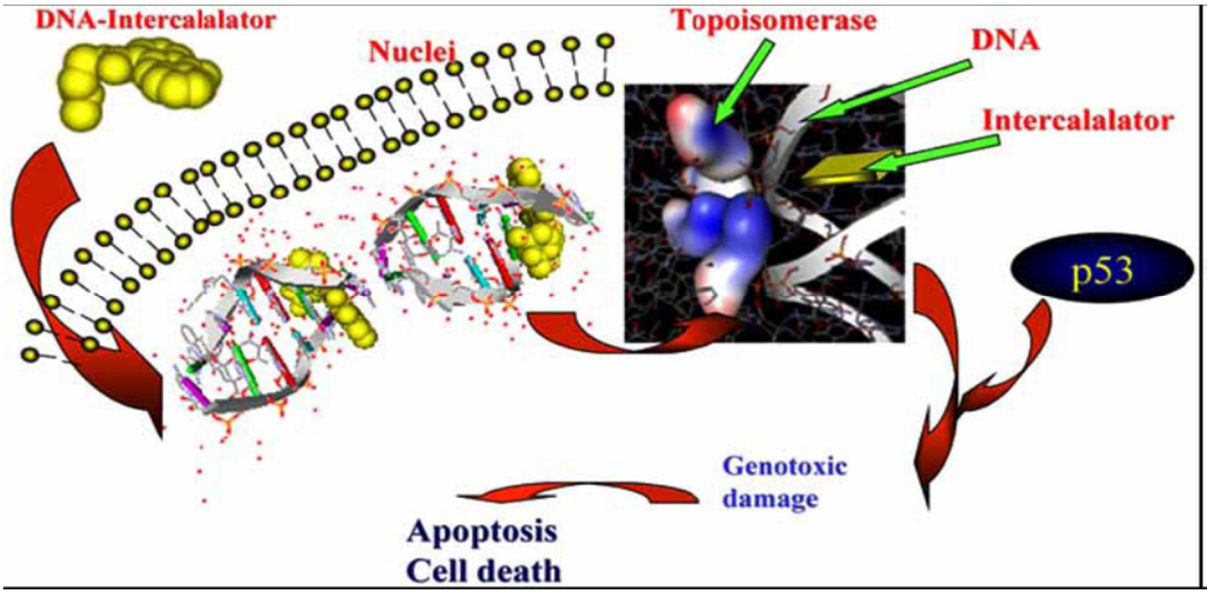

Figure 3: Schematic diagram of DNA intercalation [63]

2.4.1.2. Some Anti-Cancer Agents and their Reaction Schemes

Ramesh *et. al.* [64] reported quinoline-rhodanine derivatives as anti-cancer agents. The synthetic strategies involved condensation of 2-chloro-3-formylquinoline **(114)** and rhodanine residues **(115** and **116)**, leading to desired molecules **(117)** and **(118)**.

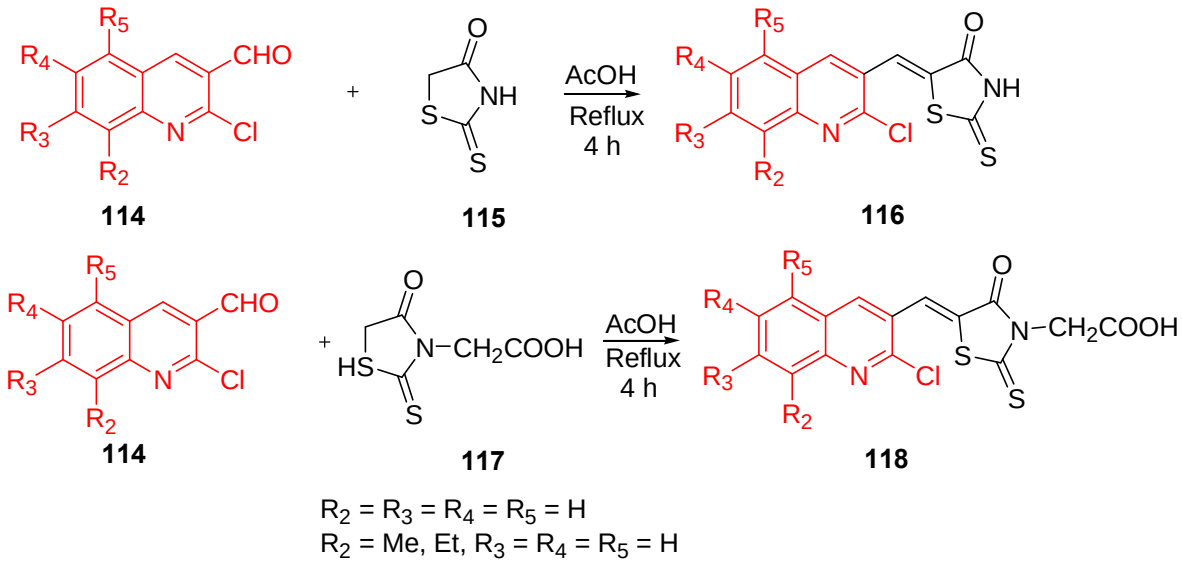

Scheme 33: Synthesis for quinoline-rhodanine derivatives 2-chloro-3-formylquinoline and rhodanine

Biginelli reactions of 2-chloro-3-formylquinoline **(114)** with urea **(3)** and active methylene compounds such as 3-methyl-1-phenyl-1*H*-pyrazol-5(4*H*)-one **(119)** and dimedone **(121)**, was performed by using microwave irradiation to give 4-(2-chloro-3-quinolinyl)-2-thio/oxo-pyrimidine **(120)** and **(122)** and they were found to be active anti-cancer agents against lung and breast carcinomas [65-67].

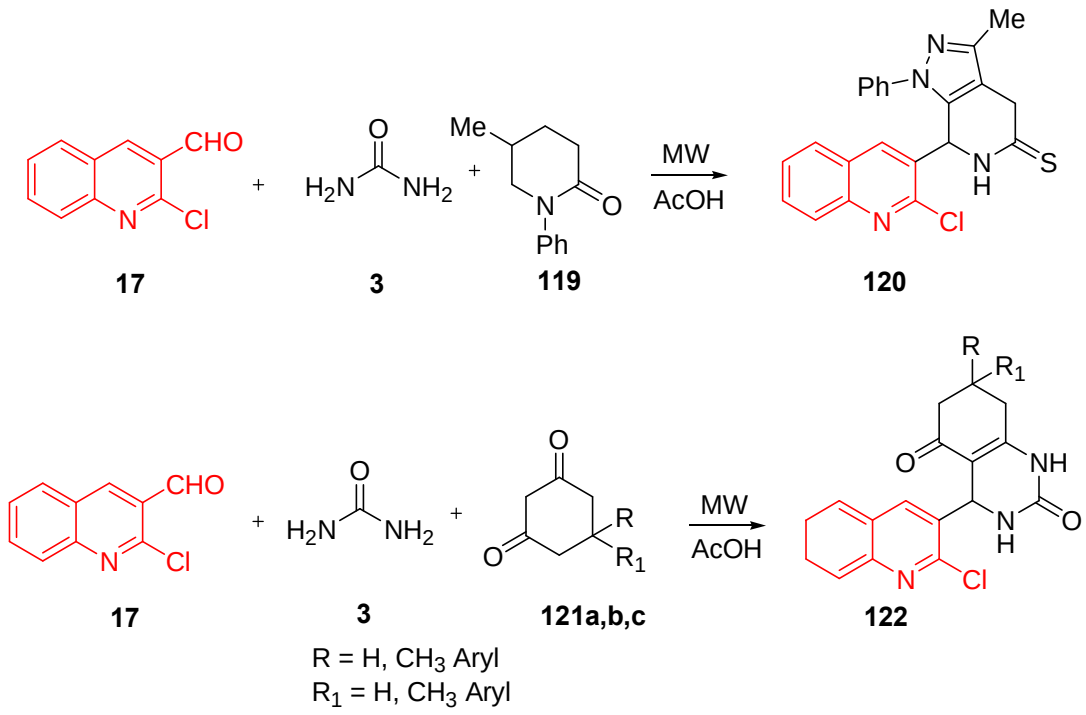

Scheme 34: Biginelli reactions for the synthesis of 4-(2-chloro-3-quinolinyl)-2-thio/oxo-pyrimidine

Cao *et. al*. [68] reported a convenient and one-pot synthesis of 1-methoxy-3-phenyl-1*H*-pyrano[4,3-*b*]-quinoline (**123)** from the reaction of 2-chloro-3-formylquinoline (**17)** with phenyl acetylene (**64a)** in acetonitrile in the presence of $Pd(OAc)_2$ and triphenylphosphine. Abeer *et. al*. [69] has also revealed that more efficient lead molecules are designed by joining two or more pharmacologically active heterocyclic systems together in a single molecular framework; doxorubicin **(124)**, amptothecin **(125)** and adriamcin **(126)** as presented in **Figure 4.**

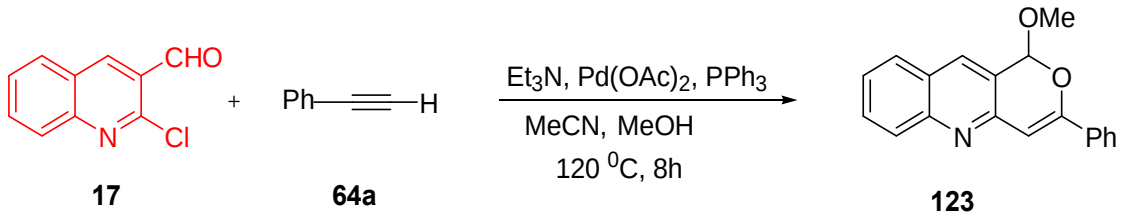

17 64a 123

Scheme 35: Synthesis 1-methoxy-3-phenyl-1*H*-pyrano[4,3-*b*]- quinoline from 2-chloro-3-formylquinoline and phenyl acetylene

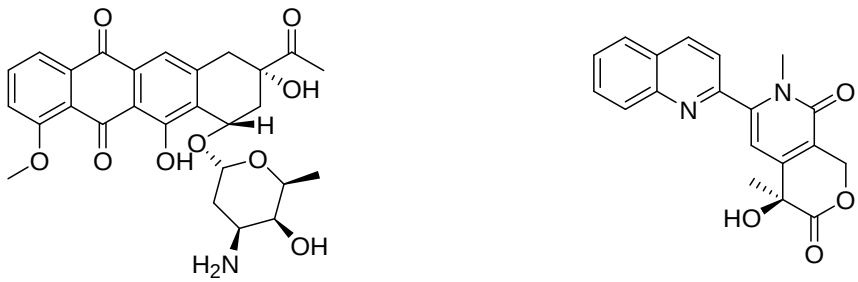

124

125

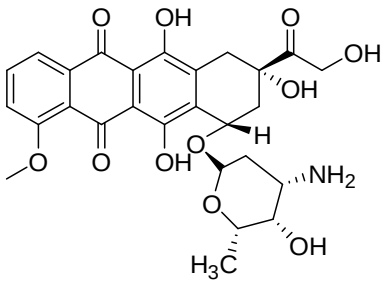

126

Figure 4: Molecules with anti-cancer activity

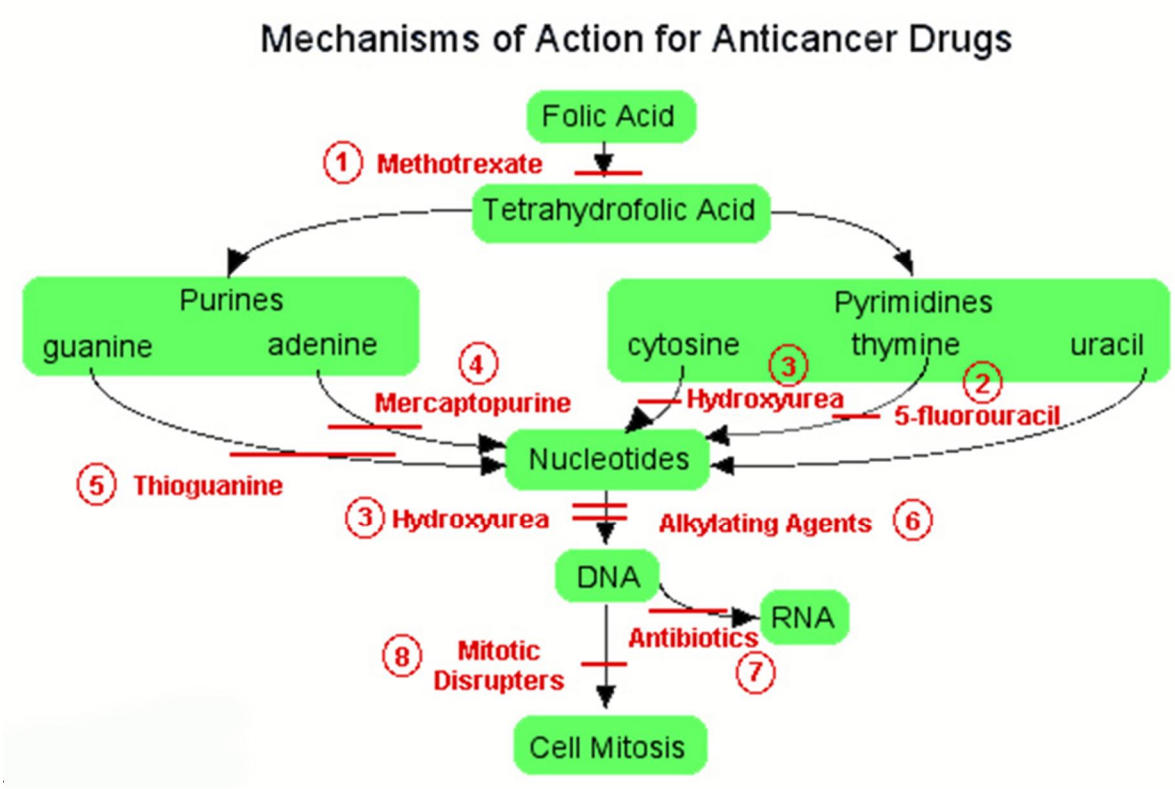

Figure 5: Schematic diagram for the mechanism of action for anticancer drugs [70]

2.4.2. Molecular Docking Studies

Docking is a method which predicts the preferred orientation of one molecule to a second when bound to each other to form a stable complex [71]. Knowledge of the preferred orientation in turn may be used to predict the strength of association or binding affinity between two molecules using, for example, scoring functions. The association between biologically relevant molecules such as proteins, nucleic acids, carbohydrates and lipids play a central role in signal transduction. Furthermore, the relative orientation of the two interacting partners may affect the type of signal produced. Therefore docking is useful for predicting both the strength and type of signal produced. Docking is frequently used to predict the binding orientation of small molecule drug candidates to their protein targets in order to predict the affinity and activity of the small molecule. Hence docking plays an important role in rational design of drugs [72]. Given the biological and pharmaceutical significance of molecular docking, considerable efforts have been directed towards improving the methods used to predict docking. **Figure 6** represents a schematic diagram illustrating the docking of a small molecule ligand (brown) to a protein receptor (green) to produce a complex and **Figure 7** represents an example of a small molecule docked to a protein.

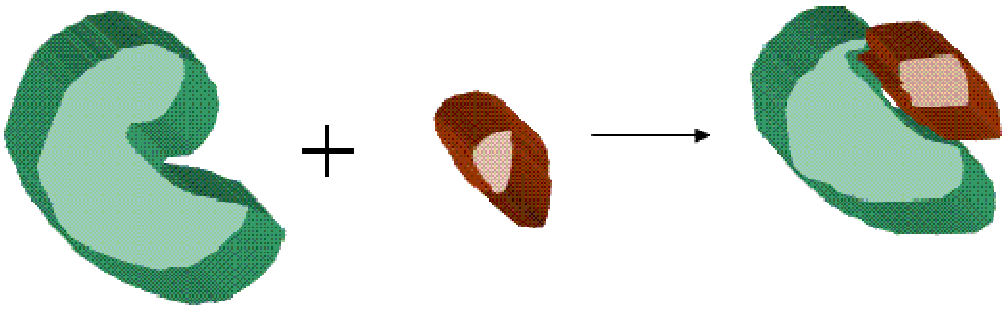

Figure 6: Docking of a small molecule ligand to a protein receptor to produce a complex [72]

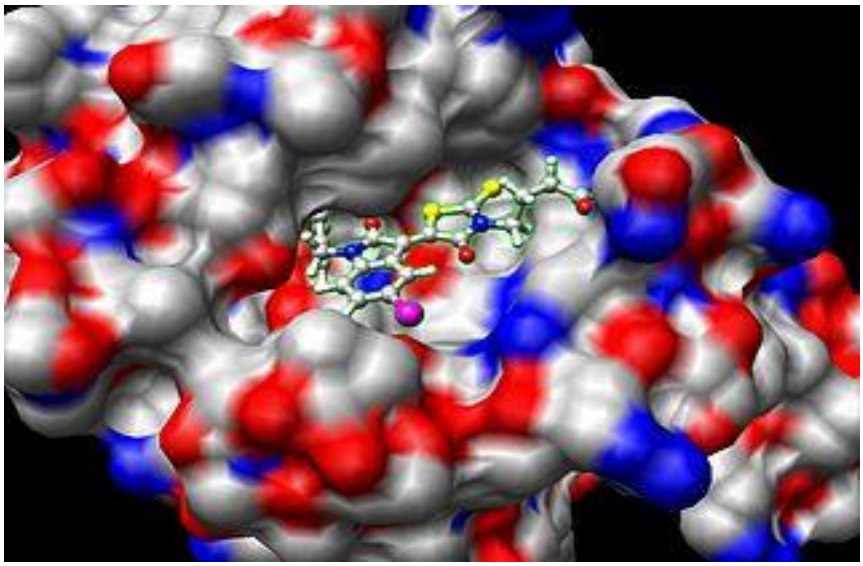

Figure 7: A small molecule docked to a protein [72]

2.4.2.1. Some Molecular Docking Properties and Their Reaction Schemes

Sharath *et. al.* [73] presented a rapid synthesis of quinoline isoxazoles **(114)**. The synthesized compounds exhibited good anti-tumor and anti-bacterial activities and were carefully examined for B-DNA molecular docking. According to a criterion used, docking of quinoline isoxazole to DNA resulted in compounds being actively favorable in binding mode and binding site as shown in **Figure 8**.

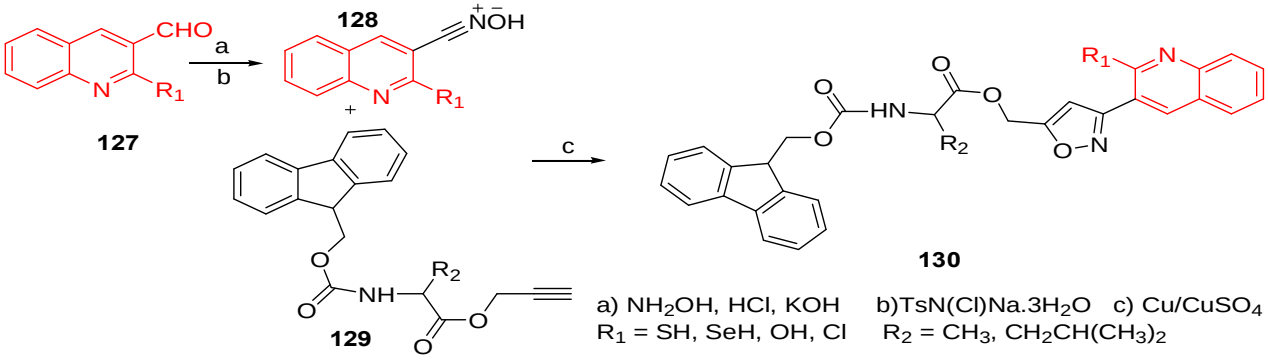

Scheme 36: Synthesis of quinoline isoxazole derivatives

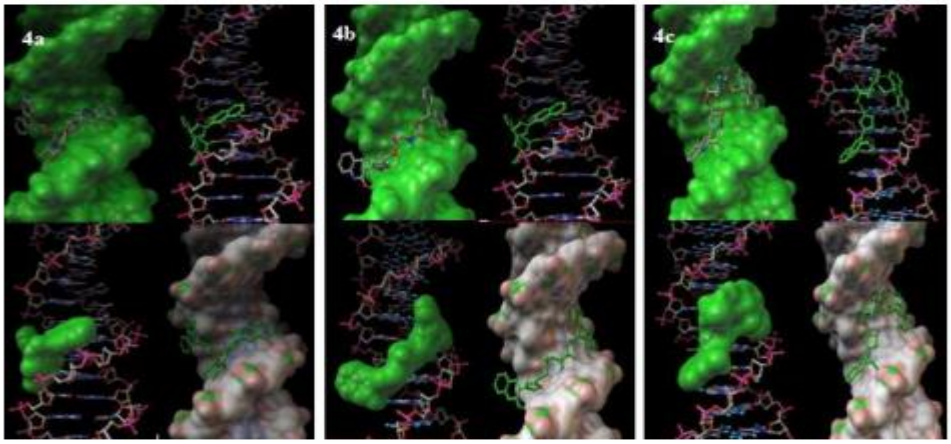

Figure 8: Example for B-DNA molecular docking [73]

Sharma *et. al.* [74] explored the binding interactions of the non-peptide based compounds **(131, 132)** with the receptor. His aim was to understand the binding mode of these molecules and to cross-check whether the developed pharmacophore model fits properly to the active site which was achieved by performing flexible docking using the Glide SP mode.

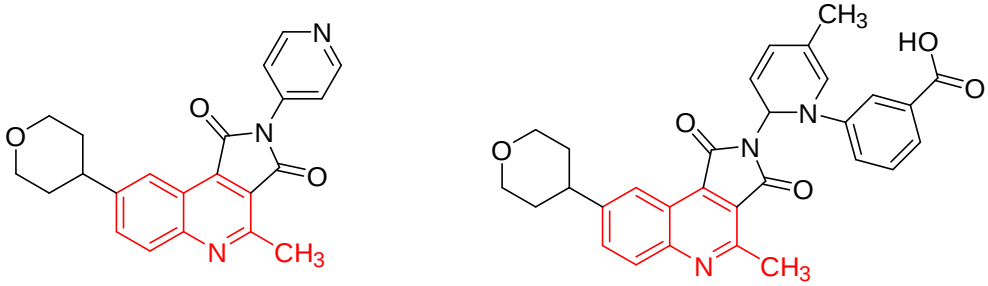

131 **132**

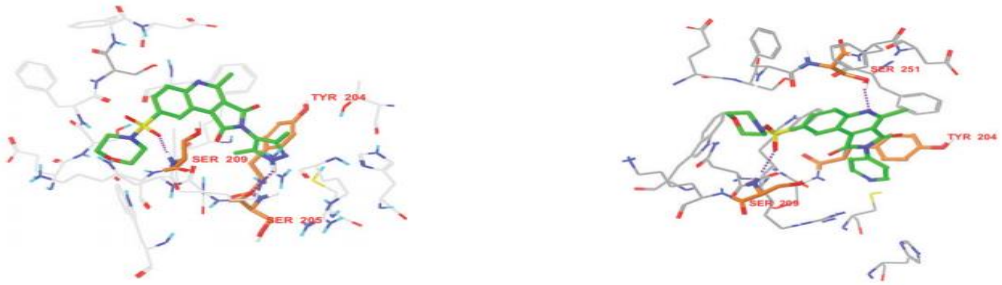

Figure 9: Binding interactions of compounds at the active site where the non-peptide interact with the receptor ligand (green), hydrogen bonds are expressed as dotted lines (purple), and active site residues are demonstrated in orange [74]

2.4.3. Bacterial Studies

2.4.3.1. History of Bacteria

Bacteria represent a huge area of prokaryotic micro-organisms. Bacteria were amongst the first life forms to appear on earth and are present in most habitats on the planet, growing in soil, water, acidic hot springs, radioactive waste [75], and deep in the earthôs crust, as well as in organic matter and the live bodies of plants and animals. According to the literature, there are typically 40 million bacteria cells in a gram of soil and there is a million bacterial cells in a millilitre of fresh water. In all, there are approximately five nonillion (5 x10^{30}) bacteria on earth [76], forming a biomass that exceeds that of all plants and animals. [77] **Figure 10** gives an overview of bacterial infections in the human body.

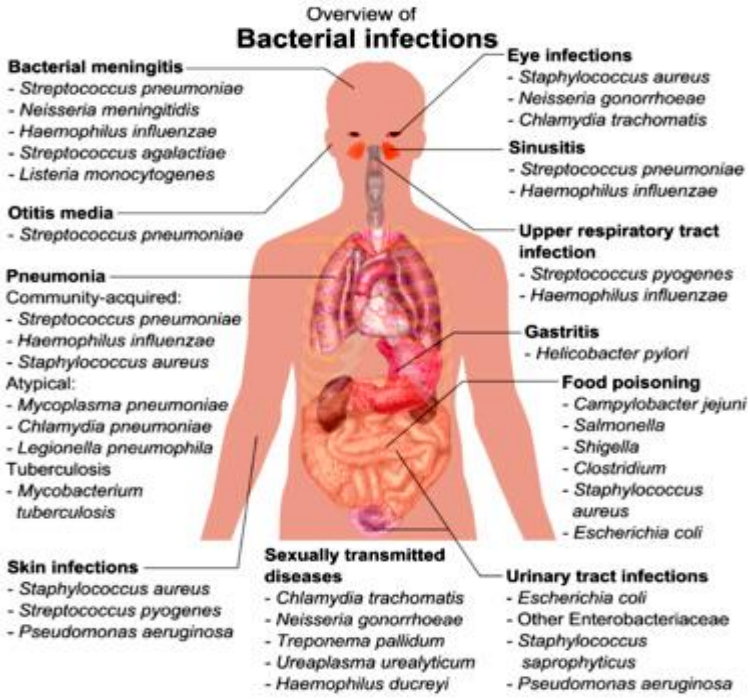

Figure 10: An overview of bacterial infections in the human body [77]

2.4.3.2. Anti-microbial Activity of Quinoline

Tuberculosis is an infection caused by *mycobacterium tuberculosis*, which commonly affects the respiratory tract, i.e. lungs. [78] The ýrst line of drugs used in the treatment of tuberculosis was a combination of rifamycin **(133)**, isoniazid **(134)**, pyrazinamide **(135)** and ethambutal **(136)**. The high concentration of lipids in the cell wall of *Mycobacterium tuberculosis* has been attributed to its resistance to antibiotics. Thus the increasing clinical importance of tuberculosis has lent additional urgency to researchers to identify new and effective anti-mycobacterial compounds. [79-80]

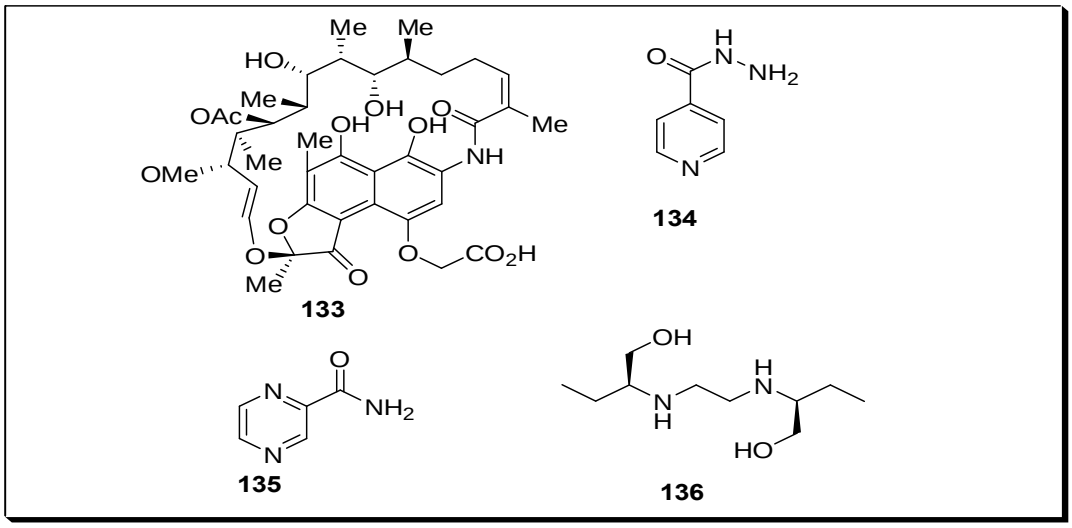

2.4.3.3 Some Quinolones and Quinolines Anti-bacterial Drugs and their Reaction Schemes

Mitscher *et. al*. [81] found that the quaternary alkaloid pteleatinium chloride and the *O*-methylptelefolonium salt isolated from Pteleatrifoliate showed anti-microbial activity towards *S. aureus* and *Mycobacterium tuberculosis*. Sadana [82] has reported the hypervalent iodine mediated synthesis of 1-aryl/hetryl-1,2,4-triazolo[4,3-*a*]pyridines **(140)**.

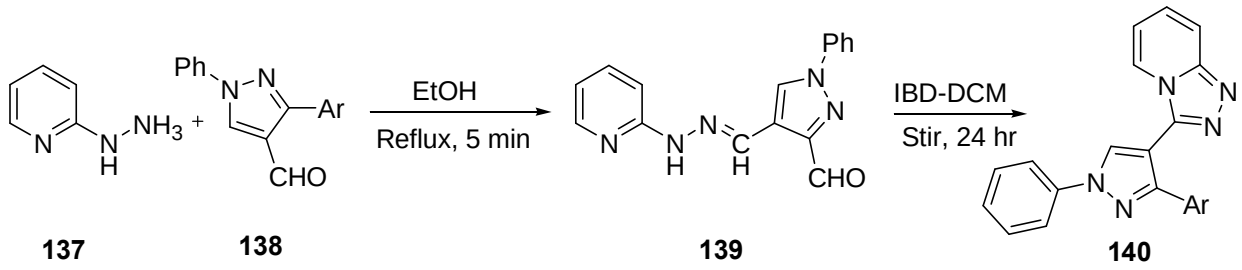

Ar = Phenyl, CH_3-Phenyl, OCH_3-Phenyl, NO_2-Phenyl, F-Phenyl,

Scheme 37: Synthesis of 1-aryl/hetryl-1,2,4-triazolo[4,3-*a*]pyridines

Nalidixic acid **(141)** [83] is a powerful anti-bacterial agent; numerous publications describing its derivatives, detection, physiological and chemical properties has been documented. This drug has high efficacy against gram negative bacteria [84]. Some essential structures of quinolone antibiotics, norfloxacin **(142)**, ciprofloxacin **(143)**, fluoroquinolone **(144)** are shown below. The blue R is usually piperazine. If the connection contains fluorine (green), it is a fluoroquinolone [85-86].

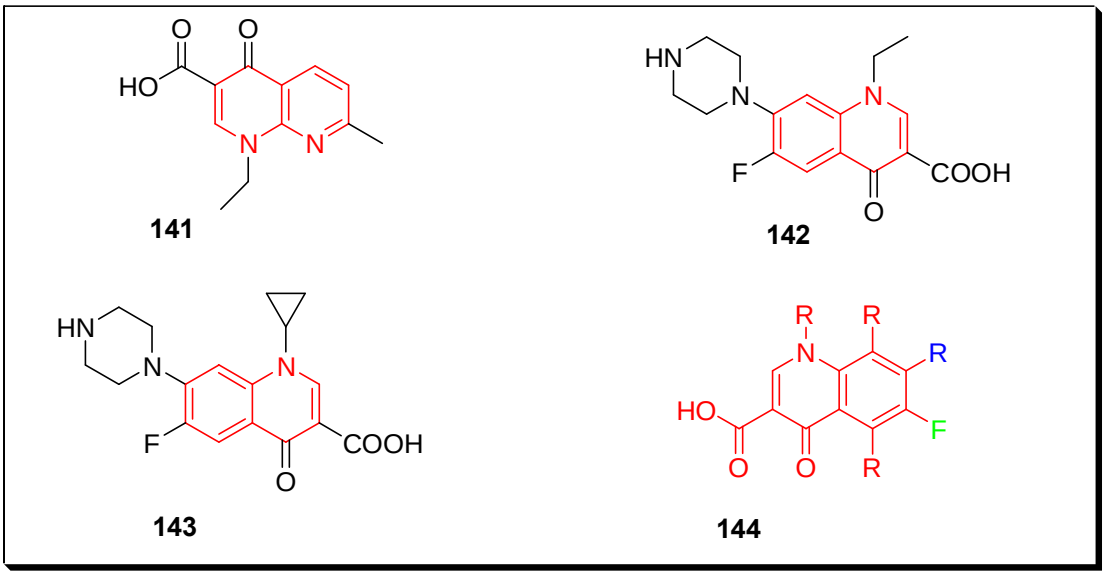

Parikh *et. al.* [87] reported the synthesis of cyanopyridines **(145)** and cyanopyrans **(146)** bearing 2-chloro-6-bromoquinoline nucleus as potential anti-microbial and anti-cancer agents.

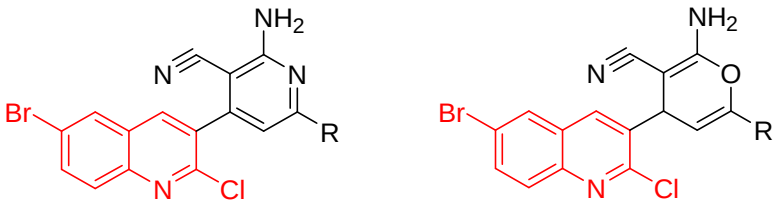

R = C_6H_5, 2-Br-C_6H_4, 4-Br-C_6H_4, 4-Cl-C_6H_4

Miniyar *et. al.* [88] reported the synthesis of 1-(5-(2-chloroquinolin-3yl)3-phenyl-1*H*-pyazol-1-yl)etha-none derivatives **(148)** as potent anti-microbial agents.

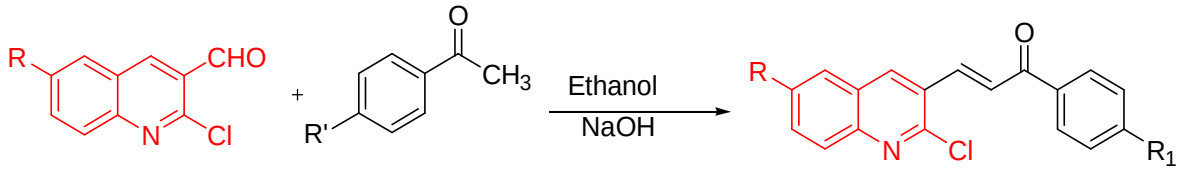

R = H, NO_2, Br
R_1 = H, NH_2, F

Scheme 38: Synthesis of synthesis of 1-(5-(2-chloroquinolin-3yl)3-phenyl-1*H*-pyazol-1-yl)etha-none derivatives

3-Formyl-2-(3-hydroxy-1,4-naphthoquinon-2-yl)-quinoline **(150)** was synthesized by Bekhit *et. al.* [89] by a reaction of 2-chloro-3-fomylquinoline **(17)** with 2-hydroxy-1,4-naphthoquinone **(149)** in basic alumina using microwave irradiation.

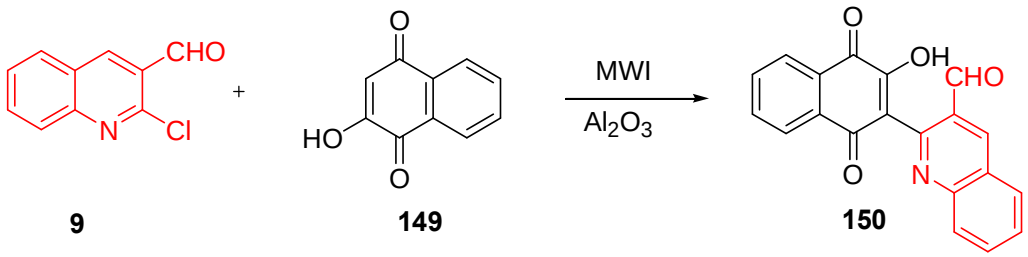

9 **149** **150**

Scheme 39: Synthesis of 3-Formyl-2-(3-hydroxy-1,4-naphthoquinon-2-yl)-quinoline from 2-chloro-3-fomylquinoline and 2-hydroxy-1,4-naphthoquinone

Nirav *et. al*. [90] reported the synthesis of 2-(2-chloro-6-quinolin-3-yl)-2,3,4,12-tetrahydro-1*H*-benzothiazolo[2,3-b]quinazolin-1-one (**152)** by a one pot condensation of 2-chloro-3-formylquinoline **(9)**, 2-amino-6-methoxybenzothiazole **(151)** and 5-dimethyl-1,3-cyclohexanedione **(105)** in ethanol. The synthesized compounds showed promising anti-bacterial activity.

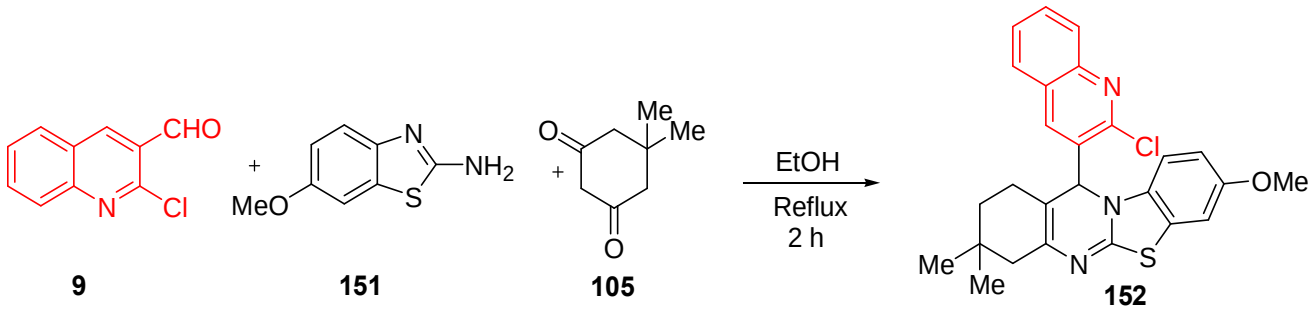

9 **151** **105** **152**

Scheme 40: 2-(2-chloro-6-quinolin-3-yl)-2,3,4,12-tetrahydro-1*H*-benzothiazolo[2,3-b]quinazolin-1-one 2-chloro-3-formylquinoline 2-amino-6-methoxybenzothiazole and 5-dimethyl-1,3-cyclohexanedione

A three-component reaction of 2-chloro-3-formylquinoline **(9)**, malononitrile **(40)**, and either 4-hydroxycoumarin **(153)** or resorcinol **(154)** was performed by Kidwai *et. al*. [91] in aqueous K_2CO_3 under microwave irradiation to give anti-bacterial active 2-amino-4-(2-chloroquinolin-3-yl)-5-oxo-4,5-dihydropyrano[3,2]chromene-3-carbonitrile **(155)** and 2-amino-4-(2-chloroquinolin-3-yl)-7-hydroxy-4*H*-chromene-3-carbonitrile **(156)**.

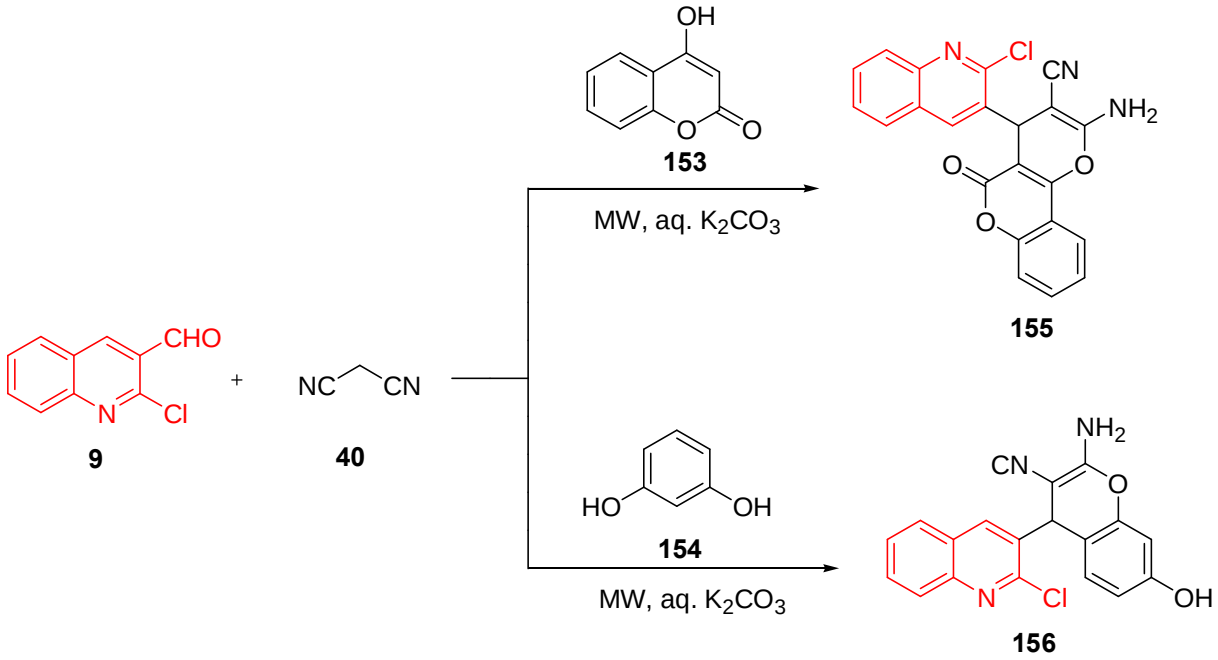

Scheme 41: Synthesis of 2-amino-4-(2-chloroquinolin-3-yl)-5-oxo-4,5-dihydropyrano[3,2]chromene-3-carbonitrile derivatives

Rahatgaonkar and Dave [92] reported the synthesis of substituted 2-[2-amino-6-(2-chloroquinolin-3-yl)-5,6-dihydropyrimidine-4-yl]phenol **(159)** by condensing differently substituted (*E*)-3-(2-chloroquinolin-3-yl)-1-(2-hydroxyphenyl)prop-2-en-1-ones **(158)** with guanidine carbonate in the presence of ethanolic potassium hydroxide.

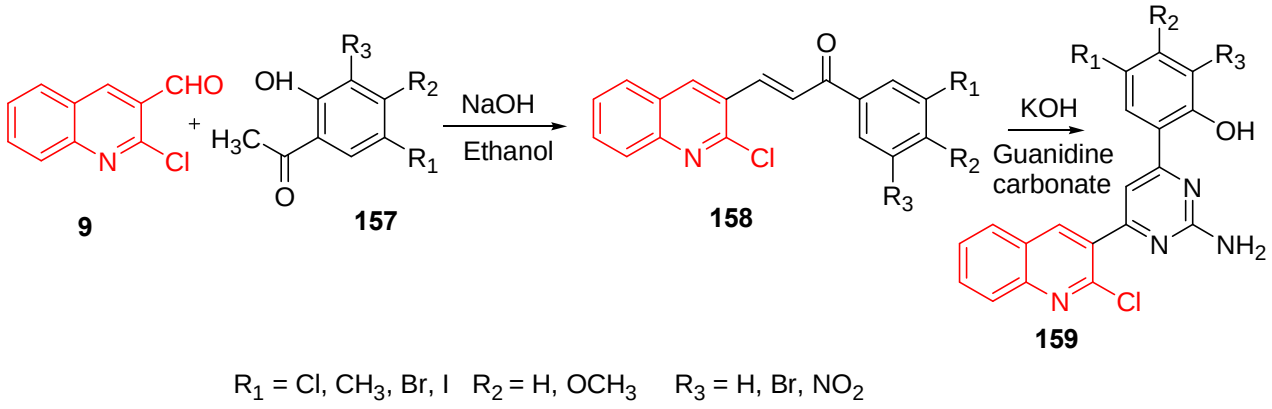

Scheme 42: Synthesis of synthesis of substituted 2-[2-amino-6-(2-chloroquinolin-3-yl)-5,6-dihydropyrimidine-4-yl]phenol

2.5. Structural elucidation

Structural determination in chemistry is the process of determining the chemical structure of molecules. Practically, the end result of such process is attaining the coordinates of the atoms in a molecule.[93] The methods by which one can determine the structure of a molecule include spectroscopy, such as nuclear magnetic resonance, infrared and mass spectroscopy. Proton **NMR** is the application

of nuclear magnetic resonance in **NMR** spectroscopy with respect to hydrogen-1 nuclei within the molecules of a substance [93]. Carbon-13 **NMR** is the application of nuclear magnetic resonance spectroscopy to carbon; it is an important tool in chemical structure elucidation in organic chemistry; it detects only the ^{13}C isotope of carbon, whose natural abundance is only 1.1%, because the main carbon isotope ^{12}C, is not detectable by **NMR** since it has zero net spin [93]. Mass spectrometry is a technique that helps identify the amount and type of chemicals present in a sample by measuring the mass-to-charge ratio and abundance of gas-phase ions. Infrared spectroscopy deals with the infrared region of the electromagnetic spectrum, that is light with a longer wavelength and lower frequency than visible light. It covers a range of techniques, mostly based on absorption spectroscopy [94].

As a typical example of synthesis and structural characterization, we report the research investigation of Nirmal *et. al.* [95] for the synthesis of biquinolines **4a-t**, which was catalyzed by DMAP by microwave irradiation. They used 2-chloro-3-formyl quinoline as a starting material and confirmed the structure by elemental analysis, IR and NMR.

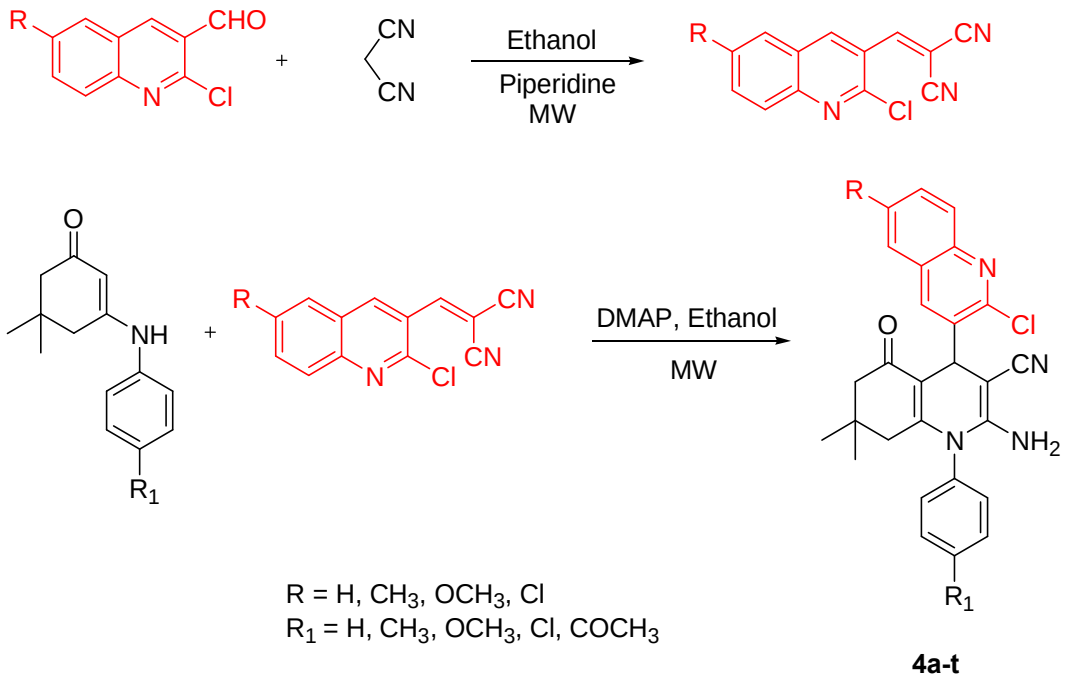

Scheme 43: Synthesis of biquinoline derivatives

As a typical example they used **4k** and elaborated on the characterization; their interpretation of spectroscopic data is presented below. We used the same methodology in our investigation to characterize the novel compounds synthesized in our laboratory. The **IR** spectrum of **4k** showed bands at 3320 (asymmetry N-H stretch) and 3250 cm^{-1} (symmetry N-H stretch) for ï NH_2, 2220 cm^{-1} for CN and 1650cm^{-1} for C=O stretching. The **^{1}H NMR** spectrum showed singlets at ŭ 0.93 and 0.97 for two methyl groups and multiplet of two methylene groups at ŭ 1.69-2.20. The singlets at ŭ 4.18 and 5.17 appeared for

amine and methine group, respectively. The aromatic protons appeared at ŭ 7.08-8.15. The **^{13}C NMR** spectrum was in good agreement with the structure assigned. The peaks at ŭ 27.3 and 29.4 were assigned to two methyl carbons, the peaks at ŭ 55.6 and 55.7 were assigned to two methylene carbons. The peak at ŭ 60.0 was assigned to carbon of carbonitrile; the peak at ŭ 195.8 was assigned to carbonyl carbon and the peaks at ŭ 105.2-160.6 were attributed to aromatic carbons.

Table 1: ^{1}H and ^{13}C NMR structural elucidation of 4k

No.	^{1}H NMR	^{13}C NMR	Compound 4k
CH_3 (C-11ô)	0.93	27.3	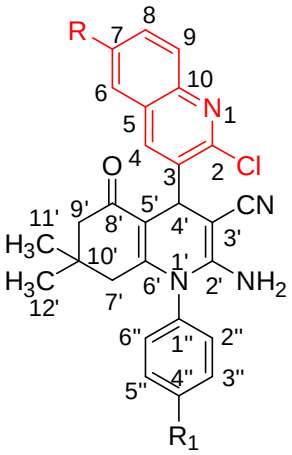
CH_3 (C-12ô)	0.97	29.4	
C-4ô	5.17	17.5	
NH_2	4.18	-	
Ar-H	7.08-8.15	-	
C-2		147.1	
C-3		105.2	
C-4		139.2	
C-5		131.3	
C-6		127.9	
C-7		41.8	
C-8		129.3	
C-9		128.4	
C-10		158.0	
C-2ô		160.6	
C-3ô		60.0	
C-5ô		108.2	
C-6ô		151.6	
C-7ô		55.7	
C-8ô		195.8	
C-9ô		55.6	
C-10ô		18.8	
C-1ôô		134.2	
C-2ôô		120.7	
C-3ôô		109.5	
C-4ôô		151.8	
C-5ôô		115.8	
C-6ôô		122.9	

In the above work, there was no information of any other **NMR** techniques, however, we found a need to unambiguously assign proton and carbon **NMR**, hence we chose two-dimensional nuclear magnetic resonance spectroscopy (**2D NMR**). This is a set of nuclear magnetic resonance spectroscopy **(NMR)** methods which give data plotted in a space defined by two frequency axes rather than one. Types of **2D NMR** include correlation spectroscopy (COSY), *J*-spectroscopy, exchange

spectroscopy (EXSY), and nuclear Overhauser effect spectroscopy (**NOESY**). Two-dimensional **NMR** spectra provide more information about a molecule than one-dimensional NMR spectra and are especially useful in determining the structure of a molecule, particularly for molecules that are too complicated to work with using one-dimensional **NMR** [96].

Since the use of two-dimensional **NMR** for correlating the spectra of coupled heteronuclei was first proposed in 1977, a considerable number of papers have appeared describing different techniques for heteronuclear correlation. The most widely used method produces a two-dimensional spectrum in which one signal appears for each directly bonded carbon-hydrogen pair in a molecule [97]. Recently, Kumar *et. al*. [98] reported the structure elucidation of dispiro substituted benzo[*H*]quinoline compounds using **1D** and **2D NMR** spectroscopy. **Figure 11** shows the particular HMBC correlations.

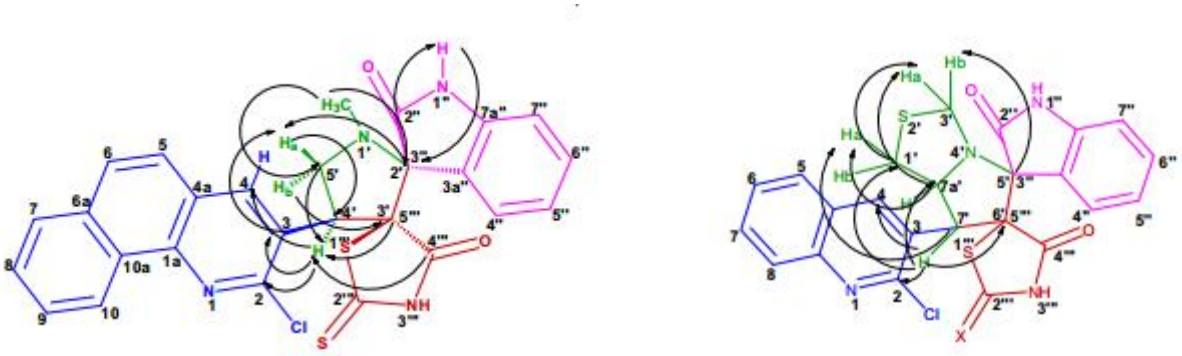

Figure 11: Selected HMBC correlations for dispiro substituted benzo[*H*]quinoline compounds

References

1. P A Wender, S T Handy, D L Wright, Molecular Sieves: From basic research to industrial applications, *Chem. & Ind.* **1997**, 765-773.
2. N N Greewood, A Earnshaw, Chemistry of Elements (2nd Ed.), *Butterworth Heinemann*, **1997**, 540-555.
3. G Abbiati, E M Beccalli, G Broggini, C Zoni, Heterocyclic communications, *Tetrahedron,* 59, **2003**, 9887-9890.
4. L Weber, S Wallbaum. S Broger. The biology-chemistry interface, *Angew. Chem. Int. Ed.* **1994**, 2280-2287.
5. I Ugi, A Domling, M Goebel, W Horl, M Gruber, Combinational chemistry & high throughput screening, *Angew. Chem. Int. Ed.* **1995**, 113-120.
6. R J K Taylor, M Reid, J Foot, S A Raw, Organic syntheses, collective, *Acc. Chem. Res.* 12, **2005**, 66-71.
7. L F Tietze, U Beifuss, Functional Organic Materials: Syntheses, strategies and applications, *Angew. Chem. Int. Ed*. 32, **1993**, 131-135.
8. D Kumar, S J Sanghu, Microwave enhanced, solvent free green protocol for the production of 3,4-dihydropyrimidine-2-(1*H*)-ones using $AlCl_3.6H_2O$ as a catalyst, *Indian J. Chem*. 49, **2010**, 360-362.
9. V Nadaraj, S Selvi, M Abirami, T D Thangadurai, Multi-component and sequential reactions in polymer synthesis, *Res J. Recent. Sci.* 3, **2013**, 370-375.
10. N K Ladani, D C Mungra, M P Patel, Microwave assisted synthesis of novel Hantzsch 1,4-dihydropyridines, acridine-1,8-diones and polyhydroquinolines bearing the tetrazolo[1,5-*a*]quinoline moiety and their antimicrobial activity assessment, *Chin. Chem. Lett*. 22, **2011**, 1407-1410.
11. F F Blicke, Derivatives of thianaphthene, *J. Am. Chem. Soc.,* 70, **1948**, 3768-3773.
12. S G Subramaniapillai, Mannich reaction: A versatile and convenient approach to bioactive skeletons. *J. Chem. Sci.* 125, **2013**, 467-470.
13. S Ramalingam, P Kumar, Multi-component carbonï carbon bond forming Mannich reaction catalyzed by yttriaï zirconia based Lewis acid, *Catal. Commun.* 9, **2008**, 2445-2449.
14. H Pellissie, Asymmetric Domino reactions, *Catalysis Series,* **2013**, 110-115.
15. K Gewald, E Schinke, Cyclization of nitriles as synthetic route to 2- and 3-aminothiophenes, *Ber*. 99, **1966**, 94-100.

16. K Wang, K Dabin, A Domling, Cyanoacetamide MCR III: Three-component Gewald reactions, *J. Comb. Chem*. 12, **2010**, 111-119.
17. T J J Müller, Multicomponent reactions, *Science of Synthesis.* 1, **2004**, 8482-8491.
18. L Umkehrer, Heterocyclic compounds, *Heterocycles*, 73, **2007**, 145-150.
19. S Makarem, A R Fakhari, A A Mohammadi, An efficient method for the preparation of nanosized particles of phthalazine derivatives via one-pot multicomponent reactions, *Analyt. & Bioanalyt. Chem. Res.* 2, **2015**, 85-98.
20. R Lavilla, M Carmen Bernabeu, I Carranco, Dihydropyridine-based multicomponent reactions. Efficient entry into new tetrahydroquinoline systems through Lewis Acid-catalyzed formal [4 + 2] cycloadditions, *Org. Lett*. 5, **2003**, 717-725.
21. A S Trifilenkov, A P Ilyin, V M Kysil, Y B Sandulenko, One pot tandem complexity-generating reaction based on Ugi four component condensation and intramolecular cyclization, *Tetrahedron, 48*, **2007**, 2563-2571.
22. M H F Wilkins, Molecular configuration of nucleic acids, *Science*, 140, **1963**, 941-950.
23. W H Brown, Introduction to Organic chemistry, *Sauders College Publishing*, 4, **1997**, 40-45.
24. M Alizadeh, N Babaki, Zohreh, One-pot solvent-free three-component synthesis of conjugated enaminones containing three alkyl carboxylate groups, *J. Chem*. 64, **2013**, 1115-1119.
25. R Sleath. Synthesis of 7,9-didecarboxymethoxatin(4,5-dihydro-4,5-dioxo-1*H*-pyrrolo[2,3-f]quinoline-2-carboxylic acid) and comparison of its chemical properties with those of methoxatin and analogous *o*-quinones, *J. Chem. Soc*. 107, **1985**, 3328-3330.
26. E Shinagawa, Biochemical and physiological functions of pyrroloquinoline quinone, *Vitamins & Hormones,* 46, **1991**, 229-235.
27. Y Ohshiro, Synthesis and characterization of dimethyl 9,10-dihydro-9,10-dioxobenzo[f] quinoline-2, 4-dicarboxylate. Effect of the pyrrole nucleus on the reactivity of coenzyme, *J. Org. Chem*. 57, **1992**, 4452-4460.
28. G Caeiro, P Magnoux, J M Lopes, Deactivating effect of coke and nitrogen basic compounds, *J. Mol. Catal. Chem*. 249, **2006**, 149-157.
29. A Alizadeh, A simple and efficient approach to the synthesis of highly functionalized benzochromenes, *Tetrahedron*, 59, **2003**, 1289-1292.
30. M M Alam, Synthesis of quinoline-attached furan-2(3*H*)-ones having anti-inflammatory and antibacterial properties with reduced gastro-intestinal toxicity and lipid peroxidation, *J. Serb. Chem. Soc*. 76, **2011**, 1617-1620.
31. T L Gilchrist, Synthesis of aromatic heterocycles, *J. Chem. Soc*. 1, **1999**, 2849-2853.

32. L Ackerman, H K Potukuchi, D Landsberg, R Vicente, Copper-catalyzed ñclickò reaction/direct arylation sequence: modular syntheses of 1,2,3-triazoles, *Org. Lett*. 10, **2008**, 3081-3090.
33. K K Kumar, P S Seenivasan, V Kumar, D T Mohan, Synthesis of quinoline coupled [1,2,3]-triazoles as a promising class of anti-tuberculosis agents, *Carbohydr. Res.* 346, **2011**, 2063-2066.
34. H Walba, R Isensee. Acidity constants of some arylimidazoles and their cations, *J. Org. Chem*. 26, **1961**, 2789-2793.
35. B Jiang, X Wang, F Shi, S J Tu, T Ai, A Ballew, G Li, Microwave enabled umpulong mechanism based rapid and efficient four- and six-component domino formations of 2-(2Ñjzaaryl)imidazoles and anti-1,2-diarylethylbenzamides, *J. Org. Chem.* 74, **2009**, 9489-9493.
36. N C Desai, A S Maheta, K M Rajpara, V V Joshi, H V Vaghani, H M Satodiya, Green synthesis of novel quinoline based imidazole derivatives and evaluation of their antimicrobial activity, *J. Saudi Chem. Soc.* 18, **2014**, 971-982.
37. L David, M Michael, Loose-leaf version for principles of biochemistry (6^{th} Ed.), *W. H. Freeman,* **2012**, 985-100.
38. V Sridar, Microwave assisted one-pot synthesis of substituted tetrahydrocarbozole and 8,9,10,11 tetrahydro-7*H*-Pyrido (9) carbazoles, *Indian J. Chem*. 36, **1997**, 86-90.
39. R Linnel, Dissociation constants of 2-substituted pyridines, *J. Org. Chem.* 25, **1960**, 290-295.
40. B Jiang, W J Hao, X Wang, F Shi, S J Tu, Diversity-oriented synthesis of Kröhnke pyridines, *J. Comb. Chem*. 11, **2009**, 846-850.
41. M Avalos, R Babiano, F R Clemente, J L Jimenez, Application of microwave heating techniques for dry organic reactions, *J. Org. Chem*. 64, **1999**, 6297-6300.
42. J C Anderson, D G Lindsay, C B Reese, The reaction between 2,3-dihydrofuran and dihalocarbenes: An attempted 2*H*-pyran synthesis, *Tetrahedron,* 20, **1964**, 2091-2098.
43. B M Laloo, H Mecadon, M R Rohman , I Kharbangar, I Kharkongor, M Rajbangshi, R Nongkhlaw, B Myrboh, Reaction of selenium dioxide with aromatic ketones in the presence of boron triflouride etherate: a protocol for the synthesis of triarylethanones., *J. Org. Chem.* 6, **2012**, 707-710.
44. Ugi, Multicomponent reactions in organic chemistry, *Endeavour*, 18, **1994**, 115-120.
45. B Suresh, Y T Reddyb, J V Madhava, 3-[Benzimidazo- and 3-[benzothiadiazoleimidazo-(1,2-c)quinazolin-5-yl]-2*H*-chromene-2-ones as potent antimicrobial agents, *Bioorg. & Med. Chem.* 21, **2011**, 524-528.
46. J P Michael. Green chemistry approach to synthesis of some new trifluoromethyl containing tetrahydropyrimidines under solvent free conditions, *J. Comb. Chem.* 11, **2007**, 612-618.

47. B Gabriele, R Mancuso, G Salerno, Novel and convenient synthesis of substituted quinolines by copper- or palladium-catalyzed cyclodehydration of 1-(2-Aminoaryl)-2-yn-1-ols, *J. Org. Chem*. 72, **2007**, 6873-6877.
48. G Roma, M D Braccio, G Grossi, 1,8-Naphthyridines IV. 9-substituted *N*,*N*-dialkyl-5-(alkylamino or cycloalkylamino) [1,2,4]triazolo[4,3-a][1,8]naphthyridine-6-carboxamides, new compounds with anti-aggressive and potent anti-inflammatory activities, *Eur. J. Med. Chem.* 35, **2000**, 1021-1025.
49. V V Kouznetsov, Recent synthetic developments in a powerful imino Dielsï Alder reaction (Povarov reaction): Application to the synthesis of *N*-polyheterocycles and related alkaloids, *Tetrahedron.* 65, **2009**, 2721-2726.
50. D Anju, J P Singh, J Neetu, R Renu, Microwave assisted synthesis, spectral studies and antibacterial activity of 1,5-benzodiazepines derivatives on a solid surface, *Asian J. Chem.* 24, **2012**, 5914-5916.
51. C G Yan, X M Cai, Q F Wang, A novel four component one-pot access to 4,6-diaryl-2-pyridinone and 4-aryl-5,6,7,8-tetrahydro-2-quinolinones, *Lett. Org. Chem*. 5, **2008**, 282-285.
52. X L Zhang, S Shang, X Liu, Solvent-free liquid-phase synthesis of polyhydroquinoline derivatives under microwave irradiation, *Arkivoc*, 13, **2007**, 79-82.
53. H R P Naik, T Aravinda, T. Synthesis, characterization, and photoactivated DNA cleavage by copper (II)/cobalt (II) mediated macrocyclic complexes, *Nucleosides, Nucleotides, Nucleic Acids*, 29, **2010**, 39-44.
54. T J Silhavy1, D Kahne, S Walker, The bacterial cell envelope, *CHS Prosectives,* 44, **2010**, 423-428.
55. M Kidwai, K R Bhushan, P Sapra. Alumina-supported synthesis of antibacterial quinolines using microwaves, *Bioorg. & Med. Chem.* 8, **2000**, 69-74.
56. M Kidwai, P Sapra, K Ranjan, Fluorination of 2-chloroquinoline-3-formaldehyde under microwave irradiation, *Indian. J. Chem*. 38. **1999**, 114-120.
57. P M Fresneda, P Molina and S Delgado, A divergent approach to cryptotackieine and cryptosanguinolentine alkaloids, *Tetrahedron,* 40, **1999**, 7275-7279.
58. B Carboni, L Monnier, Recent developments in the chemistry of amine- and phosphine-boranes, *Tetrahedron,* 55, **1999**, 1197-1199.
59. R A De Silva, S Santra, P R Andreana, A Tandem one-pot, microwave-assisted synthesis of regiochemically differentiated 1,2,4,5-tetrahydro-1,4-benzodiazepin-3-ones, *Org. Lett.* 10, **2008**, 4541-4545.

60. J D Watson, F H C Crick, The complementary structure of deoxyribonucleic acid, *The Royal Society*, 171, **1954**, 964-970.

61. P G Corrie, G Pippa. Cytotoxic chemotherapy: clinical aspects, *Medicine,* 36, **2008**, 24-28.

62. L S Goodman, M M Wintrobe, The effect of nitrogen mustards on proliferating embryonic tissues, *Cancer Res*. 7, **1947**, 49-55.

63. L H Hurley, DNA and its associated processes as targets for cancer therapy, *Nature Reviews Cancer*, 2, **2000**, 188-193.

64. V. Ramesh, Synthesis and biological evaluation of new rhodanine analogues bearing 2-chloroquinoline and benzo[*H*]quinoline scaffolds as anticancer agents, *Eur. J. Med. Chem.* 83, **2014**, 569-572.

65. M Kidwai, S Saxena, R Mohan, Environmentally benign synthesis of benzopyranopyrimidines, *Russian J. Org. Chem.* 42, **2006**, 52-60.

66. N K Ladani, M P Patel, R G Patel, An efficient three component one-pot synthesis of some new octahydroquinazolinone derivatives and investigation of their antimicrobial activities, *Arkivoc,* 6, **2009**, 292-295.

67. M Kidwai, S Saxena, M K R Khan, S S Thukral, Synthesis of 4-aryl-7,7-dimethyl-1,2,3,4,5,6,7,8-octahydroquinazoline-2-one/thione-5-one derivatives and evaluation as antibacterial, *Eur. J. Med. Chem.* 40, **2005**, 816-820.

68. H T Cao, R Grée, Diethyl azodicarboxylate-(cat)$ZnBr_2$ an efficient system for the oxidation of alcohols to carbonyl compounds, *Tetrahedron Lett. 50,* **2009**, 1493-1498.

69. A Abeer, M Daneshtalab, Nonclassical biological activities of quinolone derivatives, *J. Pharm. Scie*. 15, **2011**, 52-57.

70. L S Lerman, Acridine mutagens and DNA structure, *J. Cell. Comp. Physiol.* 1, **1964**, 64-67.

71. E Hirschberg, Patterns of response of animal tumors to anticancer agents. A systematic analysis of the literature in experimental cancer chemotherapy, *Cancer Res*. 23, **1963**, 521-525.

72. T Lengauer, M Rarey, Computational methods for biomolecular docking, *Biol.* 6, **1996**, 402-410.

73. N Sharath, H S B Naik, V Kumar B, J Hoskeri, Synthesis, antibacterial, molecular docking, DNA binding and photonuclease activity of quinoline isoxazoles, *Der Pharmacia Sinica*, 3, **2012**, 254-257.

74. S Sharma, A Basu, K R Agrawal, Pharmacophore modeling and docking studies on some nonpeptide-based caspase-3 inhibitors, *Biomed Res Int.* 2013, **2013**, 306-309.

75. B Fisher, R P Harvey, Champe, P C, Microbiology (Chapter 33*), Lippincott Williams & Wilkins*, **2007**, 367-375.

76. J K Fredrickson, Geomicrobiology of high-level nuclear waste-contaminated vadose sediments at the Hanford site, Washington State*, Applied & Environ. Microbio.* 70, **2004**, 4230-4235.
77. W B Whitman, Prokaryotes: The unseen majority*, Scie. Amer.* 95, **1998**, 6578-6580.
78. C M Hogan, C J Cleverland, Linking environmental nutrient enrichment and disease emergence in humans and wildlife*, Ecological Applications, 2,* **2010**, 20-27.
79. S H Gillespie, Evolution of drug resistance in *Mycobacterium tuberculosis*: Clinical and molecular perspective, *Antimicrob. Agents Chemother.* 46, **2002**, 267-270.
80. P M Sivakumar, D Mukesh, Synthesis, antimycobacterial activity evaluation and QSAR studies of chalcone derivatives, *Bioorg. & Med. Chem. Lett*. 17, **2007**, 1695-1698.
81. L A Mitscher, M S Bathala, G W Clark, J L Beal, Antimicrobial agents from higher plants. The quaternary alkaloids of Ptelea trifoliate, *Lloydia*, 38, **1975**, 109-112.
82. A K Sadana, Y Mirza, Hypervalent iodine mediated synthesis of 1-aryl/hetryl-1,2,4-triazolo[4,3-*a*] pyridines and 1-aryl/hetryl-5-methyl-1,2,4-triazolo[4,3-*a*]quinolines as antibacterial agents, *Eur. J. Med. Chem*. 38, **2003**, 533-537.
83. A M Emmerson, A M Jones, The quinolones: decades of development and use, *J. Antimicrob. Chemother.* 51, **2003**, 13-20.
84. R H Meyboom, Thrombocytopenia induced by nalidixic acid, *British Med. J.* 289, **1984**, 962-969.
85. M A Cohen, M D Huband, G B Mailloux, S L Yoder, G E Roland, C L Heifetz, In vitro antibacterial activities of the fluoroquinolones, *Diagnosis and Microbiology of Infectious Diseases*, 14, **1991**, 245-250.
86. M Buchbinder, J Webb, L Anderson, W McCabe, Laboratory studies and clinical pharmacology of nalidixic acid, antimicrob. *Agents Chemother.* 6, **1962**, 308-321.
87. A R Parikh, J R Patel, A V Dbaria, B P Kansagra, Synthesis of cynopyridines and cynopyrans bearing 2-chloro-6-bromoquinoline nucleus as potential antimicrobial and anticancer agents. *Indian J. Heterocycl. Chem*. 12, **2003**, 237-245.
88. P B Miniyar, M Barmade, Synthesis and biological evaluation of 1-(5-(2-chloroquinolin-3-yl)-3-phenyl-1*H*-pyrazol-1-yl)ethanone derivatives as potential antimicrobial agents, *J. Saudi Chem. Soc.* 44, **2014**, 221-228.
89. A A Bekhit, O A El-Sayed, E Aboulmag, Tetrazolo[1,5-*a*]quinoline as a potential promising new scaffold for the synthesis of novel anti-inflammatory and antibacterial agents, *Eur. J. Med. Chem*. 39, **2004**, 249-256.

90. Nirav K. Shaha, Manish P. Patela & Ranjan G. Patel, One-pot, multicomponent condensation reaction in neutral conditions: Synthesis, characterization, and biological studies of fused thiazolo[2,3-*b*]quinazolinone derivatives, *Phosphorus, Sulfur, and Silicon and the Related Elements,* 184, **2009**, 2719-2722.
91. M Kidwai, S Saxena, M K Rahman Khan, Aqua mediated synthesis of substituted 2-amino-4*H*-chromenes and in vitro study as antibacterial agents, *Bioorg*. *Med. Chem. Lett.* 15, **2005**, 4295-4299.
92. A M Rahatgaonkar, S S Dave, Syntheses and anti-microbial evaluation of new quinoline scaffold derived pyrimidine derivatives, *Arabian J. Chem.* 2, **2011**, 10-19.
93. R M Silverstein, G C Bassler, T C Morrill, Spectrometric identification of organic compounds, *Wiley Chichester*, **1991**, 419-423.
94. K Downard, Francis William Aston: the man behind the mass spectrograph, *Eur. J.Mass Spec.* 13, **2007**, 177-178.
95. J P Nirmal, M P Patel, R M Patel, Microwave-assisted synthesis of some new biquinoline compounds catalyzed by DMAP and their biological activities, *Indian J. Chem*. 48, **2009**, 712-718.
96. W P Bartholdi, R R Ernst, Two-dimensional spectroscopy. Application to nuclear magnetic resonance, *J. Chemical Physics*, 64, **1976**, 2229-2238.
97. G A Morris, An improved method for heteronuclear chemical shift correlation by two-dimensional NMR, *J. Magnetic Resonance*, 42, **1981**, 501-510.
98. G S Kumar, R Satheeshkumar, W Kaminsky, J Platts, K J R Prasad, A facile regioselective 1,3-dipolar cycloaddition protocol for the synthesis of new class of quinolinyl dispiro heterocycles, *Tetrahedron*, 55, **2014**, 5475-5480.

Chapter Three: Synthesis of Poly-Functional Dihydropyridine Quinoline Derivatives

3.1. Introduction

Multi-component reactions are convergent reactions, in which three or more starting materials react to form a product, where basically all or most of the atoms contribute to the newly formed product. In MCRs, a product is assembled according to a cascade of elementary chemical reactions. Thus, there is a network of reaction equilibria, which all finally flow into an irreversible step yielding the product. The challenge is to conduct a MCR in such a way that the network of pre-equilibrated reactions channel into the main product and do not yield side products. The result is clearly dependent on the reaction conditions, i.e. solvent, temperature, catalyst, concentration, the type of starting materials and functional groups. Such considerations are of particular importance in connection with the design and discovery of novel MCRs.

MCRs have become a high profile reaction since it could be used to produce important scaffolds for pharmaceutical applications. Hence our laboratory has embarked on MCRs to achieve synthetic targets in an ideal and expeditious way. We decided to focus on poly-functionalised dihydropyridine type molecules containing a quinoline moiety with the intention of improving the biological activity of the final product; as mentioned earlier in the thesis, quinoline derivatives display a wide range of activities such as anti-malaria, anti-cancer, anti-fungicidal, anti-bacteria etc. Furthermore we wanted to increase our research synthetic activity in terms of a Green approach. Since our research plan was to use a simple quinoline derivative as one of the substrates in a MCR, we therefore decided to start by synthesizing a chloro formyl quinoline derivative via the Vilsmeir-Haack reaction; [1] the protocol is well established in our laboratory. This reaction and mechanism is presented in this chapter. Also more importantly, we report a clean and efficient method for the synthesis of poly-functionalized dihydropyridine quinoline derivatives in excellent yields through a one-pot condensation and cyclisation containing four substrates viz., chloro formyl quinoline, malononitrile, aromatic amine and dimethyl acetylenedicarboxylate in the presence of a catalytic amount of triethylamine. This reaction is presented in **Scheme 49** (page 50).

3.2. Experimental

3.2.1. Instrumental

Melting points were determined on a Stuart Digital apparatus and were corrected and expressed in degree Celsius (ºC). The **IR** spectra were recorded on either PerkinElmer 537 spectrophotometer or a Shimadzu-8201 FT instrument, using **ATR** disc and the absorption frequencies were expressed in reciprocal centimeters (cm^{-1}). The mass spectra were recorded on either PerkinElmer **GCMS** or **TOF-MS** and the molecular weight expressed in atomic mass units. The optical activity was recorded on a Bellingham + Stanley Model D Polarimeter using a sodium lamp and the specific rotation expressed in degrees. The **^{1}H NMR, ^{13}C NMR** and **^{19}F NMR, COSY, NOESY, HSQC** and **HMBC** spectra were recorded on either Bruker (600 MHz) or Bruker (400 MHz) spectrophotometers in $CDCl_3$ or DMSO using tetramethylsilane (TMS) as an internal reference. The chemical shifts were quoted in parts per million (ppm). The following abbreviations were used:

s ï singlet

d ï doublet

t ï triplet

q ï quartet

m ï multiplet

bs ï broad singlet band

J ï spin-spin splitting constant in Hertz (Hz)

3.2.2. Methods and Materials

Solvents and commercially available reagents such as aniline, *o*-anisidine, *m*-toluidine, phosphoryloxychloride, fluoroaniline, aniline hydrochloride, dimethyl formamide, petroleum ether, ethanol, ethyl acetate, hexane and methanol were purchased from Lasec S.A, Aldrin, Fluka and Merck. These reagents and solvents were used without further purification.

Thin Layer Chromatography (TLC) was performed using TLC plates. When conducting TLC analysis, a pencil line was drawn 2 cm above and below the rim of a pre-cut TLC plate and approximately 10 εL of a solution of the crude mixture was placed on the bottom line and air dried. The mobile phase consisting of petroleum ether and ethyl acetate (4:1, v/v) was placed in a TLC chamber, closed and

allowed to equilibrate until the atmosphere was saturated with the solvent vapour. The TLC plate was placed gently in the chamber and allowed to run until the mobile phase reached the top pencil mark. It was removed, air dried and viewed under the UV lamp followed by staining in an iodine chamber containing sea sand and iodine crystals.

When conducting column chromatography purification, the pre-weighed crude synthesized mixture was dissolved in a minimum amount of chloroform and about 100 mg of silica gel was used. The beaker with the mixture was placed on a boiling water bath until the solvent evaporated and only a dry powder remained. The dry powder was transferred into a glass column and petroleum ether or hexane was added and elution process started. Equal sized fractions were collected sequentially and carefully labelled for further analyses. The polarity of the mobile phase was changed by varying the composition of the solvent mixture. All fractions were analyzed by TLC and similar fractions were combined.

3.2.2.1. Synthesis of the Starting Compound 2-Chloro-3-Formyl Quinoline

Procedure for the synthesis of 2-chloro-3-formyl quinoline (64). Dry DMF (3 mmol, 35 mL) was cooled to 0ºC in a þask equipped with a drying tube and then $POCl_3$ (12 mmol, 168.2 mL) was added drop-wise with stirring. To this solution, acetanilide (1 mmol, 20.27 g) was added in small portions and after 25-30 minutes the reaction mixture was heated for 24 hours on a boiling water bath. The reaction mixture was poured into ice water and stirred for 30 minutes. The work-up was performed with aqueous NaOH to form a precipitate, to hydrolyse the imine salt and remove any acid formed. The solid was filtered, dried and purified from ethyl acetate to give 2-chloro-3-formyl quinoline in high yield (90 %).

3.2.2.2. Synthesis of Poly-Functionalised Dihydropyridine Quinoline Derivatives by Multi Component Reactions

Procedure for the synthesis of A1-A8: In a round bottom flask, a mixture of 2-chloro-3-formyl quinoline (2 mmol, 0.3831 g), malononitrile (2 mmol, 0.144 g) and triethylamine (2 mmol, 0.202 g), in 20 mL ethanol, was stirred at room temperature for thirty minutes. Then a solution of arylamine (2 mmol, 0.2 mL) and dimethyl acetylenedicarboxylate (2 mmol, 0.284 g), in 25 mL ethanol, was added. The whole solution was stirred at room temperature for an additional ten hours. In most cases the resulting precipitates were collected by filtration and washed with cold alcohol and purified by column chromatography (50:50 Petroleum ether: Ethyl acetate).

3.3. Results and Discussion

The focus of this research was the synthesis of novel compounds, especially compounds having proper functional groups to display potential biological activities. Since heterocycles containing quinoline are reported to improve the biological activity of organic compounds, in this research investigation we have synthesized 8 novel poly-functionalised dihydropyridine quinoline derivatives (**A1-A8)**, presented in **Figure 12**, and evaluated their biological potential as described in **Chapter 4.** Since we decided to use MCR, our first goal was to synthesise a formyl quinoline derivative which could be used as one of the substrates for the one pot MCR. The other 3 types of substrates, viz malononitrile, aniline derivatives and dimethyl acetylenedicarboxylate were readily available and purchased.

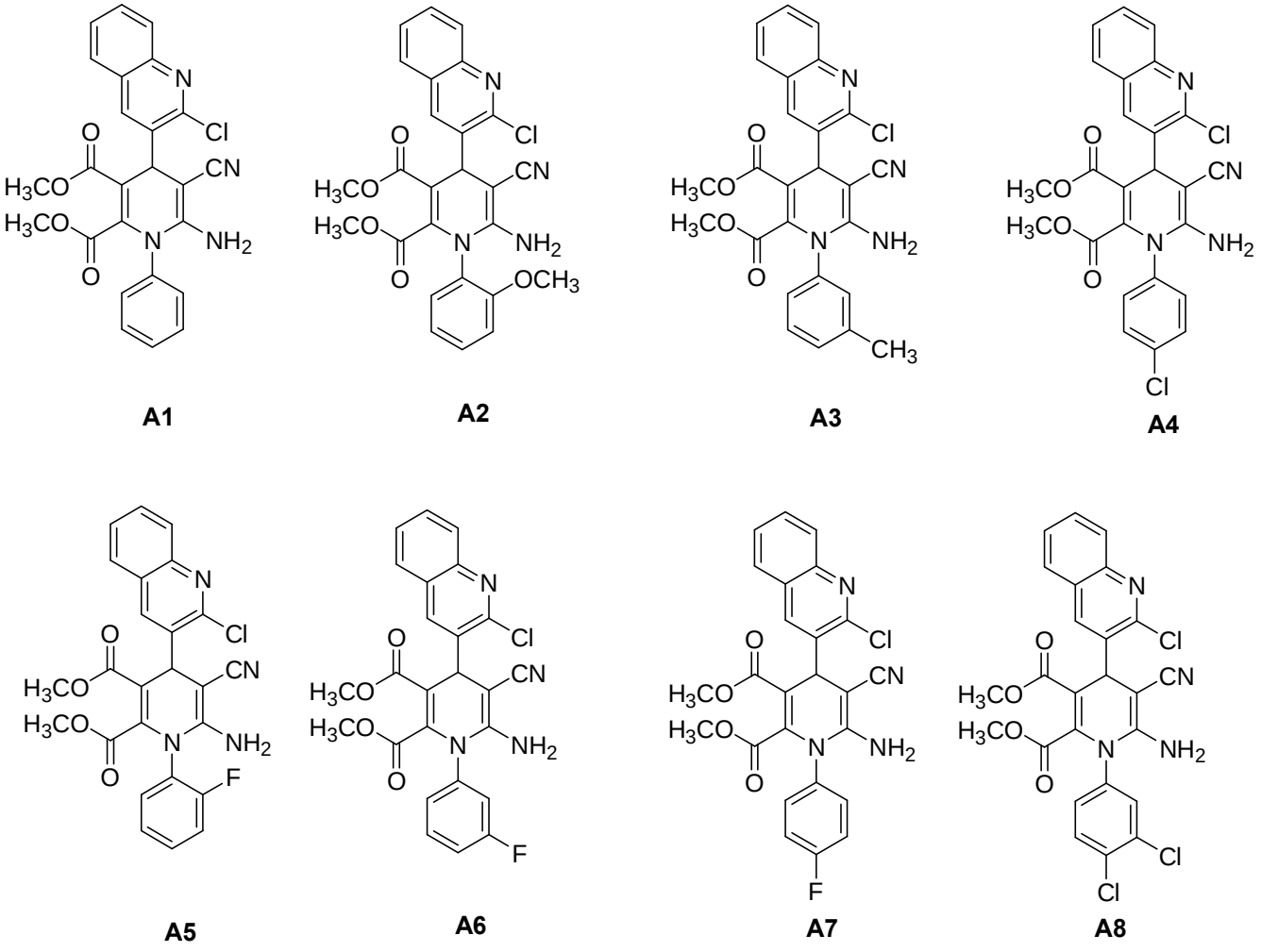

Figure 12: Novel poly-functionalised dihydropyridine quinoline derivatives

The first step of our research plan was to synthesize the formyl quinoline derivative using the Vilsmeier-Haack reaction. The Vilsmeier-Haack reaction is a standard procedure in our laboratory; it is used to synthesize new derivatives for a large variety of synthetic transformations. It finds its application in

formylation, cyclohalo-addition, cyclisation and ring annulations. This organic reaction is used to transfer an electron-rich aromatic ring to an aryl aldehyde by the use of DMF and $POCl_3$ (**Scheme 45**).

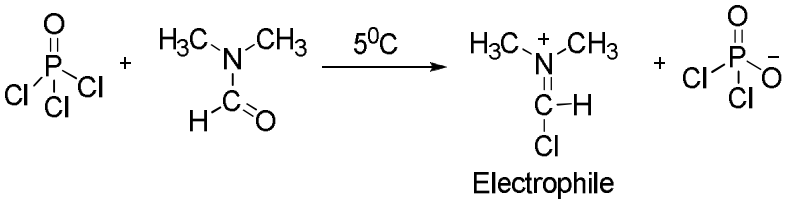

Scheme 44: The reaction of DMF and $POCl_3$

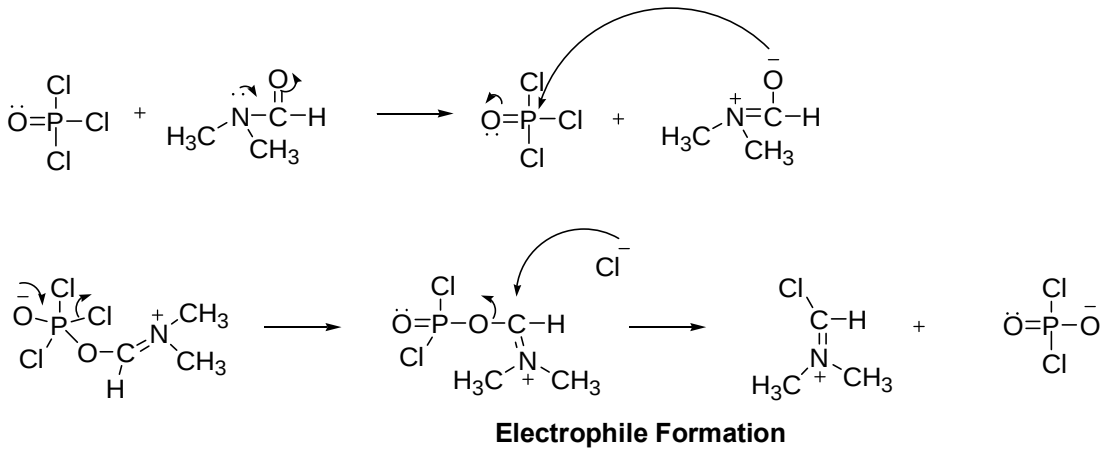

Scheme 45: The reaction mechanism illustrating the formation of an electrophile [1].

3.3.1. Synthesis of 2-Chloro-3-Formyl Quinoline

2-Chloro-3-formyl quinoline was synthesized from *N*-phenylacetamide via the Vilsmeier-Haack reaction. The reaction is presented in **Scheme 46** and **Scheme 47** (page 47) represents a proposed mechanism.

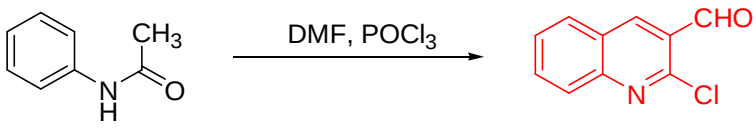

Scheme 46: Synthesis of 2-chloro-3-formyl quinoline

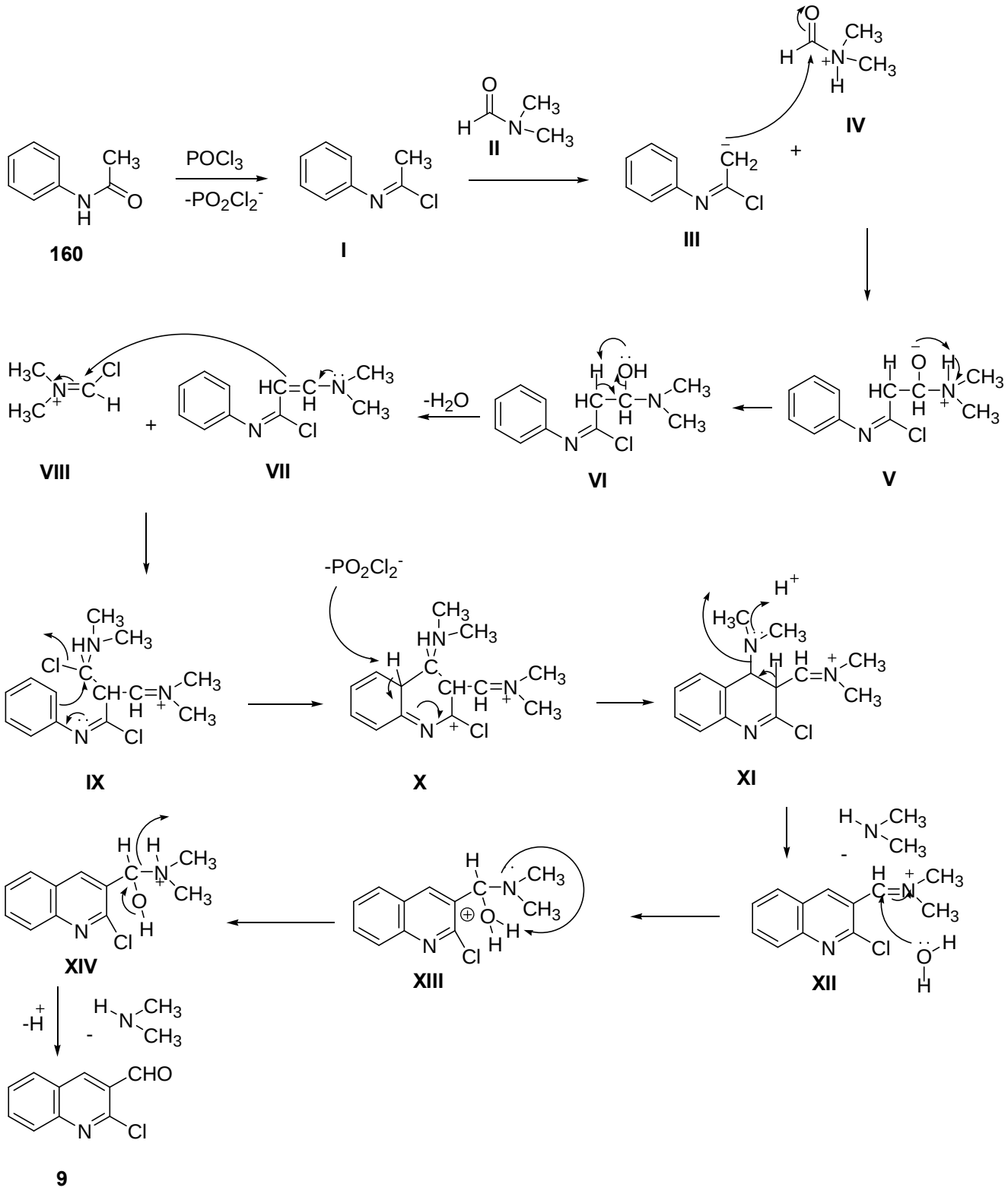

Scheme 47: A possible reaction mechanism for 2-chloro-3-formyl quinoline [2]

The mechanism starts by chlorination of the amide group (**160**) to form an intermediate chloro imine **(I)** with a loss of PO_2Cl_2. DMF (**II**) acts as a base and removes a proton from **I** to form a nucleophilic intermediate (**III**) and a quaternary ammonium species **(IV)**. These two intermediates

undergo an addition reaction to produce an intermediate **V** which undergoes subsequent intramolecular rearrangement and Knoevenagel condensation to form an enamine **VII**. The lone pair electrons on the nitrogen (**VII**) shifts towards the double bonded carbon, which results to a high electron density on the carbon thereby causing it to attack **VIII** to produce an intermediate **IX**. The latter undergoes intramolecular cyclisation and aromaticity to produce **17**.

The identity of 2-chloro-3-formyl quinoline was analysed by **IR**, **^{1}H NMR** and **^{13}C NMR** spectroscopy (**Table 2**) and confirmed by literature [3]. The **^{1}H NMR** spectrum in **Figure 26** (Appendix 1, page 86) showed the aldehydic proton (CHO) at ŭ 10.55, the aromatic protons appeared as singlet, doublet, doublet, triplet and triplet at ŭ 8.74, 7.93, 7.88, 7.87 and 7.66, respectively. The **^{13}C NMR** spectrum **Figure 27** (Appendix 2, page 87) showed the aldehydic carbon at ŭ 189.1. The remaining nine carbons appeared at ŭ 140.27-77.07. The **IR** spectrum **Figure 28** (Appendix 3, page 88) showed the main signals at 1685 cm^{-1} and 940 cm^{-1} for C=O and C-Cl, respectively.

Table 2: ^{1}H NMR and ^{13}C NMR data of 2-chloro-formylquinoline

Position	ŭ ^{13}C (ppm)	ŭ ^{1}H (ppm)
C_2	150.0	-
C_3	128.6	-
$C_{3'}$	189.1	10.55 (s, 1H, CHO)
C_4	140.2	8.74 (s, 1H, Ar)
C_5	126.1	-
C_6	129.7	7.88 (d, *J* = 8.1 Hz, 1H, Ar)
C_7	126.3	7.66 (t, 1H, *J* = 7.2 Hz, 1H, Ar)
C_8	133.6	7.87 (t, 1H, *J* = 7.2 Hz, 1H, Ar)
C_9	126.5	7.93 (d, 1H, *J* = 7.7 Hz, 1H, Ar)
C_{10}	149.5	-
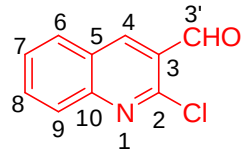		

3.3.2. Synthesis of Quinoline Derivatives by Multi Component Reactions

A mixture of 2-chloro-3-formylquinoline **(17)**, malononitrile **(40)**, arylamine **(19)** and dimethyl acetylenedicarboxylate **(161)** was used to synthesize quinoline derivatives. Different aromatic amines **(A1a-A8a)**, (**Figure 13)** were used. The mechanism for the synthesis of compounds **A1-A8** is presented in **Scheme 49** (page 50). **Table 3** shows the physicochemical data for synthesized quinoline derivatives.

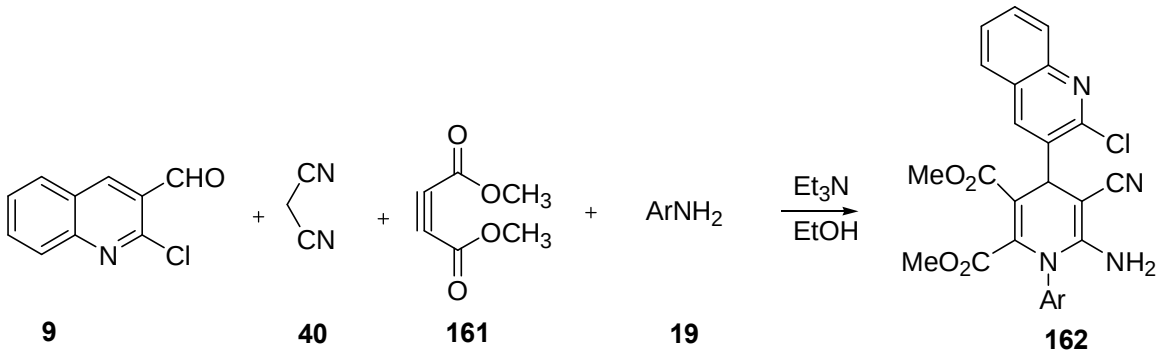

9 **40** **161** **19** **162**

Scheme 48: General reaction for the synthesis of A1-A8.

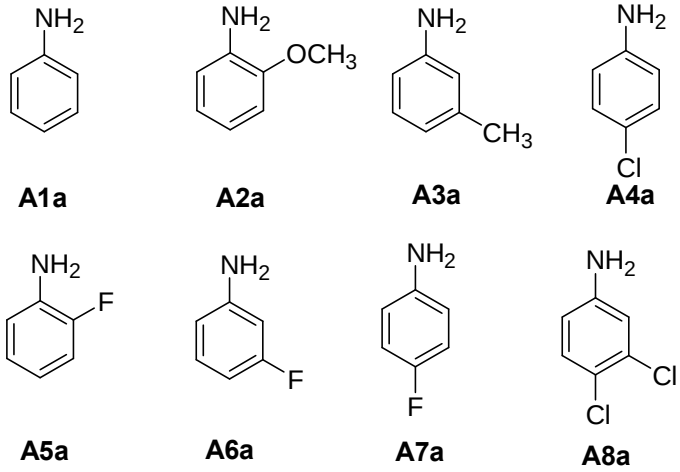

A1a **A2a** **A3a** **A4a**

A5a **A6a** **A7a** **A8a**

Figure 13: Aromatic amines A1a-A8a

Table 3: Physicochemical data for quinoline derivatives

Compound	Ar	%Yield	Melting point(°C)
A1	C_6H_4	**87**	**275-276**
A2	*o*- $OCH_3C_6H_4$	**40**	**263-265**
A3	*m*-$CH_3C_6H_4$	**73**	**237-238**
A4	*p*-ClC_6H_4	**79**	**287-289**
A5	*o*-FC_6H_4	**64**	**247-248**
A6	*m*-FC_6H_4	**31**	**269-271**
A7	*p*-FC_6H_4	**60**	**253-254**
A8	*m,p*-ClC_6H_4	**72**	**280-282**

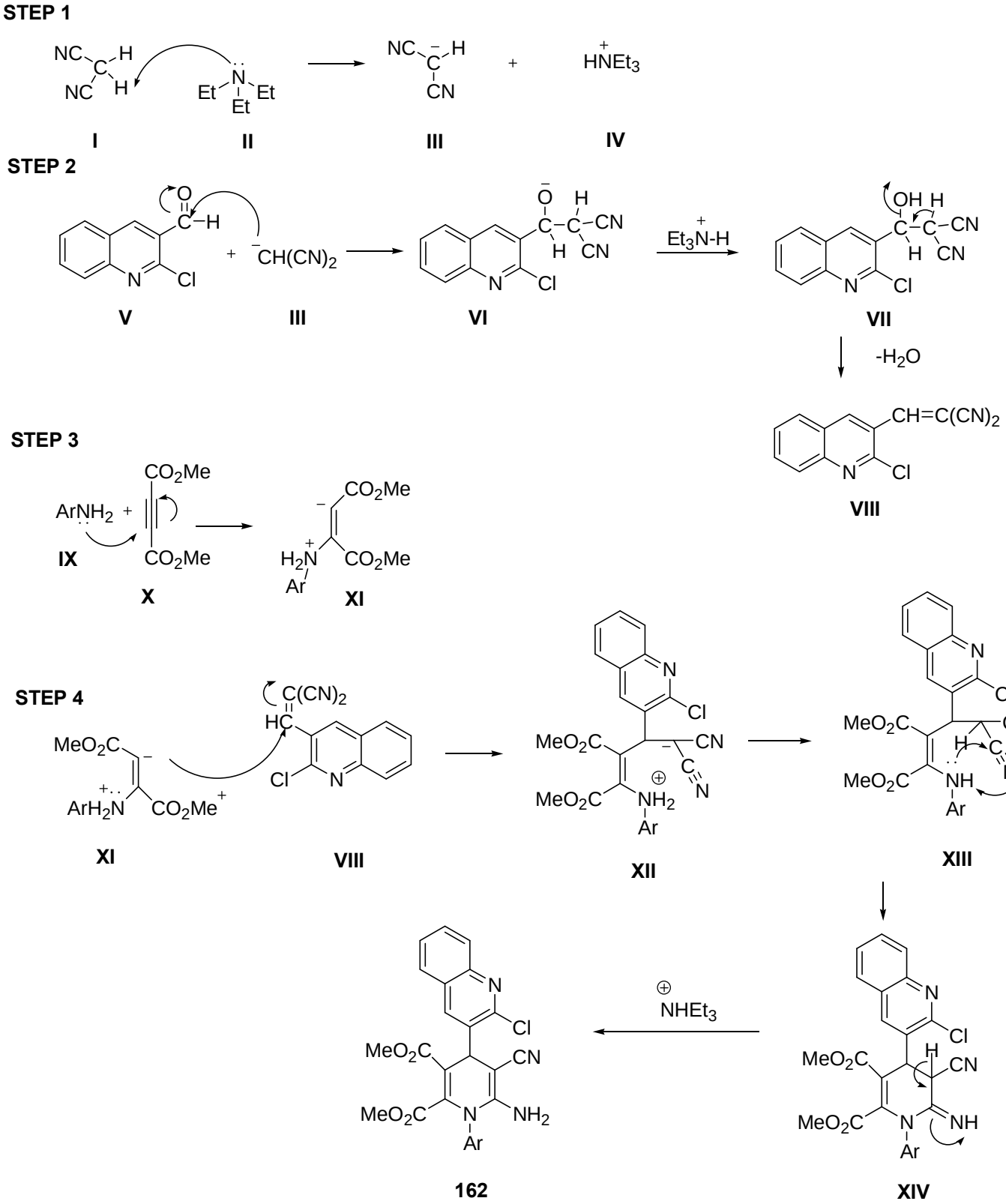

Scheme 49: The postulated reaction mechanism for the synthesised poly-functionalised dihydropyridine quinoline derivatives

In **step 1**, the acidic proton from malononitrile **(I)** is abstracted by a weak base triethylamine **(II)** to form a nucleophile **(III)** and a quaternary ammonium species **(IV)**. In **step 2**, **III** attacks the aldehydic functionality in **V** to produce an addition intermediate **VI**. This is followed by protonation and dehydration to produce **VII** and **VIII**, respectively. In **step 3**, hydroamination takes place when the lone pair of electrons on aniline **(IX)** attacks and breaks the triple bond in acetylenedicarboxylate **(X)** to form an intermediate **XI**. In **step 4**, **XI** attacks the alkenic functionality in **VIII** to produce an intermediate **XII** which further undergoes intramolecular rearrangement and cyclisation to form the final product **(162)**.

The identity of all the compounds (**A1- A8**) was confirmed by analysing the spectral data obtained from **IR**, **^{1}H NMR** and **^{13}C NMR**. All the spectra were well resolved. We selected **A1** as the template and characterised the structure fully with the aid of **2D NMR** techniques especially **HSQC**, **HMBC**, **COSY** and **NOESY** which led to the unambiguous assigning of all protons and carbons. We used the characterization of **A1** as a template to elucidate the other 7 derivatives. Hence **2D NMR** was performed on **A1** and the chemical shifts were unambiguously assigned. Furthermore, mass spectroscopy analysis was performed on, **A1**, **A2**, **A3, A4**, **A6, A7** and **A8** whilst **^{19}F NMR** was performed on **A6** and **A7**. As a typical example the optical activity of **A1** was measured using light having a wavelength of 589 nm.

The **IR** spectra of **A1-A8** exhibited an absorption band around 1748-1652 cm^{-1} which was assigned to C=O stretch whilst 1105-1153 and 932-778 cm^{-1} were assigned as the C-Cl and C-F stretch for the chloro and fluoro derivatives, respectively. The characteristic absorption bands for **A1-A8** were observed in the range 3449-3309 cm^{-1} and 3369-3218 cm^{-1} corresponding to the asymmetric and symmetric stretching of the NH_2 group whilst the CN stretch was observed at 2185-2171 cm^{-1}.

The **^{1}H NMR** spectrum of **A1**, presented in **Figure 29** (Appendix 4, page 89), shows singlets at ŭ 3.44 and ŭ 3.51 for two acetoxy groups (H-9', H-10'). The singlets at ŭ 4.13 and ŭ 5.36 are assigned to the amino (NH_2) and aliphatic proton (H-4') on the dihydropyridine ring, respectively. Ten aromatic protons were observed and unambiguously assigned by using **2D NMR** techniques. The chemical shifts, spin multiplicities and coupling constants (in Hertz) were assigned as: ŭ 8.14 (H-4, s); ŭ 7.85 (d, H-6, 8.1); ŭ 7.71 (t, H-7, 7.6); ŭ 7.55 (t, H-8, 7.4); ŭ 8.02 (d, H-9, 8.4); ŭ 7.39 (m, H-2"); ŭ 7.52 (m, H-3"); ŭ 7.38 (m, H-4", 7.4); ŭ 7.52 (m, H-5") and ŭ 7.39 (m, H-6"). The expanded **^{1}H NMR** spectrum is presented in **Figure 30** (Appendix 5, page 90).

The **COSY** spectrum, presented in **Figure 31** (Appendix 6, page 91), shows H-9 has a strong coupling with H-8 but a weaker coupling with H-7. The corresponding carbon resonances of H-7, H-8 and H-9 appeared at ŭ 130.1, 130.8 and 130.4, respectively and the absence of correlation between the

carbon to the amino protons confirm the assignment of the NH_2, according to the **HSQC** spectrum, presented in **Figure 32** (Appendix 7, page 92). The **NOESY** spectrum, presented in **Figure 33** (Appendix 8, page 93), showed the coupling of H-9 to H-8; H-6 is coupled to H-7 and H-8 whilst H-7 is coupled to H-6 and H-8. Furthermore, the **COSY** spectrum shows a strong coupling between H-6 and H-7 and between H-7 and H-8 whilst a weak coupling is observed between H-7 and H-9. Also H-4 lacked any coupling signals. Both H-4 and H-6 showed the **HMBC** correlations to C-2, C-4' and C-5, presented in **Figure 34** (Appendix 9, page 94), at ŭ 150.9, 120.3 and 134.9, respectively. The ^{4}J correlations at H-4' to C-5 and H-4' to C-8, ^{5}J correlation at H-6 to C-4' were also observed. The H-6" proton resonance shows a **COSY** correlation to H-5" and was confirmed by **HSQC** correlations between C-6" and C-5" occurring at ŭ 128.0 and 134.9, respectively. **Figure 14** shows the other selected **HMBC** correlations for **A1**.

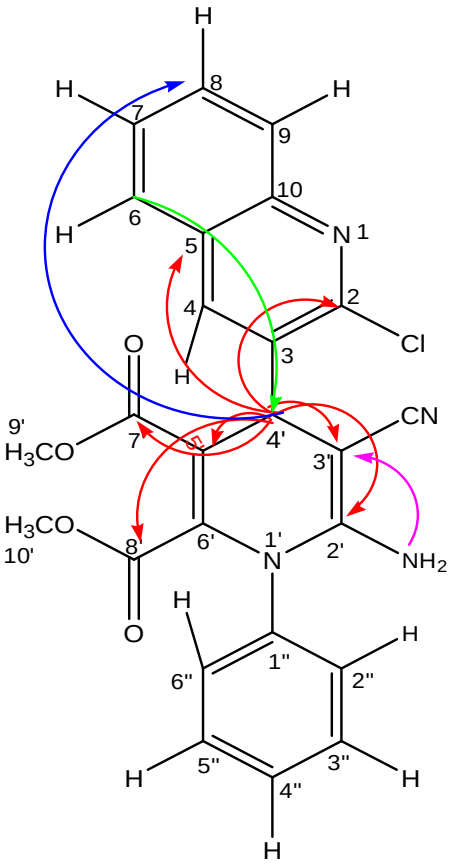

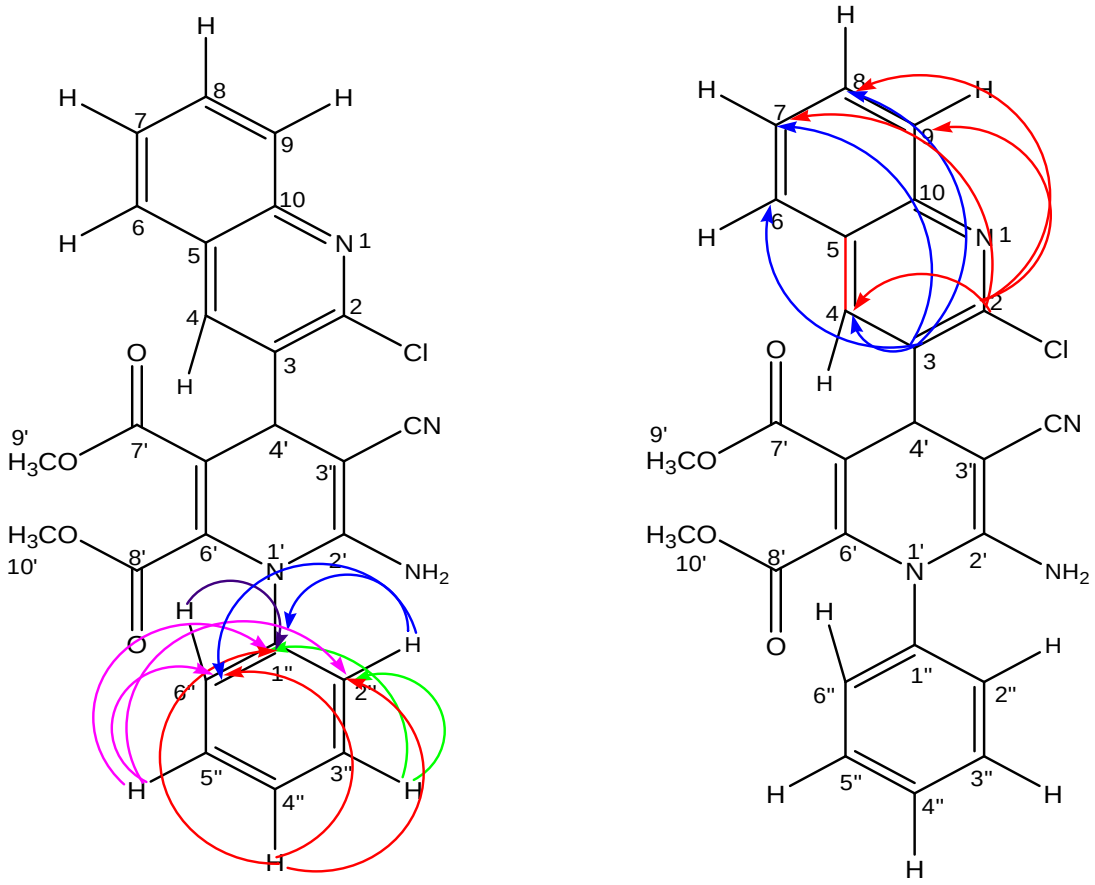

Figure 14: Selected HMBC correlations for A1

The ^{13}**C NMR** spectrum of **A1** is presented in **Figure 35** (Appendix 10, page 95). The peaks at ŭ 51.9 and ŭ 52.3 are assigned to the two acetoxy carbons (C-9', C-10'); the peak at ŭ 58.0 is assigned to carbon of CN (C-3') and the peak at ŭ 39.0 is assigned to the C-H (C-4') on the dihydropyridine ring. The peaks at ŭ 162.6 are assigned to the two C=O (C-7', C-8'); the peak at ŭ 164.7 is assigned to the C-NH_2 (C-2') whilst the peaks at ŭ 150.9-120.3 are attributed to aromatic carbons. The **IR** spectra of **A1**, presented in **Figure 36** (Appendix 11, page 96), it showed the C=O stretching at 1713 cm^{-1} and 1748 cm^{-1}, the C-N stretching at 2171 cm^{-1}, the C-Cl stretching at 669-778 cm^{-1}whilst the NH stretching at 3486 cm^{-1} and 3356 cm^{-1} was not well resolved.

The mass spectra of all the compounds that were analysed showed the *m/z* value for the molecular ion corresponding to the proposed molecular formula. The mass spectra of **A1** which is presented in **Figure 37** (Appendix 12, page 97), it shows an *m/z* of 475 which indicates the molecular ion. The isotopic ratio of 3:1 for ^{35}Cl: ^{37}Cl was not observed due to the small relative abundance of all characteristic fragments. **Scheme 50** shows possible the fragments of **A1** which was produced by the electron impact ionization technique.

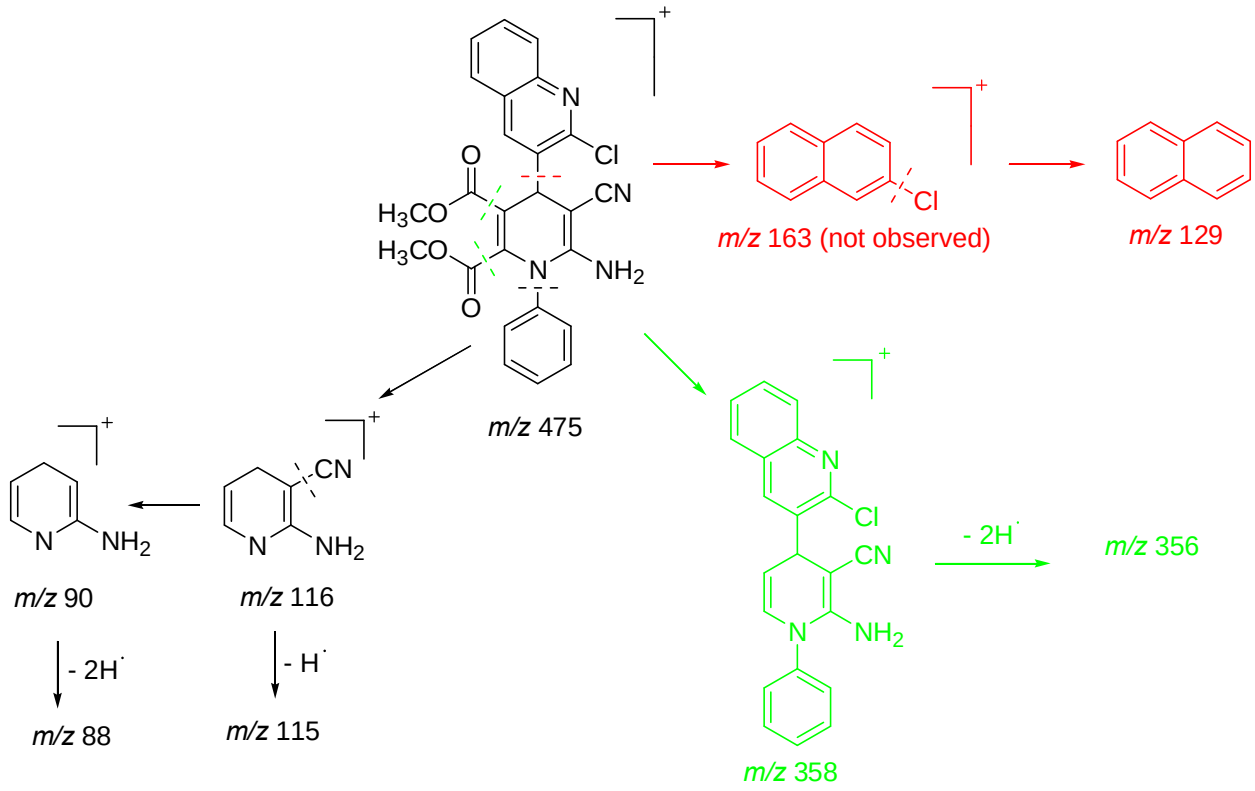

Scheme 50: Proposed fragments of A1

In the **NMR** spectra of all the related derivatives, the quinoline and dihydropyridine were similar. The differences were seen in the phenyl ring attached to the "N due to the different substituents in the ring. For instance, in the **^{1}H NMR** spectra for **A2,** presented in **Figure 38** (Appendix 13, page 98), the aromatic group methoxy proton H-7" (ŭ 3.50) of compound **A2** appears deshielded due to OCH_3 electron density attached to the nearby carbon C-7"; the H-3" resonance is now *ortho* to the OCH_3 group, is also deshielded and now occurring as a doublet at ŭ 7.84 (J = 8.1) due to OCH_3 electron density attached to the nearby carbon atom as shown in the expanded spectra, presented in **Figure 39** (Appendix 14, page 99). The mass spectra of **A2** which is presented in **Figure 42** (Appendix 17, page 102), shows an *m/z* of 504 and the isotopic ration of 3:1 for ^{35}Cl; ^{37}Cl was observed at *m/z* 427 and 429. Also, the loss of *m/z* 427 shows the benzene fragment at *m/z* 77.

In the **^{1}H NMR** spectra for **A3,** presented in **Figure 43** (Appendix 18, page 103) there is a methyl proton resonance (H-7") occurring as a singlet at ŭ 2.39. Unlike in **A1** where there was only one singlet observed in the aromatic region, a noticeable resonance H-2" (7.23) in **Figure 44** (Appendix 19, page 105) was observed. The mass spectra of **A3** which is presented in **Figure 47** (Appendix 22, page 107), the

molecular ion peak was observed at *m/z* 488. Loss of 2H· radicals gave the peak at *m/z* 486 which also showed the isotopic chlorine ratio of ^{35}Cl : ^{37}Cl as 3:1. The tropylium ion was observed at *m/z* 91.

In the expanded **^{1}H NMR** spectra for **A4,** presented in **Figure 49** (Appendix 24, page 109), resonances (H-2", H-6") and (H-3", H-5") on the phenyl ring now appears as doublets at ŭ 7.60 (*J* = 11.2) and ŭ 7.49 (*J* = 8.8), respectively. The mass spectra of **A4** which is presented in **Figure 52** (Appendix 27, page 112), it shows an *m/z* of 510. The peaks at *m/z* 509 and 508 are due to the loss of hydrogen and the two hydrogens by rearrangements, respectively.

In the **^{1}H NMR** spectra for **A5**, presented in **Figure 53** (Appendix 28, page 113), where a fluorine atom is substituted at the 2" position, causing splitting of the adjacent aromatic proton by short as well as long range coupling. The H-3" appears as a doublet at ŭ 7.33 (*J* = 7.7). The H-4", H-5" and H-6" appear at ŭ 7.37-7.64 but these assignments are not well resolved. In the **^{13}C NMR** spectrum, presented in **Figure 54** (Appendix 29, page 114), the C-F coupling is observed for C-2" and appears as a doublet at ŭ 160.6 (*J* = 254.1). The C-3" appears as doublet of doublets at ŭ 128.3 (*J* = 120.2).

In the **^{1}H NMR** expanded spectra for **A6**, presented in **Figure 56** (Appendix 31, page 116), the fluoro group is at the 3" position, causes splitting of the adjacent aromatic proton by short as well as long range coupling. The H-6" proton occurs as a doublet at ŭ 7.32 (*J* = 7.8). The H-5" occurs as a doublet doublet at ŭ 7.60 (*J* = 4.8). The H-2" and H-4" protons are split by fluorine and occurs as a doublet and doublet of doublet at ŭ 7.41 (*J* = 4.7) and ŭ 7.44 (*J* = 4.8), respectively. In the **^{19}F NMR** spectra for **A6**, presented in **Figure 58** (Appendix 33, page 118), it shows a singlet at ŭ 111.2 is attributed to C-F function. In the **^{13}C NMR** spectrum, presented in **Figure 59** (Appendix 34, page 119), the C-F coupling is observed for C-3" and appears as a doublet at ŭ 161.7 (*J* = 248.3). The C-2" and C-4" appears as doublets at ŭ 127.8 (*J* = 29.8) and ŭ 127.9 (*J* = 15.9), interchangeably. The mass spectra of **A6** which is presented in **Figure 61** (Appendix 36, page 121), it shows an *m/z* of 494. The peaks at *m/z* 493 and 492 are due to the loss of hydrogen and the two hydrogens by rearrangements, respectively.

In the **^{1}H NMR** spectra for **A7**, presented in **Figure 62** (Appendix 37, page 122), the fluoro group is at the 4" position; causing splitting of the adjacent aromatic proton by short as well as long range coupling. The H-2" and H-6" protons are equivalent and integrated to 2 protons appearing at ŭ 7.50 (*J* = 8.2). The H-3" and H-5" appears as a doublet doublet at ŭ 7.34 and 7.36 (*J* = 8.6, 8.2), respectively. In the

^{19}F NMR spectra for **A7**, presented in **Figure 63** (Appendix 38, page 123), a singlet at ŭ 110.9 is attributed to C-F function. In the **^{13}C NMR** spectrum, presented in **Figure 64** (Appendix 39, page 124), the C-F coupling is observed for C4" and appears as a doublet at ŭ 210.0 (J = 20.0). The C-3" and C-5" are equivalent and appears as doublet at ŭ 127.9 (J = 68.9). The mass spectra of **A7** which is presented in **Figure 66** (Appendix 41, page 126), it shows an *m/z* of 494. The peaks at *m/z* 493 and 492 are due to the loss of hydrogen and the two hydrogens by rearrangements, respectively.

In the expanded **^{1}H NMR** spectrum for **A8**, presented in **Figure 68** (Appendix 43, page 128), the chlorine atoms are substituted at the 3" and 4" positions, resonances H-2" and H-5" on phenyl ring now appears as doublets at ŭ 7.48 (J =7.8) and ŭ 7.47 (J = 8.2), respectively. The mass spectra of **A8** which is presented in **Figure 71** (Appendix 46, page 131), it shows an *m/z* of 544; the base peak appears at *m/z* 485 is due to the loss of the acetoxy group. **Table 4** represents the chemical shifts and coupling constants of the protons of **A1-A8**. The chemical shift of the carbons of **A1-8** is presented in **Table 5**.

Table 4: ^{1}H NMR chemical shifts for compounds A1-A8, δ of ^{1}H (*J*, Hz)

No.	A1	A2	A3	A4	A5	A6	A7	A8
NH_2	4.13(s)	4.17(s)	4.23(s)	5.86(s)	5.99(s)	5.86(s)	5.83(s)	6.02(s)
CH	5.36(s)	5.36(s)	5.33(s)	5.24(s)	5.22(s)	5.25(s)	5.23(s)	5.25(s)
OCH_3	3.51(s)	3.46(s)	3.50(s)	3.45(s)	3.46(s)	3.45(s)	3.38(s)	3.43(s)
OCH_3	3.44(s)	3.49(s)	3.44(s)	3.43(s)	3.46(s)	3.40(s)	3.43(s)	3.39(s)
4	8.14(s)	8.39(s)	8.12(s)	8.34(s)	8.33(s)	8.40(s)	8.38(s)	8.45(s)
6	7.85(d, 8.1)	7.80(d, 8.1)	7.84(d,8.2)	7.98(d, 8.5)	7.59(m)	7.99(d, 8.5)	8.17(d, 8.0)	7.99(d, 8.4)
7	7.71(t, 7.6)	7.69(7.6)	7.69(t, 10.1)	7.70(t, 7.9)	7.67(t, 7.1)	7.70(t, 6.9)	7.82(t, 7.3)	7.84(t, 7.7)
8	7.55(t, 7.4)	7.53(t, 7.1)	7.53(t, 11.2)	7.84(t, 6.9)	7.67(t, 7.1)	7.84(t, 7.0)	7.66(t, 7.2)	7.70(t, 7.6)
9	8.02(d, 8.4)	8.01(d, 8.4)	8.00(d, 9.7)	8.17(d, 8.1)	7.84(d, 7.3)	8.19(d, 8.4)	7.96(d, 7.6)	8.20(d, 8.1)
2"	7.39(m)	-	7.23(s)	7.60(d, 11.2)	-	7.41(d, 4.7)	7.50(d, 8.2)	7.47(d, 2.3)
3"	7.52(m)	7.84(d, 8.1)	-	7.49(d, 8.8)	7.33(d,d, 7.7)	-	7.34-7.36(d, 8.6)	-
4"	7.38(t, 3.5)	7.06-7.02(m)	7.16(d,7.6)	-	7.64-7.37(m)	7.44(dd, 4.8)	-	-
5"	7.52(m)	7.48(t, 7.8)	7.36(t, 9.9)	7.49(d, 8.8)	7.64-7.37(m)	7.60(d, 4.8)	7.34-7.36(d, 8.0)	7.87(d, 9.9)
6"	7.39(d, 3.4)	7.30(d, 7.3)	7.29(d,7.6)	7.60(d, 11.2)	7.64-7.37(m)	7.32(d, 7.8)	7.50(d, 8.2)	7.80(d, 7.7)
7"	-	3.50(s)	2.39(s)	-	-	-	-	-
8"	-	-	-	-	-	-	-	-

Table 5: ^{13}C NMR chemical shifts (δ in ppm) for compounds A1-A8

No.	A1	A2	A3	A4	A5	A6	A7	A8
2	150.9	150.9	150.4	151.4	151.4	151.6	149.1	151.1
3	137.3	130.4	136.5	137.7	143.2	118.7	127.4	131.3
4	138.4	138.7	138.5	139.1	146.6	139.1	142.9	131.6
5	134.9	127.6	127.7	128.0	128.7	128.0	133.3	131.8
6	139.6	139.1	128.3	128.5	128.9	131.6	133.4	132.3
7	130.2	127.0	129.8	130.2	129.1	131.6	133.3	133.5
8	130.9	128.5	131.5	132.9	133.4	131.4	133.0	133.8
9	130.5	128.3	130.4	131.4	131.5	128.6	131.1	127.9
10	149.0	149.9	149.9	149.6	143.2	149.6	149.0	142.9
2'	164.7	165.4	165.3	165.2	164.1	165.2	150.9	165.2
3'	58.0	61.8	60.8	58.5	79.6	58.8	61.7	58.6
4'	39.0	36.4	36.7	39.6	44.9	37.1	36.8	37.1
5'	120.3	119.9	127.1	120.8	120.7	120.7	120.4	120.7
6'	143.1	146.9	143.1	146.5	151.3	143.2	142.9	139.4
7'	162.6	163.3	163.2	165.2	165.7	163.3	149.1	163.1
8'	162.6	163.3	163.2	163.1	165.0	163.1	149.1	163.1
9'	52.3	52.1	52.1	52.0	53.6	52.1	57.3	52.4
10'	51.9	52.5	52.6	52.4	53.2	52.9	57.8	53.1
1"	146.0	146.9	146.9	143.3	133.5	146.6	143.1	146.5
2"	127.3	150.1	127.2	127.9	160.6 (d, 254.1)	127.8 (d, 29.8)	127.3 (d, 33.5)	128.5
3"	127.5	127.6	140.5	135.3	128.3 (dd,120.2)	161.7 (d, 248)	127.3-127.9 (dd, 180.2, 33.5)	139.4
4"	127.5	121.0	127.6	127.9	128.1 (dd,49.9)	127.9 (d, 29.8)	151.0 (d, 29.4)	137.8
5"	127.5	126.9	130.7	134.4	127.8 (dd, 180.3, 12.8)	137.9 (dd, 29.8, 15.9)	127.3-127.9 (dd, 175.0, 33.5)	135.4
6"	128.0	127.3	119.9	127.9	128.4 (d, 41.6)	128.0 (d, 52.9)	128.0 (d, 30.1)	130.1
7''	-	52.0	21.2	-	-	-	-	-

3.3.2. The Spectroscopic Data (A1-A8)

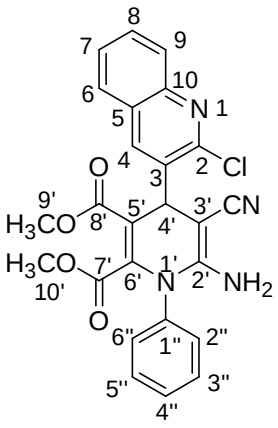

A1: Light yellow solid, 87%, m.p. 275-276ºC, **(IR) υ/cm^{-1}:** 3486, 3356, 2171, 1748, 1713, 1647, 1524, 1488, 1448, 1324, 1296, 1247, 1105, 1024, 992, 841, 835, 778, 762, 669, 667, 550; **MS** (*m/z*): 475. Anal Calculated for $C_{25}H_{19}ClN_4O_4$: C 63.23; H 4.03; Cl 7.47; N 11.80; O 13.48: Found, C 63.87; H 4.05; Cl 7.50; N 11.88; O 13.81.

A2

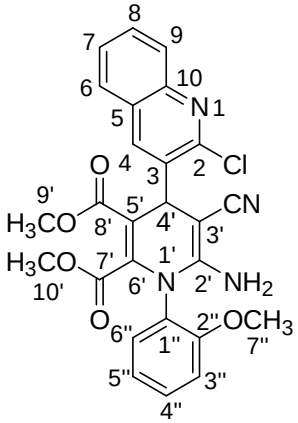

A2: Yellow solid, 40%, m.p. 263-264ºC, **(IR) υ/cm^{-1}**: 3437, 3315, 3217, 2185, 1716, 1746, 1665, 1577, 1496, 1421, 1354, 1329, 1222, 1117, 933, 932, 859, 817, 782, 755, 624; **MS** (*m/z*): 504. Anal Calculated for $C_{26}H_{21}ClN_4O_5$: C 61.85; H 4.19; Cl 7.02; N 11.10; O 15.84: Found, C 61.87; H 4.25; Cl 7.10; N 11.08; O 15.81.

A3

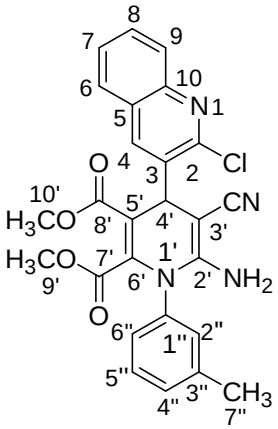

A3: Yellow solid, 73%, m.p. 237-238ºC, **(IR) υ/cm^{-1}:** 3386, 3318, 2180, 1702, 1647, 1565, 1488, 1420, 1358, 1328, 1253, 1224, 1136, 1114, 1056, 1019, 968, 928, 786, 763, 708, 686; **MS** (*m/z*) 488. Anal Calculated for $C_{26}H_{21}ClN_4O_4$: C 63.87; H 4.33; Cl 7.25; N 11.46; O 13.09: Found, C 63.20; H 4.31; Cl 7.11; N 11.36; O 13.23.

A4

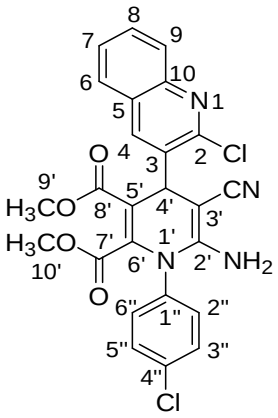

A4: Light yellow solid, 79%, m.p. 287-289ºC, **(IR) υ/cm^{-1}:** 3428, 3218, 2174, 1745, 1703, 1650, 1623, 1593, 1571, 1489, 1354, 1257, 1219, 1107, 1090, 1018, 850, 825, 780, 741, 723; **MS** (*m/z*) 510. Anal Calculated for $C_{25}H_{18}Cl_2N_4O_4$: C 58.95; H 3.56; Cl 13.92; N 11.00; O 12.56: Found, C 63.19; H 3.55; Cl 13.15; N 11.39; O 13.22.

A5

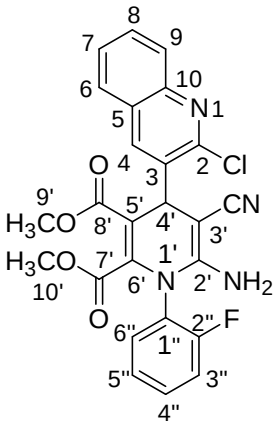

A5: White solid, 64%, m.p. 247-248ºC, **(IR) υ/cm^{-1}:** 3376, 3282, 2178, 1747, 1712, 1654, 1571, 1488, 1422, 1360, 1329, 1258, 1231, 1171, 1032, 967, 922, 872, 851, 761, 648, 644.

A6

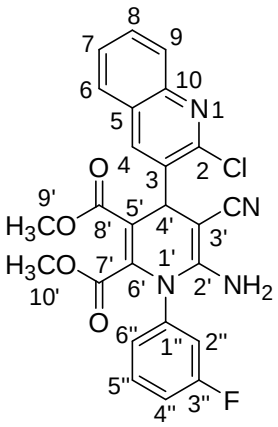

A6: White solid, 31%, m.p. 269-271ºC, **(IR) υ/cm^{-1}:** 3449, 3303, 2177, 1746, 1715, 1652, 1596, 1570, 1487, 1421, 1329, 1305, 1251, 1194, 1136, 1106, 1033, 966, 924, 819, 763, 706, 899. **^{19}F NMR (600MHz, DMSO)** ŭ**:** 111.23; **MS** (*m/z*) 494. Anal Calculated for $C_{25}H_{18}ClFN_4O_4$: C 60.92; H 3.68; Cl 7.19; F 3.85; N 11.37; O 12.98: Found, C 60.90; H 3.68; Cl 7.11; F 3.84; N 11.36; O 12.99.

A7

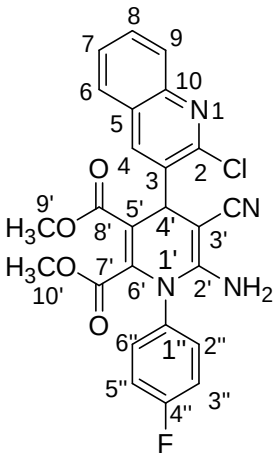

A7: White solid, 60%, m.p. 253-254ºC, **(IR) υ/cm^{-1}:** 3309, 3269, 2171, 1745, 1702, 1622, 1506, 1569, 1329, 1298, 1247, 1213, 1153, 1106, 1027, 1002, 938, 918, 840, 778, 768, 766, 741, 728, 615. **^{19}F NMR (600MHz, DMSO)** ŭ**:** 110.91; **MS** (*m/z*) 494. Anal Calculated for $C_{25}H_{18}ClFN_4O_4$: C 60.92; H 3.68; Cl 7.19; F 3.85; N 11.37; O 12.98: Found, C 60.90; H 3.68; Cl 7.11; F 3.84; N 11.38; O 12.97.

A8

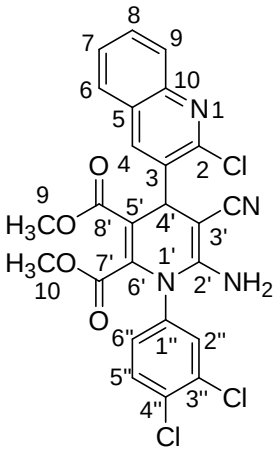

A8: Light yellow solid, 72%, m.p. 280-282ºC, **(IR) υ/cm^{-1}:** 3439, 3302, 2179, 1742, 1702, 1647, 1573, 1506, 1423, 1366, 1324, 1254, 1214, 1108, 1032, 932, 758; **MS** (*m/z*) 544. Anal Calculated for $C_{25}H_{17}Cl_3N_4O_4$: C 55.22; H 3.15; Cl 19.56; N 10.30; O 11.77: Found, C 65.19; H 3.16; Cl 19.15; N 10.39; O 11.22.

3.3.3. Conclusion

2-Chloro-3-formyl quinoline was synthesized from *N*-phenylacetamide by the Vilsmeier-Haack reaction and it was characterized by **IR**, **^{1}H NMR** and **^{13}C NMR** spectroscopy. Eight new poly-functionalised dihydropyridine quinoline derivatives were synthesized from 2-chloro-3-formyl quinoline, malononitrile, arylamine and dimethyl acetylenedicarboxylate by a one pot multi-component reaction. These compounds were produced in yields of 37-87% and were characterised by **IR**, **^{1}H NMR**, **^{13}C NMR** and **GCMS**.

References

1. A P Rajput, P D Girase, Review article on Vilsmeier-Haack reaction*, IJPCBS*, 3, **2012**, 25-40.

2. M M Ali, S Sana, K C Rajanna, P K Saiprakash, Synthetic communications: An international journal for rapid communication of synthetic organic chemistry, *Synthetic Comm*. 32, **2002**, 13-15.

3. A Srivastava, R M Singh, Vilsmeier-Haack reagent: A facile synthesis of 2-chloro-3-formyl quinolines from *N*-arylacetamides and transformation into different functionalities, *Indian J. Chem*. 44, **2005**, 1868-1876.

4. S S Pawar, N A Koorbanally, Synthesis and structure elucidation of a series of pyranochromene chalcones and flavanones using 1D and 2D NMR spectroscopy and X-ray crystallography, *Magn. Reson. Chem.* 52, **2014**, 279-288.

5. T Moodley, M Momin, C Mocktar, C Kannigadu, N A Koorbanally, The synthesis, structural elucidation and antimicrobial activity of 2- and 4-substituted-coumarinyl chalcones, *Magn. Reson. Chem*. 54, **2016**, 610ï 617.

Chapter Four: Biological studies

4.1. Cancer Studies

4.1.1. Introduction

Quinolines play a significant role in the development of new anti-cancer agents; their derivatives have shown excellent results through different mechanism of action such as growth inhibitors by cell cycle arrest, apoptosis, inhibition of angiogenesis, disruption of cell migration, and modulation of nuclear receptor responsiveness [1]. The anti-cancer potential of several of these derivatives have been demonstrated on various cancer cells including those of leukemia and other cancer cells of breast, ovary, liver, lung, pancreas and colon [2]. Owing to the previously mentioned significance, the synthesis of substituted quinolines has been a subject of great interest in organic chemistry. In addition, various fused systems of quinolines were studied for their intercalative DNA binding properties. A literature survey reveals that antitumor activity is due to the intercalation between the base pairs of DNA and interferences with the normal functioning of enzyme topoisomerase II, which is involved in the breaking and releasing of DNA strands [3]. The antitumor drugs that intercalate DNA are of growing interest in the field of anticancer derivatives. In order to add better value to our research, we investigated poly-functionalised dihydropyridine quinoline derivatives **A1-A8** and evaluated their cytotoxicity in A549 lung cancer cell lines.

4.1.2. Experimental

4.1.2.1. Materials and Methods

Lung cancer cells (A549) were purchased from Highveld Biologicals (Johannesburg, SA). Cell culture reagents were purchased from Whitehead Scientific (Johannesburg, SA). All other reagents and consumables were purchased from Merck (SA), unless otherwise stated.

4.1.2.2. Maintenance of A549 Cells in Culture

The best environment for growing cells *in vitro* should be matched as close as possible to the natural physiological conditions. The essential requirements are an environment of optimum temperature, pH, gas phases, growth substrate and media containing necessary nutrients. The optimal temperature is provided by the use of a humidified incubator supplied with 5% carbon dioxide (CO_2). The gas phases supplied to the culture includes oxygen which is maintained at atmospheric pressure, and CO_2 to ensure that the bicarbonate and CO_2 tension is in equilibrium.

A549 cells were cultured (37ºC, 5% CO_2) to 90% confluency in 25mL flasks in complete culture media (CCM) [Eagleôs minimum essential medium, 10% foetal calf serum, 1% L-Glutamine and 1%

penstrepfungizone]. The culture medium is by far the most important single factor in culturing cells. The extracellular medium must meet the essential requirements (nutritional, hormonal and stromal factors) for survival and growth.

In order to sub-culture and plate cells for the various experimental assays, the process of trypsinisation was used to detach cells once 90% confluency was reached. The process of trypsinisation involved the critical step of rinsing the cells with 3 mL aliquots of warm 0.1M PBS and incubating the cells with 1 mL of trypsin-EDTA (Lonza) for 1 minute. The cells were monitored using an inverted light microscope (Olympus IXSI; 20x magnification) and once rounded, the trypsin was discarded and CCM was added to the flask of cells. The flask was agitated to detached cells and the cell suspension was then enumerated by dye exclusion using a haemocyto meter. Trypan blue (0.4%) was utilized in a dye exclusion procedure for cell counting. The principle of dye exclusion using trypan blue is based on compromised cell membranes in dead/damaged cells which readily allow entry of the dye into the cells and are stained blue whereas viable cells remain unstained. A549 cells (15,000/well) were incubated for 24 hours with a range of concentrations of each compound in triplicate in a micro-titre plate together with an untreated control (cells incubated with CCM only). Each experiment was conducted twice on separate occasions. The data results from the first set matched the repeated experiment. The cells were then incubated (37ºC, 5% CO_2) with the MTT substrate (5 mg/mL in PBS) for 4hours. Thereafter all supernatants were aspirated, and DMSO (100 µL/well) was added to the wells. Finally the optical density was measured at 570 nm and a reference wavelength of 690 nm with an ELISA plate reader (Bio-Tek µQuant). The net MTT-dependent absorbance (optical density (OD) of each sample was calculated by subtracting the average absorbance of the blank from the average absorbance of each sample. Data are represented as mean OD plus or minus the standard deviations [4].

4.1.3 Results and Discussion

This study investigated the cytotoxicity of synthesized quinoline derivatives (**A1-A8**) in the A549 lung cancer cell line. These compounds differed in substituents like OCH_3, CH_3, F and Cl attached to the benzene ring. Herein we wished to investigate the effect of these compounds based on the different functional groups to study their anti-cancer potential. The cytotoxicity of the compounds in cancerous A549 lung cells was assessed using the MTT assay. This assay measures cell proliferation/metabolic activity *in vitro*. The technique is particularly useful for cells that are metabolically active based on their redox potential and capacity of dehydrogenase enzymes to convert yellow water-soluble salt into a purple water-insoluble formazan product. The insoluble crystals are then dissolved in DMSO and the absorbance

is read on a spectrophotometer. A549 cells were exposed to various concentrations of the synthesized compounds. A control of cells incubated with complete culture media only was used. The results were expressed as optical density. The treatment groups at various concentrations (31.25ï 500 µM) were compared to the control to determine the potential as an anti-cancer drug.

The parent compound **A1** (with no substituent in the benzene ring) is not cytotoxic but rather increases metabolic activity as all concentrations tested showed greater activity than control. The compound **A2** (with an electron donating group, OCH_3 substituent in the benzene ring), shows a dose dependent toxicity due to its substituent as the results gives evidence that the compound has potential as an anti-cancer drug. The compound **A3** (with an electron donating group, CH_3 substituent in the benzene ring) shows high toxicity but only at higher concentrations, has potential as an anti-cancer drug. Compound **A4** (with the chloro group, which withdraws electrons by induction, but donates electrons by resonance in the benzene ring) shows a dose dependent toxicity with the highest toxicity at 250 µM. The compound has potential as an anti-cancer drug. Compounds **A5**, **A6** and **A7** (with the fluoro group in the benzene ring) were not cytotoxic, whilst **A8** (with the two chloro groups, which withdraw electrons by induction, but donate electrons by resonance in the benzene ring) show a dose dependent toxicity with the highest toxicity at 125, 250 and 500 µM. The compound has potential as an anti-cancer drug.

4.1.4. A549 lung Cancer Cell Lines Raw Data and Statistical Analysis for A1-A8

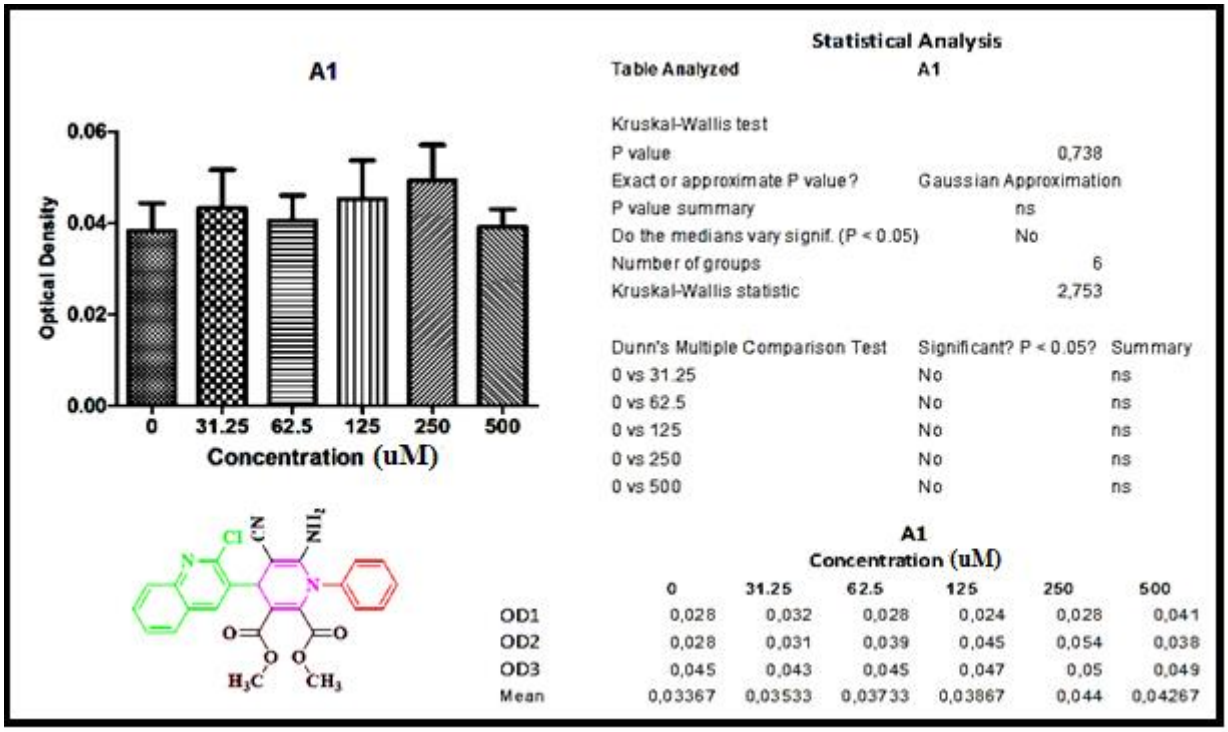

Statistical Analysis

Table Analyzed	A1
Kruskal-Wallis test	
P value	0,738
Exact or approximate P value?	Gaussian Approximation
P value summary	ns
Do the medians vary signif. (P < 0.05)	No
Number of groups	6
Kruskal-Wallis statistic	2,753

Dunn's Multiple Comparison Test	Significant? P < 0.05?	Summary
0 vs 31.25	No	ns
0 vs 62.5	No	ns
0 vs 125	No	ns
0 vs 250	No	ns
0 vs 500	No	ns

A1
Concentration (uM)

	0	31.25	62.5	125	250	500
OD1	0,028	0,032	0,028	0,024	0,028	0,041
OD2	0,028	0,031	0,039	0,045	0,054	0,038
OD3	0,045	0,043	0,045	0,047	0,05	0,049
Mean	0,03367	0,03533	0,03733	0,03867	0,044	0,04267

Figure 15: The cytotoxic effects of A1 in the A549 lung cancer cell line

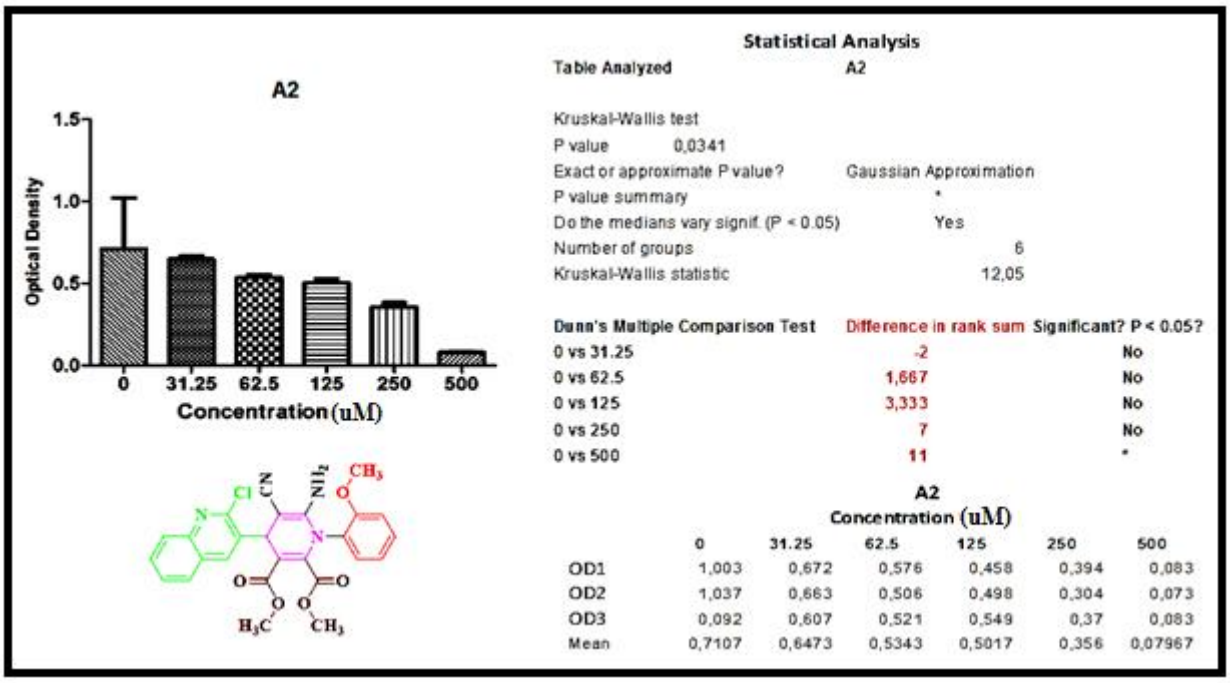

Statistical Analysis

Table Analyzed	A2
Kruskal-Wallis test	
P value	0,0341
Exact or approximate P value?	Gaussian Approximation
P value summary	*
Do the medians vary signif. (P < 0.05)	Yes
Number of groups	6
Kruskal-Wallis statistic	12,05

Dunn's Multiple Comparison Test	Difference in rank sum	Significant? P < 0.05?
0 vs 31.25	-2	No
0 vs 62.5	1,667	No
0 vs 125	3,333	No
0 vs 250	7	No
0 vs 500	11	*

A2
Concentration (uM)

	0	31.25	62.5	125	250	500
OD1	1,003	0,672	0,576	0,458	0,394	0,083
OD2	1,037	0,663	0,506	0,498	0,304	0,073
OD3	0,092	0,607	0,521	0,549	0,37	0,083
Mean	0,7107	0,6473	0,5343	0,5017	0,356	0,07967

Figure 16: The cytotoxic effects of A2 in the A549 lung cancer cell line

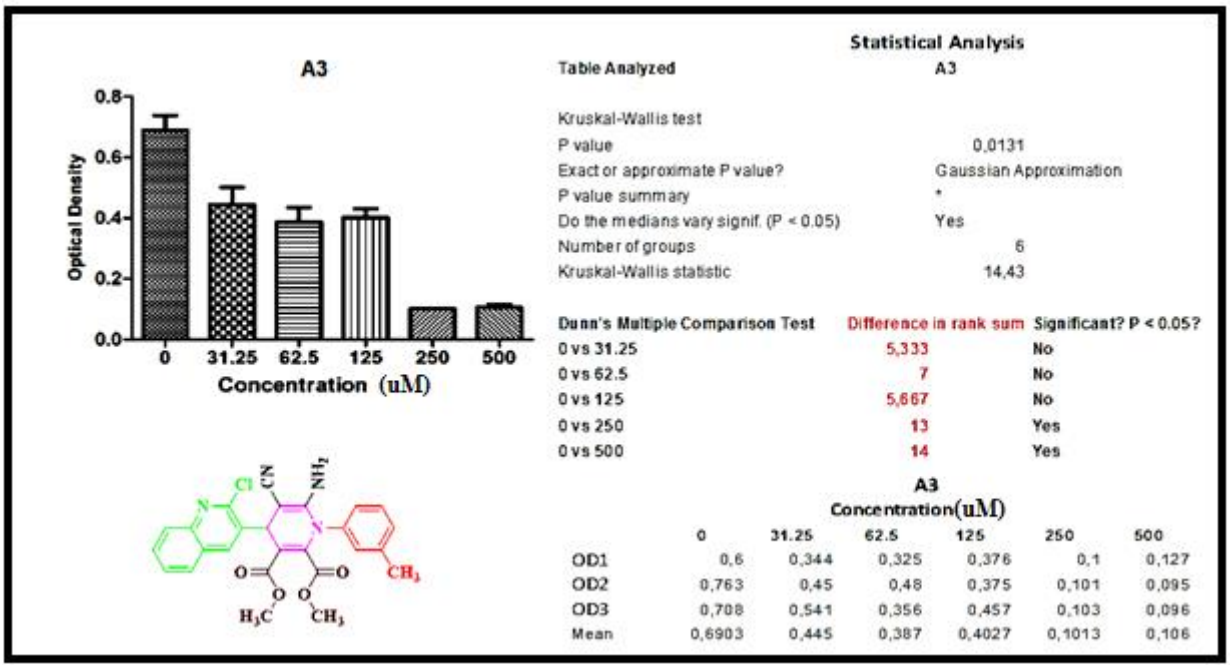

Statistical Analysis

Table Analyzed	A3
Kruskal-Wallis test	
P value	0,0131
Exact or approximate P value?	Gaussian Approximation
P value summary	*
Do the medians vary signif. (P < 0.05)	Yes
Number of groups	6
Kruskal-Wallis statistic	14,43

Dunn's Multiple Comparison Test	Difference in rank sum	Significant? P < 0.05?
0 vs 31.25	5,333	No
0 vs 62.5	7	No
0 vs 125	5,667	No
0 vs 250	13	Yes
0 vs 500	14	Yes

A3
Concentration(uM)

	0	31.25	62.5	125	250	500
OD1	0,6	0,344	0,325	0,376	0,1	0,127
OD2	0,763	0,45	0,48	0,375	0,101	0,095
OD3	0,708	0,541	0,356	0,457	0,103	0,096
Mean	0,6903	0,445	0,387	0,4027	0,1013	0,106

Figure 17: The cytotoxic effects of A3 in the A549 lung cancer cell line

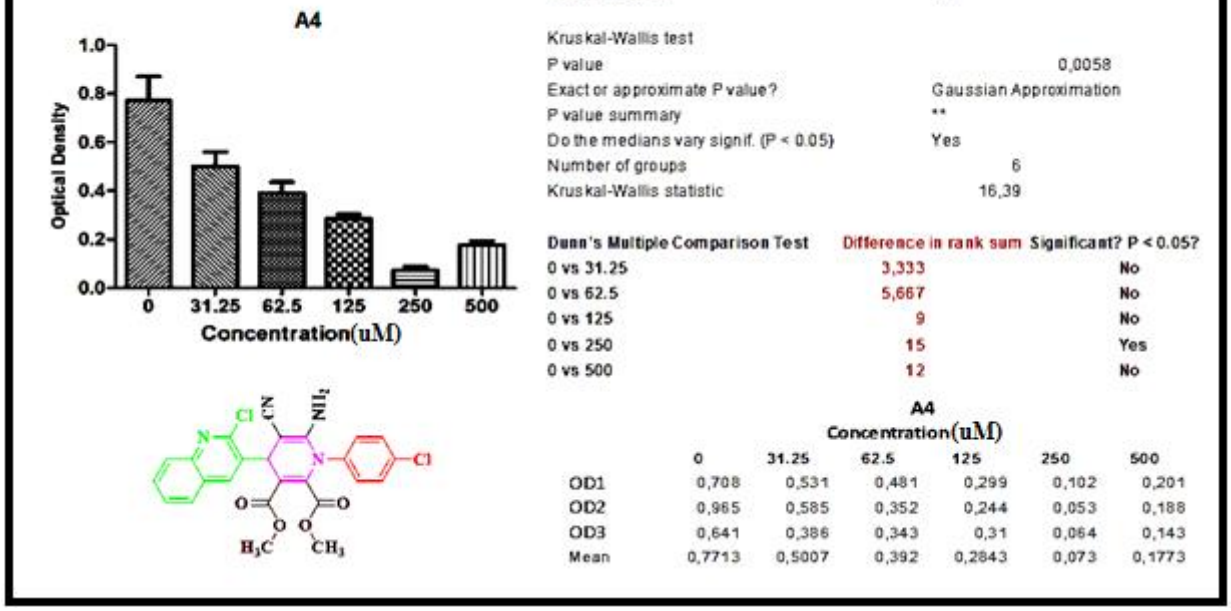

Statistical Analysis

Table Analyzed	A4
Kruskal-Wallis test	
P value	0,0058
Exact or approximate P value?	Gaussian Approximation
P value summary	**
Do the medians vary signif. (P < 0.05)	Yes
Number of groups	6
Kruskal-Wallis statistic	16,39

Dunn's Multiple Comparison Test	Difference in rank sum	Significant? P < 0.05?
0 vs 31.25	3,333	No
0 vs 62.5	5,667	No
0 vs 125	9	No
0 vs 250	15	Yes
0 vs 500	12	No

A4
Concentration(uM)

	0	31.25	62.5	125	250	500
OD1	0,708	0,531	0,481	0,299	0,102	0,201
OD2	0,965	0,585	0,352	0,244	0,053	0,188
OD3	0,641	0,386	0,343	0,31	0,064	0,143
Mean	0,7713	0,5007	0,392	0,2843	0,073	0,1773

Figure 18: The cytotoxic effects of A4 in the A549 lung cancer cell line

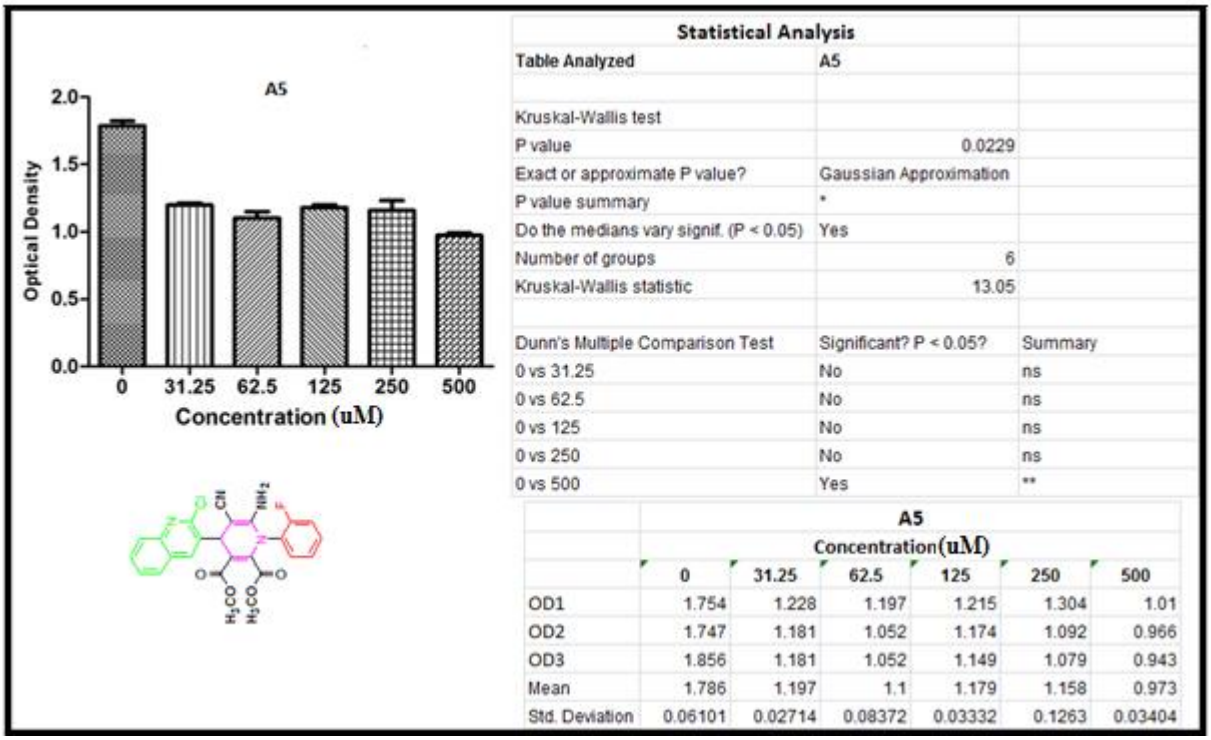

Statistical Analysis		
Table Analyzed	A5	
Kruskal-Wallis test		
P value	0.0229	
Exact or approximate P value?	Gaussian Approximation	
P value summary	*	
Do the medians vary signif. (P < 0.05)	Yes	
Number of groups	6	
Kruskal-Wallis statistic	13.05	
Dunn's Multiple Comparison Test	Significant? P < 0.05?	Summary
0 vs 31.25	No	ns
0 vs 62.5	No	ns
0 vs 125	No	ns
0 vs 250	No	ns
0 vs 500	Yes	**

	A5					
	Concentration(uM)					
	0	31.25	62.5	125	250	500
OD1	1.754	1.228	1.197	1.215	1.304	1.01
OD2	1.747	1.181	1.052	1.174	1.092	0.966
OD3	1.856	1.181	1.052	1.149	1.079	0.943
Mean	1.786	1.197	1.1	1.179	1.158	0.973
Std. Deviation	0.06101	0.02714	0.08372	0.03332	0.1263	0.03404

Figure 19: The cytotoxic effects of A5 in the A549 lung cancer cell line

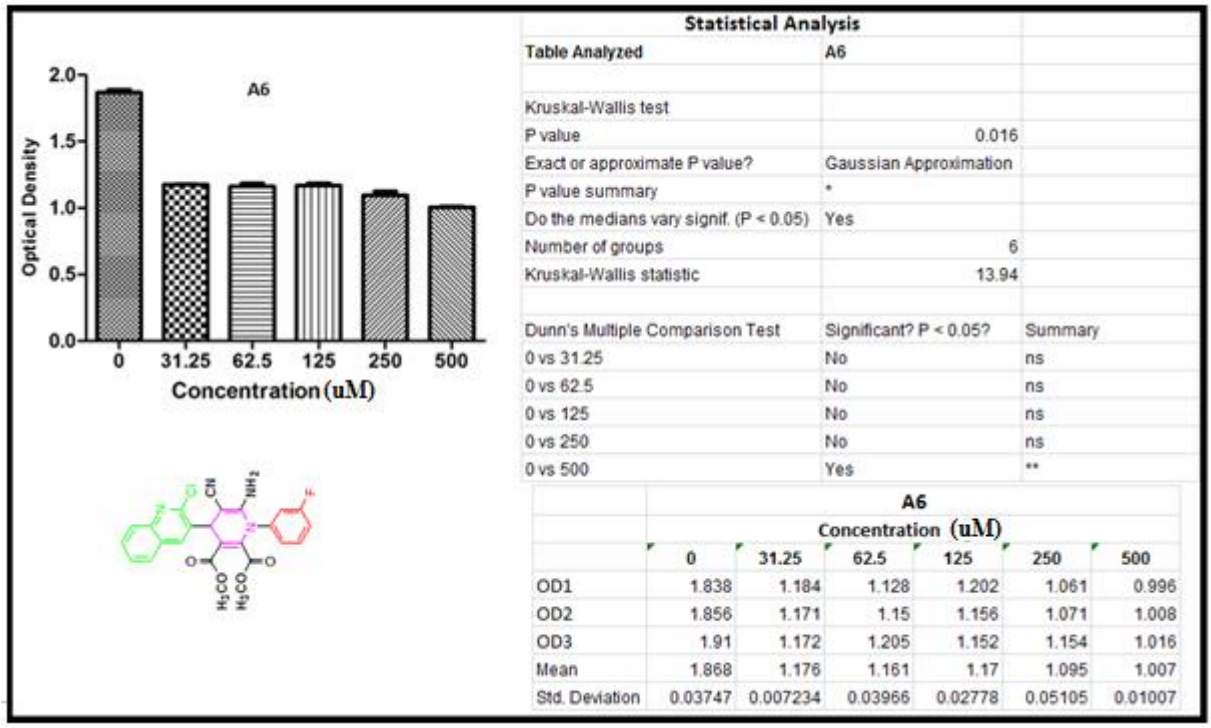

Statistical Analysis		
Table Analyzed	A6	
Kruskal-Wallis test		
P value	0.016	
Exact or approximate P value?	Gaussian Approximation	
P value summary	*	
Do the medians vary signif. (P < 0.05)	Yes	
Number of groups	6	
Kruskal-Wallis statistic	13.94	
Dunn's Multiple Comparison Test	Significant? P < 0.05?	Summary
0 vs 31.25	No	ns
0 vs 62.5	No	ns
0 vs 125	No	ns
0 vs 250	No	ns
0 vs 500	Yes	**

	A6					
	Concentration (uM)					
	0	31.25	62.5	125	250	500
OD1	1.838	1.184	1.128	1.202	1.061	0.996
OD2	1.856	1.171	1.15	1.156	1.071	1.008
OD3	1.91	1.172	1.205	1.152	1.154	1.016
Mean	1.868	1.176	1.161	1.17	1.095	1.007
Std. Deviation	0.03747	0.007234	0.03966	0.02778	0.05105	0.01007

Figure 20: The cytotoxic effects of A6 in the A549 lung cancer cell line

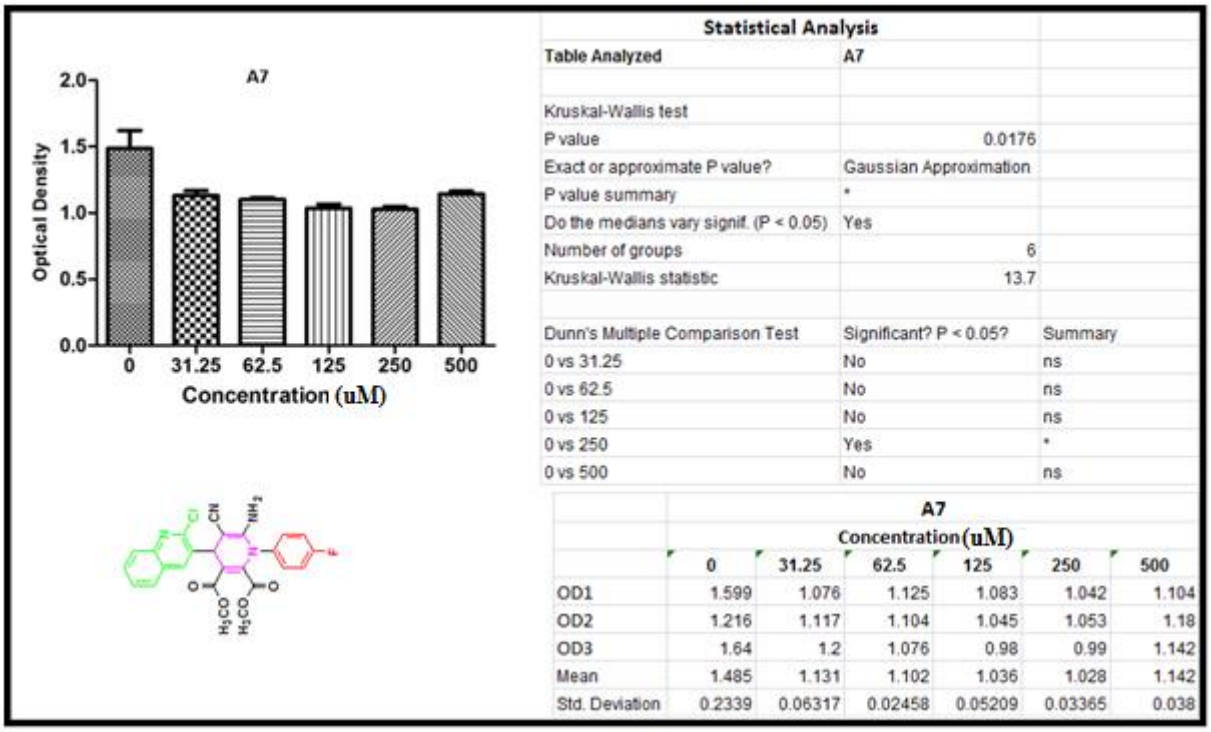

Statistical Analysis		
Table Analyzed	A7	
Kruskal-Wallis test		
P value	0.0176	
Exact or approximate P value?	Gaussian Approximation	
P value summary	*	
Do the medians vary signif. (P < 0.05)	Yes	
Number of groups	6	
Kruskal-Wallis statistic	13.7	
Dunn's Multiple Comparison Test	Significant? P < 0.05?	Summary
0 vs 31.25	No	ns
0 vs 62.5	No	ns
0 vs 125	No	ns
0 vs 250	Yes	*
0 vs 500	No	ns

	A7 Concentration (uM)					
	0	31.25	62.5	125	250	500
OD1	1.599	1.076	1.125	1.083	1.042	1.104
OD2	1.216	1.117	1.104	1.045	1.053	1.18
OD3	1.64	1.2	1.076	0.98	0.99	1.142
Mean	1.485	1.131	1.102	1.036	1.028	1.142
Std. Deviation	0.2339	0.06317	0.02458	0.05209	0.03365	0.038

Figure 21: The cytotoxic effects of A7 in the A549 lung cancer cell line

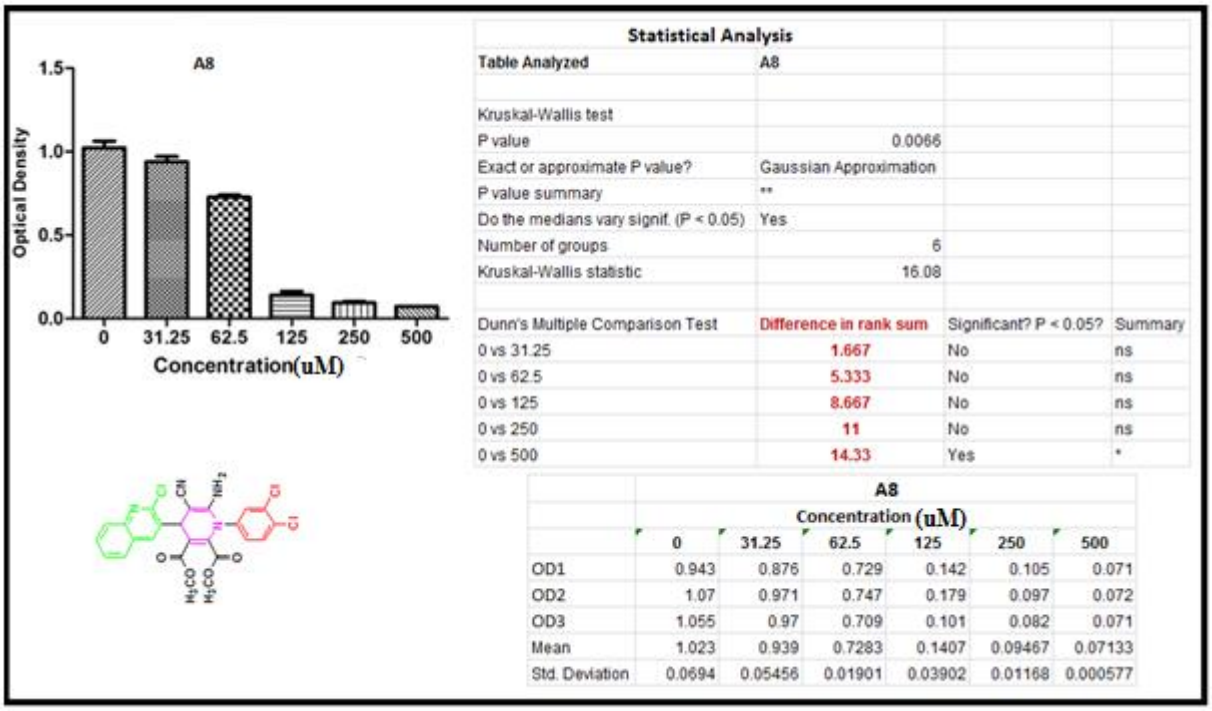

Statistical Analysis			
Table Analyzed	A8		
Kruskal-Wallis test			
P value	0.0066		
Exact or approximate P value?	Gaussian Approximation		
P value summary	**		
Do the medians vary signif. (P < 0.05)	Yes		
Number of groups	6		
Kruskal-Wallis statistic	16.08		
Dunn's Multiple Comparison Test	Difference in rank sum	Significant? P < 0.05?	Summary
0 vs 31.25	1.667	No	ns
0 vs 62.5	5.333	No	ns
0 vs 125	8.667	No	ns
0 vs 250	11	No	ns
0 vs 500	14.33	Yes	*

	A8 Concentration (uM)					
	0	31.25	62.5	125	250	500
OD1	0.943	0.876	0.729	0.142	0.105	0.071
OD2	1.07	0.971	0.747	0.179	0.097	0.072
OD3	1.055	0.97	0.709	0.101	0.082	0.071
Mean	1.023	0.939	0.7283	0.1407	0.09467	0.07133
Std. Deviation	0.0694	0.05456	0.01901	0.03902	0.01168	0.000577

Figure 22: The cytotoxic effects of A8 in the A549 lung cancer cell line

4.1.4. Conclusion

Eight novel poly-functionalised dihydropyridine quinoline derivatives were synthesized using a one pot multi-component reaction were tested for their anti-cancer potential.The anti-cancer assays indicated that compounds **A2**, **A3**, **A4** and **A8** have good potential as anti-cancer drugs by showing anti-proliferative activity. Compounds **A1**, **A5** and **A7** were not cytotoxic.

4.2. Molecular Docking Study

4.2.1. Introduction

Molecular docking is a typical computational approach of modern drug discovery that serves as a rapid method for the theoretical prediction of binding mode of the ñdrug like candidatesò with the active site of the known macromolecular structure. Despite the complexity in molecular docking algorithm and scoring function, accuracy is the only stand-alone solution of this approach leading to drug discovery. The goal of ligand-protein docking is to predict the predominant binding mode of a ligand with a protein of known three-dimensional structure. Docking can be used to perform virtual screening on large libraries of compounds, rank the results and propose structural hypotheses of how the ligands inhibit the target, which is invaluable in lead optimization. [5-6]

Glide is an esteemed docking panel which operates with the help of funnel type module that locates finely by binding the geometry of the small molecule with the protein active site. Glide is conserved as the top search algorithm in the docking community and is used for this study. The 3D co-ordinates of X-ray crystal structure of human mdm2 (PDB ID: 3VZV) was complexed from the Protein data bank. To perform docking the most crucial aspect is to prepare the protein in such a way that it can be read by the algorithm and subsequently to match it with the parameter that exists in the protein preparation. The band of operations executed in preparing the protein are assigning bond orders, adding hydrogen, treating metals, deleting water molecules, removing co-crystal ligand, treating disulfide bonds, adjusting bond order, building missing heavy atoms, formal charges and alleviating potential steric clashes. OPLS-2005 force field is employed for energy minimization at quantum level. 0.3Å RMSD cut off is taken as threshold valve to diagnose the protein refinement strategies. [7]

4.2.2. Experimental

4.2.2.1. Materials and Methods

The native structure of Human mdm2 (PDB ID: 3VZV) was retrieved from the Protein Data Bank. The compounds were drawn and converted into PDB format using Chem Draw which was used as a ligand for docking against human mdm2 protein. The Auto Dock 4.2 suite of programs which utilizes the Lamarckian Genetic Algorithm (LGA) was used for the study. All water molecules were removed and hydrogen atoms were added followed by the calculation of Gasteiger charges, as required in the Lamarckian Genetic Algorithm. The grid size along the x-, y-, z- axes was set to 52 Å, 52 Å and 52 Å respectively. The grid spacing for HSA-TBO was set as 0.425 Å. The Auto Docking parameters used were as follows: GA population size = 150; maximum number of energy evaluations = 250 000; GA crossover mode = two points. The lowest binding energy conformer was searched out of 25 different conformers for each docking simulation and the resultant one used for further analysis. The PyMoL software package was used for visualization of the docked conformations.

The prepared protein structure follows the grid ï fashion kinetic docking which commonly holds several physical parameters. It finds greater significance in prescribing the ligand interaction with the receptor. Grid files generation for protein is accomplished with ñReceptor Grid Generationò panel of Glide. The grid box is generated by assigning a common constituency point. From there a cubic grid box is extended to touch the bounty of 20Å in size or in words. The allocated size for grid generation for protein-ligand docking is 20Å since our approach is site-specific not generalized. Co-crystal ligand binding pattern with protein is well documented in recent studies. Hence, we attempted to crop the grid box to focusing on the centroid of human mdm2 (PDB ID: 3VZV). Refined structure and box coordinate X, Y, Z were set at (X=18.341215Å, Y=-3.662453Å, Z=0.929674Å). The foremost process in the hit identification pipeline docking is performed using Glide of Schrodinger [9].

4.2.2.2. Ligand Preparation

The chemical compounds of structures are not available in Pub Chem database. ChemDraw was used to draw the compound structure and all these ligands were prepared for molecular docking studies using Lig Prep version 2.3 [10]. The ligand structure energy was minimized; partial atomic charges were computed using the OPLS-2005 force field by using Schrödinger suite.

4.2.3. Results and Discussion

Since these dihydropyridine compounds are novel, we decided to include an additional application and investigated their potential to bind to proteins. Herein, docking of the ligand **A1** to Human mdm2 provides insights into the binding regions. Three hydrogen bonds were formed between GLU 25 (2.7 Å

distance), LEU 27 (3.2 Å distance) and LEU 54 (3.2 Å distance) atoms with binding energy of -8.91 kcal/mol in **Figure 23** (page 76). Docking of **A1** with Human mdm2 indicated lowest binding energy thereby showing strong affinity of the ligand molecule with the receptor which has been stabilized by strong hydrogen bond interactions in the binding pocket. This shows that **A1** is a better inhibitor for E3 ubiquitin-protein ligase mdm2 compared to the synthesized compounds **A2**-**A8**. The binding mode of **A1** within the active site of the protein was analyzed as shown in the molecular docking results in **Figure 25** (page 78). The suitable shape of this hit compound helped it to bind tightly with the active site of the ck2. Three hydrogen bond interactions were formed between the hit 6 into ck2. The hydrogen atom of the hit 6 nicely interacted with back bone oxygen atom of the hydrophobic residue of VAL 116. Then the hydrogen atom of the hit 6 nicely interacted with side chain of ASP 175. The bond length between the hit 6 into the active site of the ck2 was observed at (2.13Å, 2.06Å, 2.04Å). The glide score (-6.111 Kcal/mol) and glide energy (-62.406 Kcal/mol) was noted. Furthermore, the following residues were mainly involved in hydrophobic interaction LEU 45, VAL 116, VAL 66, VAL53, ILE 174, PHE 113, LYS 68, LEU 111, TRP 176, and LEU 85. **Table 6** shows the docking results of all of the compounds (**A1-A8**), glide score (Kcal/mol), glide energy (Kcal/mol), interacting residues, distance between the protein and ligand (Å), hydrogen bond donor and hydrogen bond acceptor. **Figure 23** (page 76), shows hydrogen bond formation of **A1** compound between GLU 25, LEU 27 and LEU 54 atoms, **Figure 24** (page 77), shows hydrogen bond formation and bond length of docking **A1** to human mdm2. **Figure 25 (**page 78), shows the binding mode of **A1** compound with E3 ubiquitin-protein ligase mdm2.

Table 6: Glide extra-precision (XP) results for 8 compounds (A1-A8) with human mdm2

Compound	Glide Score	Glide energy	No. of H bonds	Interacting Residues	Distance (Å)	Hydrogen bond donor	Hydrogen bond acceptor
A1	-6.111	-62.406	2	Tyr 104 (2)	2.20 2.15	A: TYR 104: (H)HH Ligand: (H)	Ligand: (O) Ligand: (N)
A2	-2.616	-27.659	-	-	-	-	-
A3	-4.391	-35.217	1	Thr 26	2.04	A: THR 26: (H)HG1	Ligand: (O)
A4	-3.963	-16.574	1	Thr 26	1.97	A: THR 26: (H)HG1	Ligand: (O)
A5	-4.995	-44.146	1	Thr 26	2.05	A: THR 26: (H)HG1	Ligand: (O)
A6	-4.667	-42.032	1	Thr 26	2.04	A: THR 26: (H)HG1	Ligand: (O)
A7	-1.089	-19.121	4	Arg 29 Glu 25 GLY 25	1.93 2.25 2.25 2.46	A: ARG29: (H)HH21 B: LYS 51: (H)HZ1 A: GLY 25: (O)OE1 A: GLY 25: (H)H1	Ligand: (N) Ligand: (N) Ligand: (H) Ligand: (O)
A8	-3.497	-49.899	1	Thr 26	2.15	A: THR 26: (H)HG1	Ligand: (O)

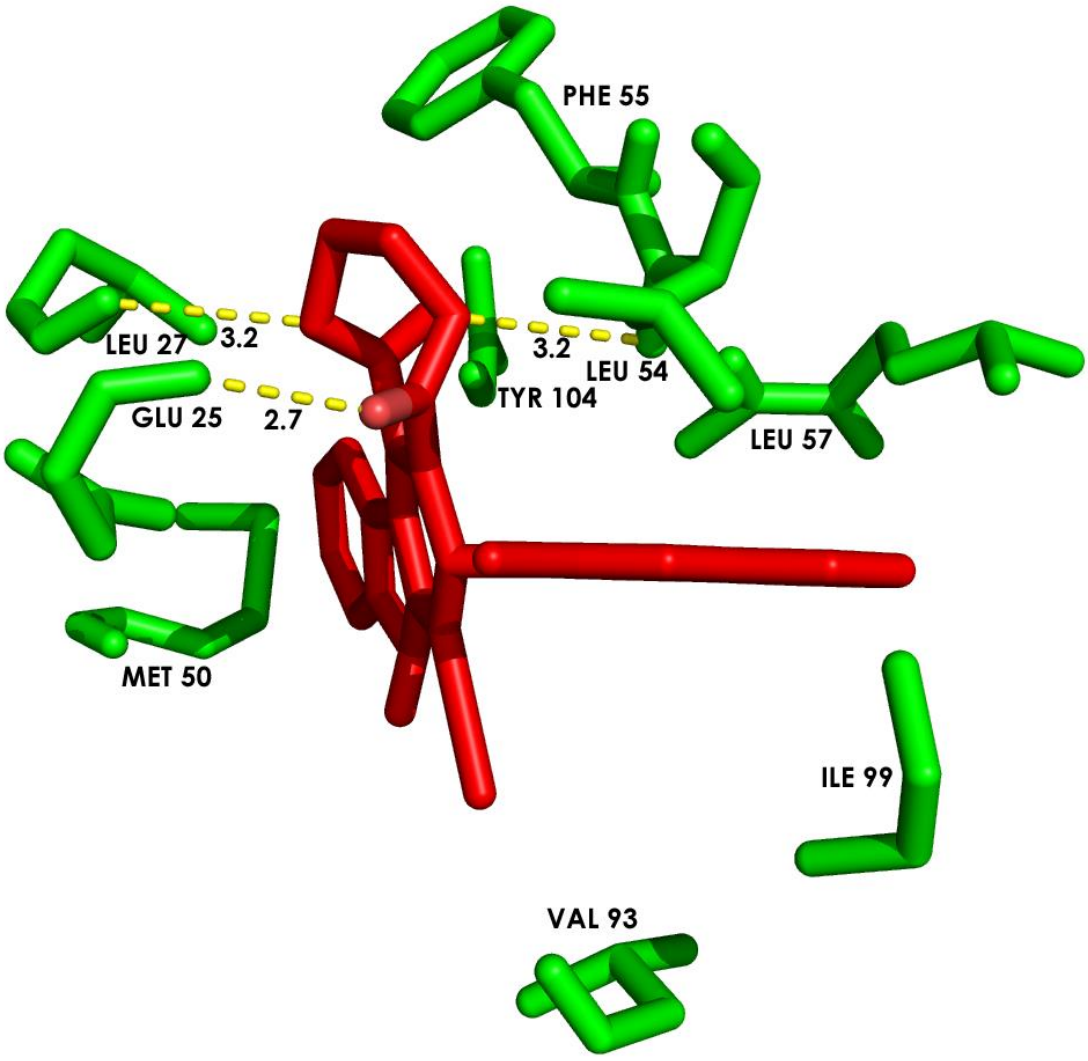

Figure 23 : Hydrogen bond formation of A1 between GLU 25, LEU 27 and LEU 54 atoms

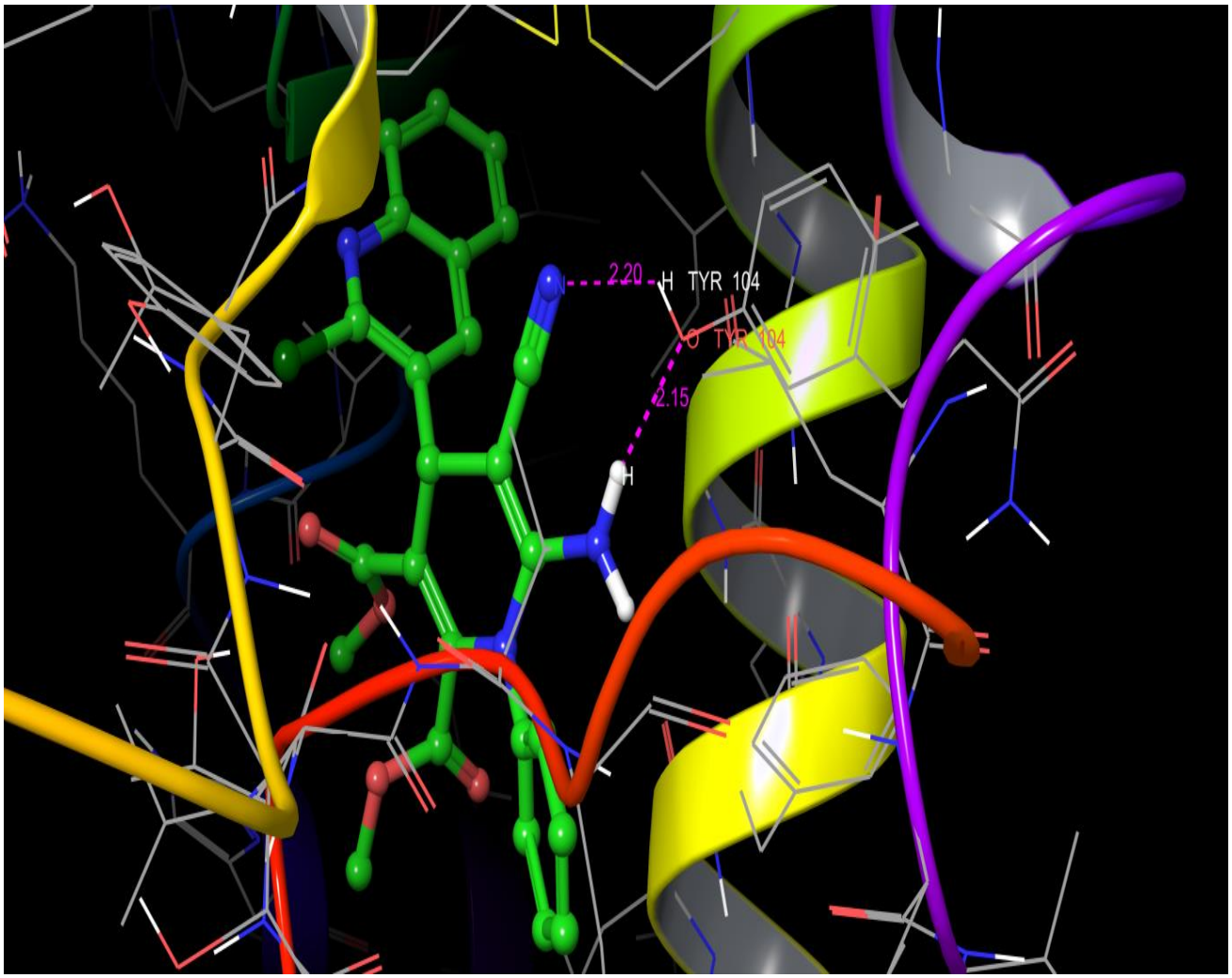

Figure 24 : Hydrogen bond formation and bond length of docking A1 compound to human mdm2

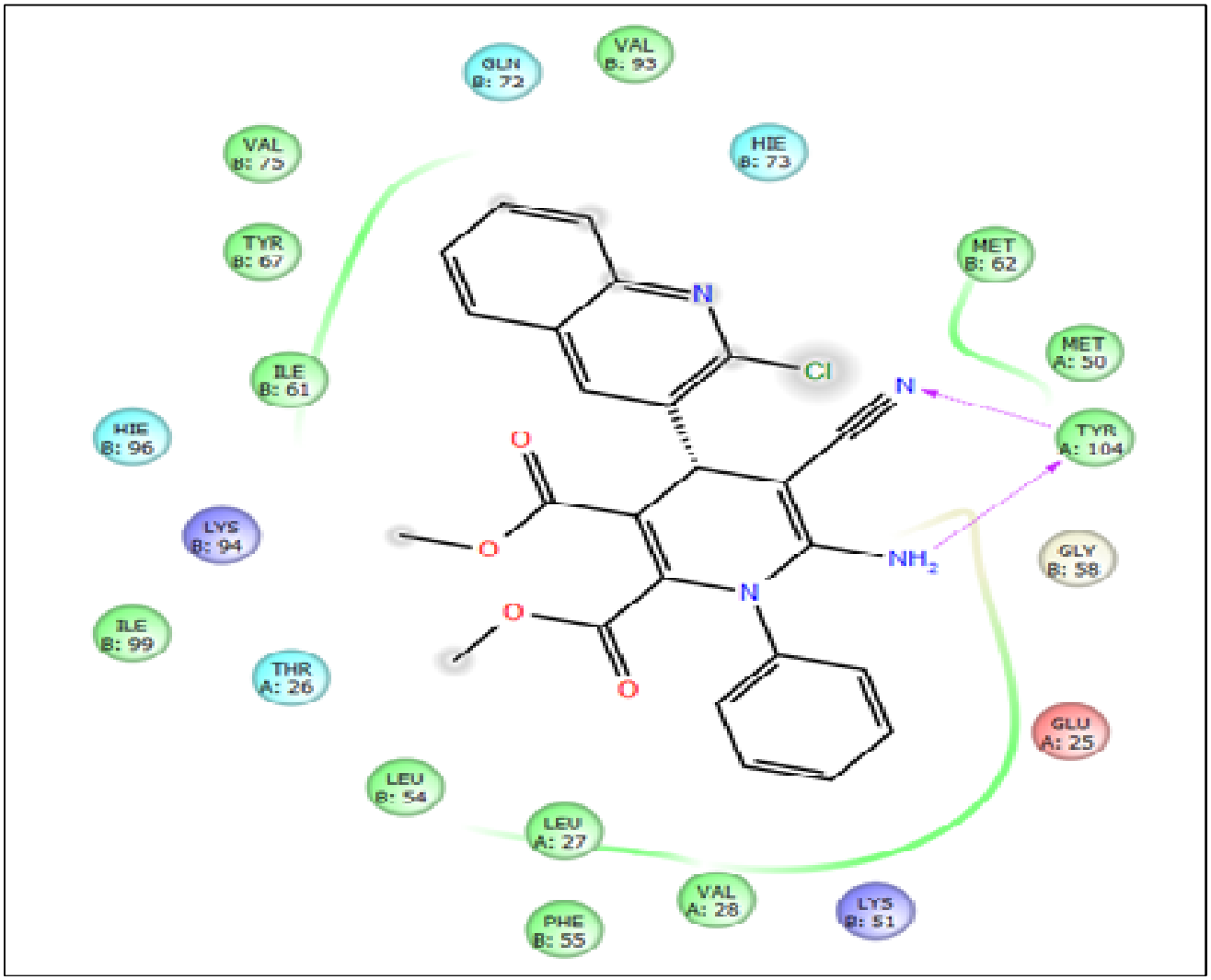

Figure 25: Binding mode of A1 compound with E3 ubiquitin-protein ligase Mdm2

4.2.4. Conclusion

Eight novel poly-functionalised dihydropyridine quinoline derivatives were subjected to molecular docking and the binding mode within the active site of protein was analysed; this was done to ascertain the possible behaviour of the newly synthesized compounds to the human mdm2 protein. On comparing the molecular docking of **A1-A8** with mdm2, **A1** showed the lowest binding energy (-6.111 Kcal/mol) thereby showing strong affinity of the ligand molecule with the receptor which has been stabilized by strong hydrogen bond interactions in the binding pocket. This interaction confirms that **A1** is the best inhibitor for mdm2 than all the other compounds tested.

4.3. Bacterial Studies

4.3.1. Introduction

Over the last decade, drug resistance to the commonly used antibiotics has become wide-spread. Therefore, the synthesis of new compounds that could be used for the effective treatment of infectious diseases without side effects is an urgent biomedical necessity [11]. Various heterocyclic compounds have shown anti-microbial potential and quinoline is one of the most promising. Quinoline heterocycles occur widely among medicinally important natural products. Realizing the medicinal importance of quinoline compounds, it was considered worthwhile to incorporate this moiety as a dihydropyridine.

Although many quinoline and quinolones have been synthesized and reported, the most notable ones used in veterinary medicine worldwide include, amifloxacin, benofloxacin, ciprofloxacin, danofloxacin, difofloxacin, norfloxacin, sarafloxacin. Other major quinolones in human medicine include enoxacin, ofloxacin, tosufloxacin etc. These fluoroquinolones share a great oral bioavailability in all monogastric species, a large volume of distribution and a low binding to plasma proteins that allows them to cross membranes and reach the most remote parts of the body at concentrations above the minimum inhibitory concentrations (MICôs) of most pathogens [12].

4.3.1.1. Experimental

4.3.1.2. Materials & Methods

4.3.1.3. The Preparation of Media

Fresh Nutrient Agar, Oxoid LTD (Hampshire, England) was prepared according to the manufacturerôs instruction as follows:

- 28g was weighed out into 3 separate one litre glass bottles each
- Distilled water was added until the one litre mark of each bottle was reached using measuring cylinder.
- The solution was mixed until the powder completely dissolved.
- Bottles were sterilized by autoclaving for 15 minutes at 121^0C
- The agar was poured into plates to solidify

4.3.1.4. The Preparation of the Nutrient Broth

Fresh Mueller Hinton Broth (Sigma-Aldrich) was made up according to manufacturerôs instruction as follows:

- 23g of Nutrient Broth powder was weighed into a 1L glass bottle

- Distilled water was added until the 1L mark was reached
- The solution was mixed until the powder completely dissolved
- This was dispensed into bijou bottles before autoclaving
- Bijou bottles were sterilized by autoclaving for 15 minutes at 121ºC

4.3.1.5. Microbial Cultures

The cultures of *S. aureus, E. coli and P. aeruginosa* were maintained on nutrient agar slopes at 4ºC and sub cultured on to blood agar plates for 24 hours before use.

4.3.1.6. Preparation of Reagent: Microplate Alamar Blue Assay (MABA)

An amount of 0.2g of Resazurin powder was dissolved in 10 mL autoclaved distilled water. The dye solution was vortexed vigorously; the solution was immediately covered with aluminium foil to keep away from light as it is light sensitive [13].

4.3.2. Results and Discussion

The minimum inhibitory concentration (MIC) was determined by serially diluting the extracts using nutrient broth. Each test tube was inoculated with a bacterial suspension containing 1 x 10^6 CFU/mL and incubated at 37ºC for 24 hours. The MIC was regarded as the lowest concentration of the extract which would not permit any visible growth when compared with extract free broths inoculated with each of the bacterial suspensions. They were incubated at 37ºC for 24 hours and were examined for growth. Each extract was tested twice with each bacterium. The activities of the synthesized compounds were studied by Microplate Alamar Blue Assay (MABA) using 96-wells microplates including a 40 εL positive control (containing 20 εL standard antibiotic) and growth control (containing 20 εL culture broth without testing materials). Then 100 εL of each concentration of the synthesized compounds were added to two neighbor wells except for the positive and growth control wells. After adding Alamar Blue (20 εL) to all of 96 wells, the total volume in each well reached 200 εL. The final concentrations of the tested compounds were 256, 128, 64, 32, 16, 8, 4, 2, 1 εM etc.

After incubation, results were recorded as MIC. A series of eight novel poly-functionalised dihydropyridines quinoline (**A1-A8**) were evaluated for antibacterial activity against two Gram-negative bacteria, *E. coli* and *P. aeruginosa* and one Gram-positive bacterium, *S. aureus*. Standard antibiotics, ciprofloxacin and nalidixic acid were used as positive controls and DMSO used as negative control. DMSO had no effect on the bacteria at the concentrations used. The anti-microbial activity results, presented in **Table 7**, revealed that the synthesized poly-functionalized dihydropyridine quinoline

derivatives showed moderate to good activity towards the mentioned panel of bacteria strains compared to standard antibiotics. It is interesting to note that compounds with substituted anilines in the *para* position (**A4, A7 & A8**) showed very good activity against all strains. These compounds (**A4, A7 & A8**) were found more potent than both standards, ciprofloxacin (MIC = 50 µM) and nalidixic acid (MIC = 50 µM) towards *S. aureus* and *P. aeruginosa.* Moreover, compound **A8** (MIC = 16 µM) was found equipotent to nalidixic acid (MIC = 16 µM) towards *E. coli*. Compound **A1** (MIC = 128 µM) exhibited comparable activity as the standard nalidixic acid (MIC = 128 µM) against *P. aeruginosa*. Compound **A1** and **A6** showed no inhibitory effect against *S. aureus* and **A6** indicated no inhibitory effect against *E. coli* as well. Compounds **A5** showed moderate activity against *S. aureus* and *E. coli,* **A2** and **A3** showed poor activity towards all strains compared with the standard antibiotics.

Table 7: Antibacterial activities of quinoline derivatives: Minimum Inhibitory Concentration (µM)

Compound	***S. aureus***	***P. aeruginosa***	***E. coli***
A1	-	128	256
A2	256	256	256
A3	256	256	256
A4	16	32	32
A5	128	256	128
A6	-	256	-
A7	32	32	32
A8	8	16	16
Ciprofloxacin	50	25	25
Nalidixic Acid	50	128	16
DMSO	-	-	-
Standard anti-bacterial drugs: Ciprofloxacin and Nalidixic acid. **(-): Has no bacterial effect.**			

4.3.3. Conclusion

Eight novel poly-functionalised dihydropyridine quinoline derivatives were evaluated for their anti-bacterial activity. The results showed that compounds **A4**, **A7** and **A8** have good activity compared to that of ciprofloxacin and nalidixic acid. Compounds **A8** showed the best activity with MIC of 8 µM, 16 µM and 16 µM for *S. aureus, P. aeruginosa and E. coli,* respectively.

Chapter Five: Summary

Green chemistry calls attention to the development and improvement of environmentally kind chemical methods and technologies. Besides typical multi-step synthesis, an increasing number of organic chemical compounds are formed by MCRôs. The quinoline nucleus is one of the active constituents present in many standard drugs and is known to increase the pharmacological activity of the molecule. The presence of substituents like chlorine, fluorine and methyl groups in quinoline compounds contribute to the net biological activity. In this study, we have embarked on MCRôs based approach to achieve our synthetic targets in an ideal and speedy way. Since the synthesis of organic compounds used to be dull and lengthy, we decided to use our current knowledge of simple synthesis and expand it to MCRôs. The exceptional structural design of quinoline has been used as a starting point for an elegant design of potential drugs and novel heterocycles. As mentioned earlier in the thesis, quinoline derivatives display a wide range of activities. Very few approaches have been directed at the synthesis of heterocycles containing both quinoline and pyridine nuclei within a single molecular framework. Thus, in the synthetic part of this study, we reported the synthesis of novel quinoline derivatives. The focus was on the poly-functional dihydropyridine containing quinoline moiety with the intention of improving the biological activity of the final product i.e anti-cancer assay, anti-bacterial activity and molecular modeling. Furthermore, we wanted to increase our research synthetic activity in terms of green chemistry. Eight poly-functionalised dihydropyridine quinoline derivatives were successfully synthesized by a one pot, four-component reaction; cyclocondensation of 2-chloro-3-formyl quinoline, arylamines, malononitrile and dimethyl acetylenedicarboxylate in the presence of catalytic amount of triethylamine. The compounds were prepared in good yield in a minimum reaction time of ten hours at ambient temperature.

The anti-cancer assay indicated that poly-functionalised dihydropyridine quinoline derivatives, **A2**, **A3, A4** and **A8** having OCH_3, CH_3 and Cl substituents in the benzene ring, respectively, has the potential to be anti-cancer drug. Among them, **A2, A4** and **A8** proved to be dose dependent with **A4** having the highest toxicity at 250 µM and **A8** having the highest toxicity at 125, 250 and 500 µM.

In addition, **A1, A5, A6** and **A7** were not cytotoxic; however, the cytotoxicity of **A2**, **A3, A4** and **A8** was enhanced by the presence of the substituent (OCH_3, CH_3 and Cl) in the benzene ring. The docking result in the form of XP Glide scores of the 8 poly-functionalised dihydropyridine quinoline derivatives (**A1-A8**) with E3 ubiquitin-protein ligase mdm2 was investigated. The stability of docking between ligand and the target protein depended on the binding interactions and thus the Glide score (-6.111 Kcal/mol) of **A1** describes how well the drug has interacted with the protein. The results revealed

that **A1** has minimum binding and docking energy and may be considered a good inhibitor of mdm2 and it may be an important molecule for researchers to develop cancer drugs. Hence compound **A2-A8** showed an interesting correlation between docking scores and experimental binding data. The novel synthetic compounds were further evaluated for their anti-bacterial activities by serial dilution method. The organisms employed were *E. coli, P. aeruginosa and P. aureus*. Ciprofloxacin and nalidixic acid were employed as the standard drugs. Compounds (**A4, A7 & A8**), were found to be more potent compared to that of standard drugs, ciprofloxacin and nalidixic acid.

References

1. G L Firestone, Anticancer activities of artemisinin and its bioactive derivatives, *Rev. Mol. Med.* 1, **2009**, 11-15.
2. J J Lu, Dihydroartemisinin induces apoptosis in HL-60 leukemia cells dependent of iron and p38 mitogen-activated protein kinase activation but independent of reactive oxygen species, *Cancer Biol*. 1, **2008**, 1017-1025.
3. G Caeiro, J M Lopes, P Magnoux, P Ayrault, F R Ribeiro, A FT-IR study of deactivation phenomena in catalytic cracking: Nitrogen poisoning, coke formation and acidity-activity correlations, *J. Catal.* 249, **2007**, 234-236.
4. R Supino, MTT assays, *Methods Mol. Biol*. 43, **1995**, 137-140.
5. S Zhou, Y Li, T Hou, Human infection with a novel avian-origin influenza A (H7N9) virus, *N Engl. J. Med.* 368, **2013**, 1888-18890.
6. M Frank, Computational docking as a tool for the rational design of carbohydrate-based drugs, *Carbohydrates as Drugs,* 12, **2014**, 53-54.
7. T A Halgren, R B Murphy, R A Friesner, H S Beard, L L Frye, W T Pollard, J L Banks, Glide: A new approach for rapid, accurate docking and scoring. 2. Enrichment factors in database screening, *J. Med. Chem*. 47, **2004**, 1750-1759.
8. R T Kroemer, Structure-based drug design: Docking and scoring, current protein and peptide science, *Curr. Protein Pept. Sci.* 8, **2007**, 328-338.
9. Glide, Version 5.5, Schrodinger, LLC, New York, NY, **2009**.
10. Ligprep, Version 2.3. Schrodinger, LLC, New York, NY, **2009**.
11. A J Alanis, Resistance to antibiotics: are we in the post-antibiotic era, *Archives of Med. Res.* 36, **2005**, 697-700.
12. G Sarkozy, Quinolones: a class of antimicrobial agents, *Vet. Med. Zchech*, 46, **2001**, 257-259.
13. A W Fothergill, M G Rinaldi. Comparative evaluation of macrodilution and alamar colorimetric microdilution broth methods for antifungal susceptibility testing of yeast isolates, *J. Clin. Microbiol*. 33, **1995**, 2660-2665.

APPENDICES

Appendix 1

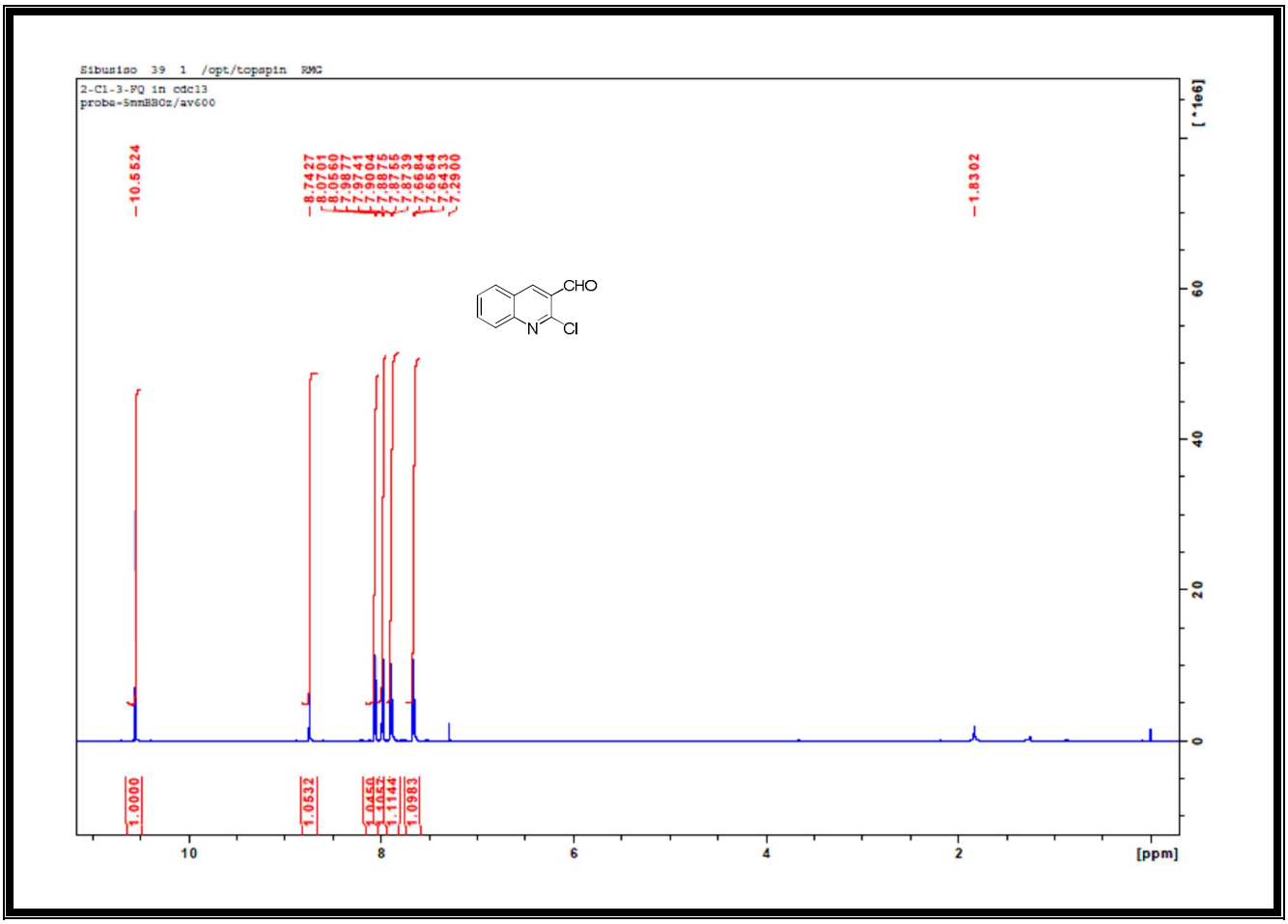

Figure 26: ^{1}H NMR Spectrum of 2-chloro-3-formylquinoline

Appendix 2

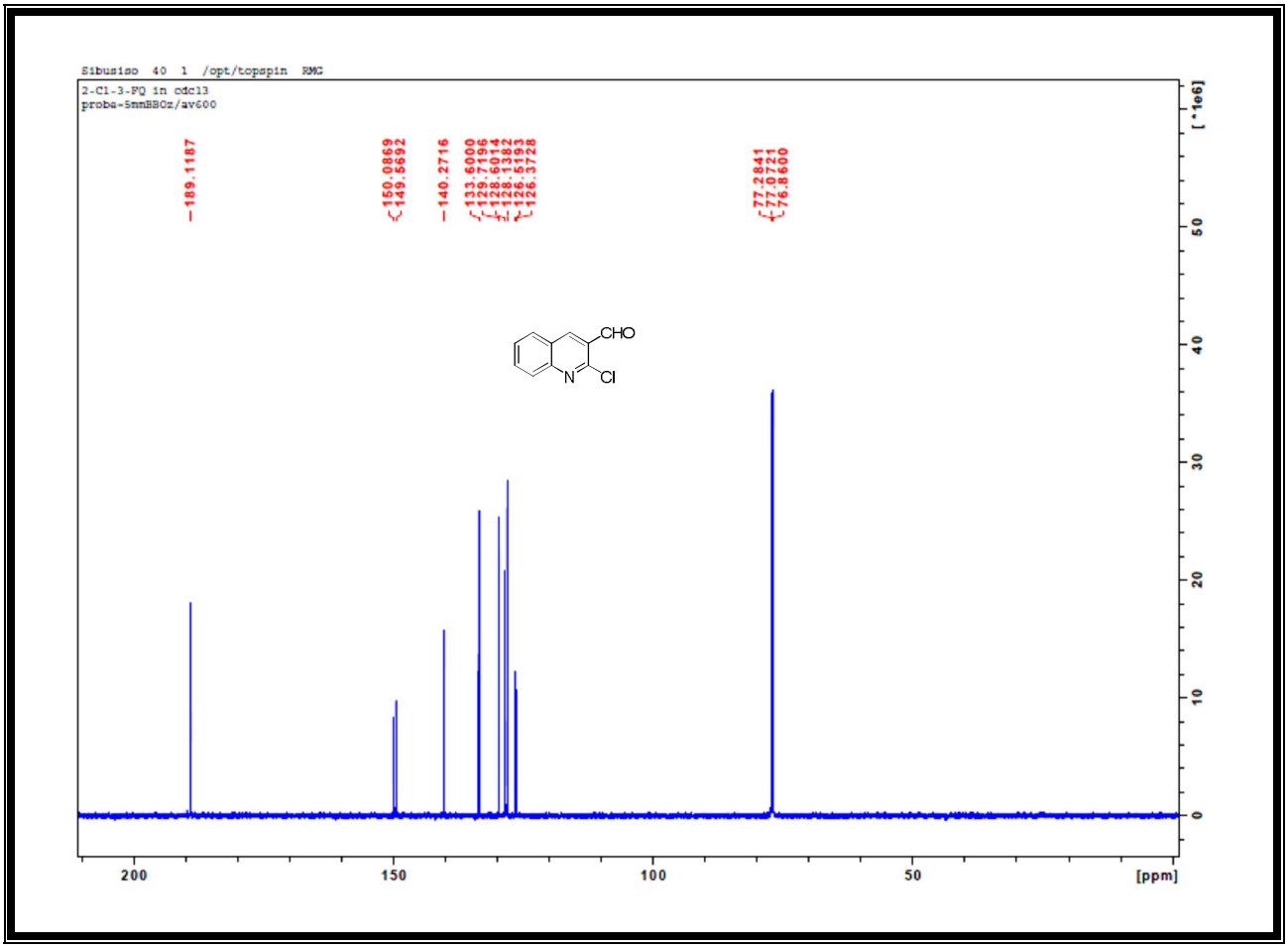

Figure 27: ^{13}C NMR Spectrum of 2-chloro-3-formylquinoline

Appendix 3

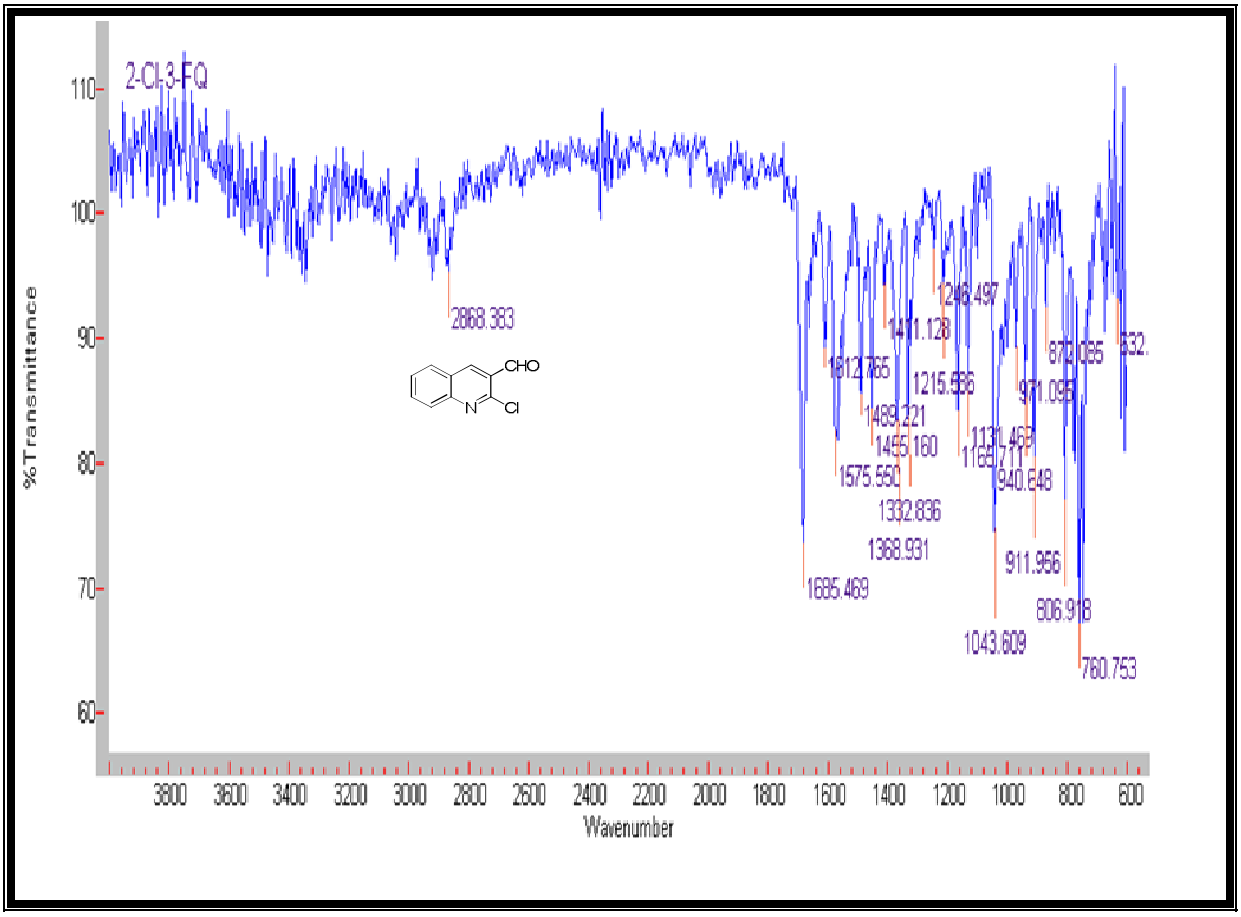

Figure 28: IR Spectrum of 2-chloro-3-formylquinoline

Appendix 4

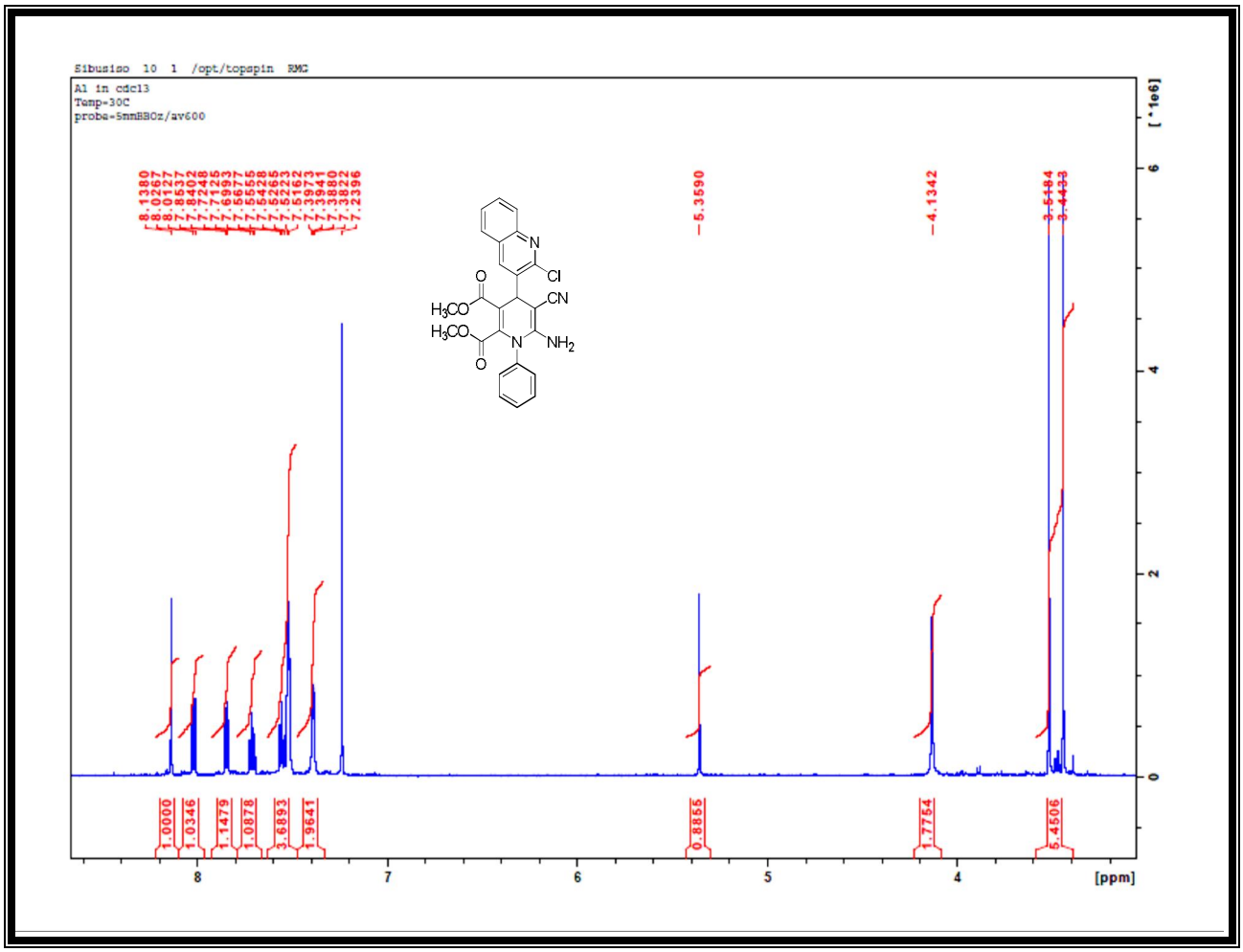

Figure 29: ^{1}H NMR Spectrum of A1, dimethyl 6-amino-4-(2-chloroquinolin-3-yl)-5-cyano-1-phenyl-1,4-dihydropyridine-2,3-dicarboxylate

Appendix 5

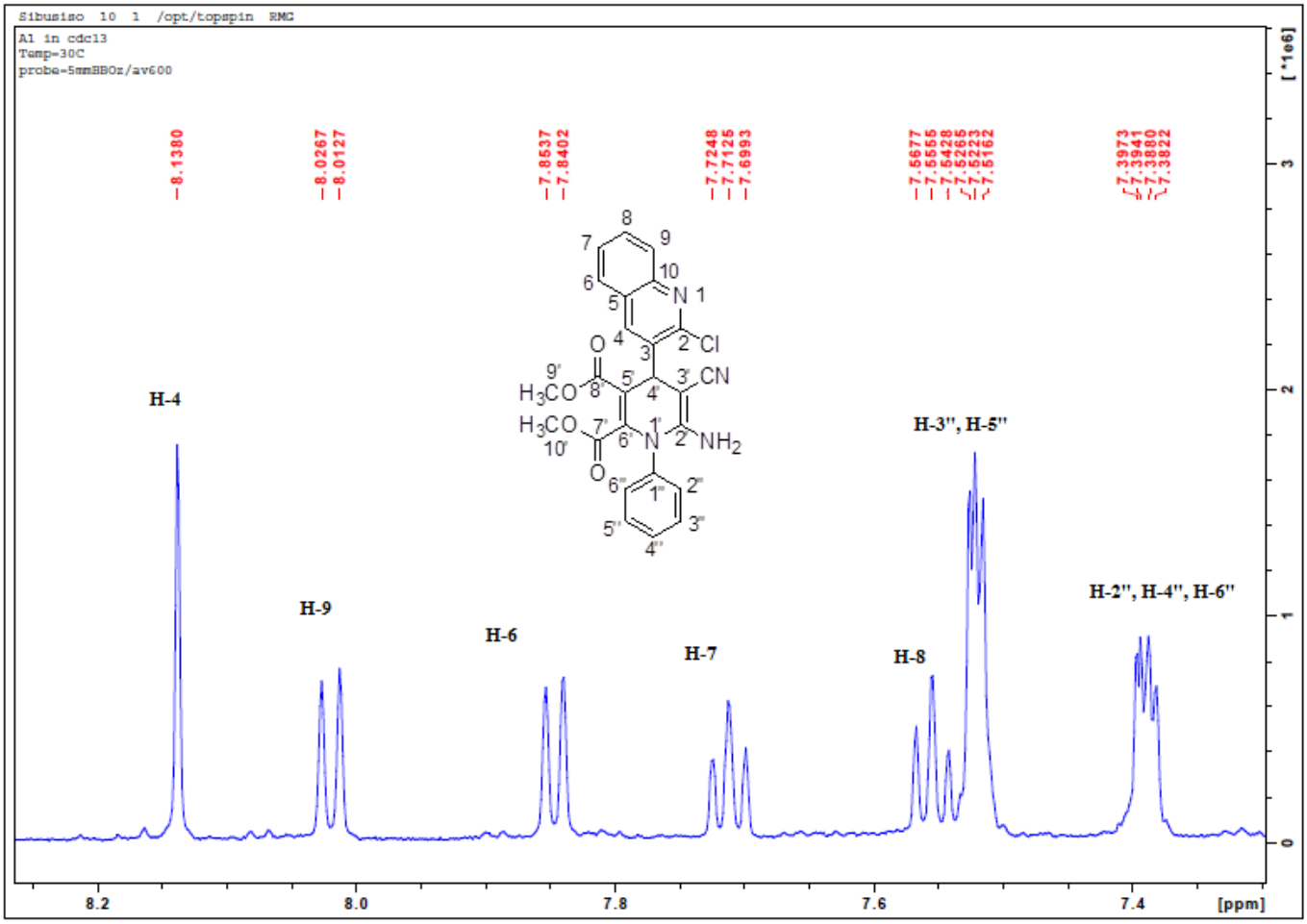

Figure 30: ^{1}H NMR Expanded spectrum of A1, dimethyl 6-amino-4-(2-chloroquinolin-3-yl)-5-cyano-1-phenyl-1,4-dihydropyridine-2,3-dicarboxylate

Appendix 6

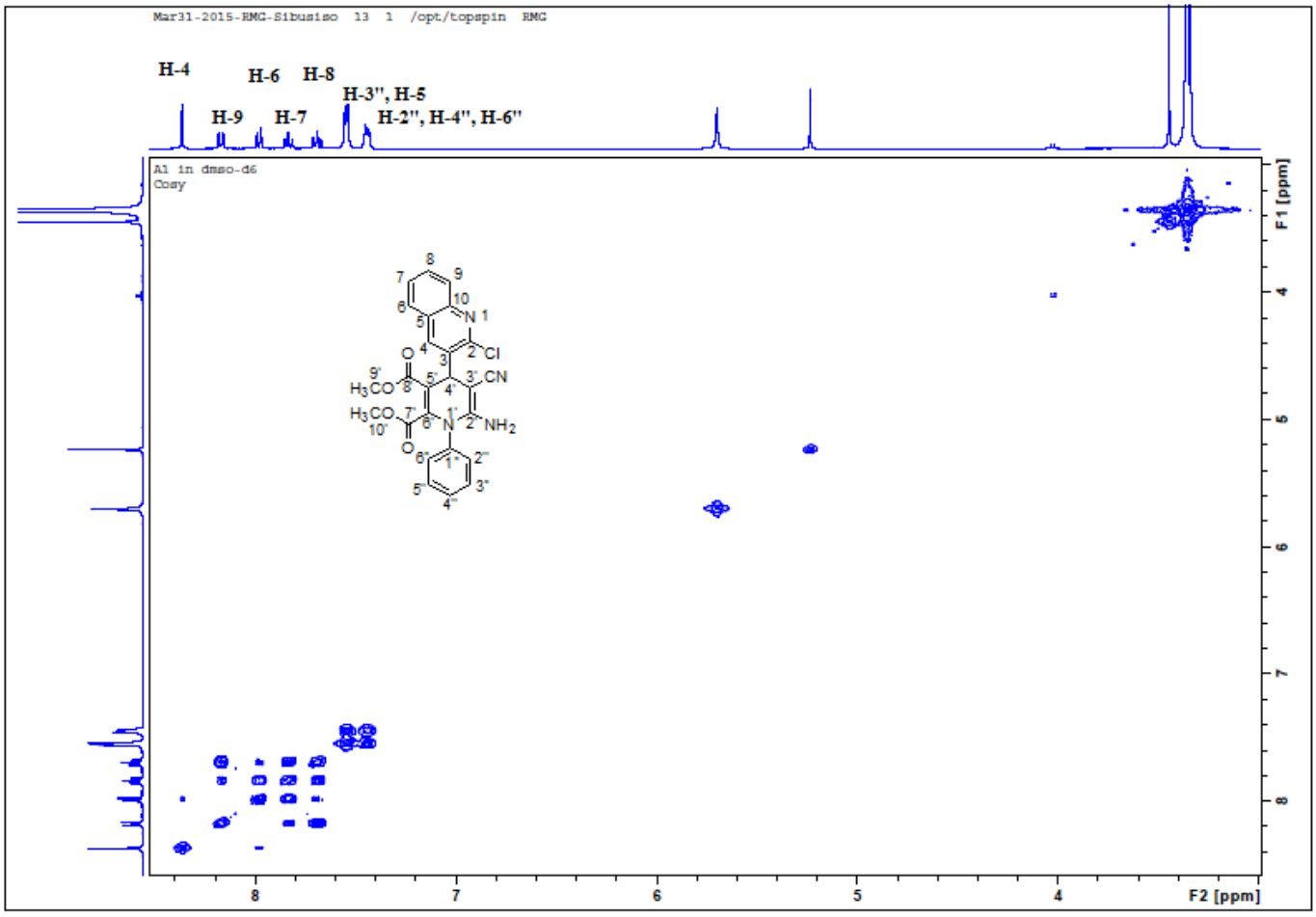

Figure 31: COSY Spectrum of A1, dimethyl 6-amino-4-(2-chloroquinolin-3-yl)-5-cyano-1-phenyl-1,4-dihydropyridine-2,3-dicarboxylate

Appendix 7

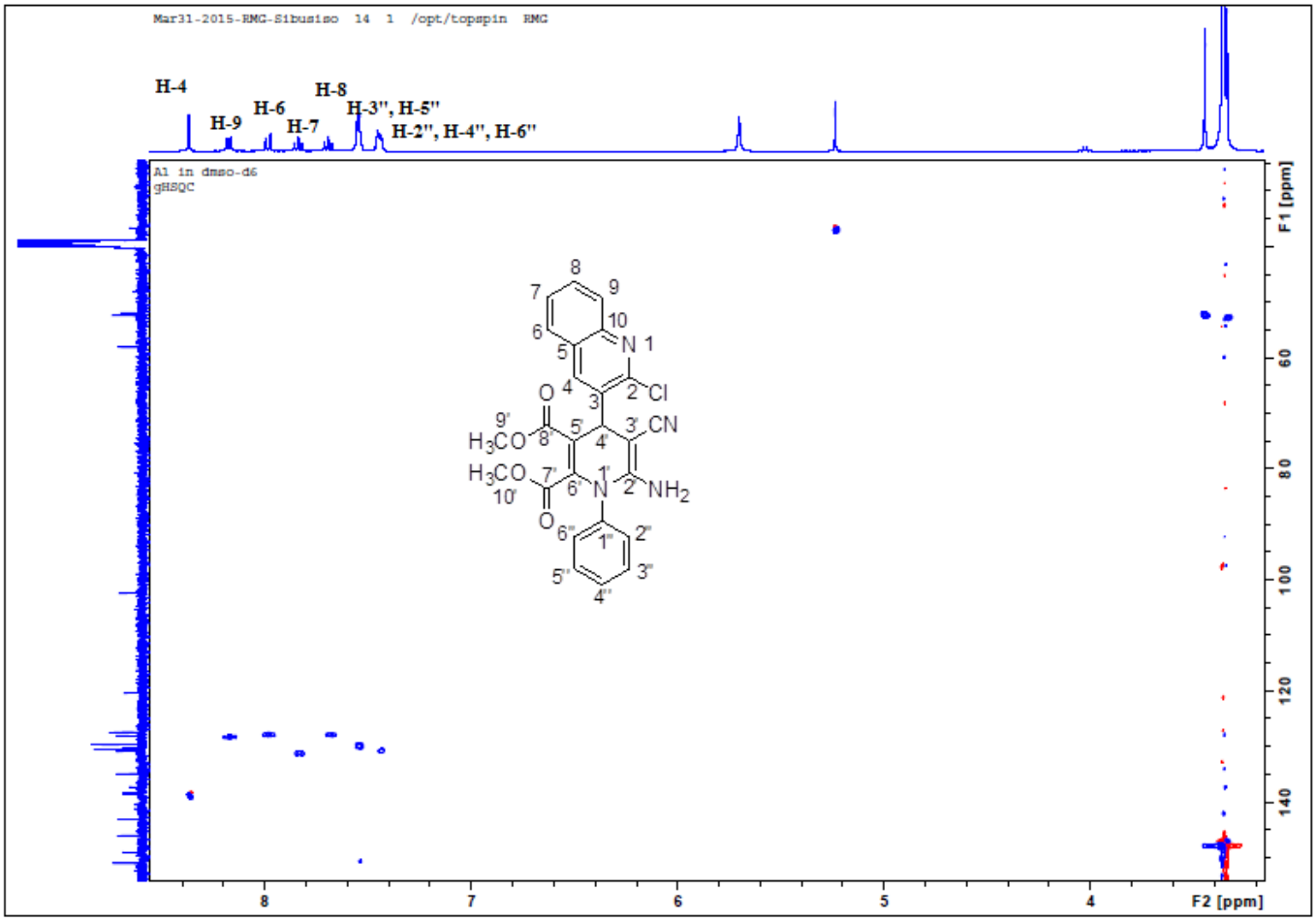

Figure 32: HSQC Spectrum of A1, dimethyl 6-amino-4-(2-chloroquinolin-3-yl)-5-cyano-1-phenyl-1,4-dihydropyridine-2,3-dicarboxylate

Appendix 8

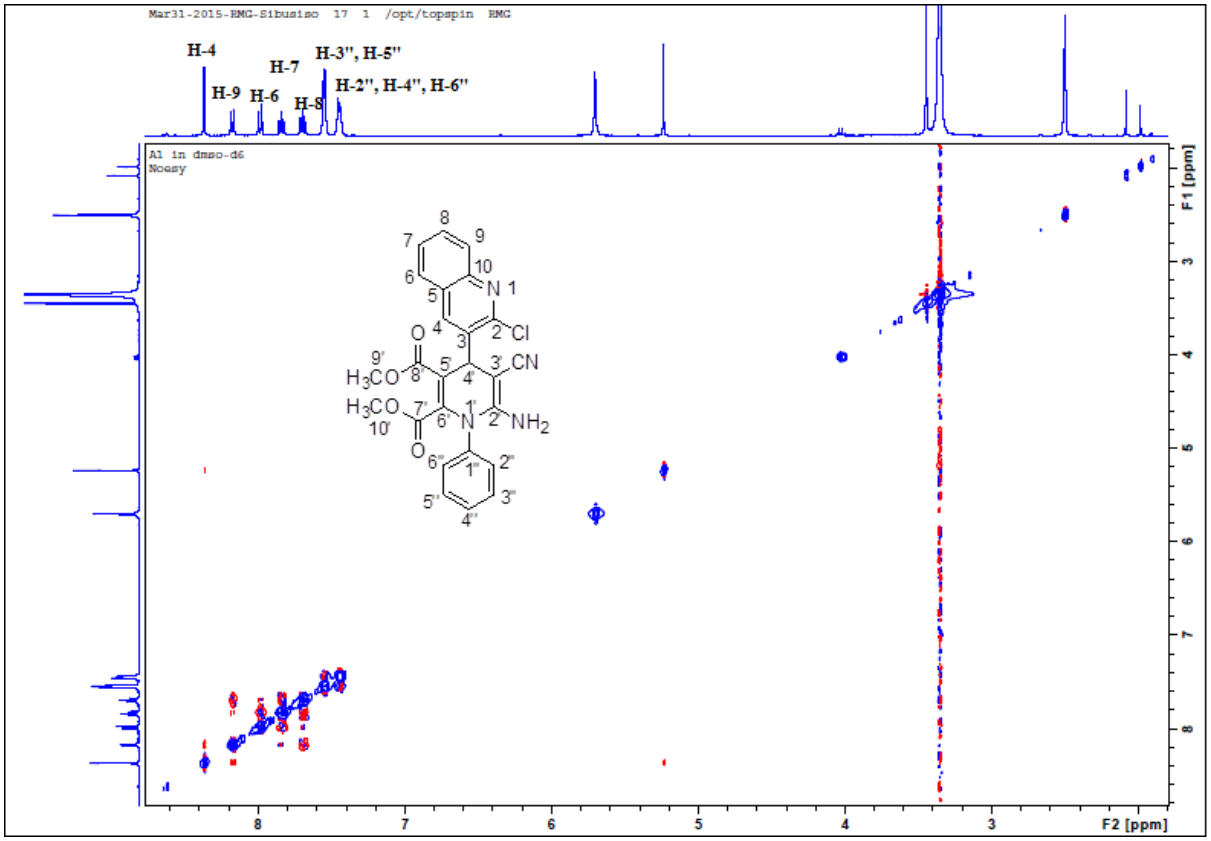

Figure 33: NOESY Spectrum of A1, dimethyl 6-amino-4-(2-chloroquinolin-3-yl)-5-cyano-1-phenyl-1,4-dihydropyridine-2,3-dicarboxylate

Appendix 9

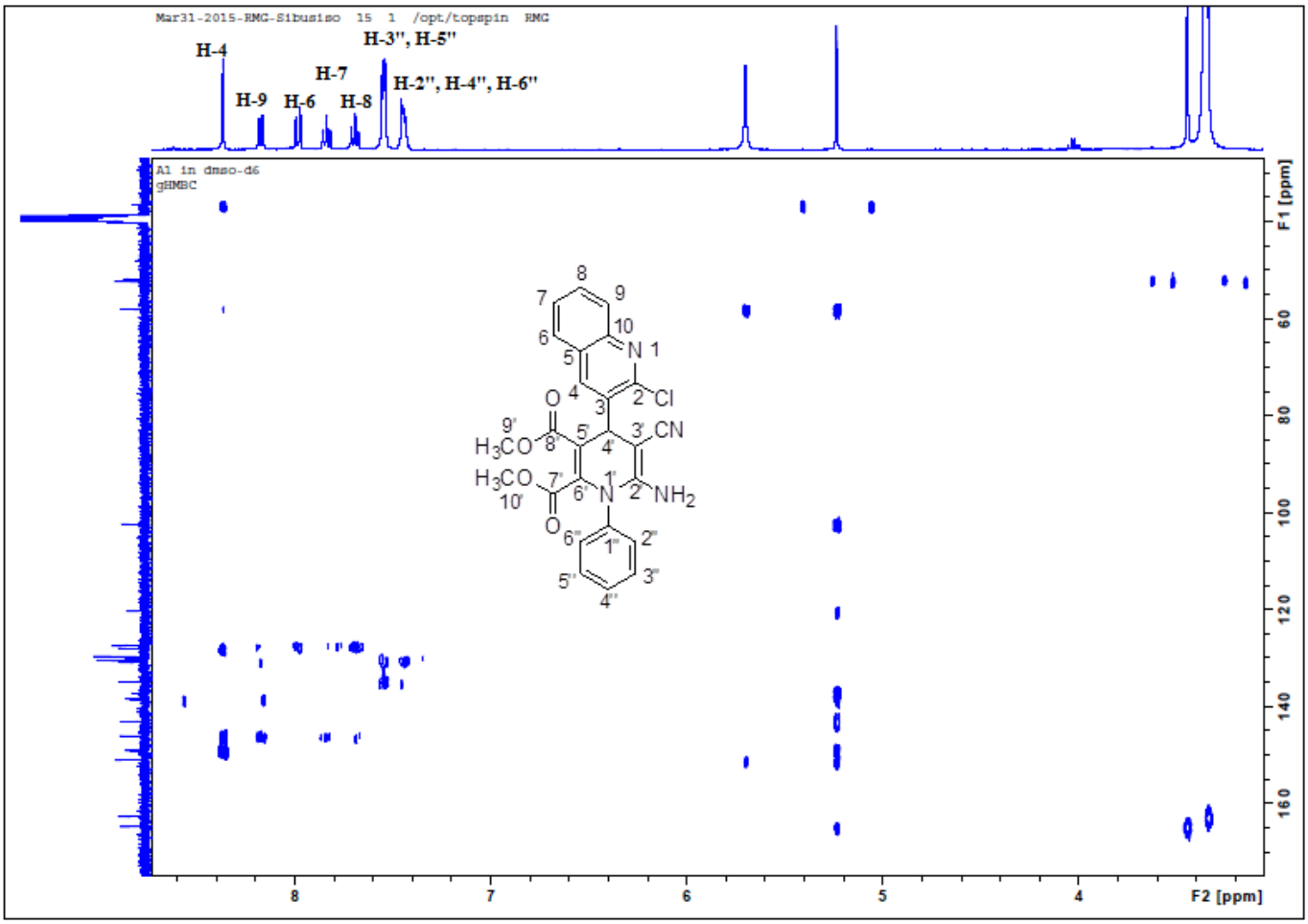

Figure 34: HMBC Spectrum of A1, dimethyl 6-amino-4-(2-chloroquinolin-3-yl)-5-cyano-1-phenyl-1,4-dihydropyridine-2,3-dicarboxylate

Appendix 10

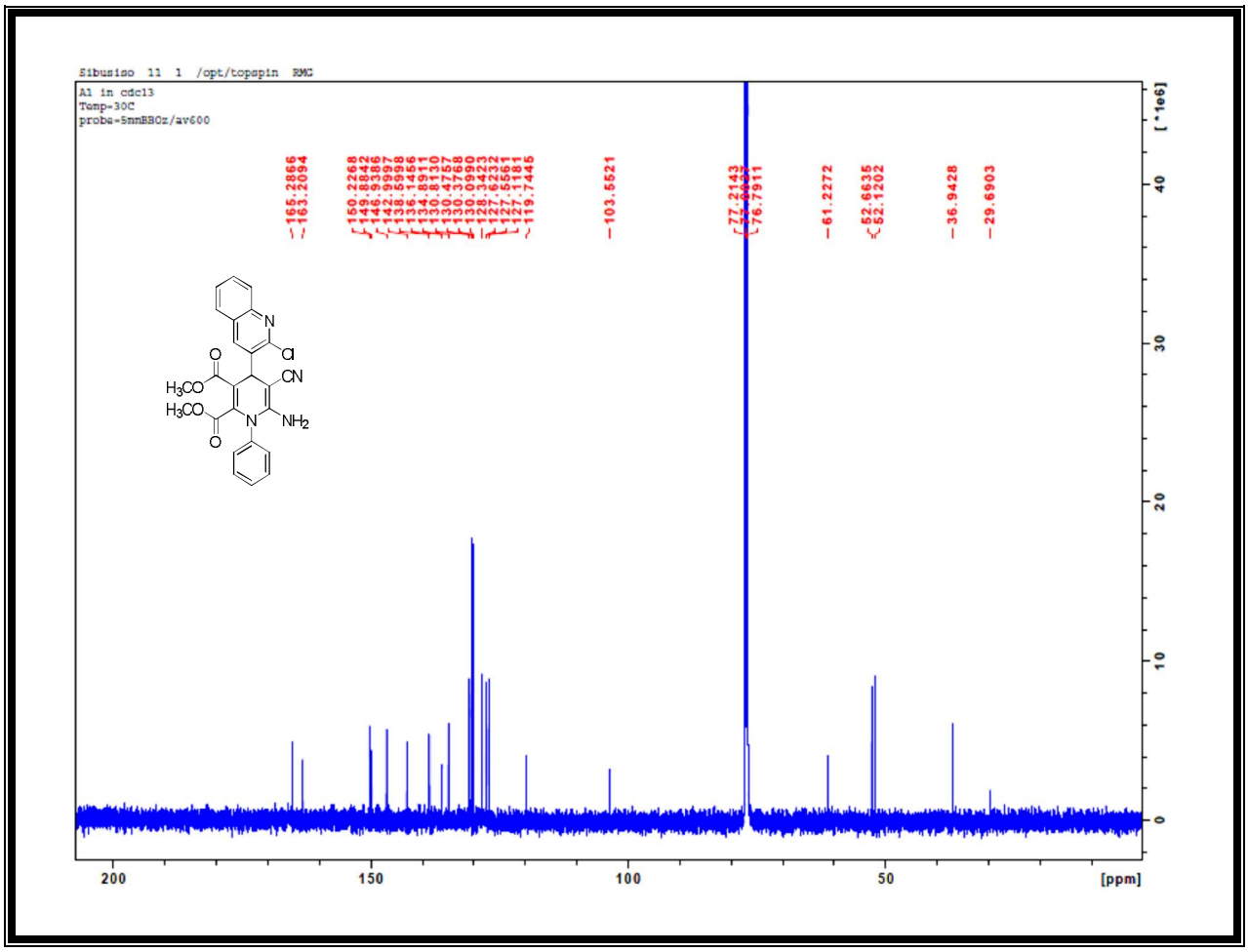

Figure 35: ^{13}C NMR Spectrum of A1, dimethyl 6-amino-4-(2-chloroquinolin-3-yl)-5-cyano-1-phenyl-1,4-dihydropyridine-2,3-dicarboxylate

Appendix 11

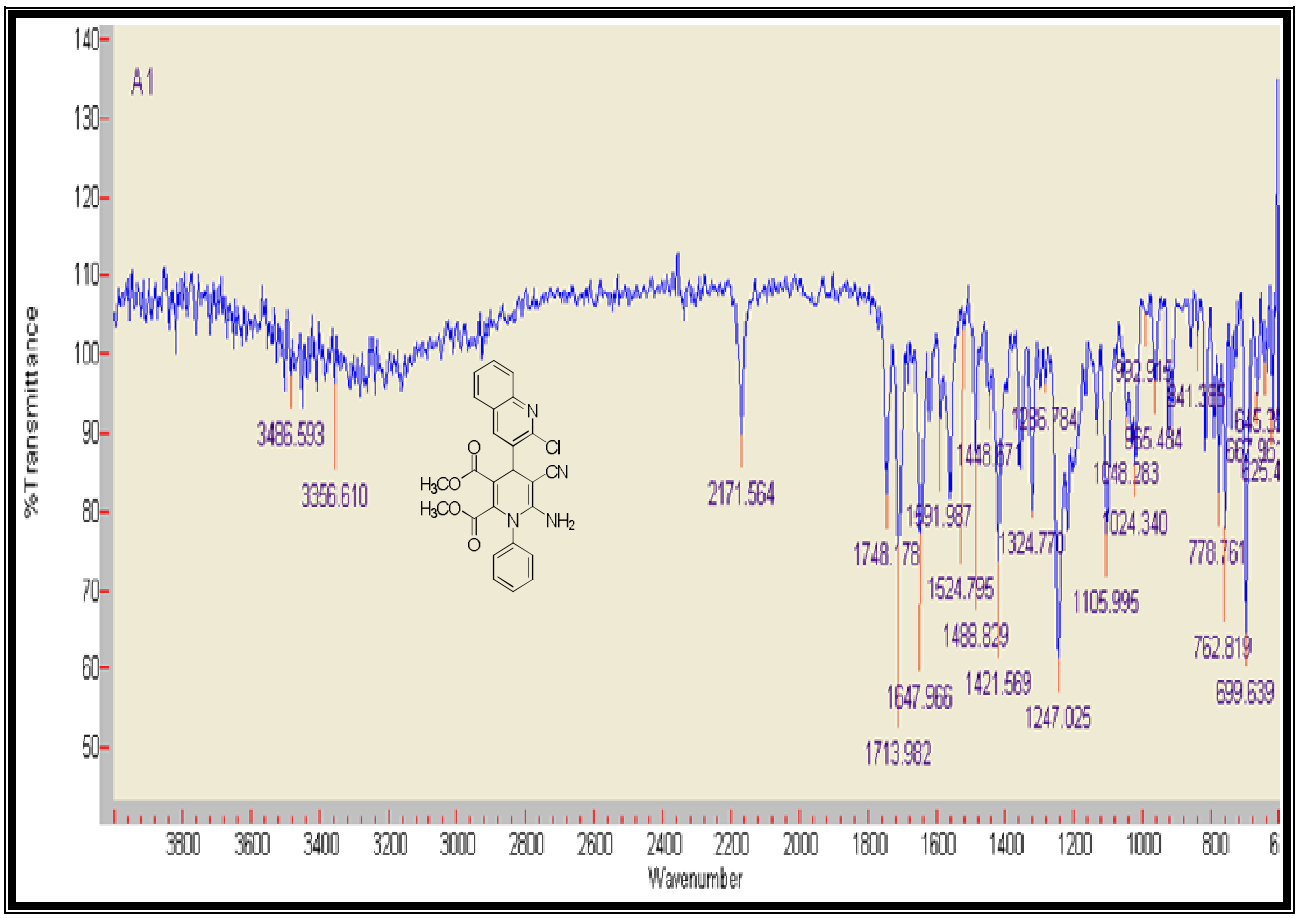

Figure 36: The IR Spectrum of A1, dimethyl 6-amino-4-(2-chloroquinolin-3-yl)-5-cyano-1-phenyl-1,4-dihydropyridine-2,3-dicarboxylate

Appendix 12

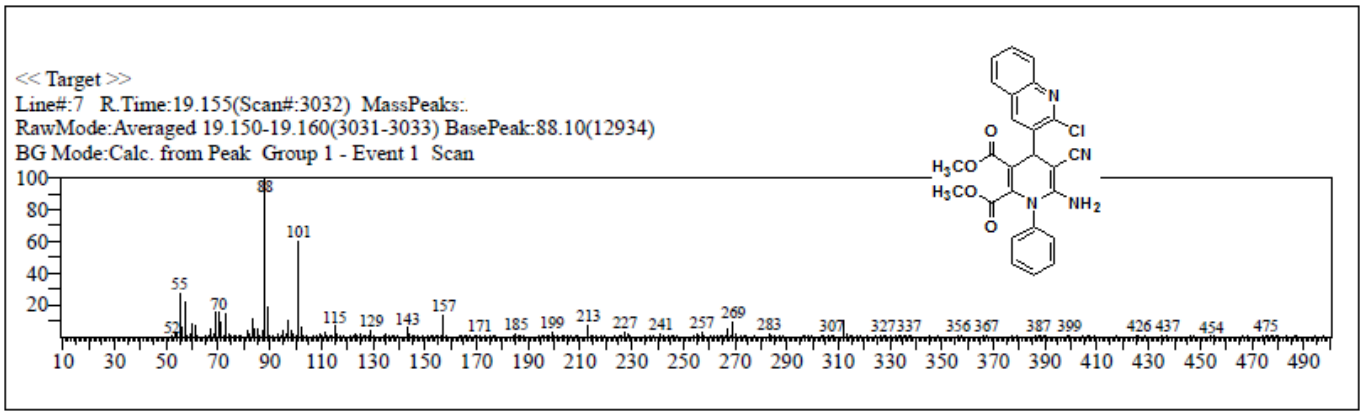

Figure 37: The Mass Spectrum of A1, dimethyl 6-amino-4-(2-chloroquinolin-3-yl)-5-cyano-1-phenyl-1,4-dihydropyridine-2,3-dicarboxylate

Appendix 13

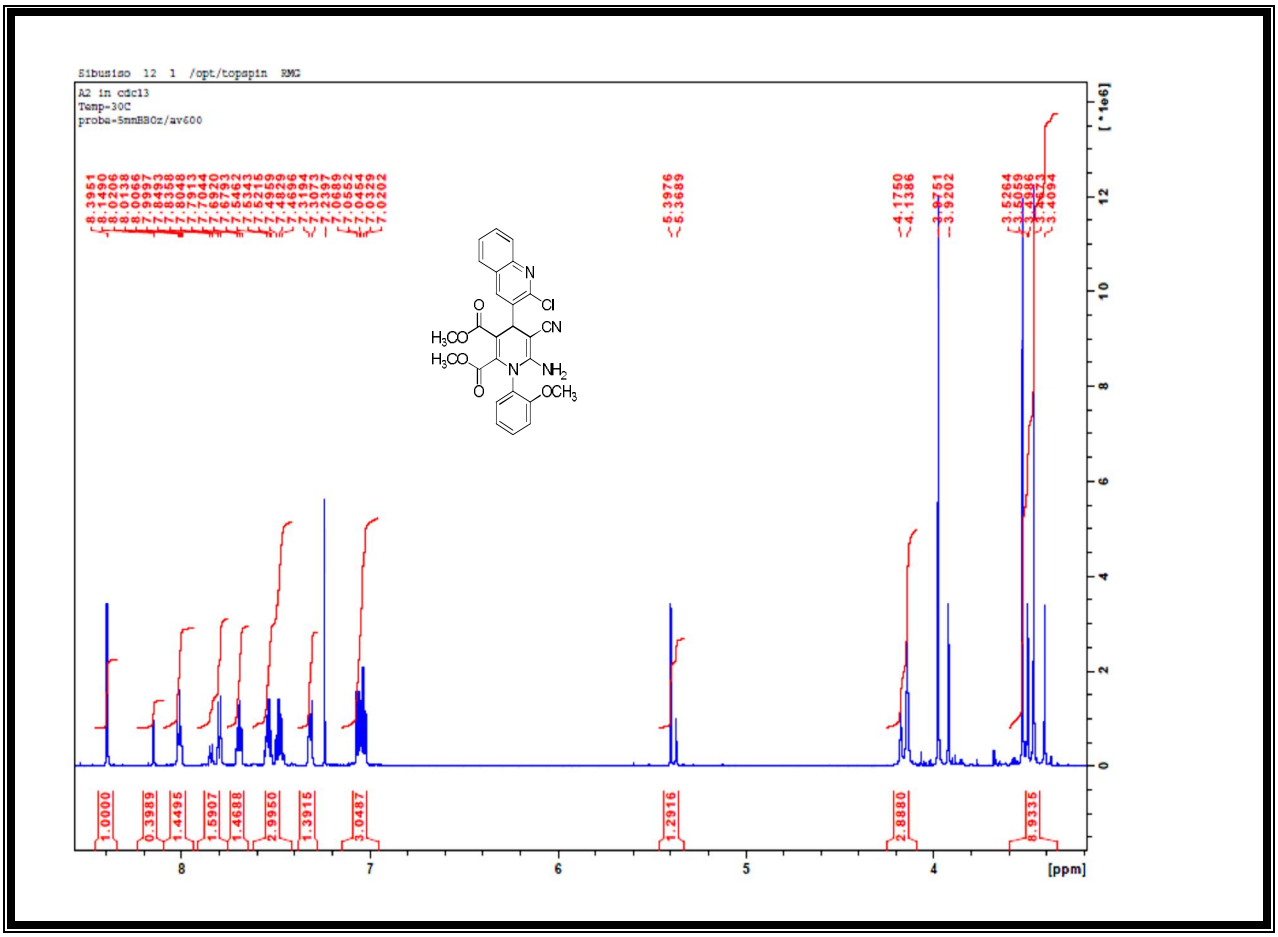

Figure 38: ^{1}H NMR Spectrum of A2, dimethyl 6-amino-4-(2-chloroquinolin-3-yl)-5-cyano-1-(2-methoxyphenyl)-1,4-dihydropyridine-2,3-dicarboxylate

Appendix 14

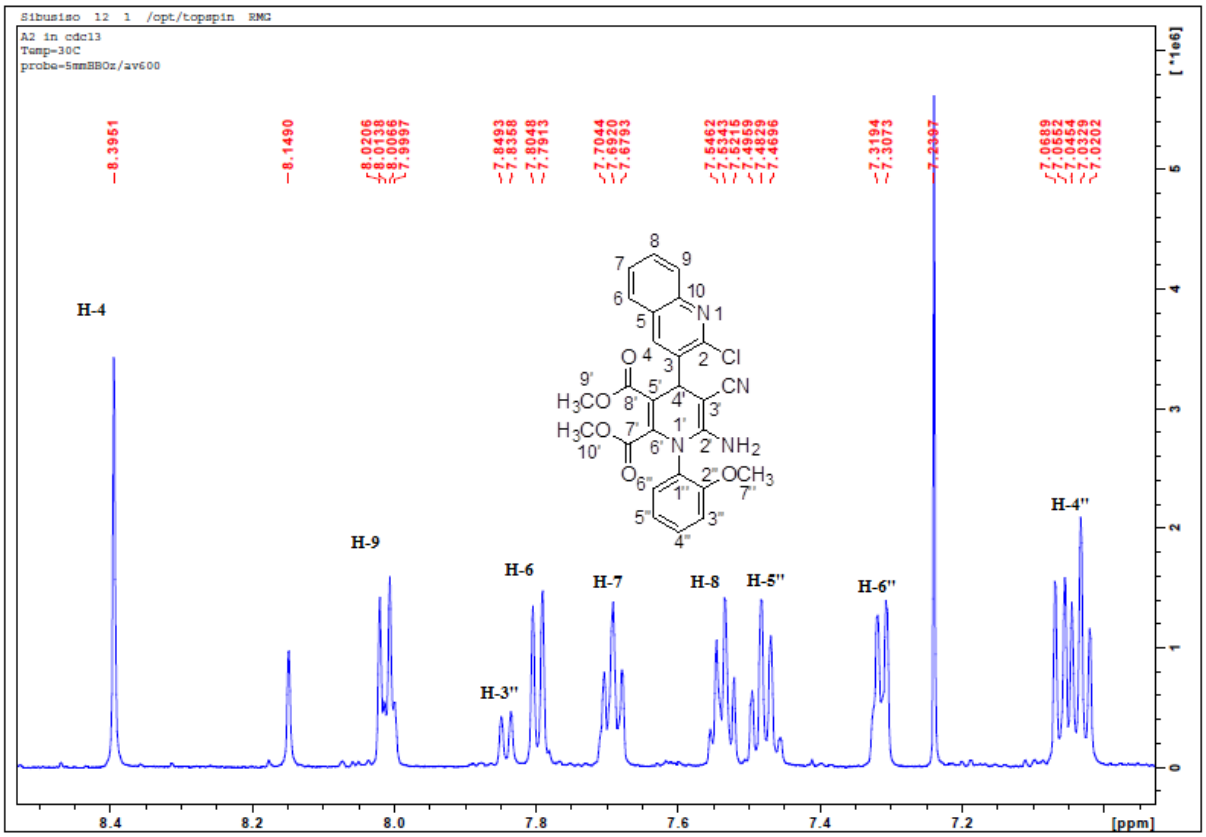

Figure 39: ^{1}H NMR Expanded spectrum of A2, dimethyl 6-amino-4-(2-chloroquinolin-3-yl)-5-cyano-1-(2-methoxyphenyl)-1,4-dihydropyridine-2,3-dicarboxylate

Appendix 15

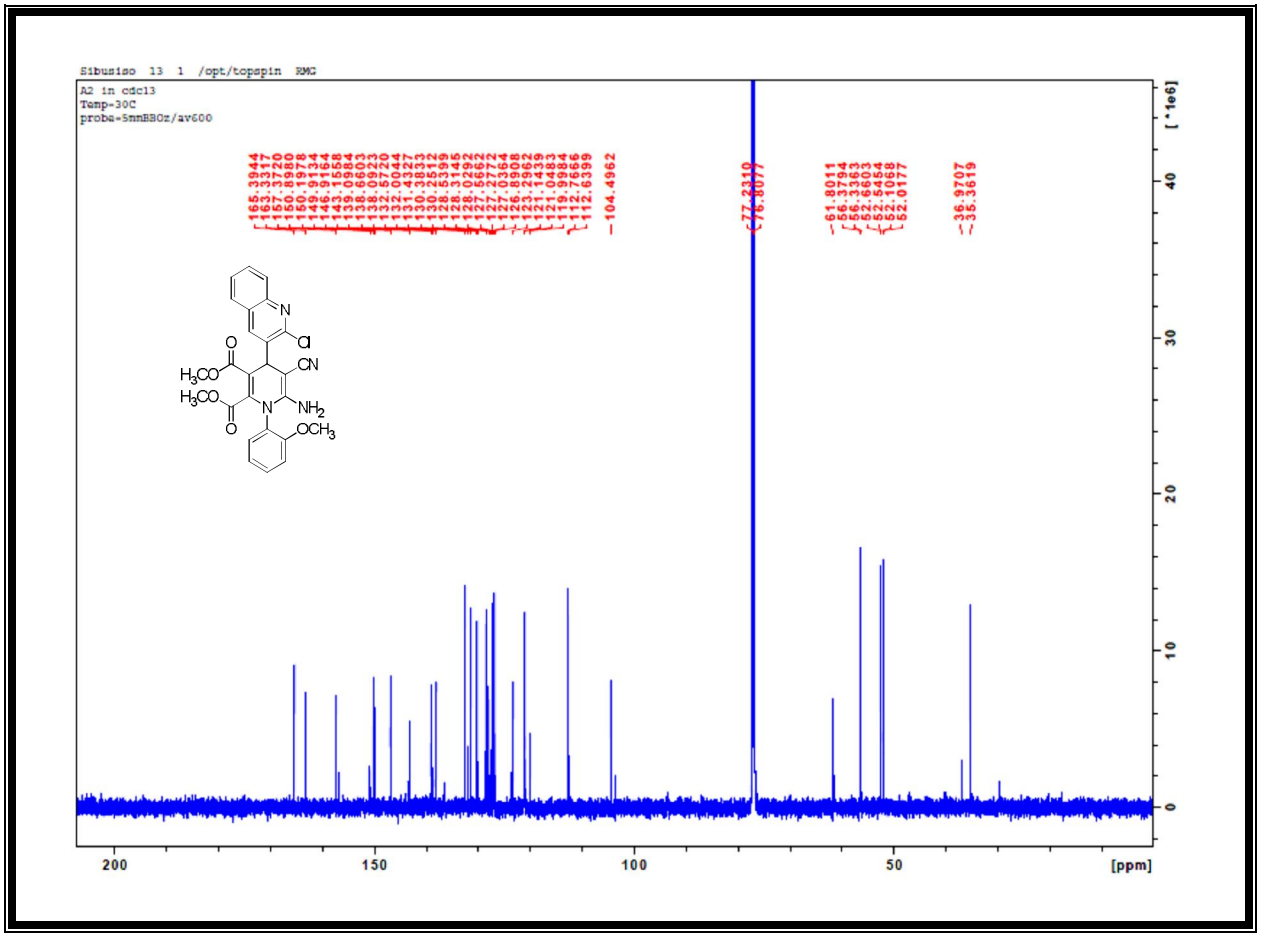

Figure 40: ^{13}C NMR Spectrum of A2, dimethyl 6-amino-4-(2-chloroquinolin-3-yl)-5-cyano-1-(2-methoxyphenyl)-1,4-dihydropyridine-2,3-dicarboxylate

Appendix 16

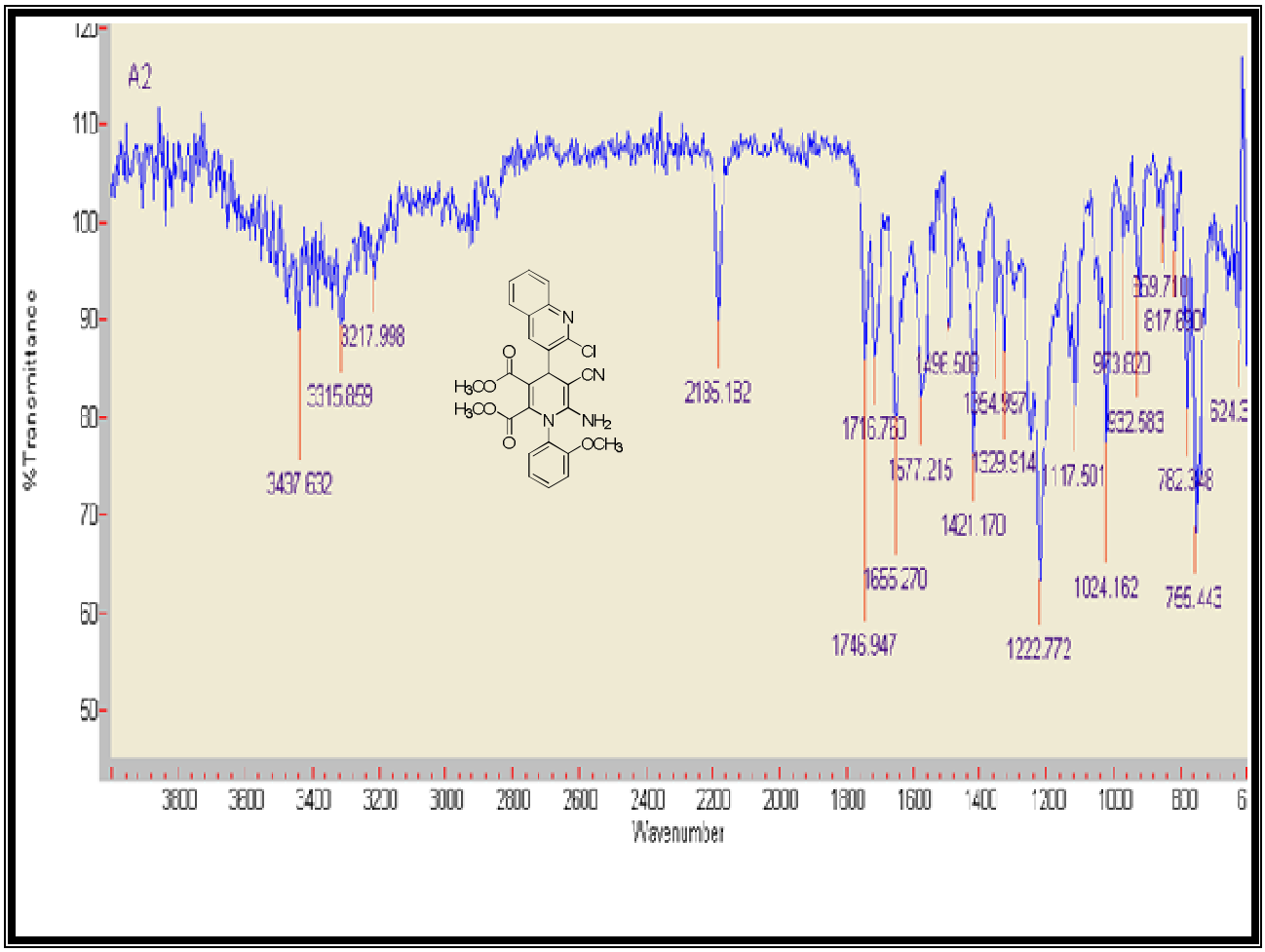

Figure 41: The IR Spectrum of A2, dimethyl 6-amino-4-(2-chloroquinolin-3-yl)-5-cyano-1-(2-methoxyphenyl)-1,4-dihydropyridine-2,3-dicarboxylate

Appendix 17

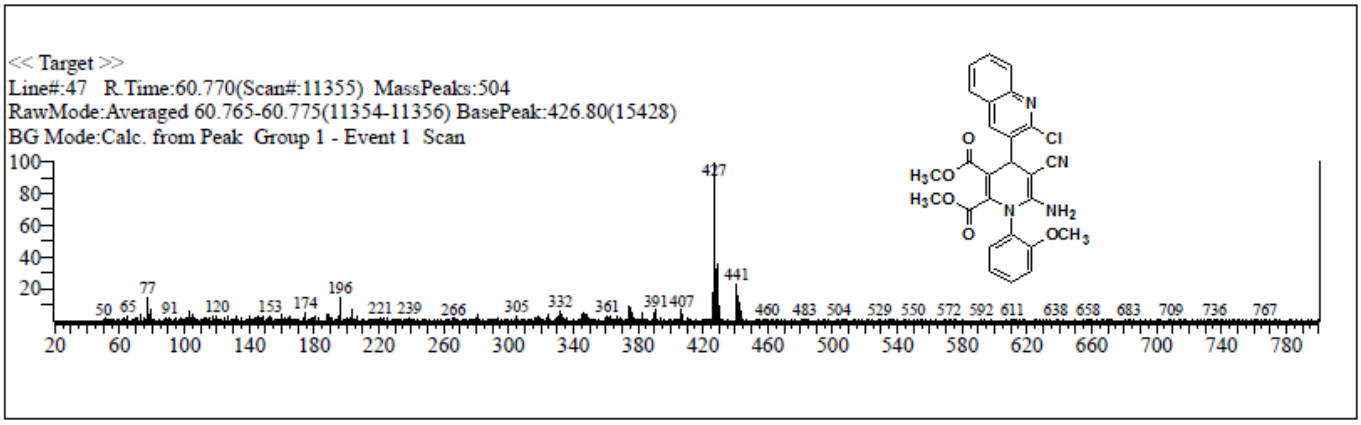

Figure 42: The Mass Spectrum of A2, dimethyl 6-amino-4-(2-chloroquinolin-3-yl)-5-cyano-1-(2-methoxyphenyl)-1,4-dihydropyridine-2,3-dicarboxylate

Appendix 18

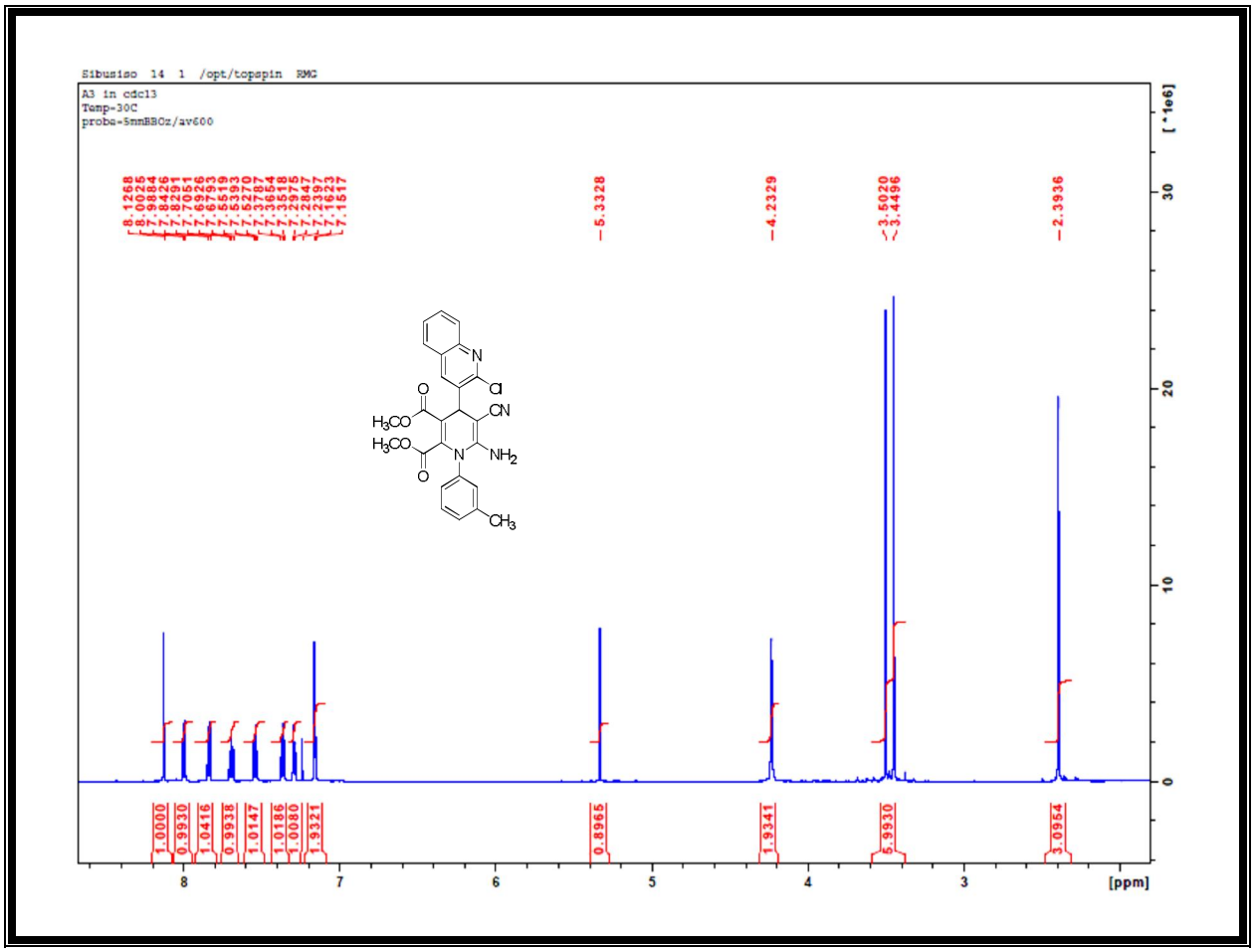

Figure 43: ^{1}H NMR Spectrum of A3, dimethyl 6-amino-4-(2-chloroquinolin-3-yl)-5-cyano-1-m-tolyl-1,4-dihydropyridine-2,3-dicarboxylate

Appendix 19

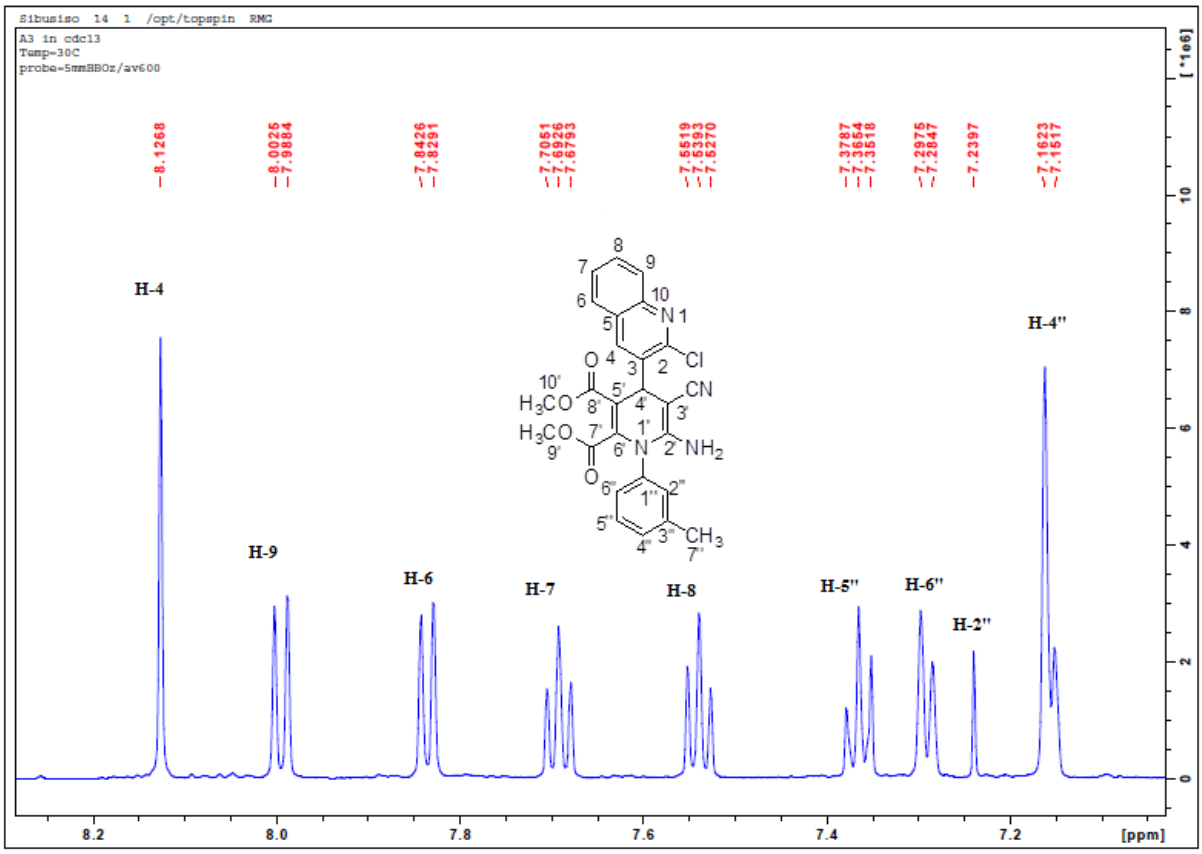

Figure 44: ^{1}H NMR Expanded spectrum of A3, dimethyl 6-amino-4-(2-chloroquinolin-3-yl)-5-cyano-1-m-tolyl-1,4-dihydropyridine-2,3-dicarboxylate

Appendix 20

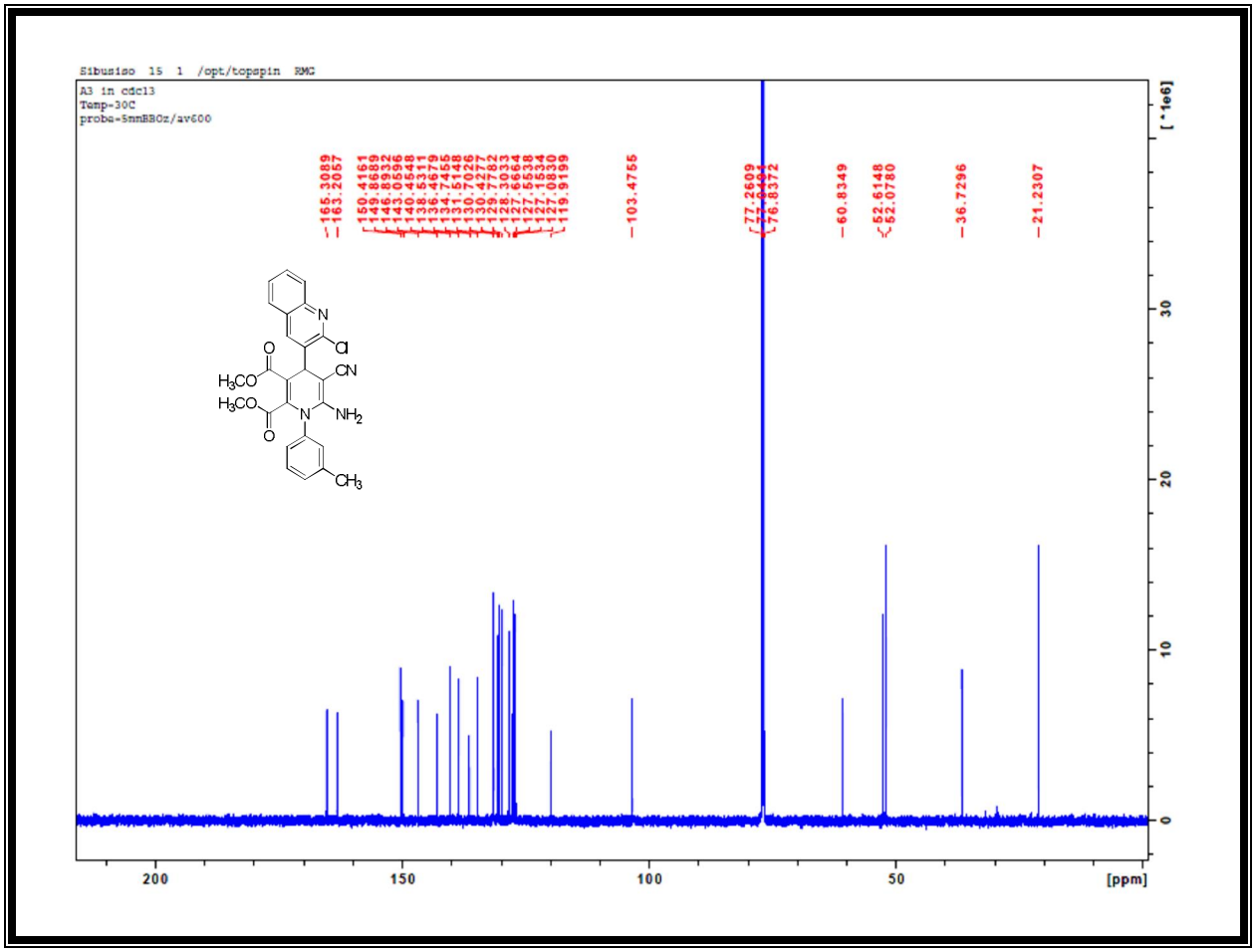

Figure 45: ^{13}C NMR Spectrum of A3, dimethyl 6-amino-4-(2-chloroquinolin-3-yl)-5-cyano-1-m-tolyl-1,4-dihydropyridine-2,3-dicarboxylate

Appendix 21

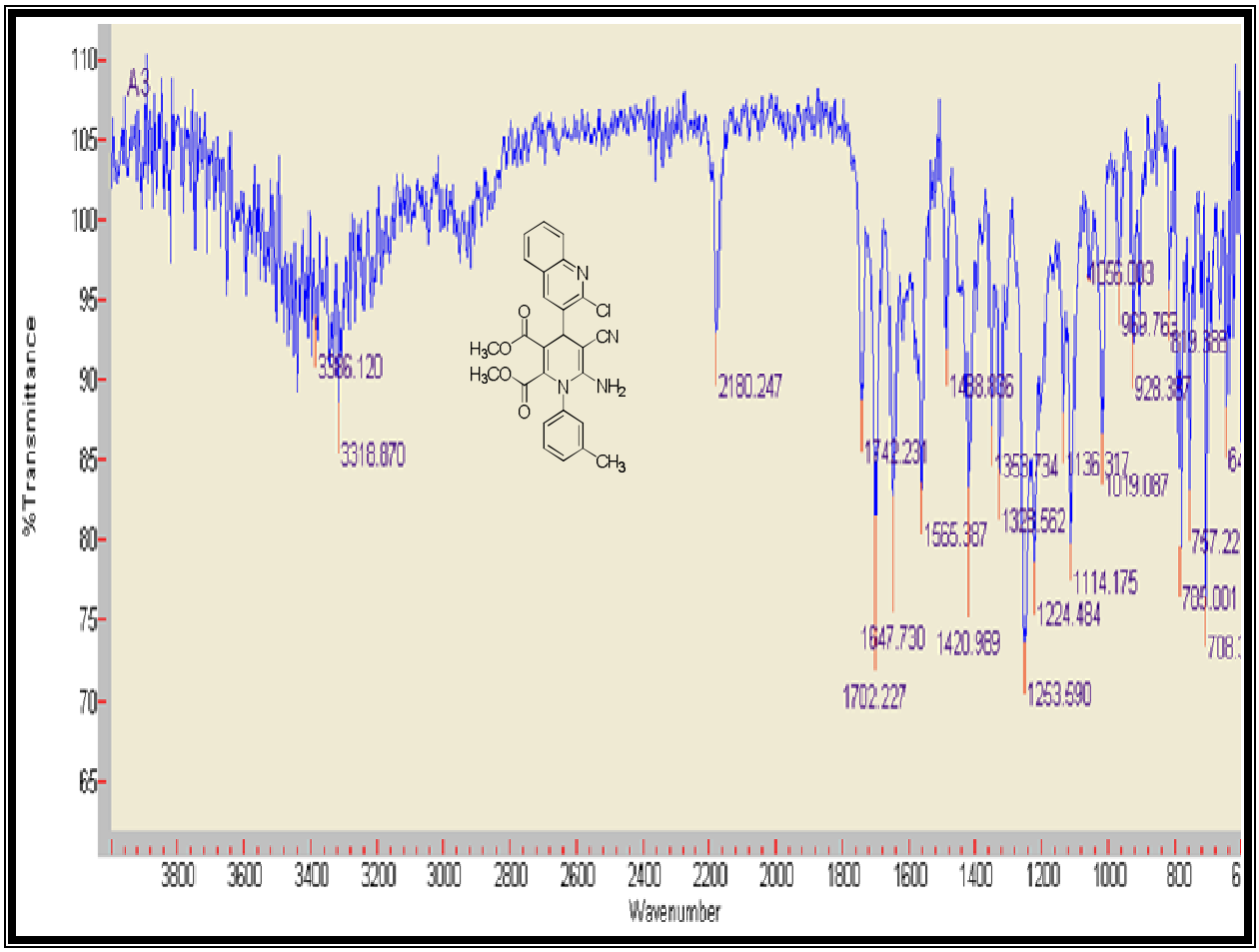

Figure 46: The IR Spectrum of A3, dimethyl 6-amino-4-(2-chloroquinolin-3-yl)-5-cyano-1-m-tolyl-1,4-dihydropyridine-2,3-dicarboxylate

Appendix 22

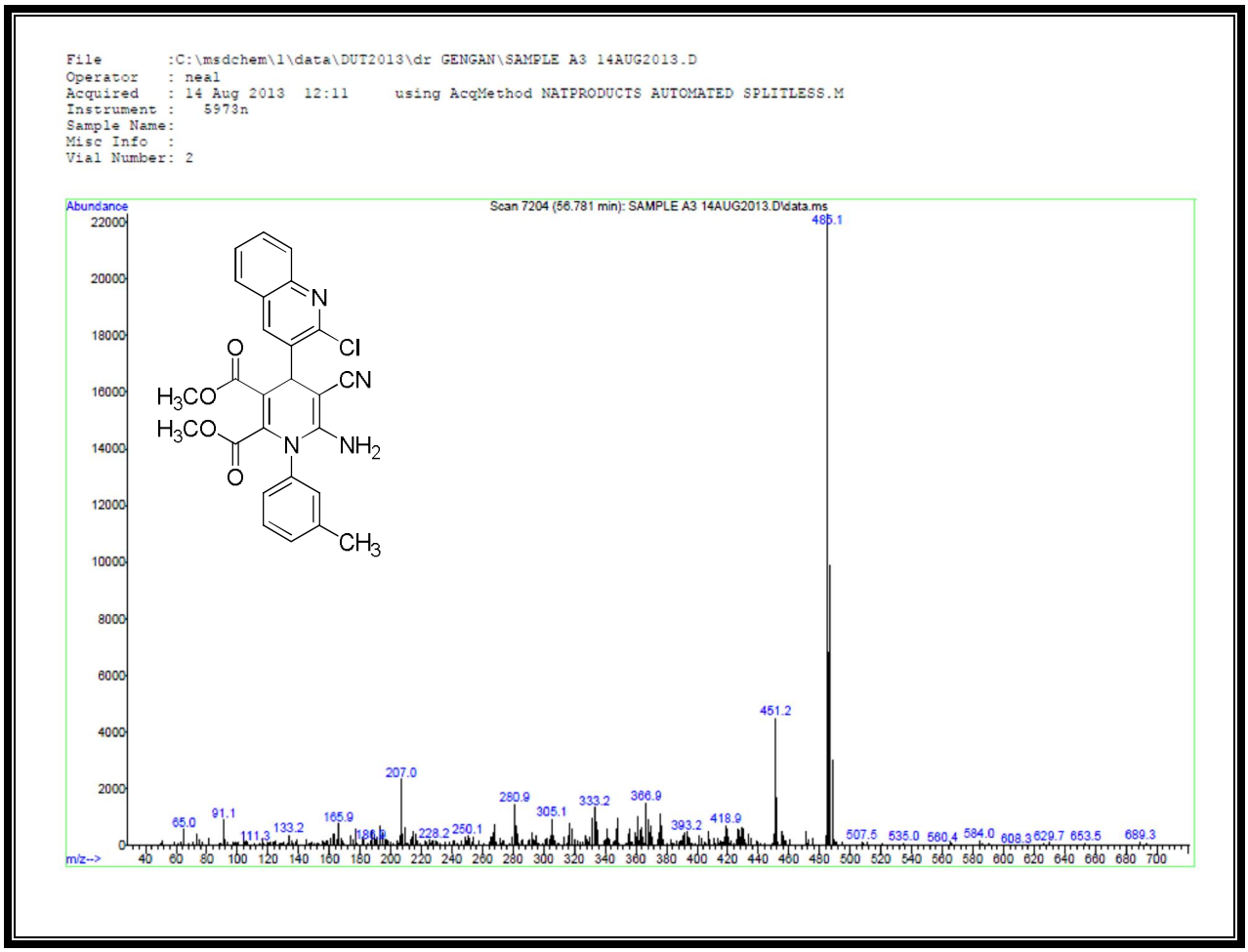

Figure 47: Mass spectrum of A3, dimethyl 6-amino-4-(2-chloroquinolin-3-yl)-5-cyano-1-m-tolyl-1,4-dihydropyridine-2,3-dicarboxylate

Appendix 23

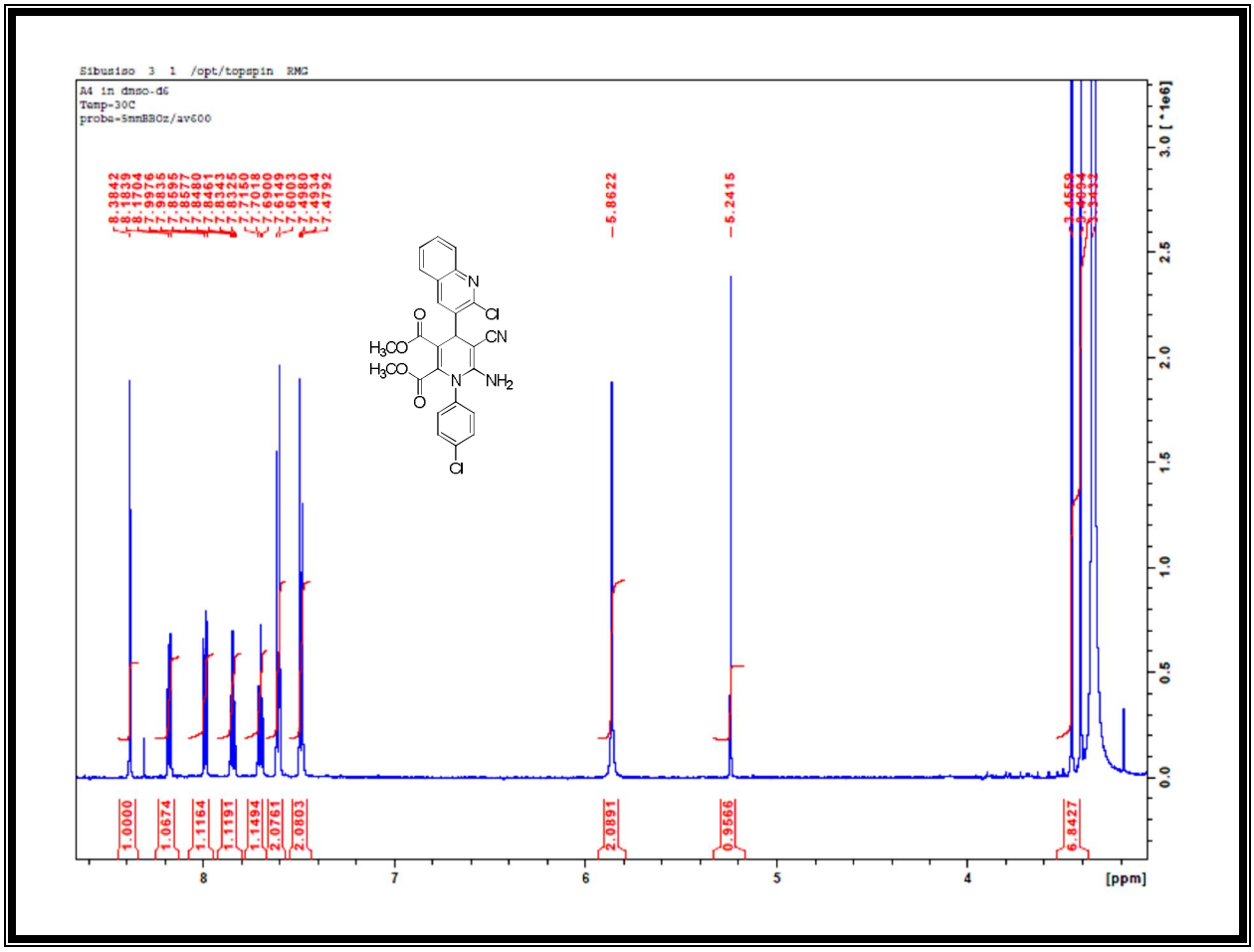

Figure 48: ^{1}H NMR Spectrum of A4, dimethyl 6-amino-1-(4-chlorophenyl)-4-(2-chloroquinolin-3-yl)-5-cyano-1,4-dihydropyridine-2,3-dicarboxylate

Appendix 24

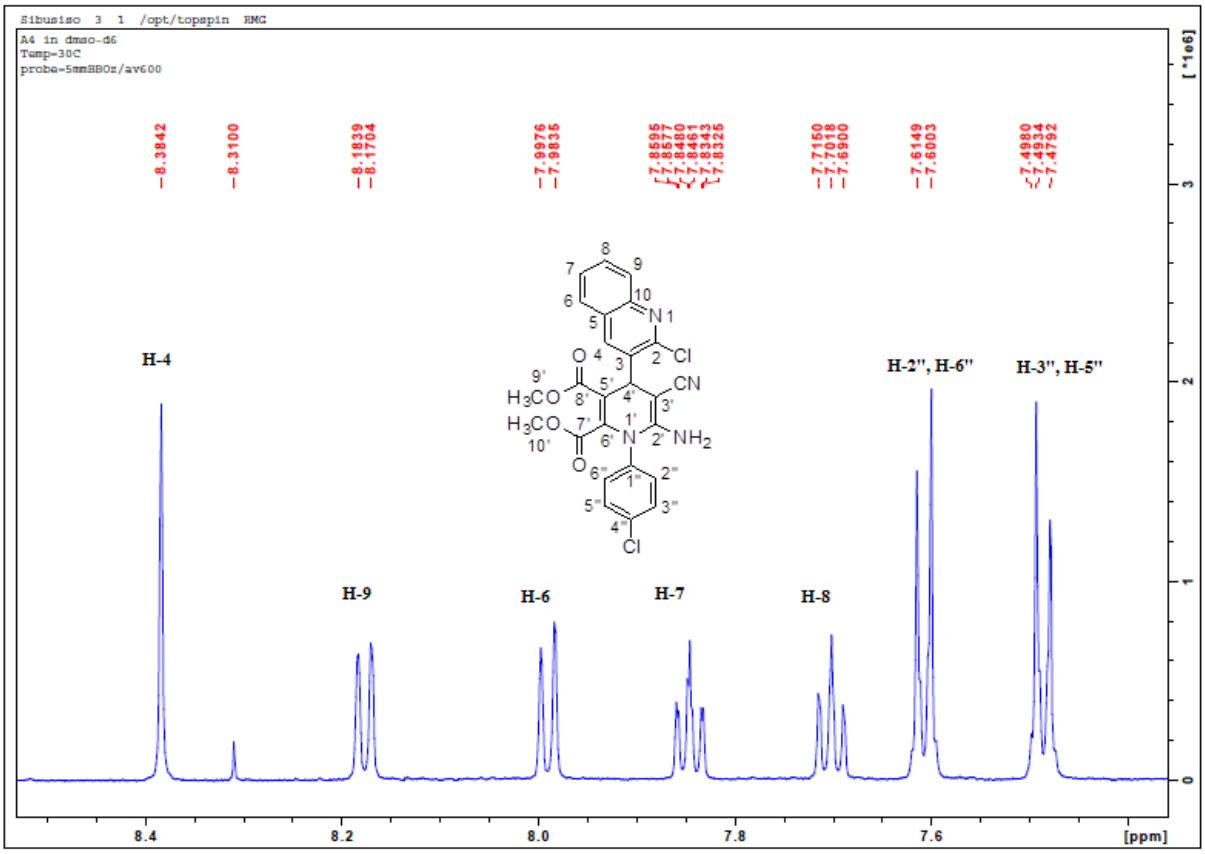

Figure 49: ^{1}H NMR Expanded spectrum of A4, dimethyl 6-amino-1-(4-chlorophenyl)-4-(2-chloroquinolin-3-yl)-5-cyano-1,4-dihydropyridine-2,3-dicarboxylate

Appendix 25

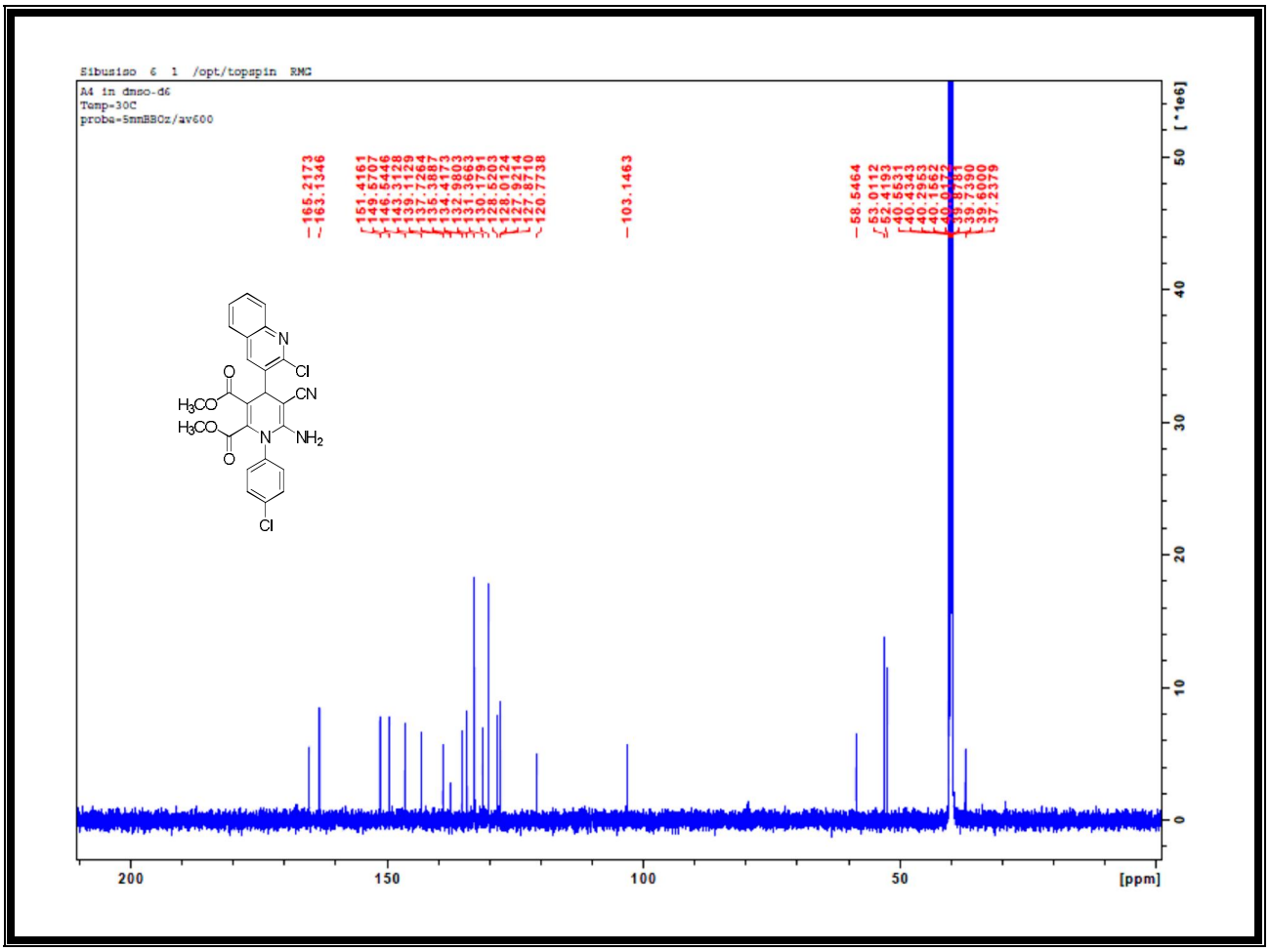

Figure 50: ^{13}C NMR Spectrum of A4, dimethyl 6-amino-1-(4-chlorophenyl)-4-(2-chloroquinolin-3-yl)-5-cyano-1,4-dihydropyridine-2,3-dicarboxylate

Appendix 26

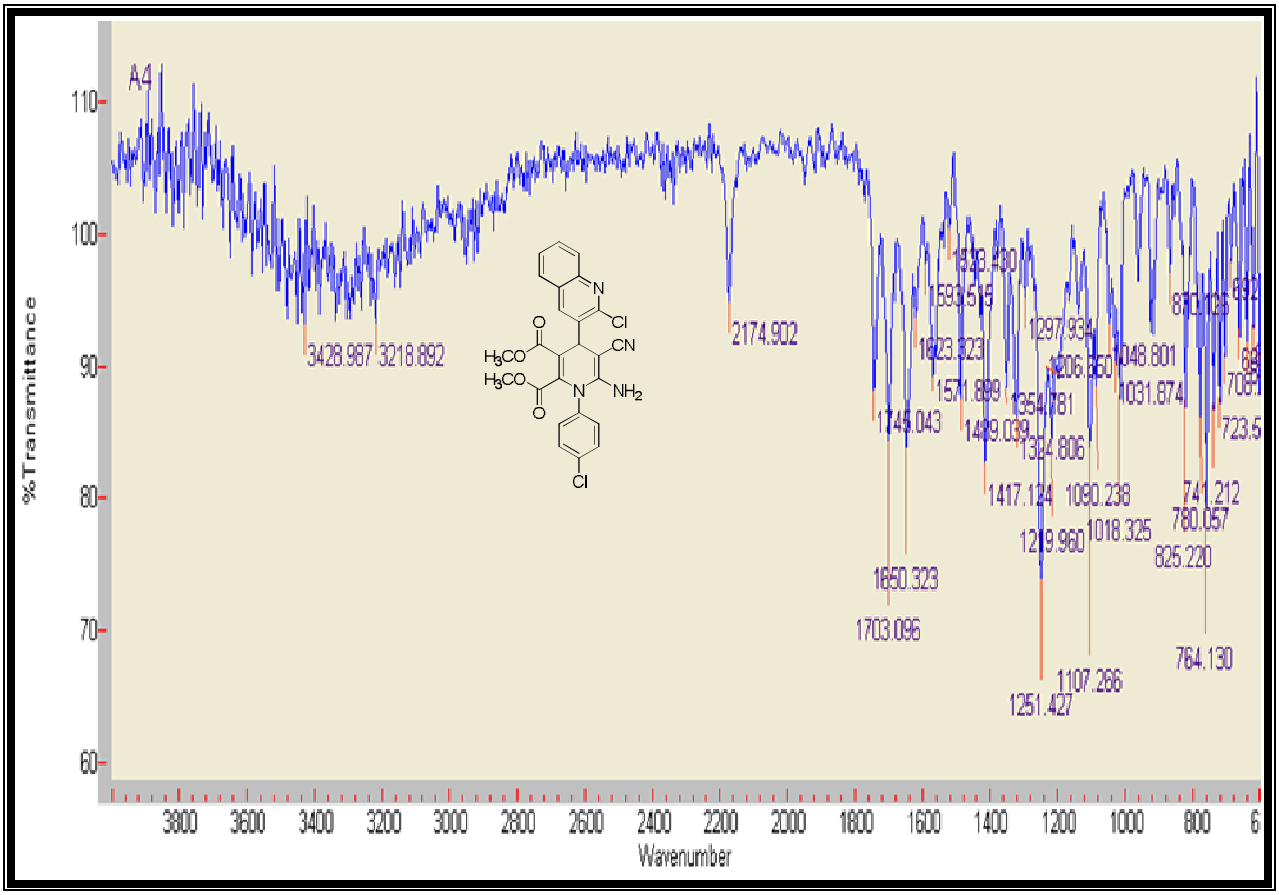

Figure 51: The IR Spectrum of A4, dimethyl 6-amino-1-(4-chlorophenyl)-4-(2-chloroquinolin-3-yl)-5-cyano-1,4-dihydropyridine-2,3-dicarboxylate

Appendix 27

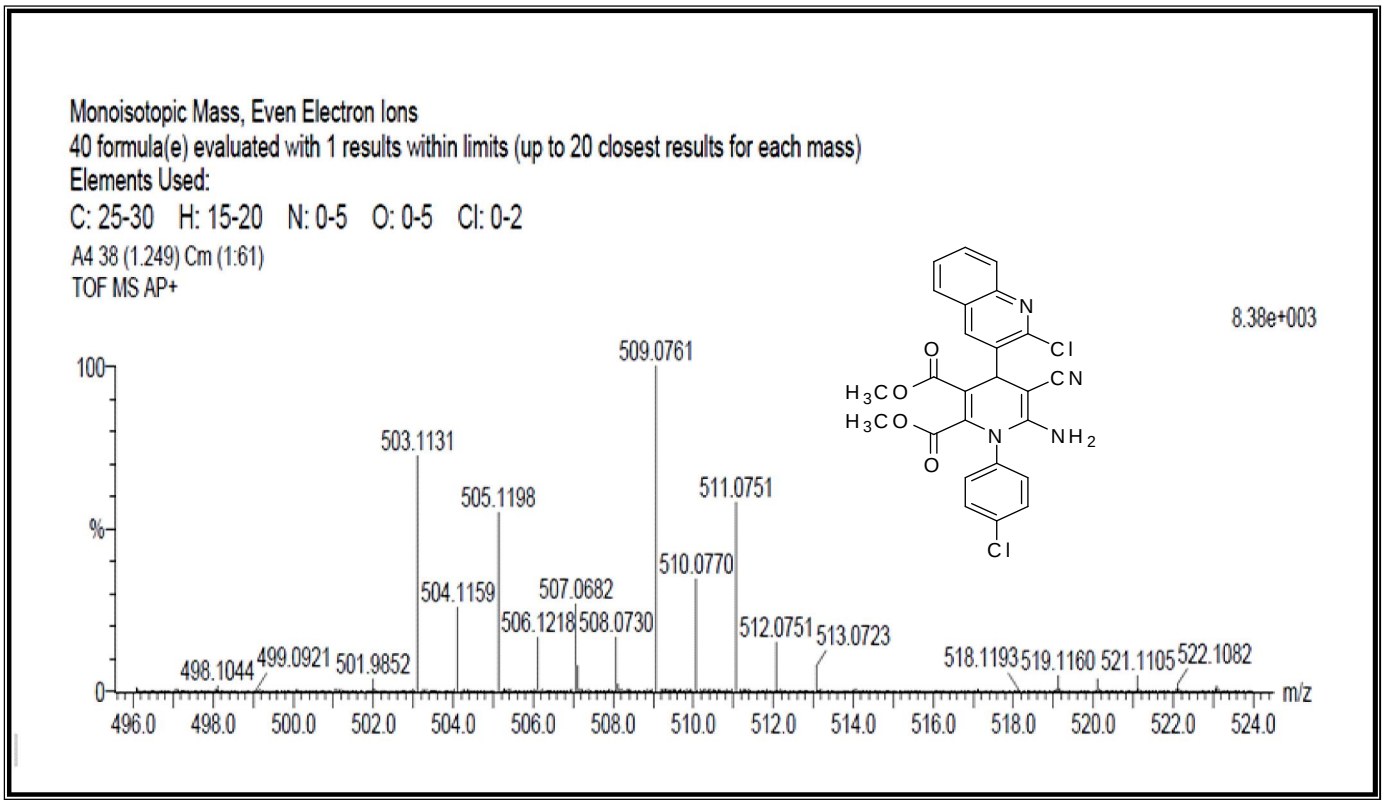

Figure 52: The Mass Spectrum of A4, dimethyl 6-amino-1-(4-chlorophenyl)-4-(2-chloroquinolin-3-yl)-5-cyano-1,4-dihydropyridine-2,3-dicarboxylate

Appendix 28

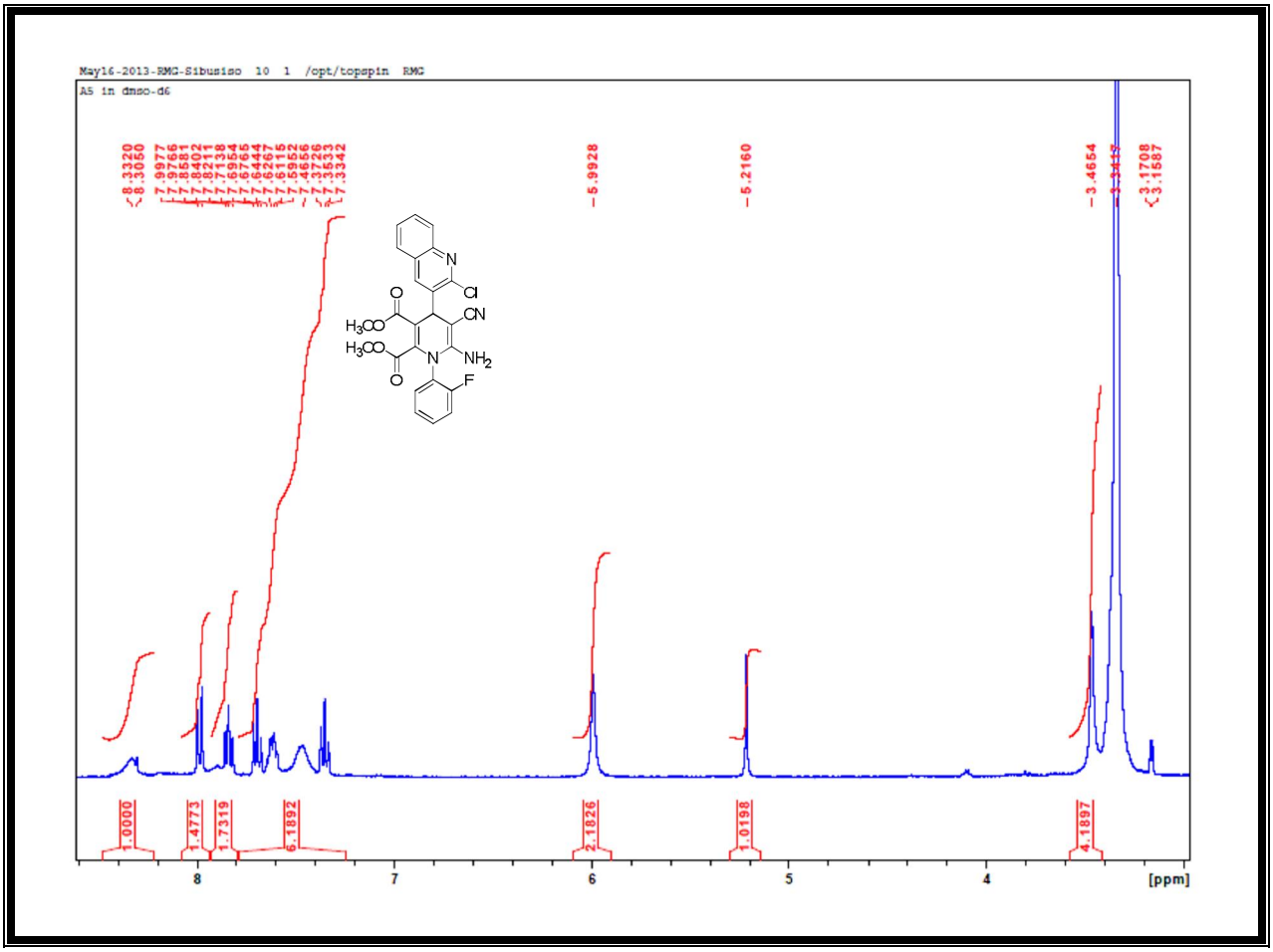

Figure 53: ^{1}H NMR Spectrum of A5, dimethyl 6-amino-4-(2-chloroquinolin-3-yl)-5-cyano-1-(2-fluorophenyl)-1,4-dihydropyridine-2,3-dicarboxylate

Appendix 29

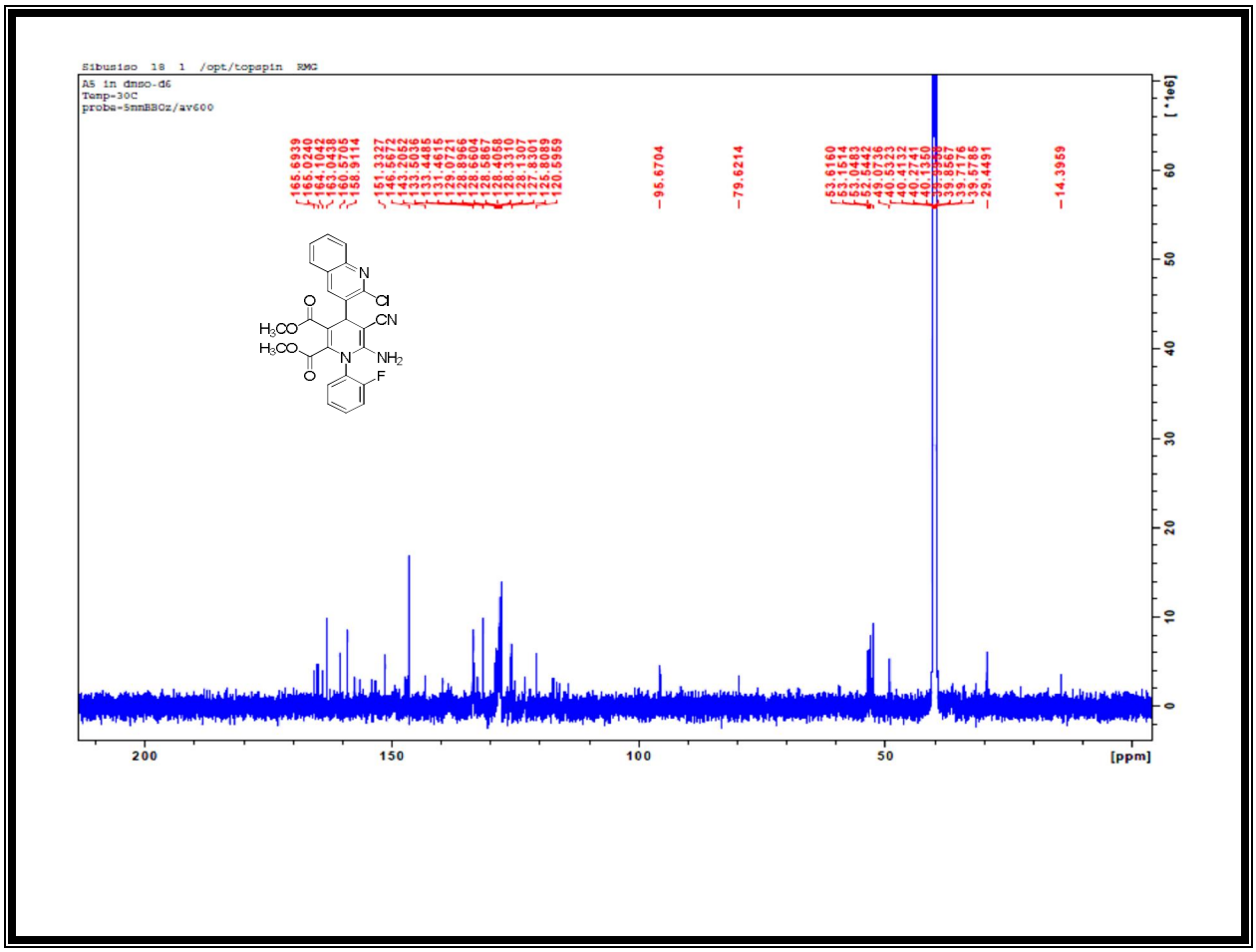

Figure 54: ^{13}C NMR Spectrum of A5, dimethyl 6-amino-4-(2-chloroquinolin-3-yl)-5-cyano-1-(2-fluorophenyl)-1,4-dihydropyridine-2,3-dicarboxylate

Appendix 30

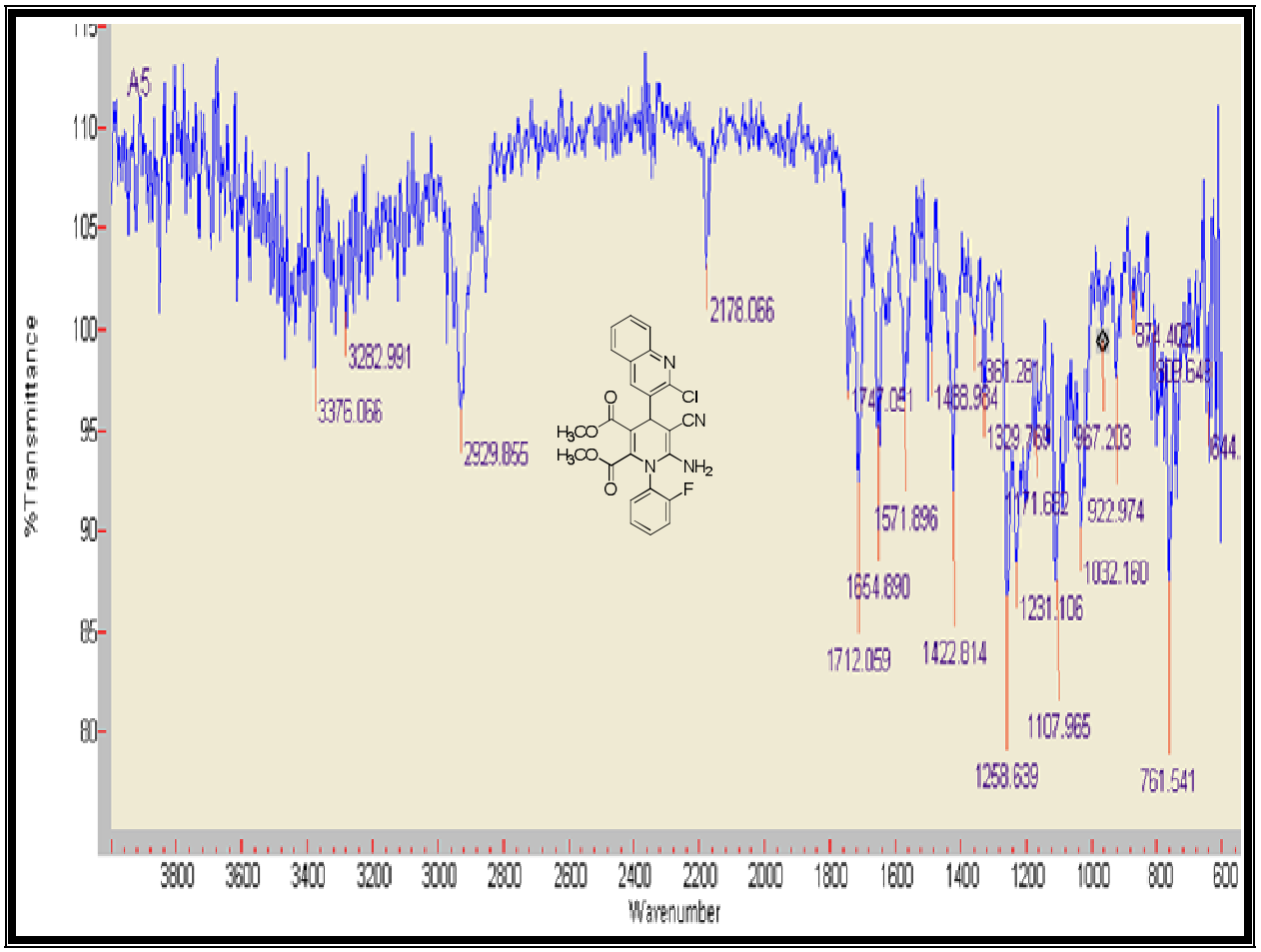

Figure 55: The IR Spectrum of A5, dimethyl 6-amino-4-(2-chloroquinolin-3-yl)-5-cyano-1-(2-fluorophenyl)-1,4-dihydropyridine-2,3-dicarboxylate

Appendix 31

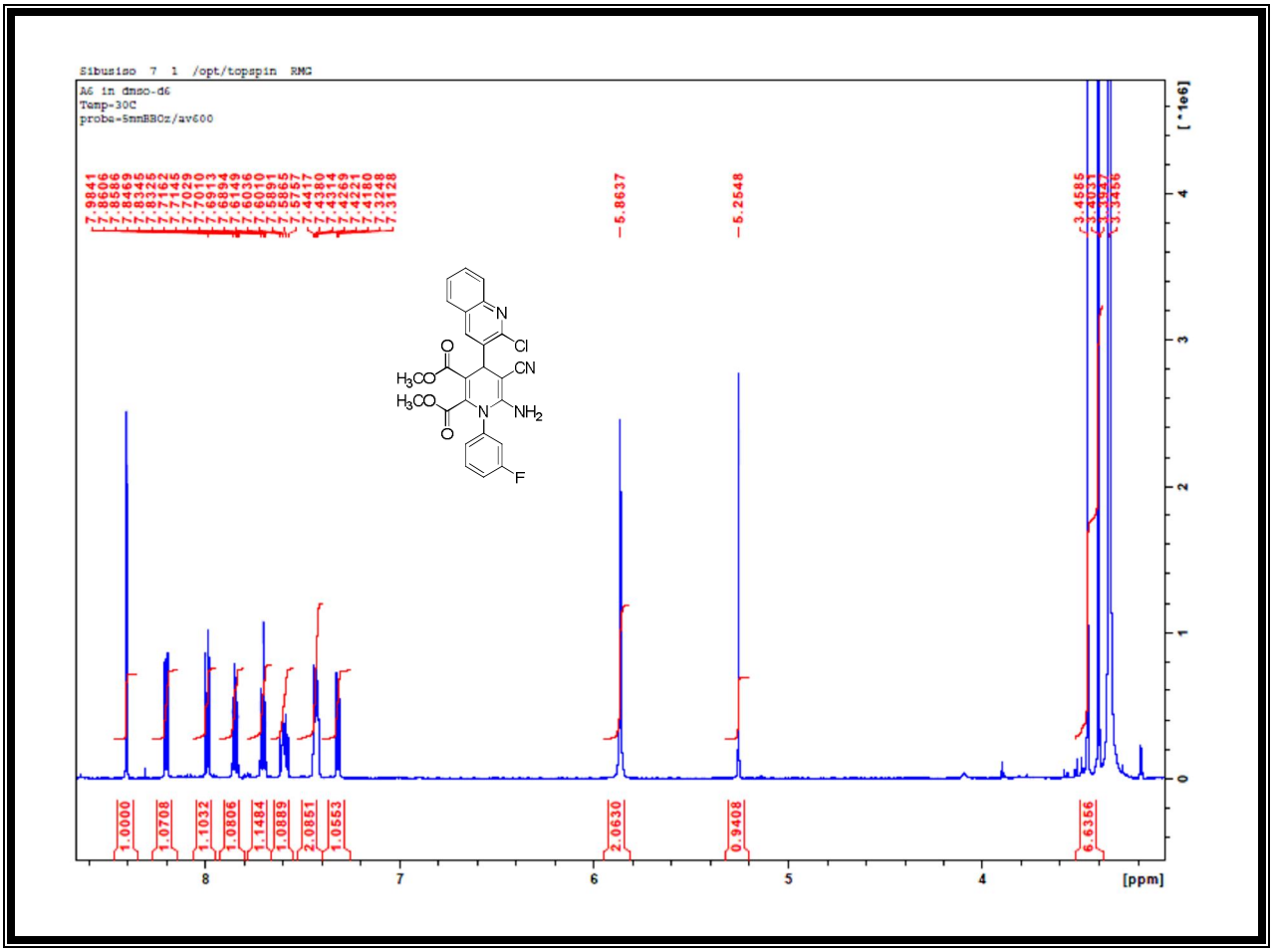

Figure 56: ^{1}H NMR Spectrum of A6, dimethyl 6-amino-4-(2-chloroquinolin-3-yl)-5-cyano-1-(3-fluorophenyl)-1,4-dihydropyridine-2,3-dicarboxylate

Appendix 32

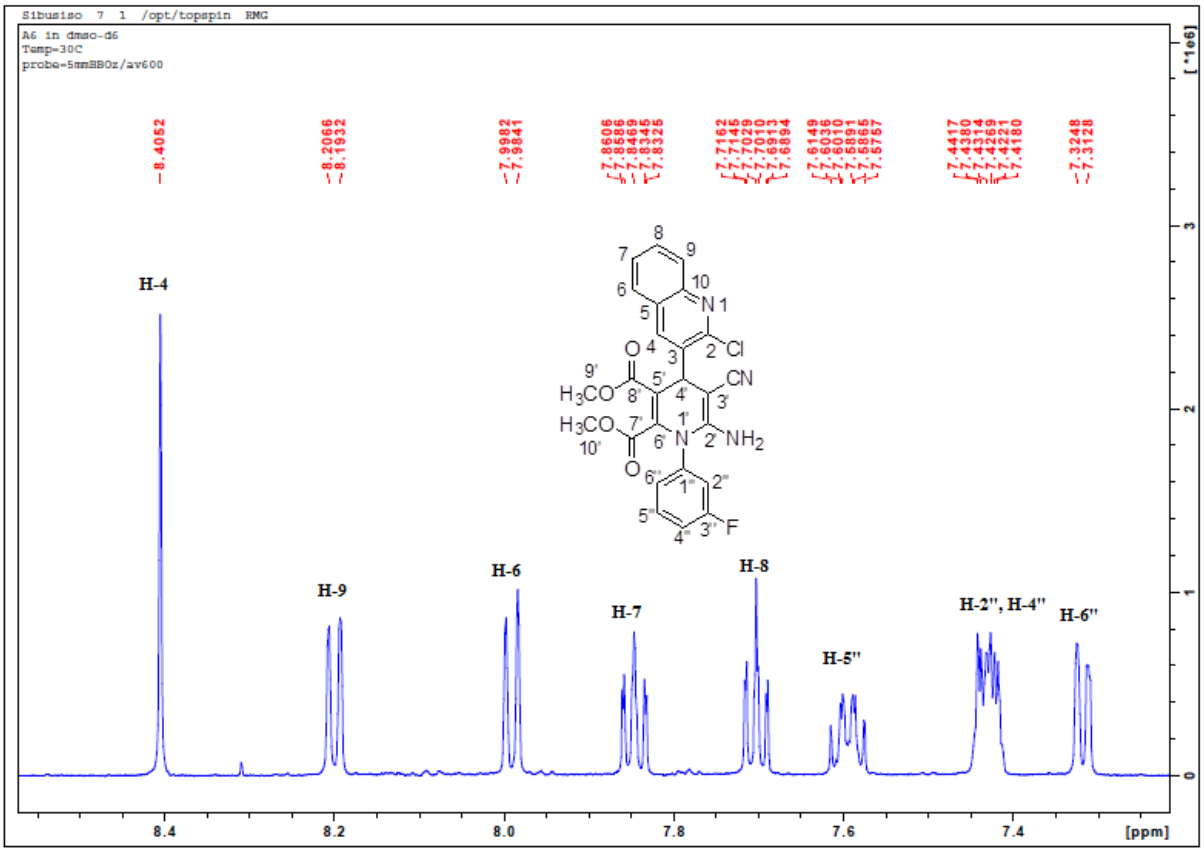

Figure 57: ^{1}H NMR Expanded spectrum of A6, dimethyl 6-amino-4-(2-chloroquinolin-3-yl)-5-cyano-1-(3-fluorophenyl)-1,4-dihydropyridine-2,3-dicarboxylate

Appendix 33

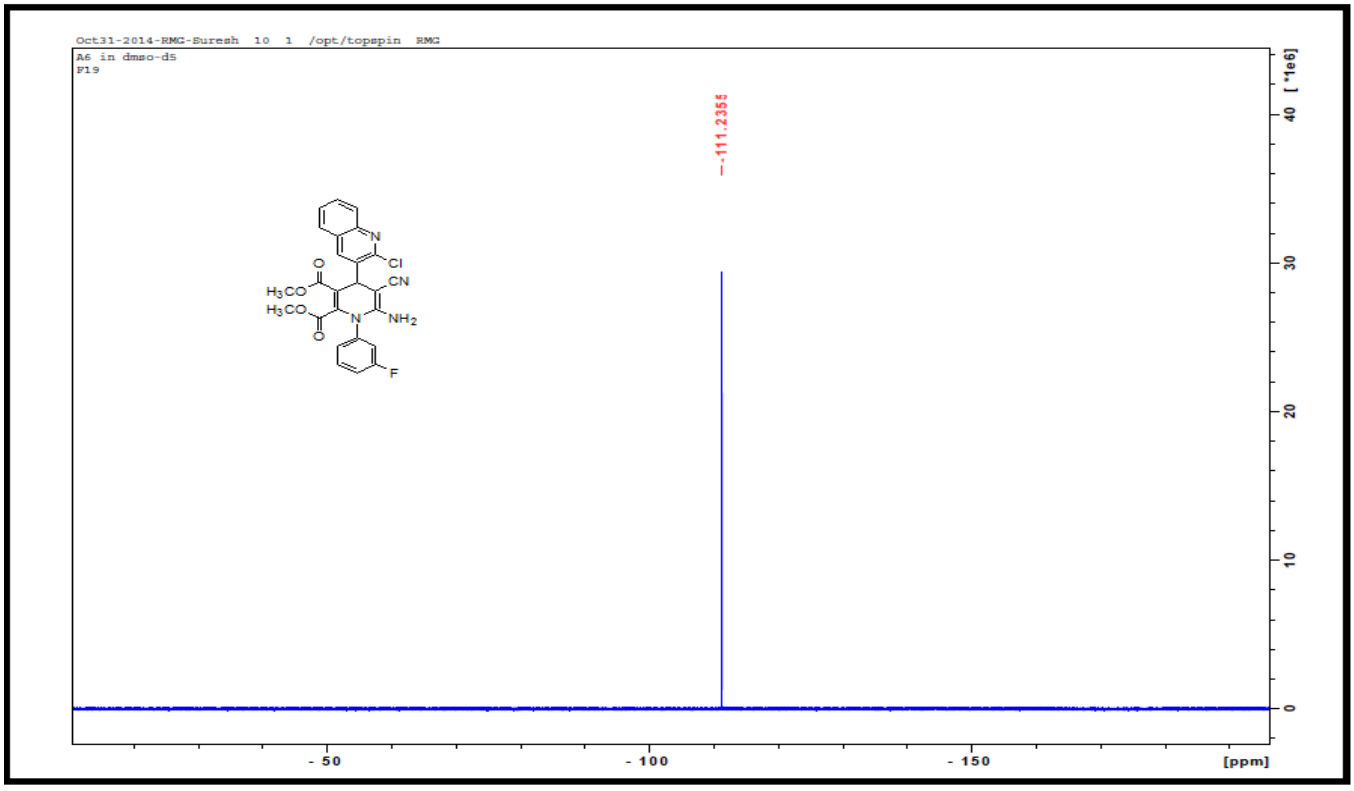

Figure 58: ^{19}F NMR Spectrum of A6, dimethyl 6-amino-4-(2-chloroquinolin-3-yl)-5-cyano-1-(3-fluorophenyl)-1,4-dihydropyridine-2,3-dicarboxylate

Appendix 34

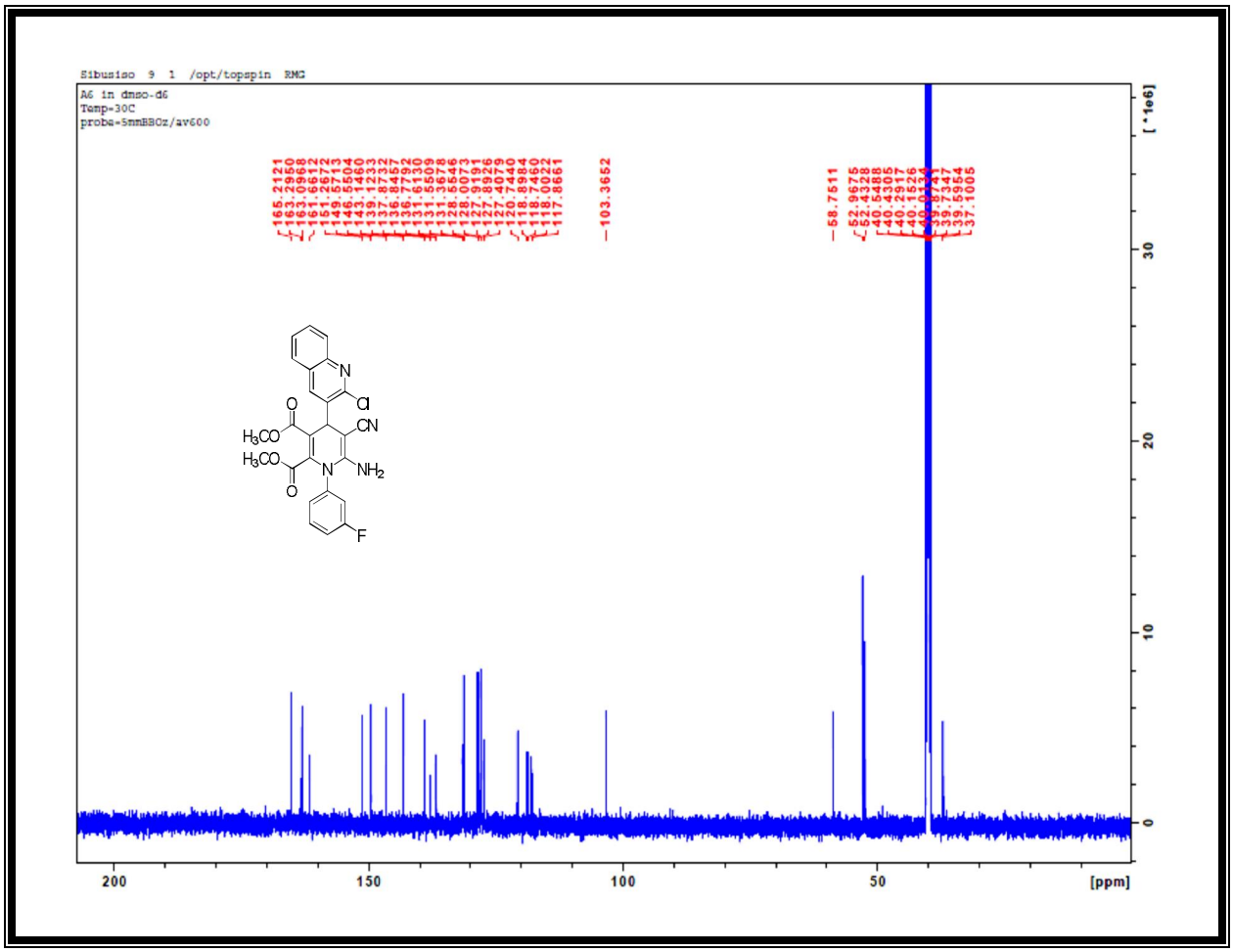

Figure 59: ^{13}C NMR Spectrum of A6, dimethyl 6-amino-4-(2-chloroquinolin-3-yl)-5-cyano-1-(3-fluorophenyl)-1,4-dihydropyridine-2,3-dicarboxylate

Appendix 35

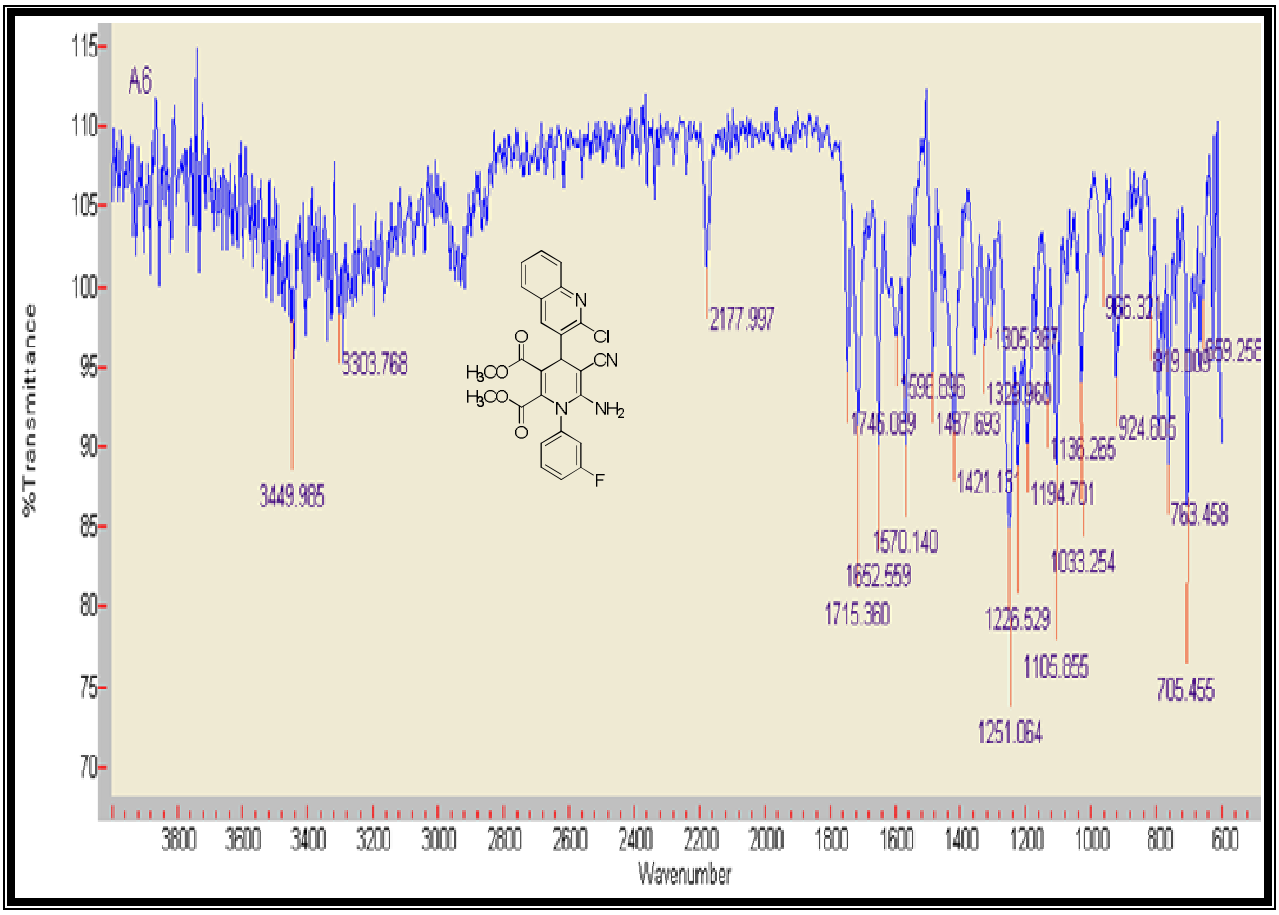

Figure 60: The IR Spectrum of A6, dimethyl 6-amino-4-(2-chloroquinolin-3-yl)-5-cyano-1-(3-fluorophenyl)-1,4-dihydropyridine-2,3-dicarboxylate

Appendix 36

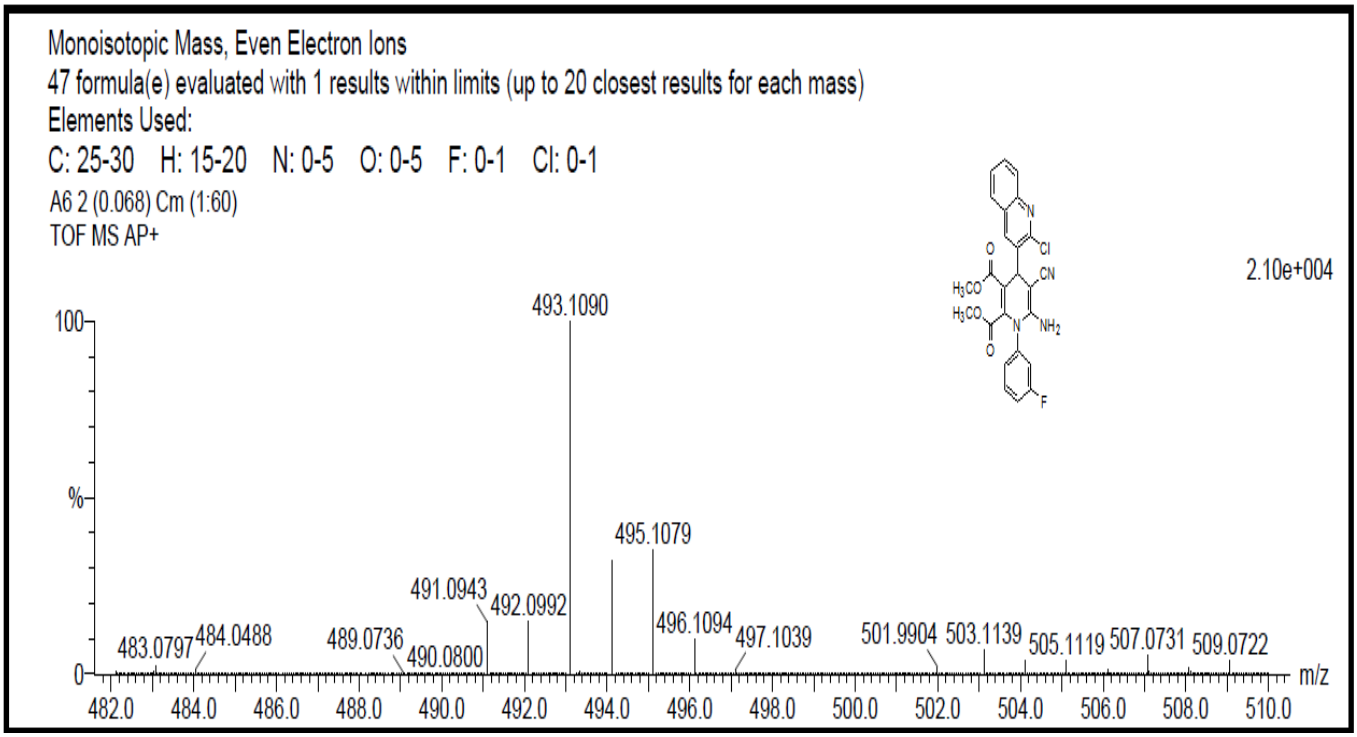

Figure 61: The Mass Spectrum of A6, dimethyl 6-amino-4-(2-chloroquinolin-3-yl)-5-cyano-1-(3-fluorophenyl)-1,4-dihydropyridine-2,3-dicarboxylate

Appendix 37

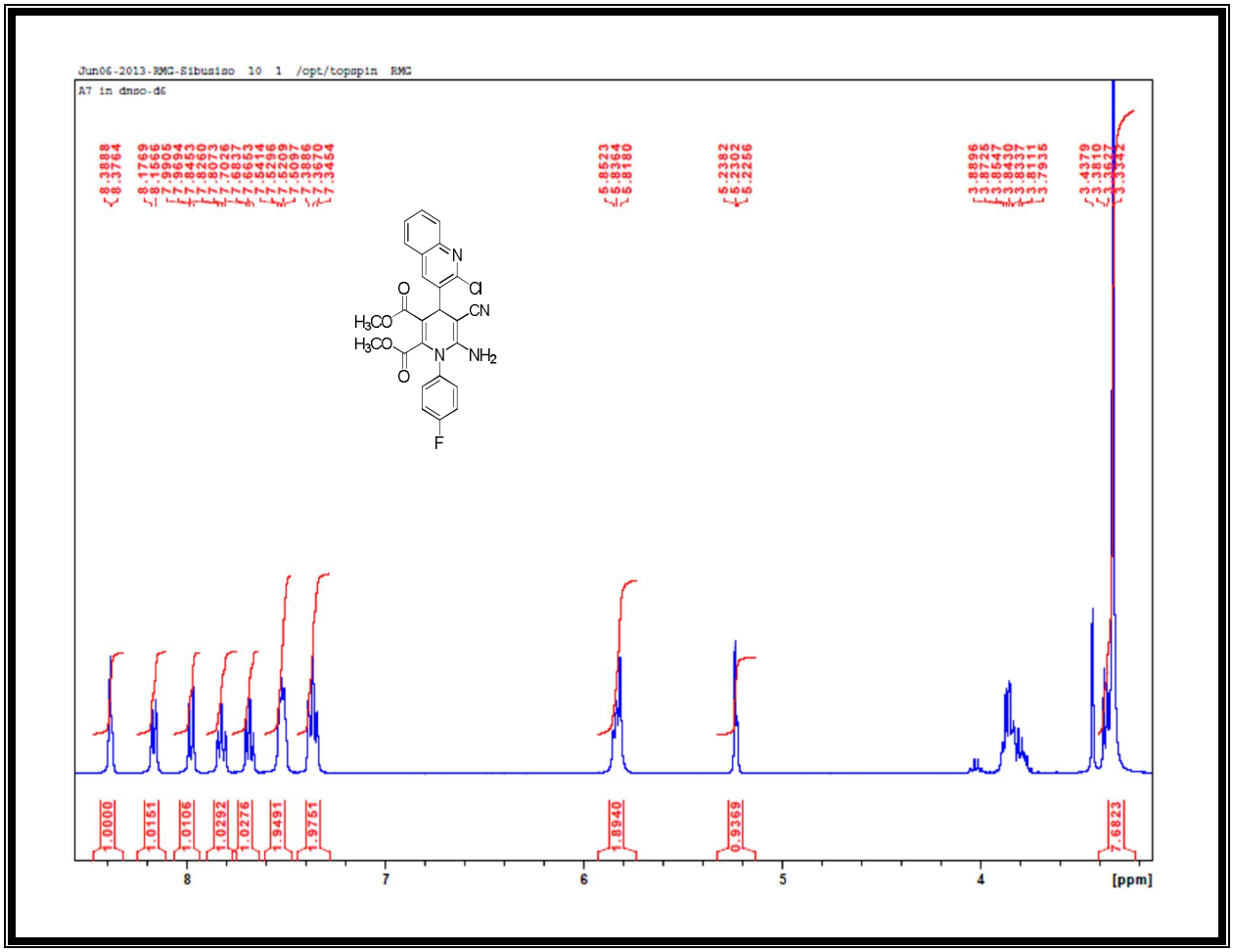

Figure 62: ^{1}H NMR Spectrum of A7, dimethyl 6-amino-4-(2-chloroquinolin-3-yl)-5-cyano-1-(4-fluorophenyl)-1,4-dihydropyridine-2,3-dicarboxylate

Appendix 38

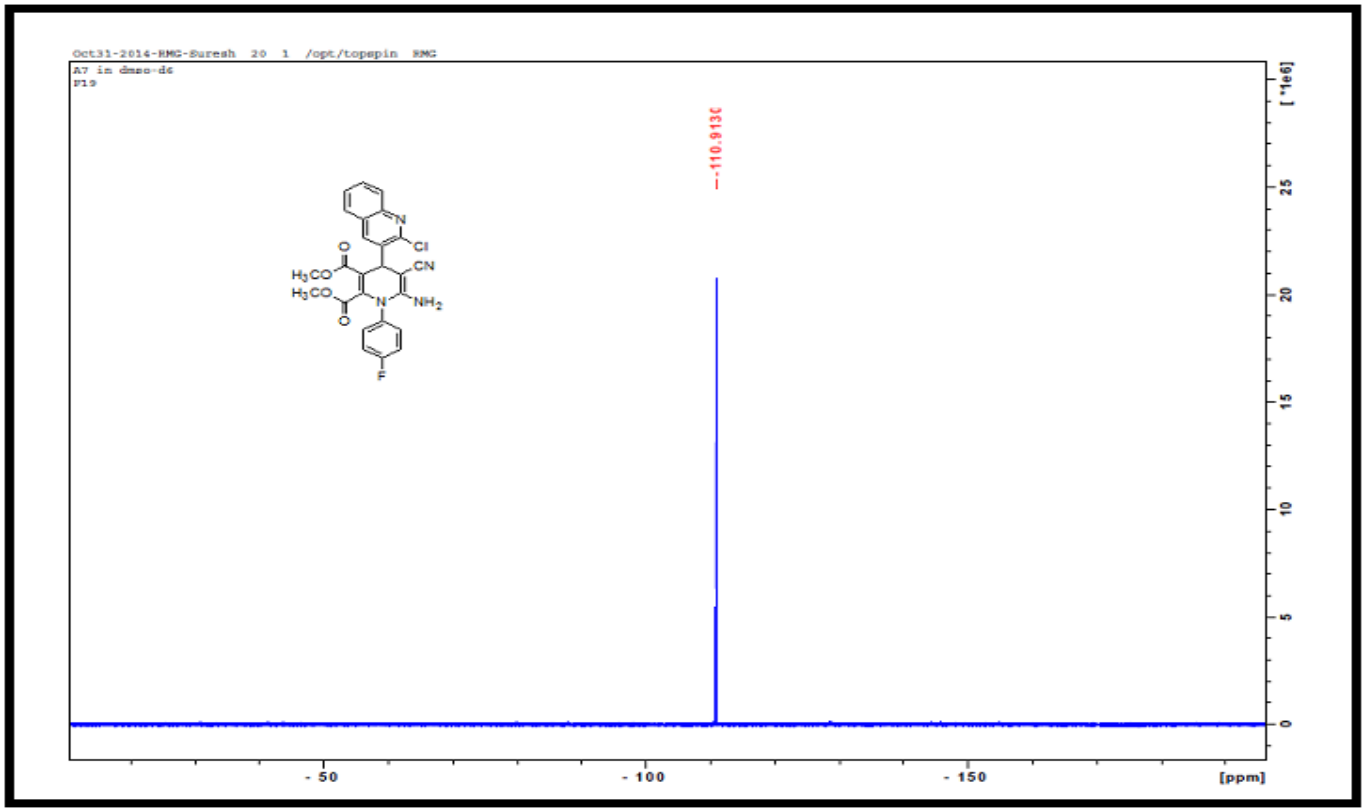

Figure 63: ^{19}F NMR Spectrum of A7, dimethyl 6-amino-4-(2-chloroquinolin-3-yl)-5-cyano-1-(4-fluorophenyl)-1,4-dihydropyridine-2,3-dicarboxylate

Appendix 39

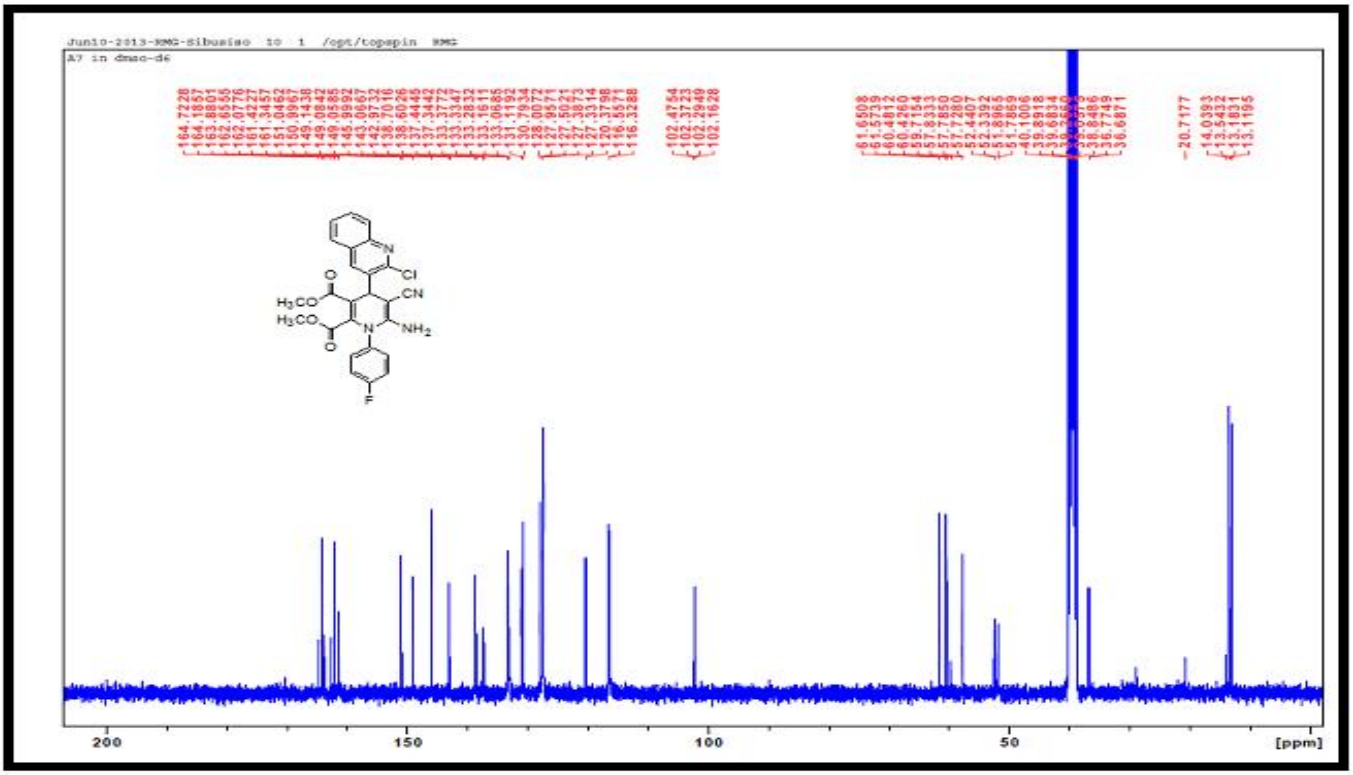

Figure 64: ^{13}C NMR Spectrum of A7, dimethyl 6-amino-4-(2-chloroquinolin-3-yl)-5-cyano-1-(4-fluorophenyl)-1,4-dihydropyridine-2,3-dicarboxylate

Appendix 40

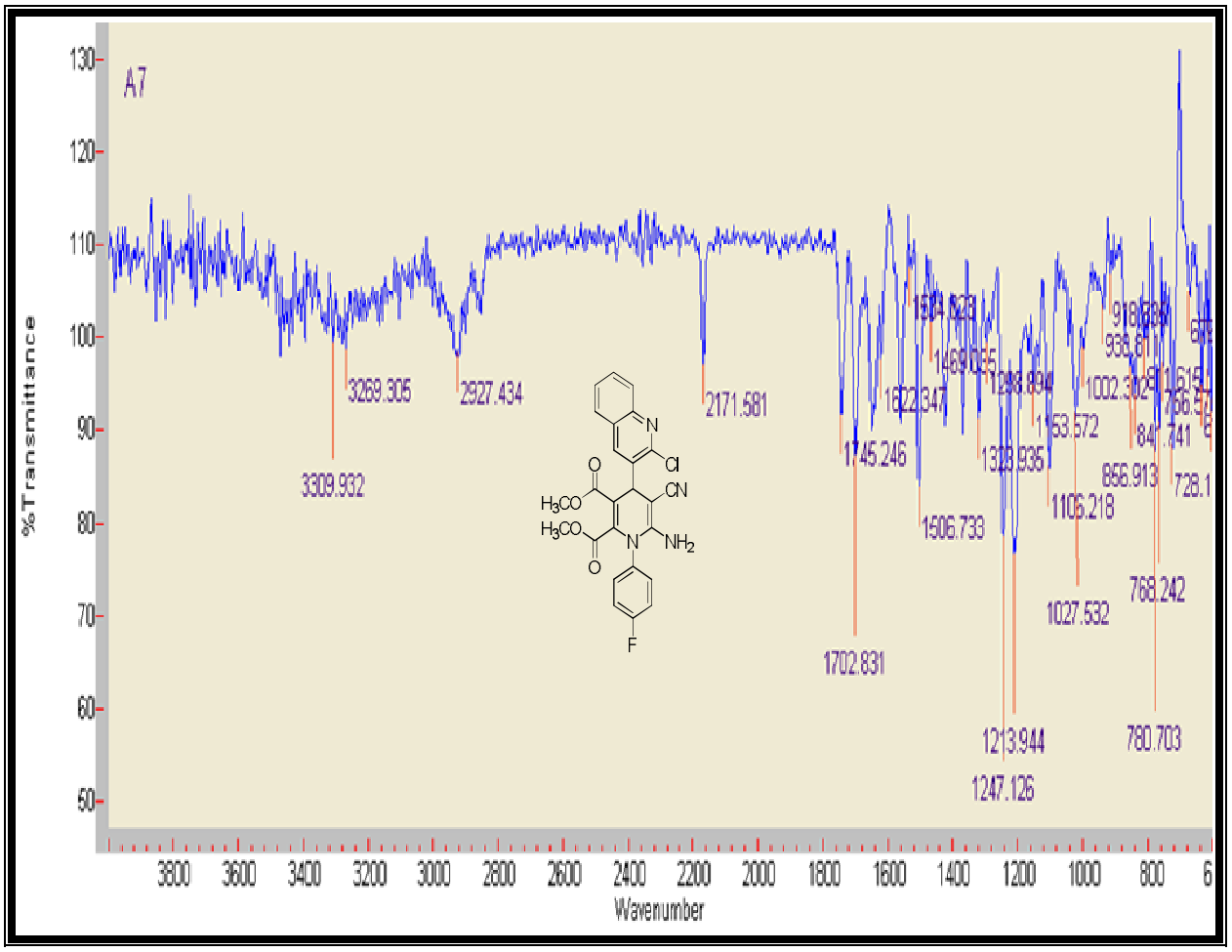

Figure 65: The IR Spectrum of A7, dimethyl 6-amino-4-(2-chloroquinolin-3-yl)-5-cyano-1-(4-fluorophenyl)-1,4-dihydropyridine-2,3-dicarboxylate

Appendix 41

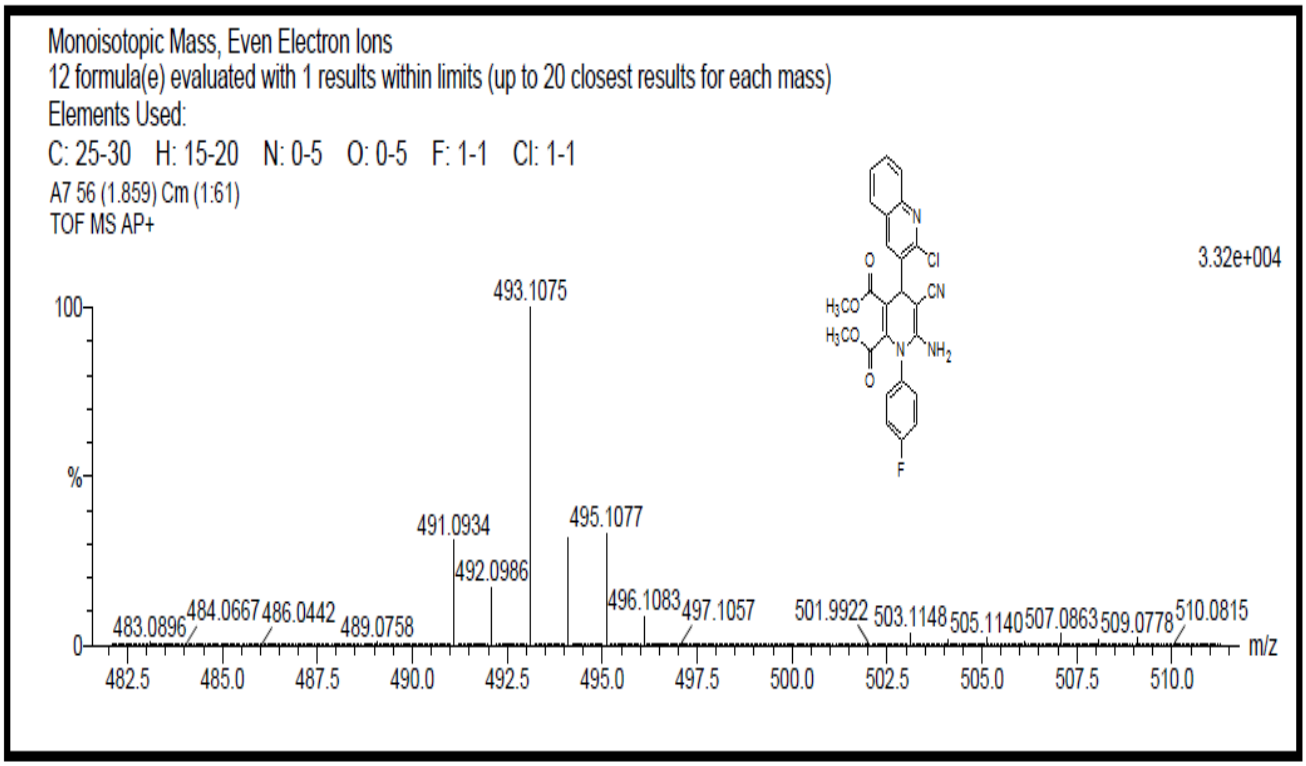

Figure 66: The Mass Spectrum of A7, dimethyl 6-amino-4-(2-chloroquinolin-3-yl)-5-cyano-1-(4-fluorophenyl)-1,4-dihydropyridine-2,3-dicarboxylate

Appendix 42

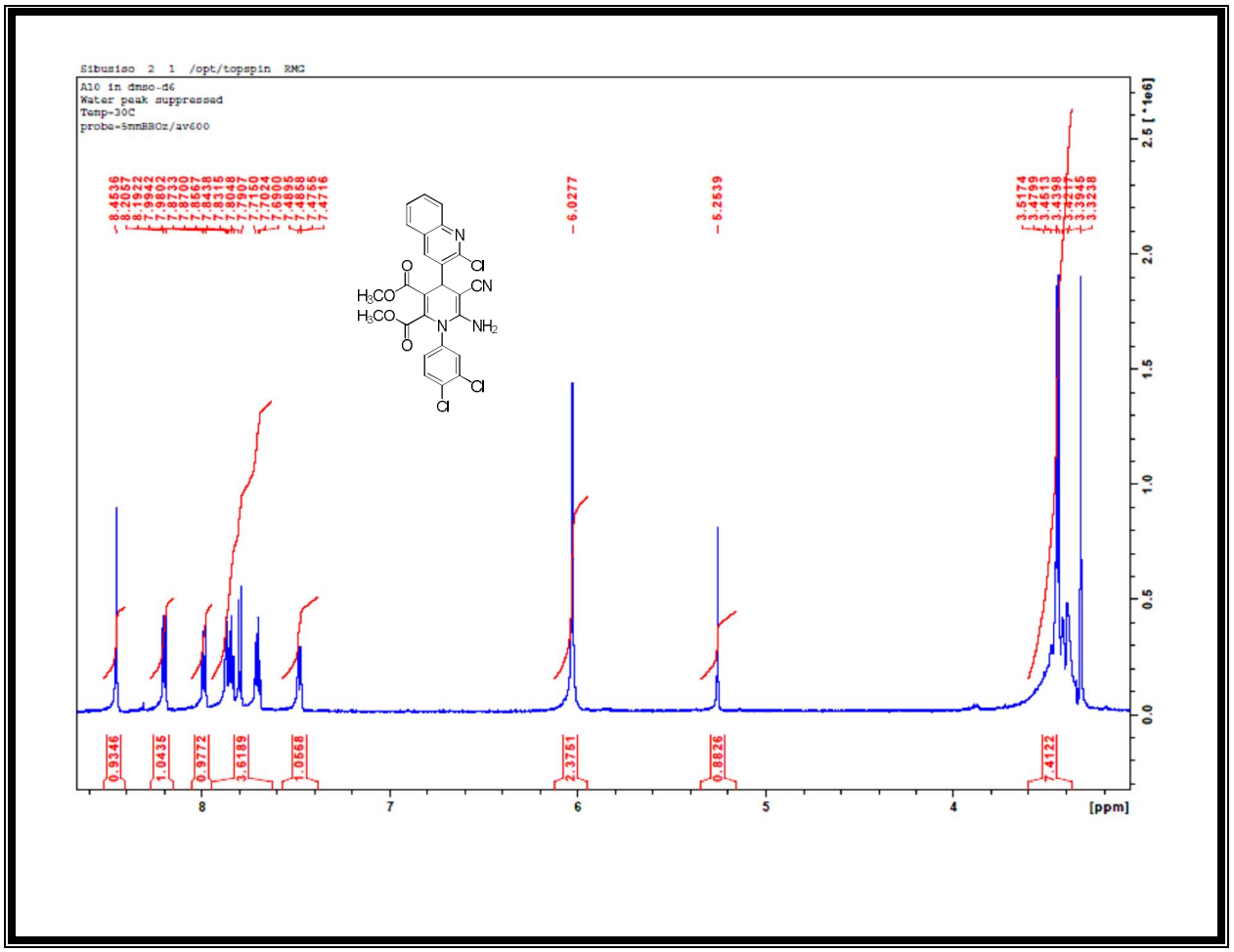

Figure 67: ^{1}H NMR Spectrum of A8, dimethyl 6-amino-4-(2-chloroquinolin-3-yl)-5-cyano-1-(3,4-dichlorophenyl)-1,4-dihydropyridine-2,3-dicarboxylate

Appendix 43

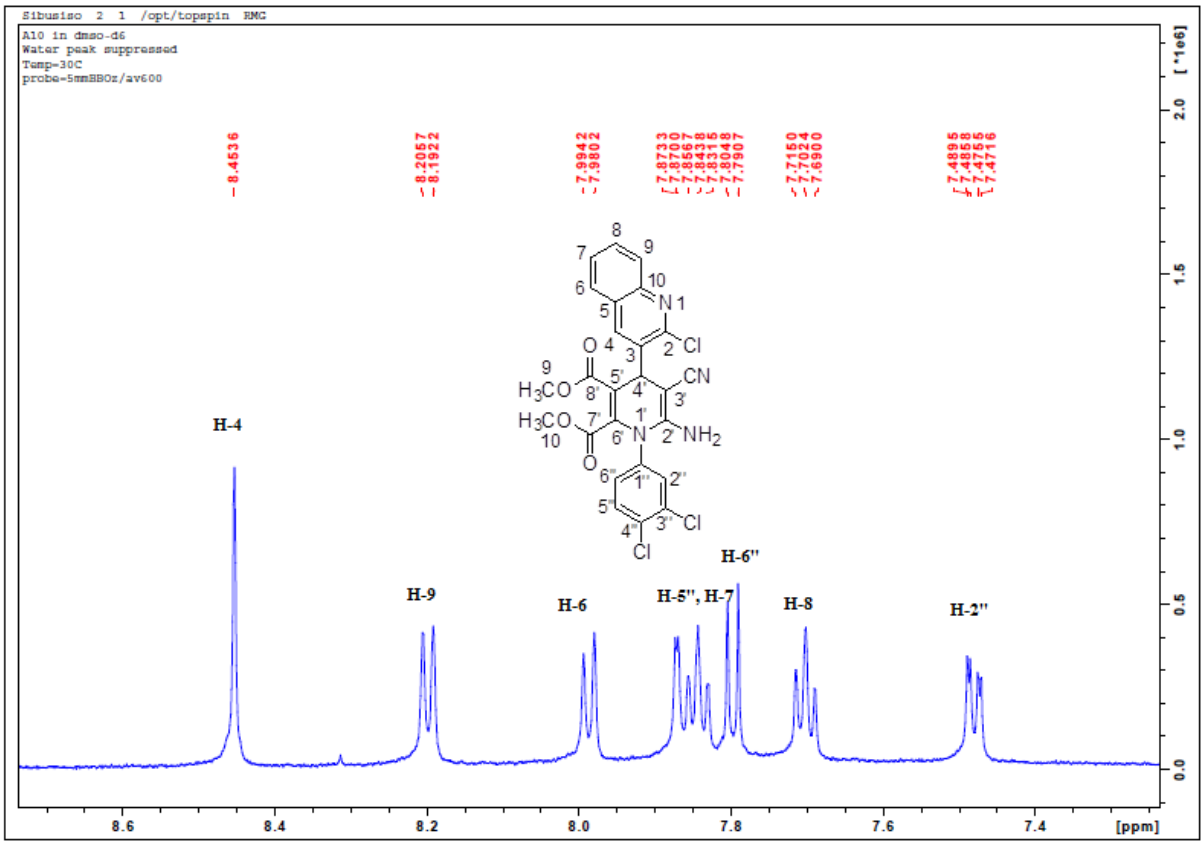

Figure 68: ^{1}H NMR Expanded spectrum of A8, dimethyl 6-amino-4-(2-chloroquinolin-3-yl)-5-cyano-1-(3,4-dichlorophenyl)-1,4-dihydropyridine-2,3-dicarboxylate

Appendix 44

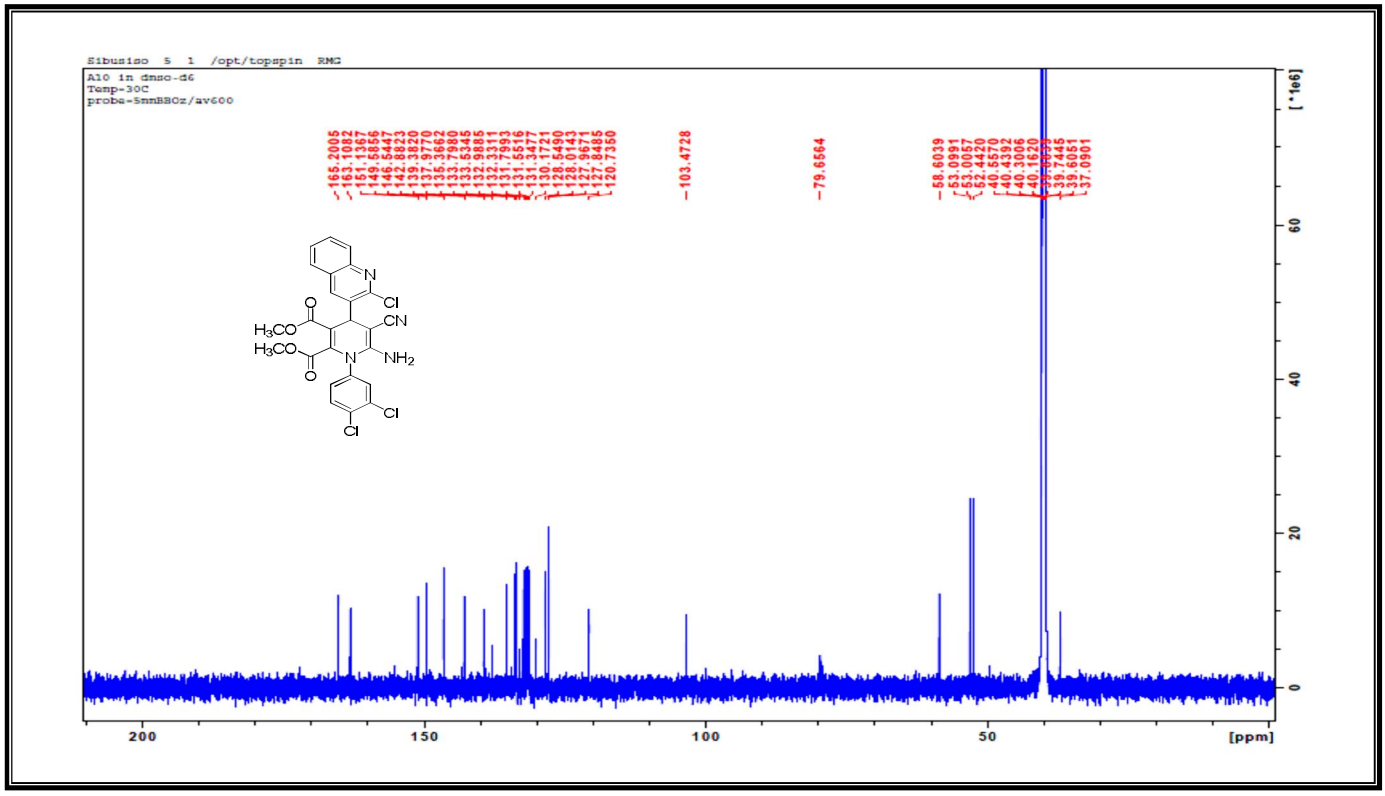

Figure 69: ^{13}C NMR Spectrum of A8, dimethyl 6-amino-4-(2-chloroquinolin-3-yl)-5-cyano-1-(3,4-dichlorophenyl)-1,4-dihydropyridine-2,3-dicarboxylate

Appendix 45

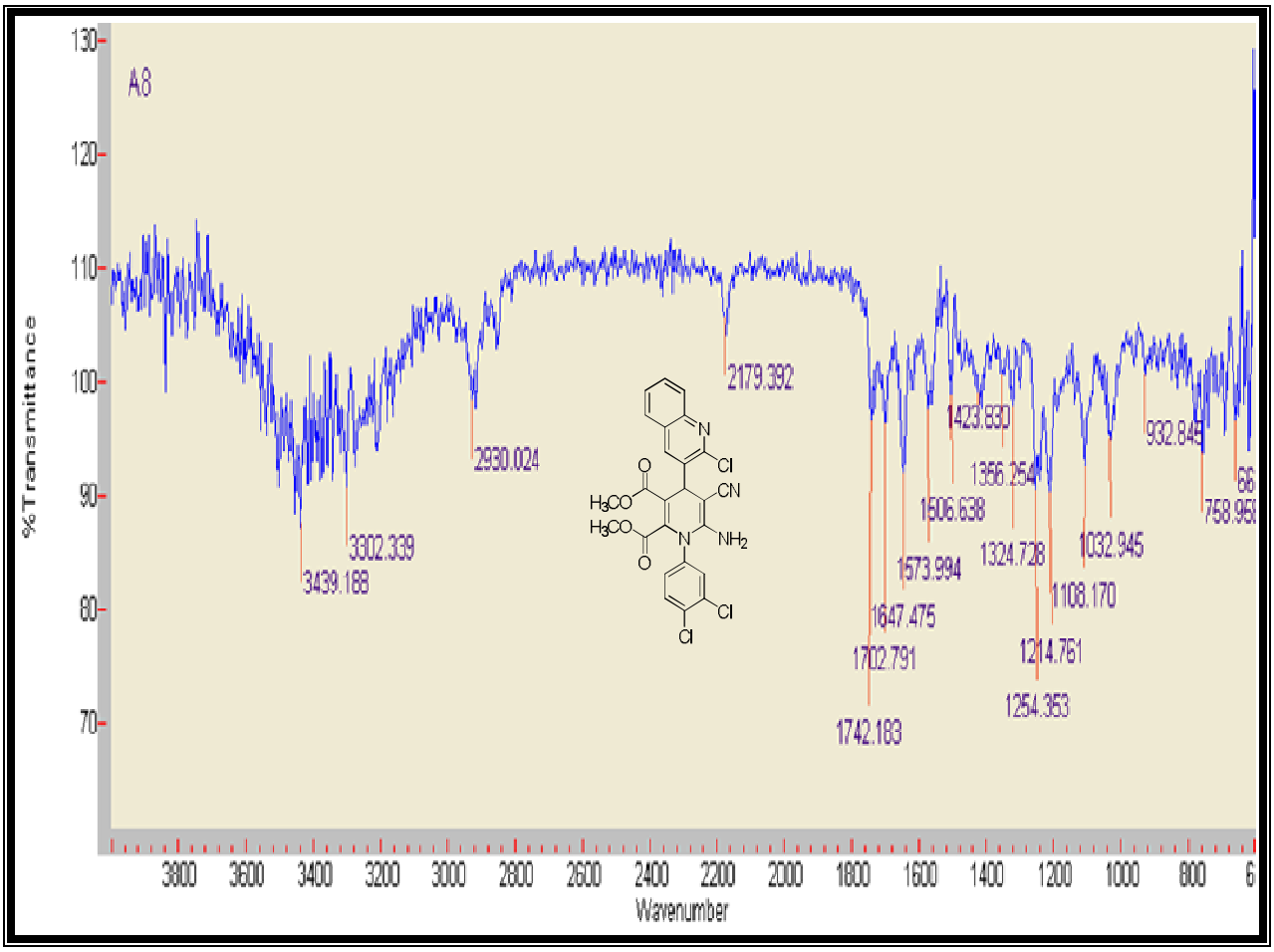

Figure 70: IR Spectrum of A8, dimethyl 6-amino-4-(2-chloroquinolin-3-yl)-5-cyano-1-(3,4-dichlorophenyl)-1,4-dihydropyridine-2,3-dicarboxylate

Appendix 46

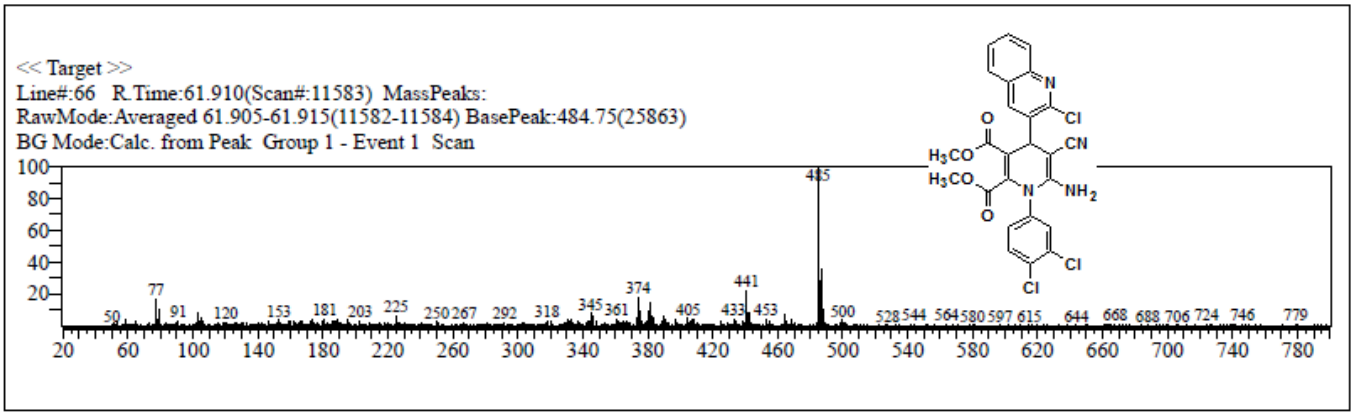

Figure 71: The Mass Spectrum of A8, dimethyl 6-amino-4-(2-chloroquinolin-3-yl)-5-cyano-1-(3,4-dichlorophenyl)-1,4-dihydropyridine-2,3-dicarboxylate

PUBLISHED RESEARCH PAPER

Journal of Photochemistry & Photobiology, B: Biology 165 (2016) 266–276

Contents lists available at ScienceDirect

Journal of Photochemistry & Photobiology, B: Biology

journal homepage: www.elsevier.com/locate/jphotobiol

Design, synthesis, anticancer, antimicrobial activities and molecular docking studies of novel quinoline bearing dihydropyridines

S'busiso Mfan'vele Nkosi [a], Krishnan Anand [a], S Anandakumar [b], Sanil Singh [c], Anil Amichund Chuturgoon [d], Robert Moonsamy Gengan [a,*]

[a] Department of Chemistry, Faculty of Applied Science, Durban University of Technology, Durban 4001, South Africa
[b] Department of Biotechnology, Bhupath and Jothi Mehtha School of Bioscience, Indian Institute of Technology-Madras, Chennai – 600 036, Tamil Nadu, India
[c] Department of Biomedical Resource Centre, University of KwaZulu-Natal, Westville, Durban 4001, South Africa
[d] Discipline of Medical Biochemistry, School of Laboratory Medicine and Medical Sciences, University of KwaZulu-Natal, Durban 4001, South Africa

ARTICLE INFO

Article history:
Received 1 September 2016
Received in revised form 3 October 2016
Accepted 11 October 2016
Available online 20 October 2016

Keywords:
2-Chloro-3-formylquinoline
Dihydropyridines
Molecular docking
Anti-cancer
Human mdm2

ABSTRACT

A new series of eight quinoline bearing dihydropyridine derivatives (**A1–A8**) were synthesized in high yield and in short reaction time by a four component reaction of 2-chloro-3-fomyl quinoline, malononitrile, arylamines and dimethyl acetylenedicarboxylate in the presence of a catalytic amount of triethylamine. The compounds were fully characterized by IR, NMR and GC–MS. These compounds were screened for potential biological activity in an A549 lung cancer cell line and were also evaluated for their antibacterial activities against *Pseudomonas aeruginosa* ATCC 27853, *Escherichia coli* ATCC 25922 and *Staphylococcus aureus* ATCC 29213 whilst their molecular docking properties in an enzymatic system were also determined. Compounds A2, A3, A4 and A8 showed anti-proliferative activity; with A4 having the highest toxicity at 250 μg/mL and A8 has high toxicity at 125, 250 and 500 μg/mL, respectively. Antibacterial results indicated that A4 have significant activity against tested microorganisms at the minimum inhibitory concentration (MIC) values of 32 μg/mL against *Pseudomonas aeruginosa* and *Escherichia coli*, and 16 μg/mL against *Staphylococcus aureus*. Docking of **A1** with human mdm2 indicated the lowest binding energy (−6.111 Kcal/mol) thereby showing strong affinity of the ligand molecule with the receptor which has been stabilized by strong hydrogen bond interactions in the binding pocket. This confirms that **A1** is a better inhibitor for E3 ubiquitin-protein ligase mdm2.

1. Introduction

Quinolines and their derivatives represent an important class of nitrogen-containing heterocycles as they are useful dyes and intermediates in organic synthesis [1]. In recent years, much attention has been focused on their synthesis as they possess useful biological activities such as anti-malarial [2], anti-inflammatory [3], bactericidal [4], fungicidal [5] and anti-cancer [6]. Because of their important role in the pharmaceutical field [7], the profiles of quinolines and their pharmaceutical properties are well documented [8,9].

On the other hand, many naturally occurring and synthetic compounds bearing pyridine scaffold possess interesting biological properties and they are well known for their versatile biological activities like antimicrobial [10], antitubercular [11,12], anticancer [13] and antitumor activity [14]. The polysubstituted pyridine represent molecular framework that serves as a platform for development of pharmaceutical agents. Thus, the synthetic of highly functionalized pyridine derivatives has become an active area of research [15–18]. Encouraged by quinolines and pyridines potent clinical applications and in continuation of our previous investigations on biopotent heterocycles [19], in this study, our efforts focused on the design and synthesis of more biological potent heterocyclic systems *via* combination of both therapeutically active moieties of quinoline and pyridine in a single scaffold.

Tandem multi-component reactions, in which multiple reactions are simulated in one synthetic operation, have been used comprehensively to form carbon-carbon bonds [20]. Such reactions offer a wide range of possibilities for the efficient formation of highly complex molecules in a single operation. Multi-component reactions (MCRs) are reactions using more than two starting materials that form a product which contains the key parts of all of the starting materials [21] in a few *in-situ* reaction steps. Compared with conventional organic reactions, MCRs are more profitable and requires minimum energy to complete the reaction. Several MCRs are known which include the Ugi 4 component condensation of amine, ketone, carboxylic acid and isocyanide [22]. The Strecker reaction, documented in 1850, was the first MCR described [23]. Recently, there has been a tremendous development in three and four-component reactions and huge attempts have been made are continuously being made to

* Corresponding author.
E-mail address: genganrm@dut.ac.za (R.M. Gengan).

http://dx.doi.org/10.1016/j.jphotobiol.2016.10.009
1011-1344/

discover and amplify new MCRs. Therefore, the development of new synthetic approaches using MCRs remains an active research area of study [24]. The literature reveals that quinoline bearing dihydropyridine derivatives in Fig. 1 have received much interest in the field of chemistry owing to their association with a variety of biological activities [25,26].

Cancer, a worldwide epidemic and one of the leading causes of death in developed countries, is responsible for 20–25% of all deaths [27,28]. Lung cancer in humans is common and often fatal [29]. Quinolines play a significant role in the development of new anti-cancer agents; their derivatives have shown excellent results through different mechanism of action such as growth inhibitors by cell cycle arrest, apoptosis, inhibition of angiogenesis, disruption of cell migration, and modulation of nuclear receptor responsiveness [30].

A number of developments have advanced drug discovery [31,32]. Increasingly, as the structures of more potential compounds are becoming available, molecular docking is progressively being studied for pharmacologically or biologically active chemical compounds [33]. Docking is a method which predicts the preferred orientation of one molecule to a moment when they bound to each other to form a stable complex. Docking it is a key tool in structural molecular biology and computer-assisted drug design. The goal of ligand-protein docking is to predict the predominant binding mode of a ligand with a protein of known three-dimensional structure [34].

Pathogenic bacteria are becoming resistance to anti-microbial treatment because of acquired resistance genes in the DNA of the micro-organism. Therefore, the antibiotic resistance problem demands continuous discovery and development of new antibacterial agents that could be used for the effective treatment of infectious diseases [35]. Realizing the medicinal importance of quinoline and pyridine based compounds; we undertook an investigation to synthesize novel quinoline bearing dihydropyridine derivatives and study their application in biological systems. The scope of this study was to synthesize novel quinoline bearing dihydropyridine type molecules from simple and cost effective starting materials, hence, purify the compounds by chromatographic techniques and characterize them by spectroscopy. Furthermore, the study seeks to also, assess and compare their potential as anti-cancer drugs in A549 lung cancer cell lines, evaluate their molecular modeling properties and anti-microbial activities.

2. Materials and Methods

2.1. Chemistry

All reagents and solvents such as aniline, *m*-toluidine, *o*-anisidine, fluoroaniline, chloroaniline, petroleum ether, ethanol, ethyl acetate and triethylamine were purchased from Lasec SA, Aldrich, Fluka and Merck. These reagents and solvents were used without further purification. Melting points were recorded on Stuart Digital melting point apparatus. The ^{1}H and ^{13}C NMR, ^{19}F NMR, COSY, NOESY, HSQC and HMBC spectra were recorded either on Bruker (600 MHz) or Bruker (400 MHz) spectrophotometers in $CDCl_3$ or DMSO using tetramethylsilane (TMS) as an internal reference. The chemical shifts were quoted in parts per million (ppm). The IR spectra were recorded on Perkin Elmer 537 spectrophotometer and Shimadzu-8201 FT instrument, using ATR. Lung cancer cells (A549) were purchased from Highveld Biologicals (Johannesburg, SA). Cell culture reagents were purchased from Whitehead Scientific (Johannesburg, SA). Fresh Nutrient Agar, Oxoid LTD was purchased from Hampsphire, England and Fresh Mueller Hinton Broth from Sigma-Aldrich, (SA) all other reagents and consumables were purchased from Merck (SA), unless otherwise stated.

2.2. Synthesis of a Starting Compound 2-Chloro-3-formyl Quinoline

Dry DMF (3 mmol) was cooled to 0 °C in a flask equipped with a drying tube and then $POCl_3$ (12 mmol) was added drop-wise with stirring. To this solution, acetanilide (1 mmol) was added in small portions and after 25–30 min the reaction mixture was heated for 24 h on a boiling water bath. The reaction mixture was poured into ice water and stirred for 30 min. The work-up was performed with aqueous NaOH to form a precipitate, to hydrolyse the imine salt and remove any acid formed. The solid was filtered, dried and purified from ethyl acetate to give 2-chloro-3-formyl quinoline in high yield (90%).

2.3. General Procedure for Synthesis of Quinoline Bearing Dihydropyridine Derivatives (A1–A8)

In a round bottom flask, a mixture of 2-chloro-3-formyl quinoline (2.0 mmol, 0.3831 g), malononitrile (2.0 mmol, 0.1324 g) and triethylamine (1.0 mL) in 20 mL ethanol was stirred at room for 30 min. Then a solution of arylamines (2.0 mmol) and dimethyl acetylenedicarboxylate (2.0 mmol, 0.284 g) in 25.0 mL ethanol was added to it. The solution was stirred at room temperature for 10 h. The resultant precipitate was collected by filtration and washed with cold ethanol to give the pure product and purified by column chromatography (50:50 petroleum ether:ethyl acetate) (Scheme 1).

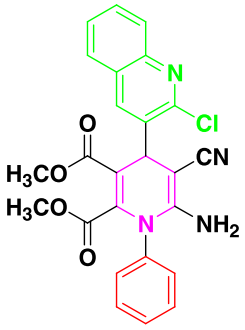

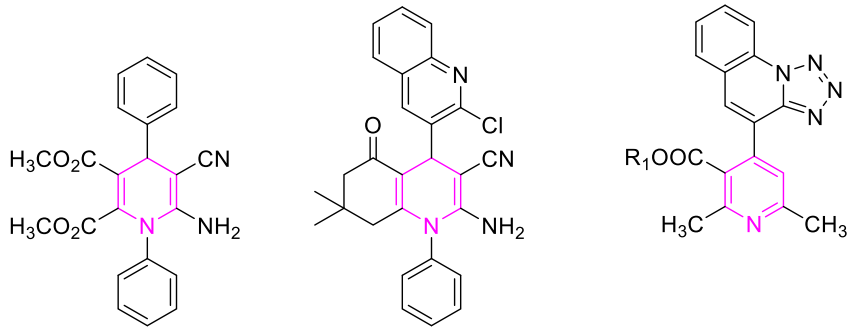

Anticancer Agent Antifungal Agent Anticancer Agent

Fig. 1. Dihydropyridine-based bioactive compounds.

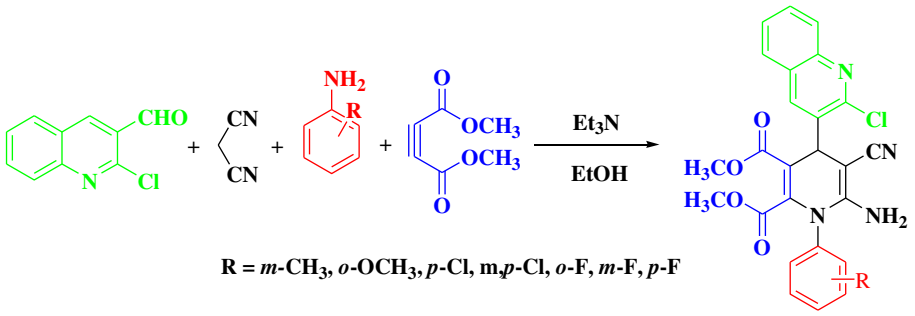

Scheme 1. Synthesis of quinoline bearing dihydropyridines.

Dimethyl-6-amino-4-(2-chloroquinolin-3-yl)-5-cyano-1-phenyl-1,4-dihydropyridine-2,3-dicarboxylate (**A1**): Light yellow solid, 87%, m.p. 275–276 °C, ^{1}H NMR (600 MHz, $CDCl_3$) δ: 8.14 (s, 1H, ArH), 8.02 (d, J = 8.4 Hz, 1H, ArH), 7.84 (d, J = 8.1 Hz, 1H, ArH), 7.71 (t, J = 7.3 Hz, 2H, ArH), 7.55 (t, J = 7.6 Hz, 1H, ArH), 7.52–7.51 (m, 2H, ArH), 7.39–7.38 (m, 2H, ArH), 5.36 (s, 1H, CH), 4.13 (s, 2H, NH_2), 3.51 (s, 3H, OCH_3), 3.44 (s, 3H, OCH_3); ^{13}C NMR (600 MHz, $CDCl_3$) δ: 165.28, 163.20, 150.22, 149.88, 146.93, 142.99, 138.59, 136.14, 134.89, 130.81, 130.47, 130.37, 130.09, 128.34, 127.62, 127.55, 127.11, 119.74, 103.55, 61.22, 52.66, 52.12, 36.94; (IR) υ/cm^{-1}: 3486, 3356, 2171, 1748, 1713, 1647, 1524, 1488, 1448, 1324, 1296, 1247, 1105, 1024, 992, 841, 835, 778, 762, 669, 667, 550. MS (m/z): 475. Anal. calculated for $C_{25}H_{19}ClN_4O_4$: C 63.23; H 4.03; Cl 7.47; N 11.80; O 13.48: Found, C 63.87; H 4.05; Cl 7.50; N 11.88; O 13.81.

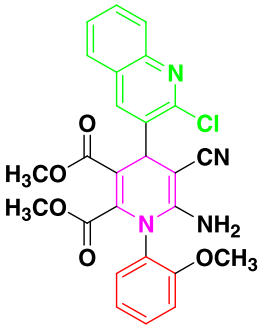

Dimethyl-6-amino-4-(2-chloroquinolin-3-yl)-5-cyano-1-(2-methoxyphenyl)-1,4-dihydropyridine-2,3-dicarboxylate (**A2**): Yellow solid, 40%, m.p. 263–264 °C, ^{1}H NMR (600 MHz, $CDCl_3$) δ: 8.39 (s, 1H, ArH), 8.01 (d, J = 8.4 Hz, 1H, ArH), 7.84 (d, J = 8.1 Hz, 1H, ArH), 7.80 (d, J = 8.1 Hz, 1H, ArH) 7.69 (t, J = 7.6 Hz, 1H, ArH), 7.53 (d, J = 7.1 Hz, 1H, ArH), 7.49 (d, J = 7.8 Hz, 1H, ArH), 7.30 (d, J = 7.3 Hz, 1H, ArH), 7.06–7.02 (m, 1H, ArH), 5.36 (s, 1H, CH), 4.17 (s, 2H, NH_2), 3.50 (s, 3H, OCH_3), 3.49 (s, 3H, OCH_3), 3.46 (s, 3H, OCH_3); ^{13}C NMR (600 MHz, $CDCl_3$) δ: 165.39, 163.33, 157.37, 150.89, 149.91, 146.91, 138.66, 132.57, 130.38, 128.53, 128.31, 127.56, 127.31, 127.03, 121.14, 121.04, 119.99, 112.7, 112.63, 61.80, 52.66, 52.54, 52,10, 36.36; (IR) υ/cm^{-1}: 3437, 3315, 3217, 2185, 1716, 1746, 1665, 1577, 1496, 1421, 1354, 1329, 1222, 1117, 933, 932, 859, 817, 782, 755, 624; MS (m/z): 504. Anal. calculated for $C_{26}H_{21}ClN_4O_5$: C 61.85; H 4.19; Cl 7.02; N 11.10; O 15.84: Found, C 61.87; H 4.25; Cl 7.10; N 11.08; O 15.81.

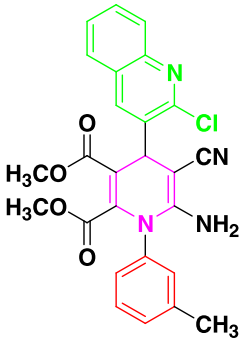

Dimethyl-6-amino-4-(2-chloroquinolin-3-yl)-5-cyano-1-*m*-tolyl-1,4-dihydropyridine-2,3-dicarboxylate (**A3**): Yellow solid, 73%, m.p. 237–238 °C, ^{1}H NMR (600 MHz, $CDCl_3$) δ: 8.12 (s, 1H, ArH), 8.00 (d, J = 9.7 Hz, 1H, ArH), 7.84 (d, J = 8.1 Hz, 1H, ArH), 7.69 (t, J = 10.1 Hz, 1H, ArH), 7.53 (t, J = 11.2 Hz, 1H, ArH), 7.36 (t, J = 9.9 Hz, 1H, ArH), 7.29 (d, J = 7.6 Hz, 1H, ArH), 7.23 (s, 1H, ArH), 7.16 (d, J = 6.4 Hz, 1H, ArH), 5.33 (s, 1H, CH), 4.23 (s, 2H, NH_2), 3.50 (s, 3H, OCH_3), 3.44 (s, 3H, OCH_3), 2.39 (s, 3H, CH_3). ^{13}C NMR (600 MHz, $CDCl_3$) δ: 165.31, 163.20, 150.41, 149.87, 146.89, 143.06, 140.45, 138.53, 136.47, 134.74, 131.51, 130.70, 130.42, 129.79, 128.30, 127.67, 127.55, 127.15, 127.08, 119.91, 60.83, 52.61, 52.07, 36.73, 21.23; (IR) υ/cm^{-1}: 3386, 3318, 2180, 1702, 1647, 1565, 1488, 1420, 1358, 1328, 1253, 1224, 1136, 1114, 1056, 1019, 968, 928, 786, 763, 708, 686; MS (m/z) 487. Anal. calculated for $C_{26}H_{21}ClN_4O_4$: C 63.87; H 4.33; Cl 7.25; N 11.46; O 13.09: Found, C 63.20; H 4.31; Cl 7.11; N 11.36; O 13.23.

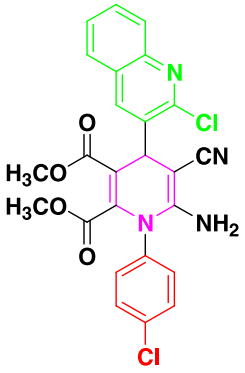

Dimethyl-6-amino-1-(4-chlorophenyl)-4-(2-chloroquinolin-3-yl)-5-cyano-1,4-dihydropyridine-2,3-dicarboxylate (**A4**): Light yellow solid, 79%, m.p. 287–289 °C, ^{1}H NMR (600 MHz, DMSO) δ: 8.38 (s, 1H, ArH), 8.17 (d, J = 8.1 Hz, 1H, ArH), 7.98 (d, J = 8.5 Hz, 1H, ArH), 7.84 (t, J = 6.9 Hz, 1H, ArH), 7.70 (t, J = 7.9 Hz, 1H, ArH), 7.60 (d, J =

8.8 Hz, 2H, ArH), 7.49 (d, $J = 11.2$ Hz, 2H, ArH), 5.86 (s, 2H, NH_2), 5.24 (s, 1H, CH), 3.45(s, 3H, OCH_3), 3.43(s, 3H, OCH_3).· ^{13}C NMR (600 MHz, DMSO) δ: 165.21, 163.13, 151.42, 149.57, 146.54, 143.31, 139.11, 137.73, 135.37, 134.41, 132.98, 131.37, 130.17, 128.52, 128.01, 127.92, 127.89, 127.87, 120.77, 103.14, 58.54, 52.43, 52.01, 39.60; (IR) υ/cm^{-1}: 3428, 3218, 2174, 1745, 1703, 1650, 1623, 1593, 1571, 1489, 1354, 1257, 1219, 1107, 1090, 1018, 850, 825, 780, 741, 723; MS (*m/z*) 510. Anal. calculated for $C_{25}H_{18}Cl_2N_4O_4$: C 58.95; H 3.56; Cl 13.92; N 11.00; O 12.56: Found, C 63.19; H 3.55; Cl 7.15; N 11.39; O 13.22.

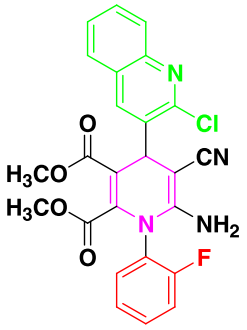

Dimethyl-6-amino-4-(2-chloroquinolin-3-yl)-5-cyano-1-(2-fluorophenyl)-1,4-dihydropyridine-2,3-dicarboxylate (**A5**): White solid, 64%, m.p. 247–248 °C, ^{1}H NMR (600 MHz, DMSO) δ: 8.33 (s, 1H, ArH), 7.84 (d, $J = 7.3$ Hz, 2H, ArH), 7.67 (d, $J = 7.1$ Hz, 2H, ArH), 7.59 (m, 2H, ArH), 7.37–7.33 (m, 2H, ArH), 5.99 (s, 2H, NH_2), 5.22 (s, 1H, CH), 3.46 (s, 6H, OCH_3). ^{13}C NMR (600 MHz, DMSO) δ: 165.59, 165.02, 164.10, 163.04, 160.57, 158.91, 151.33, 146.57, 143.21, 133.50, 133.44, 131.46, 129.07, 128.89, 128.66, 128.40, 128.07, 120.59, 79.62, 53.61, 53.15, 49.07, 40.53, 39.57, 29.44; (IR) υ/cm^{-1}: 3376, 3282, 2178, 1747, 1712, 1654, 1571, 1488, 1422, 1360, 1329, 1258, 1231, 1171, 1032, 967, 922, 872, 851, 761, 648, 644.

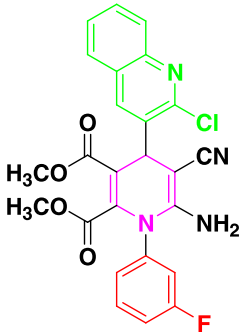

Dimethyl-6-amino-4-(2-chloroquinolin-3-yl)-5-cyano-1-(3-fluorophenyl)-1,4-dihydropyridine-2,3-dicarboxylate (**A6**): White solid, 31%, m.p. 269–271 °C, ^{1}H NMR (600 MHz, DMSO) δ: 8.40 (s, 1H, ArH), 8.19 (d, $J = 8.4$ Hz, 1H, ArH), 7.99 (d, $J = 8.5$ Hz, 1H, ArH), 7.84 (t, $J = 7.0$ Hz, 1H, ArH), 7.70 (t, $J = 6.9$ Hz, 1H, ArH), 7.61–7.56 (m, 1H, ArH), 7.42 (m, 1H, ArH), 7.31 (d, $J = 7.2$ Hz, 1H, ArH), 5.86 (s, 2H, NH_2), 5.25 (s, 1H, CH), 3.45 (m, 3H, OCH_3), 3.40 (m, 3H, OCH_3), ^{13}C NMR (600 MHz, DMSO) δ: 165.75, 163.09, 161.65, 151.60, 149.57, 145.55, 143.15, 139.12, 137.87, 136.84, 131.61, 131.56, 131.36, 128.55, 128.00, 127.74, 120.74, 121.91, 118.74, 117.86, 58.75, 52.96, 52.09, 37.10; (IR) υ/cm^{-1}: 3449, 3303, 2177, 1746, 1715, 1652, 1596, 1570, 1487, 1421, 1329, 1305, 1251, 1194, 1136, 1106, 1033, 966, 924, 819, 763, 706, 899. ^{19}F NMR (600 MHz, DMSO) δ: 111.23; MS (*m/z*) 494. Anal. calculated for $C_{25}H_{18}ClFN_4O_4$: C 60.92; H 3.68; Cl 7.19; F 3.85; N 11.37; O 12.98: Found, C 60.90; H 3.68; Cl 7.11; F 3.84; N 11.36; O 12.99.

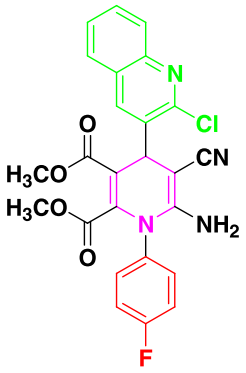

Dimethyl-6-amino-4-(2-chloroquinolin-3-yl)-5-cyano-1-(4-fluorophenyl)-1,4-dihydropyridine-2,3-dicarboxylate (**A7**): White solid, 60%, m.p. 253–254 °C, ^{1}H NMR (600 MHz, DMSO) δ: 8.38 (s, 1H, ArH), 8,17 (d, $J = 8.0$ Hz, 1H, ArH), 7.96 (d, $J = 7.6$ Hz, 1H, ArH), 7.82 (t, $J = 7.3$ Hz, 1H, ArH), 7.66 (t, $J = 7.2$ Hz, 1H, ArH), 7.54–7.52 (m, 2H, ArH), 7.38–7.34 (m, 2H, ArH), 5.83 (s, 2H, NH_2), 5.23 (s, 1H, CH), 3.43 (s, 3H, OCH_3) 3.38 (s, 3H, OCH_3); ^{13}C NMR (600 MHz, DMSO) δ: 150.99, 149.9, 149.14, 145.99, 143.03, 142.97, 138.60, 137.44, 137.34, 133.38, 133.37, 133.34, 133.33, 133.26, 113.1.1, 130.06, 128.00, 127.95, 127.38, 120.37, 116.32, 61.65, 57.83, 57.32, 36.77; (IR) υ/cm^{-1}: 3309, 3269, 2171, 1745, 1702, 1622, 1506, 1569, 1329, 1298, 1247, 1213, 1153, 1106, 1027, 1002, 938, 918, 840, 778, 768, 766, 741, 728, 615. ^{19}F NMR (600 MHz, DMSO) δ: 110.91; MS (*m/z*) 494. Anal Calculated for $C_{25}H_{18}ClFN_4O_4$: C 60.92; H 3.68; Cl 7.19; F 3.85; N 11.37; O 12.98: Found, C 60.90; H 3.68; Cl 7.11; F 3.84; N 11.38; O 12.97.

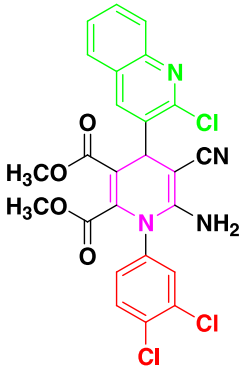

Dimethyl-6-amino-4-(2-chloroquinolin-3-yl)-5-cyano-1-(3,4-dichlorophenyl)-1,4-dihydropyridine-2,3-dicarboxylate (**A8**): Light yellow solid, 72%, m.p. 280–282 °C, ^{1}H NMR (600 MHz, DMSO) δ: 8.45 (s, 1H, ArH), 8.20 (d, $J = 8.1$ Hz, 1H, ArH), 7.99 (d, $J = 8.4$ Hz, 1H, ArH), 7.85 (d, $J = 7.7$ Hz, 1H, ArH), 7.84 (t, $J = 7.7$ Hz, 1H, ArH), 7.70 (t, $J = 7.6$ Hz, 1H, ArH), 7.48 (d, $J = 2.2$ Hz,

Table 1
Synthesis of quinoline bearing dihydropyridines derivatives.

Entry	Compound	Ar	% Yield	m.p. (°C)
1	A1	C_6H_4	87	275–276
2	A2	*o*-$OCH_3C_6H_4$	40	263–264
3	A3	*m*-CH_3-C_6H_4	73	237–238
4	A4	*p*-ClC_6H_4	79	287–288
5	A5	*o*-FC6H4	64	247–248
6	A6	*m*-FC6H4	31	269–271
7	A7	*p*-FC6H4	60	253–254
8	A8	*m,p*-ClC6H4	72	280–282

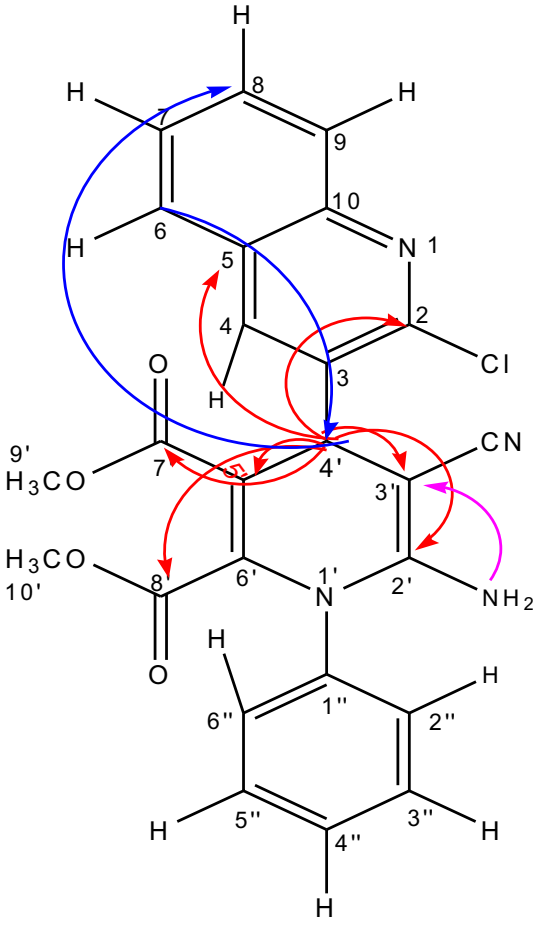

Fig. 2. Selected HMBC correlations for **A1**.

1H, ArH), 7.47 (d, $J = 2.3$ Hz, 1H, ArH), 6.02 (s, 2H, NH_2), 5.25 (s, 1H, CH), 3.43 (s, 3H, OCH_3), 3.39 (s, 3H, OCH_3); ^{13}C NMR (600 MHz, DMSO) δ: 165.20, 163.10, 151.14, 149.58, 146.54, 142.88, 139.38, 137.78, 135.36, 133.79, 133.53, 132.33, 131.79, 131.55, 131.34, 130.17, 128.54, 127.96, 127.84, 120.73, 79.65, 53.09, 53.00, 39.60; (IR) υ/cm^{-1}: 3439, 3302, 2179, 1742, 1702, 1647, 1573, 1506, 1423, 1366, 1324, 1254, 1214, 1108, 1032, 932, 758; MS (m/z) 544. Anal Calculated for $C_{25}H_{17}Cl_3N_4O_4$: C 55.22; H 3.15; Cl 19.56; N 10.30; O 11.77: Found, C 65.19; H 3.16; Cl 19.15; N 10.39; O 11.22.

2.4. Anticancer Study

2.4.1. Maintenance of A549 Cells in Culture

The best environment for growing cells *in vitro* should be matched as close as possible to the natural physiological conditions. The essential requirements are an environment of optimum temperature, pH, gas phases, growth substrate and media containing necessary nutrients. The optimal temperature is provided by the use of a humidified incubator supplied with 5% CO_2. The gas phases supplied to the culture includes oxygen which is maintained at atmospheric pressure, and CO_2 to ensure that the bicarbonate and CO_2 tension is in equilibrium. A549 cells were cultured (37 °C, 5% CO_2) to 90% confluency in 25 mL flasks in complete culture media (CCM) [Eagle's minimum essential medium, 10% foetal calf serum, 1% L-Glutamine and 1% penstrepfungizone]. The culture medium is by far the most important single factor in culturing cells. The extracellular medium must meet the essential requirements (nutritional, hormonal and stromal factors) for survival and growth.

2.4.2. Trypsinisation

In order to sub-culture and plate cells for the various experimental assays, the process of trypsinisation was used to detach cells once 90% confluency was reached. The process of trypsinisation involved the critical step of rinsing the cells with 3 mL aliquots of warm 0.1 M PBS and incubating the cells with 1 mL of trypsin-EDTA (Lonza) for 1 min. The cells were monitored using an inverted light microscope (Olympus IXSI; 20× magnification) and once rounded, the trypsin was discarded and CCM was added to the flask of cells. The flask was agitated to detached cells and the cell suspension was then enumerated by dye exclusion using a haemocytometer. Trypan blue (0.4%) was utilized in a dye exclusion procedure for cell counting. The principle of dye exclusion using trypan blue is based on compromised cell membranes in dead/damaged cells which readily allow entry of the dye into the cells and are stained blue whereas viable cells remain unstained.

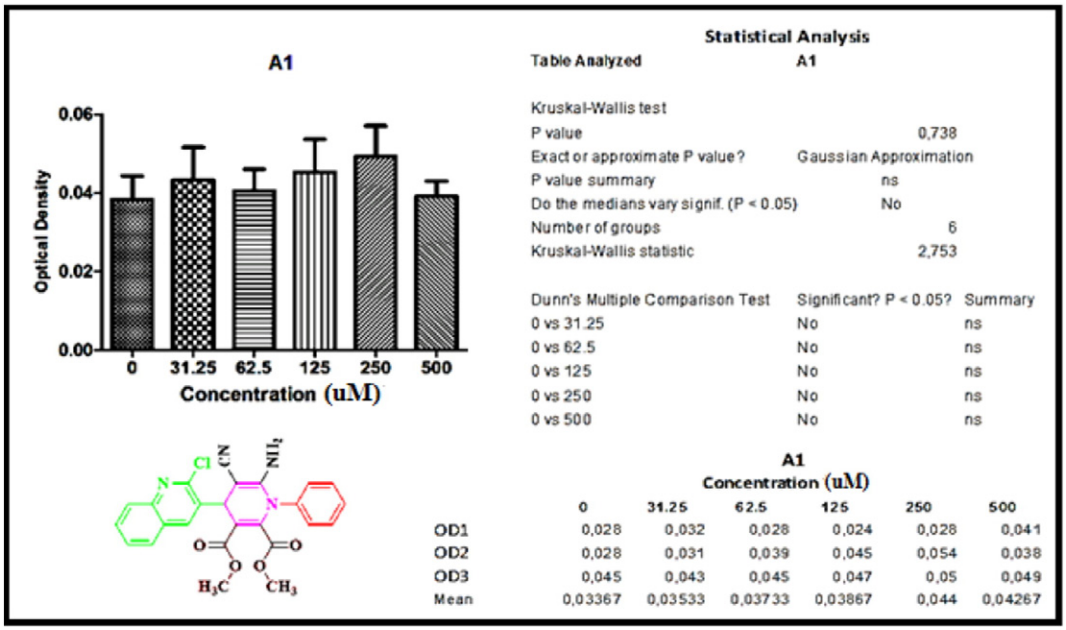

Fig. 3. The cytotoxic effects of A1 in the A549 lung cancer cell line.

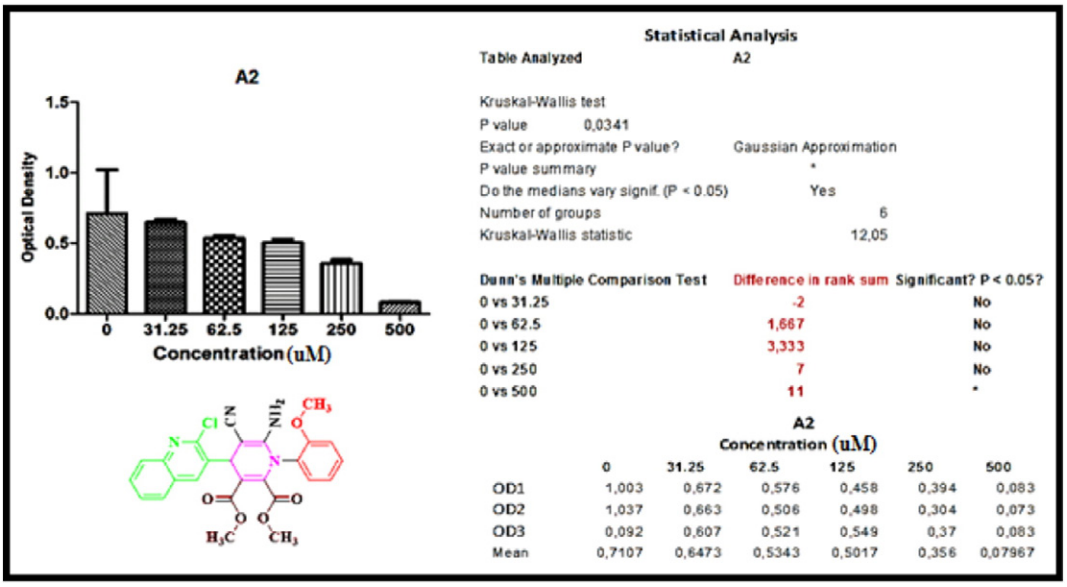

Fig. 4. The cytotoxic effects of A2 in the A549 lung cancer cell line.

2.4.3. Cell Antiproliferation Assay

The effect of newly synthesized compounds in A549 cells was measured using a methyl tetrazolium dye reduction assay, the [3,(4,5-dimethylthiazol-2-yl)-2,5-diphenyl tetrazolium bromide] (MTT) assay. This assay measures cell antiproliferative assay *in vitro*. This technique is particularly useful for cells that are metabolically active based on their redox potential and capacity of dehydrogenase enzymes to convert yellow water-soluble salt into a purple water-insoluble formazan product. The insoluble crystals are then dissolved in dimethyl sulfoxide (DMSO) and the absorbance is read on a spectrophotometer. The amount of formazan produced is directly proportional to cell number thus allowing for the determination of cell viability and proliferation [36].

A549 cells (15,000/well) were incubated for 24 h with a range of concentrations of each compound in triplicate in a micro-titre plate together with an untreated control (cells incubated with CCM only). Each experiment was conducted twice on separate occasions. The data results from the first set matched the repeated experiment. The cells were then incubated (37 °C, 5% CO_2) with the MTT substrate (5 mg/mL in PBS) for 4 h. Thereafter all supernatants were aspirated, and DMSO (100 μL/well) was added to the wells. Finally the optical density was measured at 570 nm and a reference wavelength of 690 nm with an ELISA plate reader (Bio-Tek μQuant).

2.5. Antibacterial Study

2.5.1. Preparation of Media and Nutrient Broth

Fresh nutrient agar and fresh Mueller Hinton Broth were prepared according to the manufacturer's instructions. The cultures of *Staphylococcus aureus*, *Escherichia coli* and *Pseudomonas aeruginosa* were maintained on nutrient agar slopes at 4 °C and sub cultured on to blood agar plates for 24 h before use.

2.5.2. Microplate Alamar Blue Assay (MABA)

An amount of 0.2 g of Resazurin powder was dissolved in 10 mL autoclaved distilled water. The dye solution was vortexed vigorously;

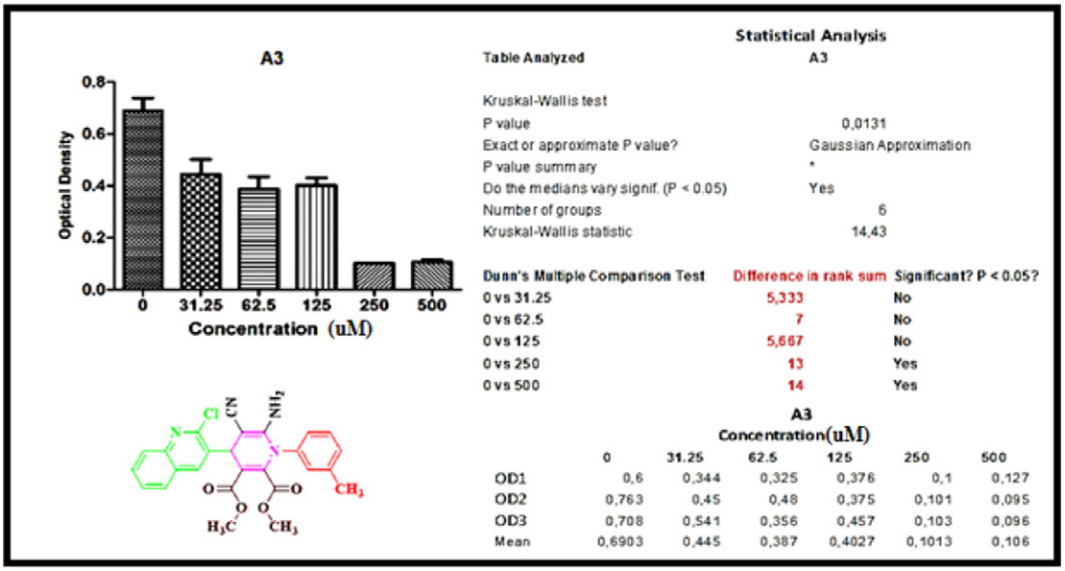

Fig. 5. The cytotoxic effects of A3 in the A549 lung cancer cell line.

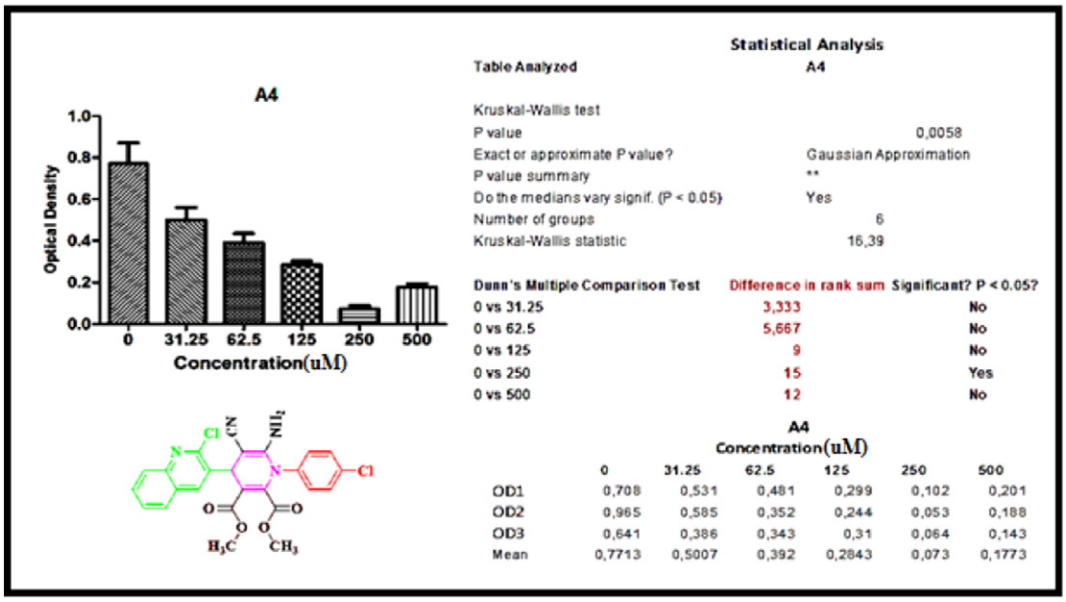

Fig. 6. The cytotoxic effects of A4 in the A549 lung cancer cell line.

the solution was immediately covered with aluminium foil to keep away from light as it is light sensitive.

The *in vitro* antibacterial activities of the synthesized compounds were studied by MABA using 96-wells microplates. Bacterial cultures were diluted in broth to turbidity comparable to that of a 0.5 McFarland turbidity standard and 20 μL of each bacterial dilution was distributed in all 96 wells of microplate including positive control (containing standard antibiotic) and growth control (containing culture broth without testing materials). Then 20 μL of each concentration of the synthesized compounds were added to two neighbour wells except for positive and growth control wells.

After adding Alamar Blue (20 μL) to all of 96 wells, the total volume in each well reached 200 μL. The final concentrations of the tested compounds were 256, 128, 64, 32, 16, 8, 4, 2, 1 μg/mL etc. After incubation, results were recorded as MIC (minimum concentration of each synthesized compound which completely inhibited growth of microorganism). The stock solutions of the synthesized compounds were prepared by dissolving in the minimum volume of DMSO.

2.5.3. Molecular Docking

The crystal structure of human mdm2 (**PDB ID: 3VZV**), were retrieved from the Protein Data Bank After selected the protein structure, protein preparation wizard of Schrodinger suite was used to prepare protein structure. All the water molecules were removed from the protein structure. Metal was treated and hydrogen atoms were added. All atom force field (**OPLS-2005**) charges and atom types were assigned. Protein structure energy was minimized. The chemical compounds structures were not available in pubchem database. Therefore, we used chem sketch to draw the compound structure. All the ligands were prepared for molecular docking studies using ligprep version 2.3 [37]. The ligand structure energy was minimized; partial atomic charges

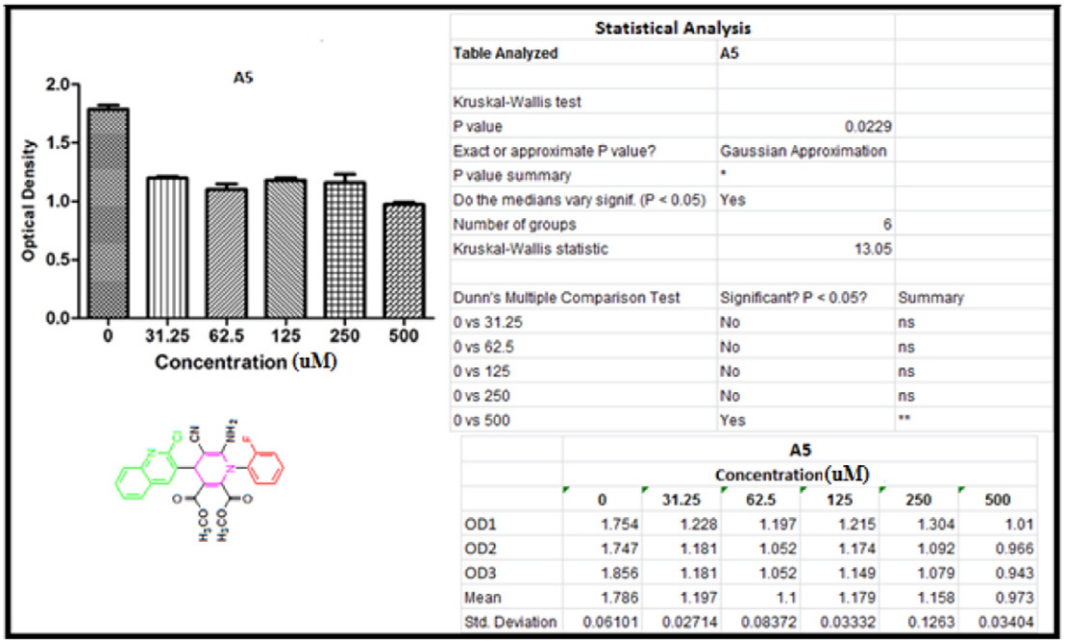

Fig. 7. The cytotoxic effects of A5 in the A549 lung cancer cell line.

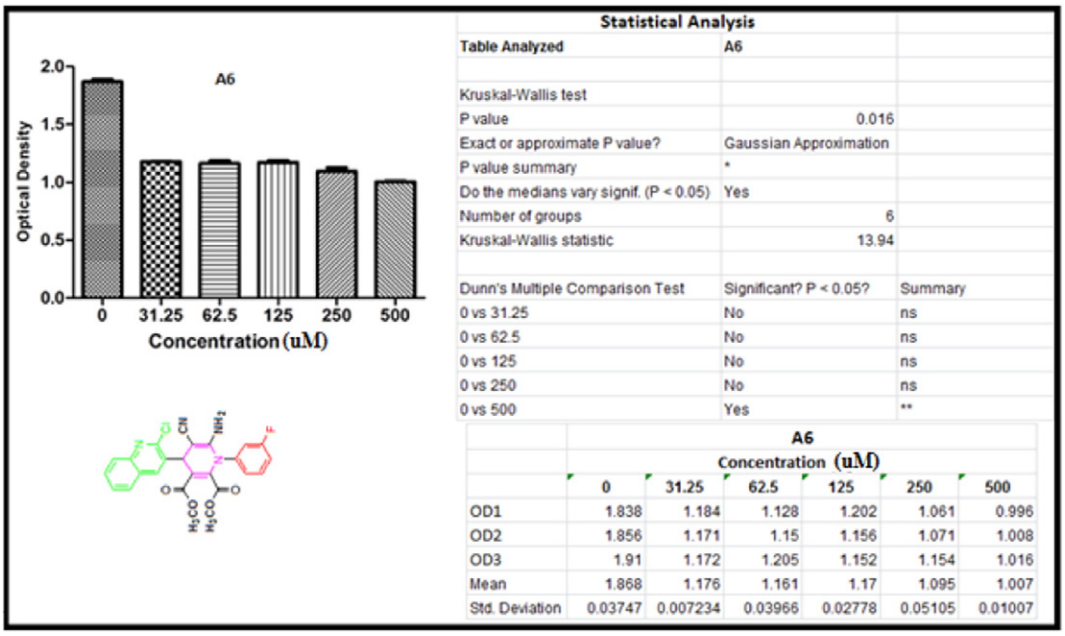

Statistical Analysis

Table Analyzed	A6	
Kruskal-Wallis test		
P value	0.016	
Exact or approximate P value?	Gaussian Approximation	
P value summary	*	
Do the medians vary signif. (P < 0.05)	Yes	
Number of groups	6	
Kruskal-Wallis statistic	13.94	
Dunn's Multiple Comparison Test	Significant? P < 0.05?	Summary
0 vs 31.25	No	ns
0 vs 62.5	No	ns
0 vs 125	No	ns
0 vs 250	No	ns
0 vs 500	Yes	**

	A6 Concentration (uM)					
	0	31.25	62.5	125	250	500
OD1	1.838	1.184	1.128	1.202	1.061	0.996
OD2	1.856	1.171	1.15	1.156	1.071	1.008
OD3	1.91	1.172	1.205	1.152	1.154	1.016
Mean	1.868	1.176	1.161	1.17	1.095	1.007
Std. Deviation	0.03747	0.007234	0.03966	0.02778	0.05105	0.01007

Fig. 8. The cytotoxic effects of A6 in the A549 lung cancer cell line.

were computed using the OPLS-2005 force field by using Schrödinger suite.

The prepared protein structure was followed up by the grid-fashion kinetic docking which commonly holds several physical parameters and finds greater significance in prescribing the ligand interaction with the receptor. Grid files generation for protein was accomplished with "Receptor Grid Generation" panel of Glide. The grid box was generated by assigning a common constituency point. From there an actually cubic grid box was extended to touch the bounty of 20 Å in size. In other words, the allocated size for grid generation of protein-ligand docking was 20 Å since our approach was site-specific not generalized. Having observed that co-crystal ligand binding pattern with protein is already well documented in recent studies, we attempted to crop the grid box to focus on the centroid of human mdm2 refined structure and box coordinate X, Y, Z were set at (X = 18.341215 Å, Y = −3.662453 Å, Z = 0.929674 Å). The foremost process in the hit identification pipeline, docking is performed using Glide of Schrodinger [38].

3. Results and Discussion

The focus of this research was to synthesize novel compounds, especially compounds that contain functional groups with potential biological activities. Since heterocycles containing quinoline are reported to improve the biological activity of organic compounds, our aim was to synthesize novel quinolone bearing dihydropyridine derivatives (Table 1). Also, we decided to use MCR, therefore, our first objective was to synthesize a formyl quinoline derivative using Vilsmeier-Haack

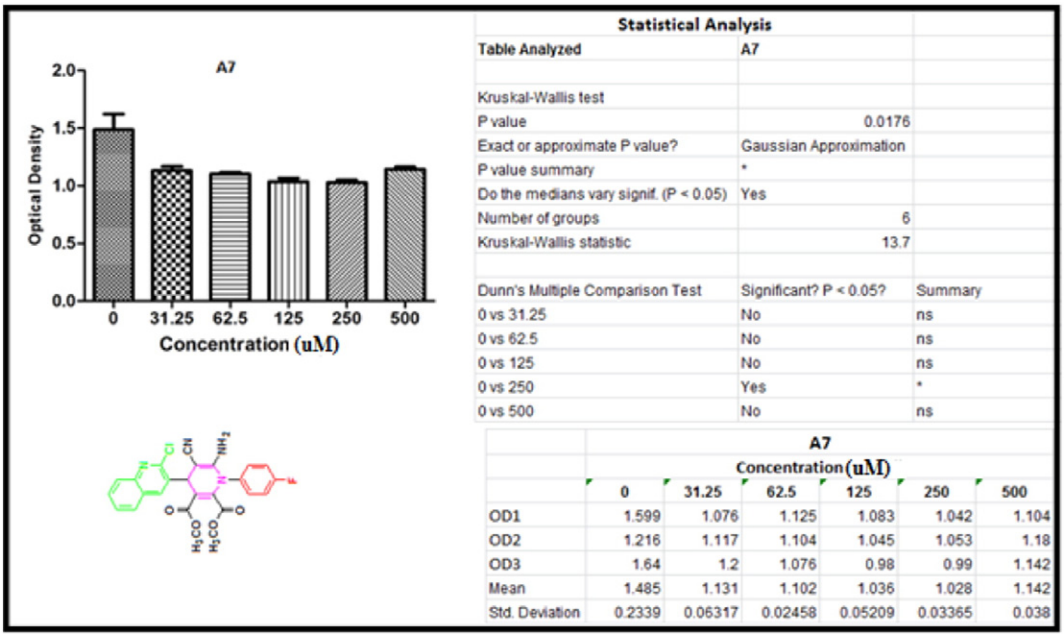

Statistical Analysis

Table Analyzed	A7	
Kruskal-Wallis test		
P value	0.0176	
Exact or approximate P value?	Gaussian Approximation	
P value summary	*	
Do the medians vary signif. (P < 0.05)	Yes	
Number of groups	6	
Kruskal-Wallis statistic	13.7	
Dunn's Multiple Comparison Test	Significant? P < 0.05?	Summary
0 vs 31.25	No	ns
0 vs 62.5	No	ns
0 vs 125	No	ns
0 vs 250	Yes	*
0 vs 500	No	ns

	A7 Concentration (uM)					
	0	31.25	62.5	125	250	500
OD1	1.599	1.076	1.125	1.083	1.042	1.104
OD2	1.216	1.117	1.104	1.045	1.053	1.18
OD3	1.64	1.2	1.076	0.98	0.99	1.142
Mean	1.485	1.131	1.102	1.036	1.028	1.142
Std. Deviation	0.2339	0.06317	0.02458	0.05209	0.03365	0.038

Fig. 9. The cytotoxic effects of A7 in the A549 lung cancer cell line.

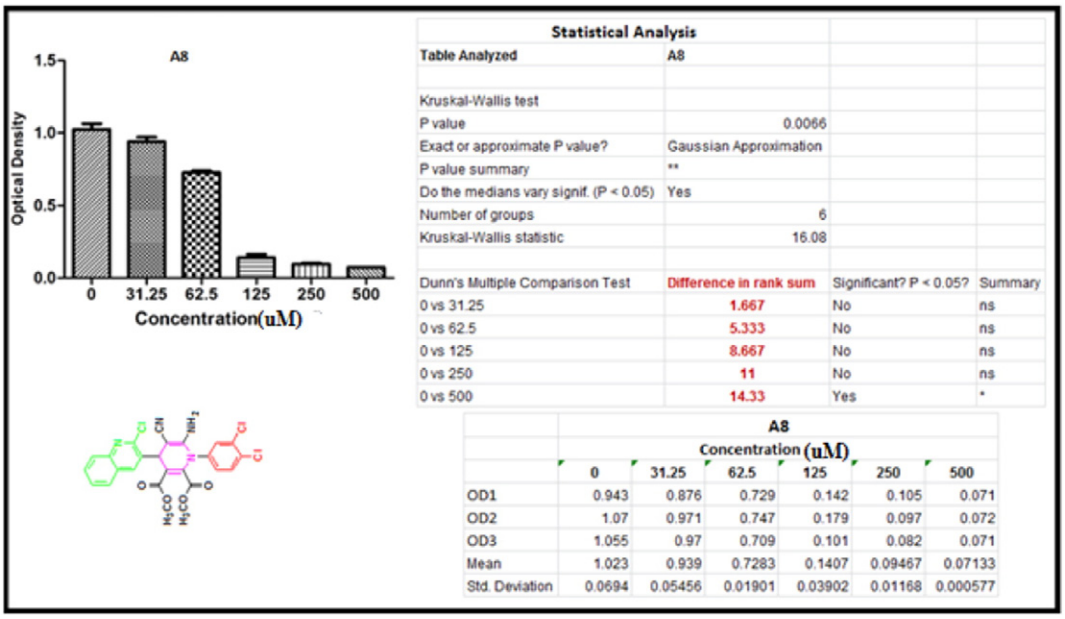

Statistical Analysis

Table Analyzed	A8		
Kruskal-Wallis test			
P value	0.0066		
Exact or approximate P value?	Gaussian Approximation		
P value summary	**		
Do the medians vary signif. (P < 0.05)	Yes		
Number of groups	6		
Kruskal-Wallis statistic	16.08		
Dunn's Multiple Comparison Test	Difference in rank sum	Significant? P < 0.05?	Summary
0 vs 31.25	1.667	No	ns
0 vs 62.5	5.333	No	ns
0 vs 125	8.667	No	ns
0 vs 250	11	No	ns
0 vs 500	14.33	Yes	*

A8

	Concentration (uM)					
	0	31.25	62.5	125	250	500
OD1	0.943	0.876	0.729	0.142	0.105	0.071
OD2	1.07	0.971	0.747	0.179	0.097	0.072
OD3	1.055	0.97	0.709	0.101	0.082	0.071
Mean	1.023	0.939	0.7283	0.1407	0.09467	0.07133
Std. Deviation	0.0694	0.05456	0.01901	0.03902	0.01168	0.000577

Fig. 10. The cytotoxic effects of A8 in the A549 lung cancer cell line.

reaction [39] which could be used as one of the substrates for the one pot MCR.

The identity of all the compounds (**A1–A8**) were confirmed by analyzing the spectral data obtained from IR, ^{1}H NMR, ^{13}C NMR and GCMS. All the spectra were well resolved. We selected **A1** as the template and characterized the structure fully with the aid of 2D NMR techniques especially HSQC, HMBC, COSY and NOESY which led to the unambiguous assigning of all protons and carbons. We used the characterization of **A1** as a template to elucidate the other 7 derivatives. The IR spectra of **A1** showed the C═O stretching at 1713 cm^{-1} and 1748 cm^{-1}, the C—N stretching at 2171 cm^{-1}, the C—Cl stretching at 669–778 cm^{-1} whilst the NH stretching at 3486 cm^{-1} and 3356 cm^{-1} was not well resolved.

The ^{1}H NMR spectrum of **A1** showed singlets at δ 3.44 and δ 3.51 for two acetoxy groups (H-9′, H-10′). The singlets at δ 4.13 and δ 5.35 were assigned to the amino (NH_2) and aliphatic proton (H-4′) on the dihydropyridine ring, respectively. The peaks at δ 8.14–7.38 were attributed to aromatic protons. The chemical shifts, spin multiplicities and coupling constants (in Hertz) were assigned as: δ 8.14 (H-4, s); δ 7.84 (d, H-6, 3.2); δ 7.71 (t, H-7, 7.6); δ 7.64 (t, H-8, 7.4); δ 8.02 (d, H-9, 8.4); δ 7.39–7.36 (m, H-2″, H-4″, H-6″); δ 7.54–7.51 (m, H-3″–H-5). The COSY spectrum, presented in Fig. S4, shows H-9 has a strong coupling with H-8 but a weaker coupling with H-7. The corresponding carbon resonances of H-7, H-8 and H-9 appeared at δ 130.17, 130.87 and 130.47, respectively and the absence of correlation between the carbons to the amino protons confirm the assignment of the NH_2, according to the HSQC spectrum, presented in Fig. S6. The NOESY spectrum, presented in Fig. S7, shows the coupling of H-9 to H-8; H-6 is coupled to H-7 and H-8 whilst H-7 is coupled to H-6 and H-8. Furthermore, the COSY spectrum shows a strong coupling between H-6 and H-7 and between H-7 and H-8 whilst a weak coupling is observed between H-7 and H-9. Also H-4 lacked any coupling signals. Both H-4 and H-6 shows the HMBC correlations to C-2, C-4′ and C-5, presented in Fig. S5, at δ 150.99, 120.33 and 134.90, respectively. The ^{4}J correlations at H-4′ to C-5 and H-4′ to C-8, ^{5}J correlation at H-6 to C-4′ were

Table 2
Antibacterial activities of (A1–A8): minimum inhibitory concentration.

Compound	*Staphylococcus aureus* (μM)	*Pseudomonas aeruginosa* (μM)	*Escherichia coli* (μM)
A1	–	128	256
A2	256	256	256
A3	256	256	256
A4	16	32	32
A5	128	256	128
A6	–	256	–
A7	32	32	32
A8	8	16	32
Nalidixic acid	50	128	16
Ciprofloxacin	50	25	25
DMSO	–	–	–

Table 3
Glide extra-precision (XP) for (A1–A8) with human mdm2 by use of Schrodinger.

Title	Glide score	Glide energy	No. of H bonds	Interacting residues	Distance (Å)	Hydrogen bond donor	Hydrogen bond acceptor
A1	−6.111	−62.406	1	Tyr 104	2.15	Ligand: (H)	A: TYR 104: (O)
A2	−2.616	−27.659	–	–	–	–	–
A3	−4.391	−35.217	1	Thr 26	2.04	A: THR 26: (H)	Ligand: (O)
A4	−3.963	−16.574	1	Thr 26	1.97	A: THR 26: (H)	Ligand: (O)
A5	−4.995	−44.146	1	Thr 26	2.05	A: THR 26: (H)HG1	Ligand: (O)
A6	−4.667	−42.032	1	Thr 26	2.04	A: THR 26: (H)HG1	Ligand: (O)
A7	−1.089	−19.121	4	Arg 29	1.93	A: ARG29: (H)HH21	Ligand: (N)
					2.25		
				Glu 25	2.25	B: LYS 51: (H)HZ1	Ligand: (N)
				GLY 25	2.46	A: GLY 25: (O)OE1	Ligand: (H)
						A: GLY 25: (H)H1	Ligand: (O)
A8	−3.497	−49.899	1	Thr 26	2.15	A: THR 26: (H)HG1	Ligand: (O)

also observed. The H-6″ proton resonance shows a COSY correlation to H-5″ and was confirmed by HSQC correlations between C-6″ and C-5″ occurring at δ 128.00 and 127.49, respectively. Fig. 2 shows the HMBC correlation for **A1**.

The ^{13}C NMR spectrum of **A1** is presented in Fig. S8. The peaks at δ 51.90 and δ 52.34 were assigned to the two acetoxy carbons (C-9′, C-10′); the peak at δ 58.06 was assigned to carbon of CN (C-3′) and the peak at δ 39.03 was assigned to the C—H (C-4′) on the dihydropyridine ring. The peaks at δ 162.64 are assigned to the two C═O (C-7′, C-8′); the peak at δ 164.73 was assigned to the C-NH_2 (C-2′) whilst the peaks at δ 150.99–120.33 were attributed to aromatic carbons. The ^{13}C NMR spectra of all compounds were appropriate to their formulas. Mass spectra of the compounds showed *m/z* in accordance with their formulas. The mass spectrum of **A1** is presented in Fig. S9, it shows the *m/z* value for the molecular ion corresponding to the proposed molecular formula at 475.

The cancer study was used to investigate the cytotoxicity of synthesized quinoline derivatives (**A1**–**A8**) in the A549 lung cancer cell line. These compounds differed in substituents like OCH_3, CH_3, F and Cl attached to the benzene ring. Herein we decided to investigate the effect of these compounds based on the different functional groups to study their anticancer potential. At this stage of our investigation, we were unable to source out a suitable standard containing the dihydropyridine nucleus and hence we selected **A1** as a reference point. Our hypothesis was that the presence of functional groups present in the phenyl part will influence cytotoxicity. The parent compound **A1** (with no substituent in the benzene ring) is not cytotoxic but rather increases metabolic activity as all concentrations tested show greater activity than control. The compound **A2** (with an electron donating group, OCH_3 substituent in the benzene ring), shows a dose dependent toxicity due to its substituent as the results gives evidence that the compound has potential as an anti-cancer drug. The compound **A3** (with an electron donating group, CH_3 substituent in the benzene ring) shows high toxicity due to its CH_3 substituent but only at higher concentrations; has potential as an anti-cancer drug. The compound A4 (with the chloro group, which withdraws electrons by induction, but donates electrons by resonance in the benzene ring) showed a dose dependent toxicity with the highest toxicity at 250 μM. The compound had potential as an anti-cancer drug. **A5**, **A6** and **A7** (with the fluoro group in the benzene ring) were not cytotoxic. A8 (with the two chloro groups, which withdrew electrons by induction, but donated electrons by resonance in the benzene ring) showed a dose dependent toxicity with the highest toxicity at 125, 250 and 500 μM. The compound had potential as an anti-cancer drug (Figs. 3–10).

All compounds (**A1**–**A8**) were evaluated for antibacterial activity against two Gram-negative bacteria, *E. coli* and *P. aeruginosa* and one Gram-positive bacterium, *S. aureus*. Standard antibiotics, ciprofloxacin and nalidixic acid were used as positive controls and DMSO used as negative control. DMSO had no effect on the bacteria in the concentrations. The antimicrobial activity results, Table 2 revealed that the synthesized compounds showed moderate to good activity towards the mentioned panel of bacteria strains. It is interesting to note that compound with substituted anilines in the *para* position (**A4**, **A7** and **A8**) showed very good activity against all strains. These compounds were found more potent than both standards, ciprofloxacin (MIC = 50 μM) and nalidixic acid (MIC = 50 μM) towards *S. aureus* and *P. aeruginosa*. Compound **A1** (MIC = 128 μM) exhibited comparable activity as the standard nalidixic acid (MIC = 128 μM) against *P. aeruginosa* but showed no inhibitory effect against *S. aureus E. coli*. Compounds **A2** and **A3** showed poor activity towards all strains compared with the standard antibiotics.

The binding mode of **A1** within the active site of the human mdm2 was analyzed and the suitable shape of the compound helped it to bind tightly with the active site of the human mdm2. There was one hydrogen bond interaction formed between the side chains of the hydrophobic residue of TYR 104. The bond lengths between **A1** into the active site of the human mdm2 were observed (2.15 Å). Docking of **A1** with human mdm2 indicated lowest binding energy, glide score −6.111 Kcal/mol and glide energy −62.406 Kcal/mol thereby showing strong affinity of the ligand molecule with the receptor which had been stabilized by strong hydrogen bond interactions in the binding pocket. Furthermore, the following residues were mainly involved in hydrophobic interaction LEU27, VAL28, MET50, LEU54, PHE55, ILE61, MET62, TYR67, VAL75, VAL93, and ILE99. Table 3 shows the docking results of all of the compounds (**A1**–**A8**), glide score (Kcal/mol), glide energy (Kcal/mol), interacting residues, distance between the protein and ligand (Å), hydrogen bond donor and hydrogen bond acceptor. Fig. 11a, b and c shows hydrogen bond formation, hydrogen bond formation

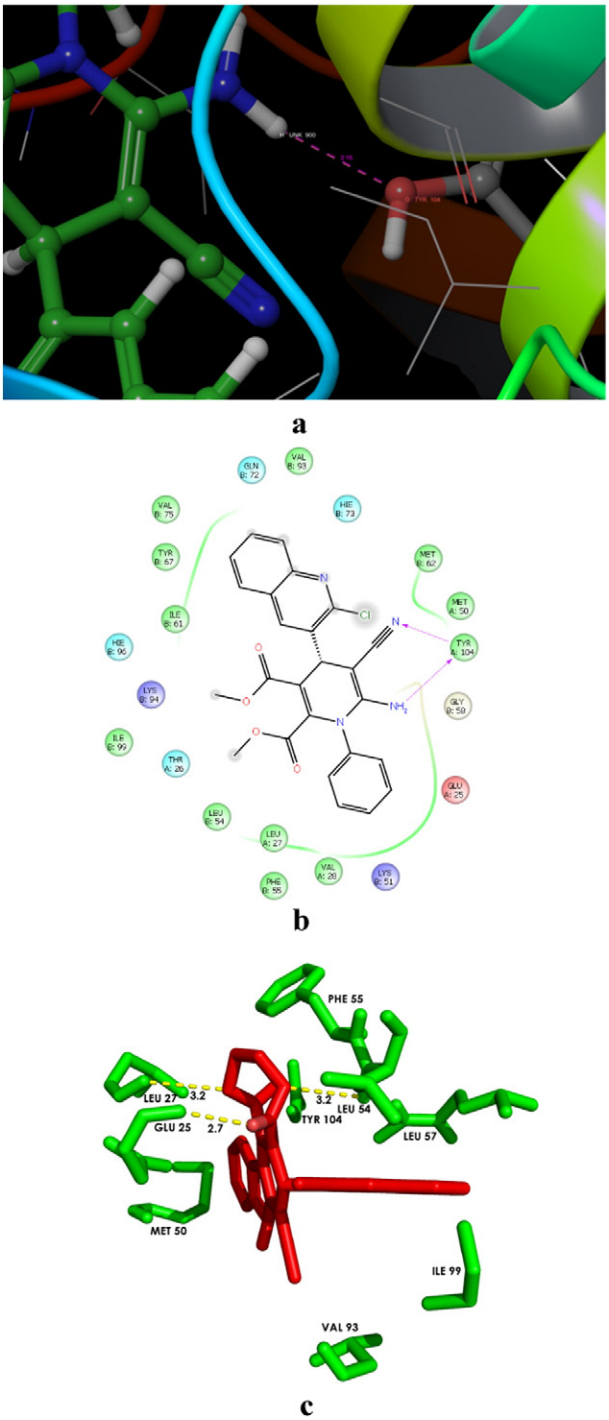

Fig. 11. a, b & c Molecular docking result of A1 with human mdm2.

and bond length and the binding mode of **A1** compound with E3 ubiquitin-protein ligase mdm2.

4. Conclusion

All compounds containing quinoline and dihydropyridine nucleus in a single molecular frame work were efficiently synthesized and fully characterized. *In vitro* anticancer and antibacterial studies were carried out; molecular docking was also investigated. The biological studies revealed that these compounds are selective in their action. The anti-cancer assay indicated that compounds **A2**, **A3**, **A4** and **A8** have good potential as an anticancer drug. The results obtained from the antibacterial assay showed that compounds A4, A7 and A8 have good activity compared to that of standard drugs, whereas **A2** and **A3** showed poor activity against the tested bacterial strains. Compound **A1** showed no inhibitory effect against *S. aureus E. coli*. Docking of **A1** with human mdm2 indicated the lowest binding energy thereby showing strong affinity of the ligand molecule with the receptor which has been stabilized by strong hydrogen bond interactions in the binding pocket. This confirms that **A1** is a better inhibitor for mdm2. Hence compound **A2–A8** showed an interesting correlation between docking scores and experimental binding data.

Acknowledgement

We are grateful to the National Research Foundation (NRF) and Durban University of Technology (DUT) for funding this project.

Appendix A. Supplementary Data

Supplementary data to this article can be found online at http://dx.doi.org/10.1016/j.jphotobiol.2016.10.009.

References

[1] M.M. Heravi, M.H. Tehrani, K. Bhakhtiari, H.A. Oskooie, Synthesis of 2,4,5-triaryl-imidazoles catalyzed by $NiCl_2 \cdot 6H_2O$ under heterogeneous system, Catal. Commun. 8 (2007) 1341–1344.
[2] E.B. Golden, H.Y. Cho, F.M. Hofman, S.G. Louie, A.H. Schönthal, T.C. Chen, Quinoline-based antimalarial drugs: a novel class of autophagy inhibitors, Neurosurg. Focus. 3 (2015) 50.
[3] D. Liu, X. Wen, S. Wang, Synthesis and evaluation of the anti-inflammatory activity of quinoline derivatives, Med. Chem. Res. 24 (2015) 2591.
[4] S. Maddela, M. Ajitha, M. Venugopal, R. Maddela, Design and synthesis of novel quinoline 3-carbohydrazone derivatives for their antimicrobial and antioxidant activity, Int. J. Pharm. Pharm. Sci. 6 (2014) 254–258.
[5] V. Nadaraj, S.T. Selvi, Synthesis and characterization of some quinoline bearing isoxazoles nucleus, J. Chem. Pharm. Res. 4 (2012) 2850–2853.
[6] D. Wu, Studies on novel heterocyclic compounds and their microbicidal efficacy, Tetrahedron 59 (2003) 8649–8687.
[7] V.P. Litvinov, Thienopyrimidines: synthesis, properties, and biological activity, Russ. Chem. Bull. 53 (2004) 487–516.
[8] A. Chipeleni, J. Gut, P.J. Rosenthal, K. Chibale, Synthesis and biological evaluation of phenolic Mannich bases of benzaldehyde and (thio) semicarbazone derivatives against the cystein protease falcipain-2 and a chloroquine resistant strain of *Plasmodium falciparum*, Bioorg. Med. Chem. 15 (2007) 273–282.
[9] S. Kumar, S. Bawa, H. Gupta, Biological activities of quinoline derivatives, Mini-Rev. Med. Chem. 9 (2009) 1650–1654.
[10] M.R. Mahmoud, E.A.A. El-Bordany, N.F. Hassan, F.S.M. Abu El-Azm, Utility of nitriles in synthesis of pyrido[2,3-d]pyrimidines, thiazolo[3, 2-a]pyridines, pyrano[2,3-b]benzopyrrole, and pyrido[2,3-d]benzopyrroles, Phosphorus Sulfur Silicon 182 (2007) 2507–2521.
[11] M. Ashrafali, M.S. Yar, M. Kumar, G. Pandian, Synthesis and antitubercular activity of substituted novel pyrazoline derivatives, Nat. Prod. Res. 21 (2010) 575–579.
[12] M.C.S. Lourenco, M.V.N. De Souza, A.C. Pinheiro, M.L. Ferreira, R.S.B. Gonçalves, T.C.M. Nogueira, M.A. Peralta, Evaluation of anti-tubercular activity of nicotinic and isoniazid, ARKIVOC 15 (2007) 181–191.
[13] M. Kawase, A. Shah, H. Gaveriya, N. Motohashi, H. Sakagami, A.J. Varga, 3,5-Dibenzoyl-1,4-dihydropyridines: synthesis and MDR reversal in tumor cells, Bioorg. Med. Chem. 10 (2002) 1051–1055.
[14] C. Safak, R. Simsek, Fused 1,4-dihydropyridine as potential calcium modulatory compounds, Mini-Rev. Med. Chem. 6 (2006) 747–755.
[15] E.R. Anabha, K.N. Nirmala, A. Thomas, C.V. Asokan, Synthesis of 3-aroylnicotinonitriles from aroylketene dithioacetals, Synthesis 3 (2007) 428–432.
[16] M.D. Fletcher, T.E. Hurst, T.J. Miles, C.J. Moody, Synthesis of highly-functionalized pyridines via hetero-diels-alder methodology: reaction of 3-siloxy-1-aza-1,3-butadienes with electron deficient, Tetrahedron 62 (2006) 5454–5463.
[17] P.V. Shinde, S.S. Sonar, B.B. Shingate, M.S. Shingare, Boric acid catalyzed convenient synthesis of 2-amino-3,5-dicarbonitrile-6-thio-pyridines in aqueous media, Tetrahedron Lett. 51 (2010) 1309–1312.
[18] M. Sridhar, B.C. Ramanaiah, C. Narsaiah, B. Mahesh, M. Kumaraswamy, K.K.R. Mallu, V.M. Ankathi, P. Rao, Novel $ZnCl_2$-catalyzed one-pot multicomponent synthesis of 2-amino-3,5-dicarbonitrile-6-thio-pyridines, Tetrahedron Lett. 50 (2009) 3897–3900.
[19] R.M. Gengan, P. Pandian, C. Kumarsamy, P.S. Mohan, Convenient and efficient microwave-assisted synthesis of a methyl derivative of the fused indoloquinoline alkaloid cryptosanguinolentine, Molecules 15 (2010) 3171–3178.
[20] R.J.K. Taylor, M. Reid, J. Foot, S.A. Raw, Organic syntheses, Collective Acc. Chem. Res. 12 (2005) 66–69.
[21] M.K. Sinha, K. Khoury, E. Herdtweck, A. Domling, Tricycles by a new Ugi variation and Pictet-Spengler reaction in one pot, Eur. J. Chem. 19 (2013) 8048–8052.
[22] I. Ugi, The solution phase synthesis of diketopiperazine libraries via the Ugi reaction: novel application of Armstrong's convertible isonitrile, Angew. Chem. Int. Ed. Eng. 1 (1962) 8–21.
[23] A.G. Degussa, Catalytic enantioselective Strecker reactions and analogous syntheses, Chem. Rev. 103 (2003) 2795–2827.
[24] A.M. Shestopalov, D.H. Evans, One-step synthesis of substituted 6-amino-5-cyanospiro-4-(piperidine-4′)-2H, 4H-dihydropyrazolo [3,4-b]pyrans, Org. Lett. 16 (2002) 423–425.
[25] N.K. Ladani, D.C. Mungra, M.P. Patel, R.G. Patel, Microwave assisted synthesis of novel Hantzsch 1,4-dihydropyridines, acridine-1,8-diones and polyhydroquinolines bearing the tetrazolo[1,5-a]quinoline moiety and their antimicrobial activity assess, Chin. Chem. Lett. 22 (2011) 1407–1410.
[26] J.P. Nirmal, M.P. Patel, R.G. Patel, Microwave-assisted synthesis of some new biquinoline compounds catalyzed by DMAP and their biological activities, Indian J. Chem. 48B (2009) 712–717.
[27] G. Bepler, Preoperative exercise Vo2 measurement for lung resection candidates: results of cancer and leukemia group B protocol 9238, J. Thorac. Oncol. 2 (2007) 619–625.
[28] A. El-Hussein, Study DNA damage after photodynamic therapy using silver nanoparticles with A549 cell line, J. Nanosci. Nanotechnol. 7 (2016) 346.
[29] A. Mehrotra, R.C. Nagarwal, J.K. Pandit, Fabrication of lomustine loaded chitosan nanoparticles by spray drying and in vitro cytostatic activity on human lung cancer cell line L132, J. Nanosci. Nanotechnol. 103 (2010) 2157–7439.
[30] G.L. Firestone, Anticancer activities of artemisinin and its bioactive derivatives, Rev. Mol. Med. 1 (2009) 11.
[31] R. Singh, P. Wagh, S. Wadhwani, S. Gaidhani, A. Kumbhar, J. Bellare, B.A. Chopade, Synthesis, optimization, and characterization of silver nanoparticles from acinetobacter calcoaceticus and their enhanced antibacterial activity when combined with antibiotics, Int. J. Nanomedicine 8 (2013) 4277–4290.
[32] K.B. Shoichet, L.S. McGovern, Molecular docking and high-throughput screening for novel inhibitors of protein tyrosine phosphatase-1B, J. Med. Chem. 45 (2002) 2213–2221.
[33] H. Clauben, C. Buninga, M. Rareya, T. Lengauera, Efficient molecular docking considering protein structure variations, J. Mol. Biol. 308 (2001) 377–395.
[34] R. Kharb, Y.M. Shahar, Recent advances and future perspectives of triazole analogs as promising antiviral agents, Rev. Med. Chem. 11 (2011) 84–96.
[35] H. Gandhi, S. Khan, Biological synthesis of silver nanoparticles and its antibacterial activity, J. Nanosci. Nanotechnol. 7 (2016) 366.
[36] R. Supino, MTT assays, Methods Mol. Biol. 43 (1995) 137.
[37] Ligprep, Schrodinger, Version 2.3., 2009. LLC, New York, NY.
[38] Glide, Schrodinger, Version 5.5., 2009. LLC, New York, NY.
[39] A. Srivastava, R.M. Singh, Vilsmeier-Haack reagent: a facile synthesis of 2-chloro-3-formylquinolines from N-arylacetamides and transformation into different functionalities, Indian J. Chem. 44 (2005) 1868.